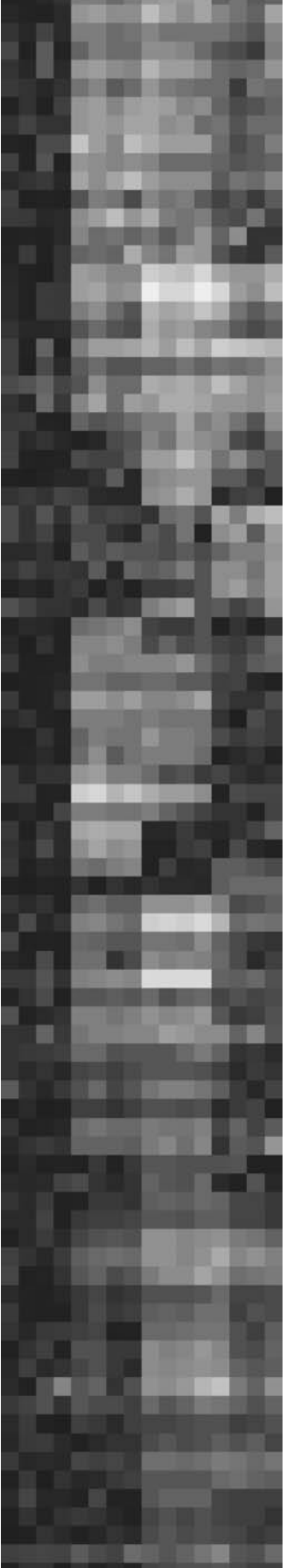

Transcriptomics as a tool to dissect copper homeostasis and COMMD protein function

Patricia Muller

ISBN 978-90-8559-362-1

Print and layout by Optima Grafische Communicatie BV, Rotterdam, The Netherlands

Transcriptomics as a tool to dissect copper homeostasis and COMMD protein function

Het gebruik van transcriptomics om koperhomeostase en de functie van COMMD eiwitten te doorgronden

(met een samenvatting in het Nederlands)

Proefschrift

ter verkrijging van de graad van doctor aan de Universiteit Utrecht op gezag van de rector magnificus, prof.dr. J.C. Stoof, ingevolge het besluit van het college voor promoties in het openbaar te verdedigen op dinsdag 25 maart 2008 des middags te 14.30 uur

door

Patricia Anthonia Johanna Muller

geboren op datum 7 oktober 1980
te Rotterdam

Promotoren: Prof. dr. C. Wijmenga
Prof. dr. R. Berger

Co-promotor: Dr. L.W.J. Klomp

Voor Oma

Contents

	Preface	000
Chapter 1	Novel perspectives in mammalian copper homeostasis through the use of genome-wide approaches	000
Chapter 2	Gene expression profiling of liver cells *in vivo* and *in vitro* reveals new copper-regulated genes	000
Chapter 3	Novel insights in the pathophysiology of Wilson disease and Hereditary hemochromatosis by a transcriptomics meta-analysis	000
Chapter 4	Increased activity of HIF-1 is associated with early embryonic lethality in COMMD1 null mice	000
Chapter 5	Distinct COMMD proteins regulate the expression of specific subsets of NF-κB target genes	000
Chapter 6	Nuclear-cytosolic transport of COMMD1 regulates NF-κB activity	000
Chapter 7	COMMD1 autoregulation is dictated by critical amino acid residues that determine XIAP binding	000
Chapter 8	General discussion	000
	References	000
	Nederlandse samenvatting	000
	Abbreviations	000
	Dankwoord	000
	Curriculum Vitae	000
	List of publications	000

Preface

Transcriptomics is a recently developed tool to characterize the genome-wide set of RNA transcripts at a given time. The overall aim of the research described in this thesis was to use transcriptomics to unravel novel aspects of copper metabolism and to gain insights in the function of COMMD proteins.

Copper is an essential trace metal that is required in several biological processes as cofactors in copper-dependent enzymes, but can be highly toxic in excess. The necessity and the toxicity of copper are illustrated in Menkes disease and Wilson disease. Menkes disease is a lethal X-linked inherited disorder that arises from various mutations in the gene encoding the copper transporting P-type ATPase ATP7A and is characterized by copper deficiency due to insufficient copper uptake from the placenta and the diet [1-3]. Patients with Menkes disease present at a very young age with a spectrum of phenotypes including neurological degeneration and growth retardation caused by a dysfunction of copper-dependent enzymes. Wilson disease is an autosomal recessive inherited disorder resulting from mutations in the gene encoding a homologous P-type ATPase, ATP7B [4, 5]. ATP7B is expressed in hepatocytes and is essential for the excretion of copper from the liver cell into the bile. Decreased biliary excretion of copper in patients with Wilson disease results in marked copper deposition in the liver and some extrahepatic organs. Patients may manifest with liver disease or neurological defects; or a combination of both. These disorders underscore that maintaining adequate copper homeostasis is crucial for health and development. The proteins responsible for maintaining intracellular copper homeostasis and human copper homeostasis disorders have been extensively reviewed in [6, 7] Nevertheless, our knowledge of the exact mechanisms responsible for the regulation of copper homeostasis is limited and the pathophysiological mechanisms leading to expression of liver disease and neurological disease are incompletely understood .In the work in this thesis we therefore first set out to dissect the pathophysiological mechanisms that underlie human copper homeostasis disorders. As an introduction to this field of research, the recent advances and future perspectives of systems biology approaches in copper metabolism, denoted as cupromics, is reviewed in **chapter 1.** Systems biology is defined as the systematic study of genome-wide changes to the genome, the transcriptome, the proteome and the metabolome and the mutual interactions between these biological components. Such approaches offer a novel and good opportunity to advance our knowledge on copper homeostasis. In **chapter 2,** we used transcriptomics, to investigate genome-wide gene expression changes in liver cells and mouse livers after copper overload. In this study, we aimed to characterize several novel copper-responsive genes, but our data indicated that direct transcriptional regulation of copper import, copper distribution, copper utilization or copper export appeared to be absent. Our second aim was to identify genes that were induced or repressed by prolonged copper exposure, to begin to define transcriptional responses associated with copper-induced liver disease. Individual

transcriptomics studies are prone to experimental variations. To overcome this issue, we performed a literature-based transcriptomics meta-analysis to dissect the underlying transcriptional pathogenic mechanisms leading to hepatic copper overload disease in **chapter 3**. In this analysis all publicly available, deposited transcriptional changes after copper overload *in vitro* and *in vivo* were listed and reanalyzed, including the data from **chapter 2**. The transcriptomics meta-analysis thus characterized several biological processes associated with copper-induced liver cirrhosis and liver failure. Similar to copper, iron is also a redox-active metal, whose accumulation in the liver also results in liver cirrhosis and liver failure. In order to determine the specificity of the copper-dependent transcriptional changes, we therefore also retrieved all available transcriptional data on iron overload and compared hepatic transcriptional changes between iron and copper overload. This comparative transcriptomics meta-analysis revealed novel biological processes specifically involved in the pathogenesis of copper overload disorders and iron overload disorders.

In chapter 2, we identified that the expression of a family of proteins was repressed after copper overload. This family, the COMMD proteins consist of 10 members that are ubiquitously expressed. Originally, one of the members of the COMMD protein family, *COMMD1* (Copper Metabolism MURR Domain protein 1), was identified as the gene mutated in Bedlington terriers that suffered from an autosomal recessively inherited condition named hepatic copper toxicosis [8]. In Bedlington terriers affected with copper toxicosis, mutations in *COMMD1* resulted in the complete absence of detectable COMMD1 protein expression. COMMD1 interacts with the hepatic copper exporter ATP7B [9, 10]. Together these data provided independent genetic and biochemical evidence implicating COMMD1 as a novel protein in cellular copper excretion. More recently COMMD1 has been implicated in other biological processes, including NF-κB (nuclear factor-kappa B) signaling [11]. Through interactions with various proteins involved in NF-κB signaling, COMMD1 could inhibit NF-κB mediated transcription. In addition, COMMD2-9 could similarly inhibit NF-κB mediated transcription [11]. The precise functions of COMMD1 and other COMMD proteins still remain elusive. The second aim of this thesis was to gain better insights into the function of COMMD proteins through the combined use of transcriptomics and molecular cell biological approaches. In order to study the function of COMMD1, a *Commd1* knockout mouse was generated **(chapter 4)**. Remarkably, *Commd1* knockout mice were embryonically lethal, indicating that COMMD1 plays a pivotal role in mouse embryogenesis. To characterize the underlying physiological mechanisms leading to embryonic lethality, we compared the genome-wide gene expression profiles of *Commd1* knockout embryos to wild type littermate embryos in **chapter 4**. From this study, we established a novel role for COMMD1 in repressing the expression of genes that are regulated by the transcription factor HIF-1 (hypoxia-inducible factor 1).

In **chapter 5**, we used transcriptomics approaches to address the function of COMMD1 and two other COMMD proteins, COMMD6 and COMMD9, in regulating NF-κB signaling in a cellular system. Gene expression profiles in COMMD deficient cells were compared to control cells cultured in the absence or in the presence of tumor necrosis factor (TNF), a well-established NF-κB stimulus. All three investigated COMMD proteins were able to modulate the expression of TNF target genes after TNF exposure.

These findings prompted us to address the specific molecular function of COMMD1 as a transcriptional regulator in relation to its cellular localization. The function of many proteins that play a role in NF-κB or HIF-1 signaling is regulated though nucleocytoplasmic shuttling. Specific NESs (nuclear export signals) or NLSs (nuclear localization signals) dominate nucleocytoplasmic shuttling of these proteins. In **chapter 6**, we characterized two functional NESs in COMMD1, which appeared to control the inhibitory role of COMMD1 in NF-κB signaling. In collaboration with Dr E. Burstein, we detected that nuclear export of COMMD1 was associated with COMMD1 polyubiquitination and COMMD1 degradation. These observations were further explored in **chapters 6 and 7**. Finally, the contribution of the results in this thesis to our current knowledge of copper metabolism and COMMD protein function are integrated and discussed in **chapter 8** in the context of transcriptional regulation.

Chapter 1

Novel perspectives in mammalian copper homeostasis through the use of genome-wide approaches

Patricia A.J. Muller, Leo W.Klomp

Laboratory for Metabolic and Endocrine Diseases,
UMC Utrecht, the Netherlands

American Journal of clinical nutrition, in press

Abstract

The transition metal copper plays an essential role in many biological processes, but is highly toxic in excess. Recent studies have characterized a highly conserved set of proteins that mediate cellular copper import, distribution, sequestration, utilization and export. Nevertheless, the pathogenesis of copper overload and copper deficiency disorders are not well understood and we are only beginning to comprehend the results of mild copper overload or deficiency in relation to nutritional uptake and common diseases at the population level. Technological advances in genetics, genomics, transcriptomics, proteomics and metabolomics open the possibility to dissect the complete genome for genetic variants predisposing to copper overload or depletion and for variations in gene expression generated by either reduced or excessive copper intake. In this respect, genome-wide gene expression analyses using cDNA microarray technology have recently provided insights on copper-mediated toxicity *in vivo* and *in vitro*. Proteomic analyses have identified novel copper-binding proteins and have revealed copper-dependent protein-protein interactions. This review will discuss the recent achievements and future potential of integrated genome-wide applications to advance our knowledge on copper homeostasis, and to develop molecular biomarker profiles as sensitive indicators of copper status.

Introduction

Copper is an essential micronutrient, which plays a critical role in various biological processes. Both shortage and excess of this trace metal can lead to serious abnormalities as illustrated by the inherited disorders Menkes disease and Wilson disease. A tight balance of copper uptake, excretion, storage and utilization is therefore crucial and is maintained by several proteins that appear to be largely conserved in evolution. Several of these proteins have been characterized in the past decades via a variety of studies including positional cloning and heterologous complementation of copper-related phenotypes in yeast.

Systems biology offers unique possibilities to identify novel regulatory mechanisms and adaptive responses involved in copper metabolism. Differences in genomic, transcriptomic, proteomic and metabolic profiles due to variations in copper exposure will characterize new genes, proteins, signaling cascades and metabolites that have a role in copper biology. The integration of these techniques will help to dissect the precise regulatory mechanisms that underlie these profiles. Individual profiles may also be used as a fingerprint for disease or nutritional state or to select for specific biomarkers that can be used for diagnostic purposes.

The implementation of such approaches is important. Copper has long been suspected to play a role in the pathogenesis of cardiovascular disease, by virtue of its capacity to oxidize arterial wall components. Similarly, copper is thought to play an important role in the pathogenesis of neurodegenerative disorders, particularly Alzheimers disease. Nevertheless, these biomedical effects of copper currently remain somewhat controversial and incompletely understood. Such disease-nutrient interactions are most probably rather subtle and will rely on the specific genetic build-up of individual patients as well as environmental aspects. An unbiased, systematic and integrated systems biology approach is therefore likely to advance our knowledge in this field.

In line with the current nomenclature and the already established term metallomics that comprises all metals, the systems biology approach to unravel copper metabolism will be designated cupromics in this review. Here, we will discuss recent advances and future perspectives in cupromics.

Achievements in cupromics and future perspectives

Advances in genome-wide screening technologies have enabled us to examine copper-dependent changes of the genome, the transcriptome, the proteome and the metabolome in a systematic and high-throughput fashion. The contribution of each of the 'omics' approaches to dissect copper metabolism and the most prominent studies in these

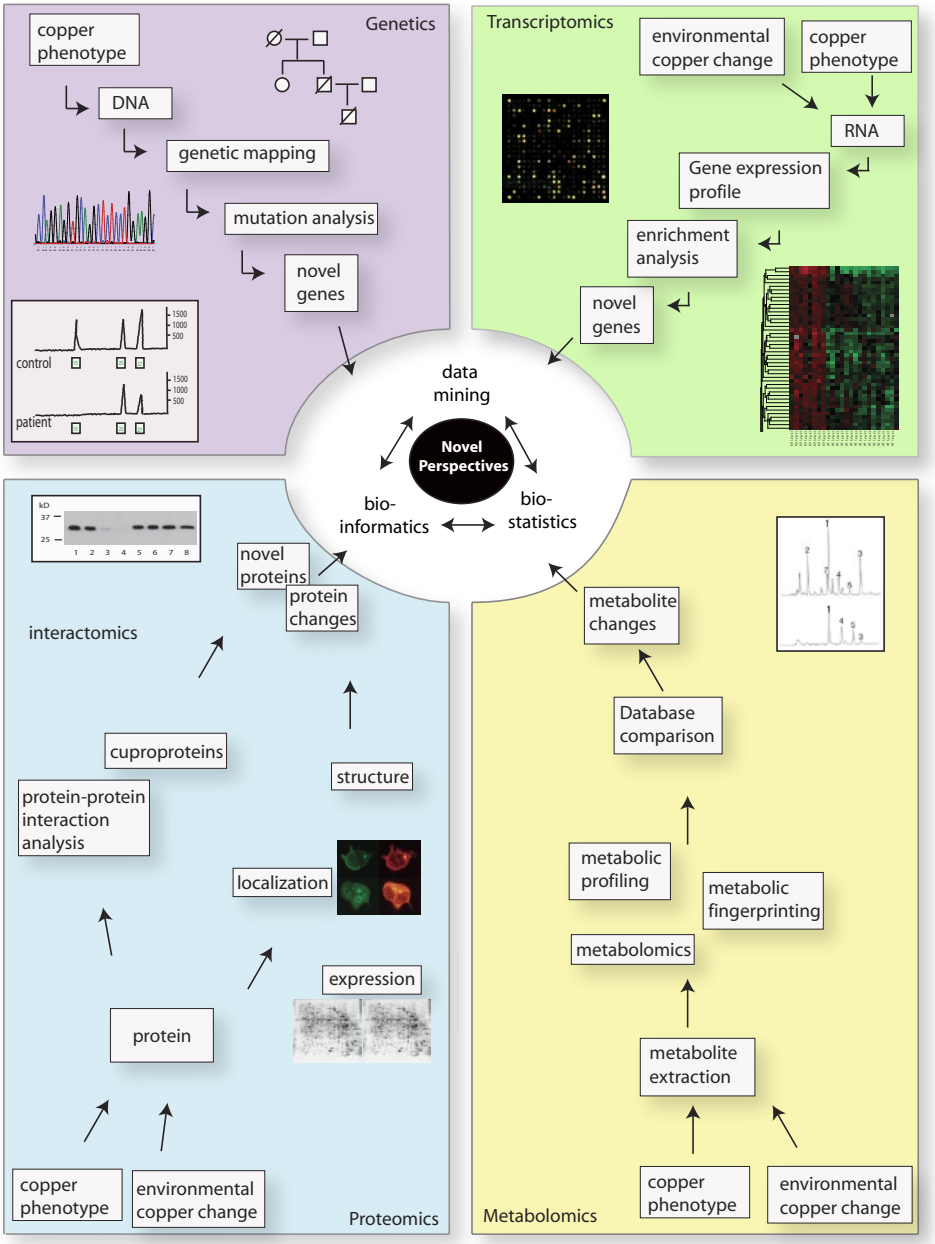

Figure 1 Flow chart of systems biology approaches in copper metabolism

areas are discussed below. Figure 1 summarizes the strategies employed to gain novel insights in the mechanisms of copper homeostasis and these strategies are described below. Table I summarizes the mostly used techniques and analysis methods.

Table 1 High-throughput strategies in cupromics approaches

objective	technique	analysis
genetics		
Novel gene discovery	Haplotype sharing	SNP-typing, microsatellites
transcriptomics		
Gene expression differences	Chip-based cDNA microarrays	DNA hybridization
Novel gene expression networks	Chip-based cDNA microarrays	DNA hybridization, enrichment analysis
Transcriptional profiling	Chip-based cDNA microarrays	DNA hybridization, cluster methods
proteomics		
Protein expression differences	protein purification, 2-D PAGE, MALDI-TOF MS	Database mass comparison analysis
	Chip-based protein microarrays	Antibody detection
Protein modifications	protein purification, MS	Database mass comparison analysis
Protein profiling	MALDI-TOF MS; SELDI-TOF MS	Proteome survey, cluster methods
proteomics/interactomics		
Novel copper binding proteins	IMAC protein purification, 2-D PAGE, MALDI-TOF MS	Database mass comparison analysis
	WCX (weak cation exchange) protein chips	SELDI-TOF mass spectrometry
Novel copper-mediated interactions	Yeast-two hybrid technology, TAP (tandem affinity purification)	Cloning strategies and subsequent interaction analysis
metabolomics		
Metabolite variations	Total metabolome analysis	Metabolite extraction via HPLC,GC-MS, LC-MS, database comparison
Novel metabolic networks	Mass isotopomer analysis	Metabolite extraction techniques including NMR in combination with MS, radio-LC-MS, database comparison
Metabolite classification	Metabolic fingerprinting	NMR, MS, cluster methods

Genetics/ genomics

Inherited disorders of copper homeostasis have rendered valuable insights on genes that critically regulate copper metabolism. Positional cloning of the *ATP7A* gene and the highly homologues *ATP7B* in Menkes disease and Wilson disease, respectively established the pivotal role of copper transporting P-type ATPases in the biosynthesis of cuproproteins in the secretory pathway and in the cellular excretion of copper. More recently, a positional cloning approach in the dog breed Bedlington terrier affected with copper-toxicosis lead to the identification of *COMMD1* as a novel gene involved in copper excretion [8]. Indian childhood cirrhosis, Tyrolean infantile cirrhosis and idiopathic copper toxicosis are human copper overload diseases that originate from a combina-

tion of high dietary copper intake and genetic predisposition. Despite some attempts, the underlying genetic defects of the latter disorders have not been identified yet. In the near future, high-density SNP arrays should help to reveal novel genes that play a role in copper metabolism in these and other diseases of aberrant copper homeostasis both in man and in several sheep and dog breeds. Subsequently, genetically engineered mouse models will be studied to clarify the precise functions of these genes in copper homeostasis.

Functional genomics also holds great potential to identify new genes that are important in copper homeostasis. It is now possible to individually over express or silence genes in mammalian cell lines using cDNA libraries or libraries encoding short hairpin RNAs, respectively. To assess the effects of such treatments on copper metabolism, highly sensitive indicators of cellular copper status are necessary, preferably at the single cell level. Several laboratories are currently developing chemical or genetically-encoded copper sensors that may aid in functional genomic screens [12].

Transcriptomics

Recent advances in microarray-based transcription analysis have increased the sensitivity, reproducibility and accuracy to a level that the expression of virtually the whole genome can be monitored. At this moment, transcriptomics is therefore the most powerful 'omics' approach for complete genome coverage. Extended sets of differentially expressed genes have been identified in various cell types and in tissues of animals that are either exposed to variable copper concentrations or that have inappropriate copper levels due to inherited gene mutations (Muller *et al*., manuscript submitted). Genome-wide time-series gene expression analyses in HepG2 cells revealed a rapid response of genes induced by copper that exclusively comprised metallothionein genes. Copper overload also resulted in a delayed induction of genes directly or indirectly involved in oxidative stress [13]. The main hepatic transcriptional response in *Atp7b-/-* mice or mice exposed to a high-copper diet represented genes involved in cholesterol synthesis, cell death and cell cycle progression [13, 14]. Fibroblasts or macrophages that were exposed to copper similarly revealed enrichment in expression of genes involved in one or more of these processes, although the individual genes were different [15, 16]. Strikingly however, none of these experiments revealed differential expression of genes directly involved in copper import or export, implying that transcriptional regulation of copper homeostasis in mammals is limited. Regulatory mechanisms involved in maintaining intracellular copper levels therefore probably result from posttranslational events. Although genome-wide transcriptional profiling will probably not identify novel 'homeostasis' genes, this approach will prove essential to elucidate the adaptive responses of cells to chronic copper deficiency or copper overload.

Proteomics

The effects of copper on proteins are broad and comprise variations in protein expression, structure, localization and post-translational modifications. Specifically, they also include variations in metal-affinity of copper binding proteins and variations in copper-dependent protein-protein interactions. MALDI-TOF mass spectrometry plays a central role in the identification of proteins and protein modifications. Mass spectrometry is often preceded by 2D PAGE to visualize changes in protein expression or by affinity purification to select for proteins with specific properties. SELDI-TOF mass spectrometry provides a quick and high throughput method to analyze protein expression, but is not followed by protein identification. Protein microarrays offer an alternative sensitive way to screen for protein expression, without using mass spectrometry. In contrast to transcriptomics, proteomics techniques are subject to detection limitations because the physicochemical properties of individual proteins differ manifold more than those of nucleic acids.

Copper-induced expression changes of several proteins have been determined in North-Ronaldsay sheep that are highly sensitive to increased dietary copper. These changes mainly comprised proteins involved in the protection against the toxic effects of copper overload [17]. Interestingly, livers of rats subjected to a low-copper diet revealed changes in expression of proteins involved in cholesterol metabolism, consistent with the transcriptional changes observed in response to copper overload in other studies [18]. In addition, copper deficiency resulted in the increased expression of several protein chaperones that promote folding, suggesting that in the absence of copper, copper-containing proteins are misfolded.

Specific purification methods (Table I) have proven useful in identifying novel copper-binding proteins, novel copper-binding motifs and copper-associated protein modifications in human hepatoma cell lines [19-21], which may serve as biomarkers for disease states. Of specific interest in the context of copper-proteomics is the study of (copper-dependent) protein-protein interactions, also termed interactomics. As an example, yeast-two hybrid studies with ATP7B as a bait revealed interactions of GRX1 (glutaredoxin), PLZF (promyelocytic leukemia zinc finger) and p62 (dynactin subunit p62) with ATP7B [22-24]. The interactions with p62 and GRX1 are copper-dependent and affect the localization or the ATPase function of ATP7B, by which these proteins might affect intracellular copper levels.

Metabolomics

Although individual metabolites have been studied for centuries, the metabolomics field is the youngest research approach in the 'omics' family. It studies, in a high-throughput and systematic manner, changes in metabolite profiles and quantities in an organism or cellular system secondary to disease state or environmental parameters. By combining

one of the various extraction methods with mass spectrometric analysis (see Table I), many different metabolites can be accurately measured. Nevertheless, a combination of multiple analysis methods is necessary to reach significant coverage of the complete metabolome. Changes in enzyme function greatly affect the variety and quantity of several metabolites. As copper is a catalyst in several enzymatic reactions, changes in metabolite quantity and variety are to be expected upon copper challenge or depletion. In addition, copper-mediated oxidative stress results in peroxidation of biomolecules that can subsequently act as signal transducers and affect metabolite quantities and diversity. Although copper-dependent metabolite profiles have not been examined extensively yet, some studies indicated that the abundance of metabolites involved in carbohydrate metabolism, dopamine metabolism and detoxification of oxidative stress vary in response to changing copper levels [25-27]. In Wilson disease patients, proton MR (magnetic resonance) spectroscopy has been conducted and provided a non-invasive way to determine metabolic changes in the brain of these patients [28], illustrating the potential of extensive metabolome profiling for clinical studies.

The development of metabolomics faces many challenges. The number of metabolites and their chemical diversity vastly exceeds the proteome. Metabolite extraction from several biological matrices, pre-MS separation, data preprocessing, metabolite identification, and data analysis all need further development. More fundamentally, as many of the metabolomics techniques rely on the calculation of mass differences that are to be expected based on known reactions or prediction models, uncommon reactions and reactions with large mass differences can not be reliably measured. Future research in which the whole metabolome can be monitored for copper-dependent variations will probably unravel new and highly important metabolome networks that will help in the understanding of copper metabolism and may serve as potential biomarkers.

Conclusions

Will systems biology completely replace recent and current methodology that appeared so successful in the characterization of the mechanisms of copper homeostasis? Obviously, this is not the case. Since genome-wide assessment of copper metabolism is a relatively new field, it needs to be developed parallel to more conventional approaches. In that respect, further development of cupromics will appear highly dependent on existing well-characterized and genetically homogeneous yeast and animal models. In this context, the incorporation of bioinformatics and biostatistics in this area will also be highly necessary. In addition, as an unbiased approach, cupromics will generate rather than test hypotheses; novel genes and novel perspectives identified in a systems biology approach need to be rigorously functionally tested.

In conclusion, the rapid evolvement of genome-wide profiling techniques set the first careful and exciting steps and will pave the way for investigating novel aspects of copper metabolism. The individual profiles established by any of the cupromics approaches may serve as a fingerprint for disease state and nutrition state. Using an integrated, multidisciplinary, systems biology approach, we will better understand the role of copper in a variety of human diseases, including cardiovascular and neurodegenerative disorders, which might provide novel therapeutic avenues.

Acknowledgements

We apologize to all our colleagues, whose work could not be cited due to space limitations. We thank Ruud Berger, Margriet Hendriks and Cisca Wijmenga and members of the Klomp-Wijmenga laboratories for helpful discussions.

Chapter 2

Gene expression profiling of liver cells *in vivo* and *in vitro* reveals new copper-regulated genes

Patricia A.J. Muller[1,2], Harm van Bakel[2,3], Bart van de Sluis[2,5], Frank Holstege[3], Cisca Wijmenga[2,5], Leo W.J. Klomp[1,5]

[1]Laboratory for Metabolic and Endocrine Diseases, UMC Utrecht, the Netherlands;
[2]Complex Genetics Section, DBG-Department of Medical Genetics, UMC Utrecht, the Netherlands; [3]Genomics Lab, UMC Utrecht, the Netherlands;
[4]Oncogenesis and Development Section, NHGRI, National Institutes of Health, Bethesda, MD 20892, USA;
[5]Equal contributions

Journal of biological and inorganic chemistry, 2007;12(4): 495-507

Abstract

Copper toxicity in the liver is mediated by free radical generation, resulting in oxidative stress. To prevent toxic accumulation of copper, liver cells adapt to high copper levels. Here, we used microarray analysis to compare the adaptive responses on global gene expression in liver cells exposed to high copper levels in vitro and in vivo.

In HepG2 cells we identified two clusters of upregulated genes over time, an "early" cluster that comprised metallothionein genes and a "late" cluster, highly enriched in genes involved in proteasomal degradation and in oxidative stress response. Concomitant with the 'late' cluster, we detected a significant downregulation of several copper metabolism MURR1 domain (COMMD) genes that were recently implicated in copper metabolism and inhibition of nuclear transcription factor κB (NF-κB) signaling. As metal-induced oxidative stress increases NF-κB activity, our data suggest a role for reduced COMMD protein levels in prolonged activation of NF-κB, thus inducing cell survival. Mice, exposed to a copper diet that highly exceeded normal daily intake, accumulated only two-fold more hepatic copper than control mice. Although a moderate, but significant upregulation of a set of 22 genes involved in immunity, iron and cholesterol metabolism was detected, these cannot account for direct mechanisms involved in copper excretion.

In conclusion, we identified a novel set of genes that represent a delayed response to copper overload, thus providing insight into the adaptive transcriptional response to copper-induced oxidative stress.

Introduction

All organisms require the uptake of the trace metal copper, which plays an essential role as a catalyst for several enzymatic reactions. In excess conditions, this capacity renders copper highly toxic, because free copper catalyzes the reaction between superoxide anion and hydrogen peroxide producing the hydroxyl radical in the Haber-Weiss reactions [29].

$$O_2^{\cdot-} + Cu^{2+} \rightarrow O_2 + Cu^{+}$$
$$Cu^{+} + H_2O_2 \rightarrow Cu^{2+} + OH^{\cdot} + OH^{-}$$

The hydroxyl radical generated can directly damage essential cellular components such as lipids, nucleic acids and proteins.

The toxic nature of copper is apparent in Wilson disease that is characterized by impaired biliary copper excretion secondary to inherited mutations in the *ATP7B* gene [5]. The concomitant accumulation of copper in the liver can result in hepatocellular injury and eventually copper overload in other tissues such as the brain. Other diseases that present with accumulation of copper in the liver are Indian childhood cirrhosis and idiopathic copper toxicosis, which are associated with high levels of dietary copper intake with exposures as high as 8 mg/L copper in drinking water [30, 31]. Healthy individuals exposed to similar concentrations of copper may experience gastrointestinal problems, but blood indicators of copper overload remain unaffected [32]. This suggests that the livers of healthy individuals adapt to changes in copper exposure by increased biliary copper excretion.

The yeast strain *Saccharomyces cerevisiae* is an important model system for the study of eukaryotic copper metabolism [33]. Many of the pathways involved in copper homeostasis were originally discovered in yeast and are conserved over a wide variety of species including mammals. Regulation of copper homeostasis occurs both on the transcriptional level by copper-responsive transcription factors, and by post-translational processes such as copper-dependent internalization of transporters [34-36]. In comparison with yeast, little is known about the transcriptional regulation of genes involved in mammalian copper homeostasis. Metallothioneins are small cytoplasmic metal-binding proteins that are upregulated during excess conditions of copper and regulated by the transcription factor *MTF1* [37]. Other transcription factors that could regulate expression of copper import or export proteins during copper overload such as seen in yeast, have not been identified in mammals.

Some contradictory results have been published on the expression of certain genes encoding proteins involved in copper import and export in both human-derived and animal-derived cellular systems, as well as in animal tissues. *Ctr1,* the gene encoding the

major copper influx carrier, was reported to be induced in the intestine of rat pups in response to a high-copper diet [38], but no differential expression of *Ctr1* was observed by others [39, 40]. Intestine-derived Caco-2 cells do not experience changes in *CTR1* expression during copper overload [39, 41]. Finally, *Atp7a* expression was reported to be increased in rat-pup intestine, but appeared unaffected during similar copper exposure conditions in other work [38, 39, 42].

The aim of our study was therefore to examine the gene expression responses of liver cells to toxic levels of copper. Previous studies in human cells have either focused on the expression of a limited set of copper transporters as a result of varying copper levels, or on a genome-wide level using expression profiles obtained for a limited number of time points [43]. Here, we have extensively studied the messenger RNA (mRNA) expression profiles in HepG2 cells in an extended time-series analysis, and determined the changes in expression profiles to characterize the genes involved in the adaptation to high-copper levels. As in vitro models may respond differently to a more physiological in vivo condition, we also examined, for the first time, the direct effects of a high-copper diet on hepatic gene expression levels in mice and compared the in vivo profile with the in vitro profile.

Materials and methods

Cell culture

HepG2 cells, derived from ATCC (HB-8065; Manassas, VA, USA), were cultured in MEM supplemented with 10% heat-inactivated fetal calf serum, 1% L-glutamine and 1% penicillin/streptomycin (37 ˚C in 5% CO_2/air). During incubation with copper or Bathocuproine disulphonic acid (BCS Sigma, Utrecht, the Netherlands) cells were grown in MEM supplemented with L-glutamine. Human embryonic kidney (HEK 293T) cells (ATCC) were cultured in DMEM supplemented with 10% heat-inactivated fetal calf serum and 1% penicillin/streptomycin (37 ˚C in 5% CO_2/air).

Transfection, constructs and luciferase assays

For luciferase assays (described in [44]) HEK 293T cells were seeded in 24 wells plates and transfected with 62.5 ng 2κB-firefly-luciferase construct (kindly provided by Dr. C. Duckett, University of Michican Medical School, Ann Arbor) and 12.5 ng TK-renilla luciferase construct in combination with either 0.5 µg pEBB-COMMD1-FLAG [11] or 0.5 µg pEBB [11] using calcium phosphate transfection [45]. After 24 hrs, cells were subjected to varying copper concentrations for 16 hrs or 500 U/ µl TNF for 12 hrs (Roche applied science, Penzberg, Germany). Cells were lysed and luciferase activity was measured in a luminometer (Berthold, LB 953, Woerden, The Netherlands). Firefly luciferase values

were corrected for Renilla luciferase values measured in the same samples and were expressed as relative light units (RLU).

Immunoblot analysis and antibodies

After copper incubation for varying periods, cells were lysed in cold lysis buffer [46] and immunoblotting was performed using anti-Flag antibodies (Sigma), anti-HMOX1 (stressgen, Victoria, BC Canada), anti-Tubulin-alpha (Sigma) and anti-COMMD1 [46] as previously described [46].

Animal groups and sample collection

129Sv/Ev mice were housed in a pathogen-free area according to NIH guidelines.

Starting at the age of six to seven weeks, drinking water in a group of eight animals was supplemented with 6 mM $CuCl_2$ for one month, while the control group of seven animals received normal drinking water. Livers were snap frozen in liquid nitrogen and stored at –80 ˚C for RNA isolation.

Intracellular copper measurements in liver cells

HepG2 cells were grown in 10-cm dishes, treated with 100 µM $CuCl_2$ or 100 µM BCS at indicated time points and were harvested at 70% confluence. Cells were trypsinized and washed three times with PBS containing 0.02 mM EDTA and subsequently lysed in 200 µl lysis buffer (25 mM HEPES, 100 mM NaCl, 1 mM EDTA, 1% Triton X-100, 10% glycerol). After incubation for 15 minutes at 4˚C, 10% of this solution was used to determine the total amount of intracellular protein in each sample, using a Bradfort assay with BSA as a standard (Biorad Laboratories BV, Veenendaal, the Netherlands). The remaining solution was dissolved in 11 M HNO_3 for 24 hrs at 20˚C. Copper measurements were performed on a Varian spectrAA 220-fast sequential flame atomic absorption spectrometer (FAAS) in 1 ml volume. Copper standards in a comparable solution were used for calibration and determination of the linear detection range.

Approximately 100 mg of mouse liver was dissolved in 11 M HNO_3 for at least 24 hrs at 20˚C and the amount of hepatic copper was determined in 1 ml solution by FAAS as described by [47]. The liver copper content was related to the wet liver weight.

RNA isolation, Microarray hybridization, normalization and analysis

Complete protocols and microarray data were deposited in the MIAME (Minimal Information About a Microarray Experiment) database at http://www.ebi.ac.uk/arrayexpress with the following accession numbers:

Microarray layout, human, A-UMCU-3; mouse A-UMCU-7; data, human, E-MEXP-753; mouse, E-MEXP-745; protocols, RNA isolation, P-UMCU-19; mRNA amplification, P-

UMCU-21; cRNA labeling, P-UMCU-22; Hybridization and washing, P-UMCU-23 and P-UMCU-24; scanning, P-UMCU-25; image analysis, P-UMCU-11.

Briefly, HepG2 cells were harvested at 70-90% confluence and total RNA was isolated with Trizol reagent (Invitrogen, Leek, the Netherlands). High-quality RNA as determined by a 28S/18S ribosomal RNA ratio >1.8 in a bioanalyzer (2100; Agilent, Amstelveen, the Netherlands) was used to create cDNA. In each reaction 30 µg total RNA was used to generate approximately 600 ng cDNA with incorporated 5-(3 aminoallyl)-dUTP. These UTP nucleotides were labeled with Cy3 or Cy5 (2-4% specific activity) and 400 ng was used to hybridize for 18 h at 42˚C. Human cDNA microarrays contained 70-mer oligonucleotides representing 16,659 human genes and 2,541 control spots.

For mice livers, approximately 25 mg tissue was solubilized in 1 ml Trizol reagent and total RNA was isolated. Amplification of total RNA (2 µg) was performed by an *in vitro* transcription reaction (Ambion, Uden, the Netherlands) on double stranded cDNA. In the *in vitro* transcription reaction 5-(3 aminoallyl)-dUTP nucleotides were incorporated into the cRNA and were subsequently labeled with Cy3 or Cy5. In the hybridization reaction of 18 hrs at 42˚C, 1 µg of cRNA was used. Mice microarrays contained 35,000 spots comprising 32,101 distinct genes and 2,891 control spots. All slides were scanned in a DNA microarray scanner (G2565AA). Quantification of the spots was performed by Imagene 4.0 software (BioDiscovery, Inc. CA, USA) for HepG2 cells and by Imagine v.5.6 (BioDiscovery, Inc. CA, USA) for mice livers. Data were normalized per subgrid using the marrayNorm R package v.1.1.3 [48, 49] and the variance stabilized with the VSN R package v.1.3.2 [50] The expression of each gene was calculated as the ratio between copper-treated samples versus normal controls. ANOVA analysis was performed using the MAANOVA R package v.0.95-3 [51] to determine the differentially expressed genes in copper-treated samples versus controls ($p < 0.05$). A standard correlation method was used to perform hierarchical clustering in the Genespring 6.1 software (Silicon Genetics, Redwood City, CA, USA). A fixed-effect model that took into account array and dye effects was used and only genes with a false-discovery rate (FDR) adjusted tabulated p-value of $q < 0.05$ were selected.

Quantitative RT-PCR analysis

Microarray analysis data were validated in quantitative reverse transcriptase-polymerase chain reaction (qRT-PCR) on the DNA engine opticon (MJ Research, Waltham, MA, USA) using a SYBR Green kit (Ambion ltd, Austin TX, USA). All RT-PCR primers (table 1) were designed to span intron-exon boundaries when possible and the expression levels of *GAPDH* (human) or *18S* ribosomal RNA (mouse) were used to normalize the data during all conditions. Linear amplification ranges were determined for all primer sets (table 1). All reactions were performed using 1.5 µg total RNA to create cDNA with the superscript first strand synthesis system (Invitrogen) according to the manufacturer's protocol. cDNA

Table 1 Quantitative real-time polymerase chain reaction primer sequences

Gene	5′–3′ forward primer sequence	5′-3′ reverse primer sequence
Human		
GAPDH	TCAACGGATTTGGTCGTATTG	TCTCGCTCCTGGAAGATGG
MT2A	TCTTCAGCTCGCCATGGAT	TTGTGGAAGTCGCGTTCTTTA
MT1X	GCTTCTCCTTGCCTCGAAA	TGACGTCCCTTTGCAGATG
CTR1	TGGAGACACACAAAACTGTTG	AGAGGAAGTATCCTGTACCG
CTR2	TACAGCGGTGCTTCTGTTTG	CAAGTACCACCTGTGGTGG
ATOX1	CCTCAATAAGCTTGGAGGAG	CCCTTTGGTCCATCCTGTG
COX 17	GCGTGTATCATCGAGAAAGG	AAAGTTCGTCAAAGAACTCCC
CCS	ATCACTTTAACCCTGATGGAG	CCCTGTGATCTTGGATAAGG
ATP7A	GGAAATGCCGCTTTTGACT	CCCGCCTTAAATTCCGTT
ATP7B	TGGCAACATTGAGCTGACAA	TGATAATATCCCGTGGACCG
COMMD1	TGTTGCCATTATAGAGCTGG	CTTAGAAAAGGTCAGTGGGG
COMMD2	GGAATTGTCCGAGGAGCATAA	CACATTGAGTTTTCTGGCGG
COMMD3	GTTTCTTGGCGCTTGGAATA	CCCACCAAGTCCTGTAATTGTT
COMMD4	TTTGAGTCAGGCGATGTGAA	TCTCCTCATAACAGCGGCA
COMMD5	GTCAGCATACCGCTTTGAGGT	TCCAAGCCGGATCTGAATG
COMMD6	AAGTGGCAGATCATTCAGGC	CACCGTTTCAATAACTGCAGC
COMMD7	CCAGGCGGATTTCATAACTCT	CCCAGATGTCACTCCAAATTTC
COMMD8	TTCCAGTGACAAGATTGCTGC	CACCTTATTCGCTGCTTCCA
COMMD9	TCAGCCCTTGGCTTGAAA	AAAGAGAGCCAGAATTGCCTC
COMMD10	ACAGTTGAAAAGTTCCGGCA	TCTCCAGGCTCTTTGAATCTTC
Mouse		
Commd1	CGCAGAACGCCTTTCACGG	TTTGCTTGACTTTAACTTCATC
18S ribosomal RNA	CCACATCCAAGGAAGGCAG	GCTGGAATTACCGCGGCTG

was diluted 10-fold and 2 µl was used in each qRT-PCR reaction. Reaction conditions consisted of an initial denaturation step at 92˚C for 2 minutes, followed by 40 cycles of 30 s. denaturation at 92˚C, 1 min. annealing at 60˚C and 30 s. elongation at 72˚C. Specificity of all products was verified both by melting curve analysis and analysis on agarose gels. Results are expressed in relative arbitrary units as fold changes in mRNA expression level and as means ± SEM. Differences between means were statistically assessed by a Student's *t* test in which the limit of statistical significance was set at $p< 0.05$.

Results

Copper status of HepG2 cells and mice livers upon copper exposure.

The total amount of intracellular copper in HepG2 cells was measured after incubation with $CuCl_2$ in a time course experiment comprising 0-72 hrs. HepG2 cells, incubated with

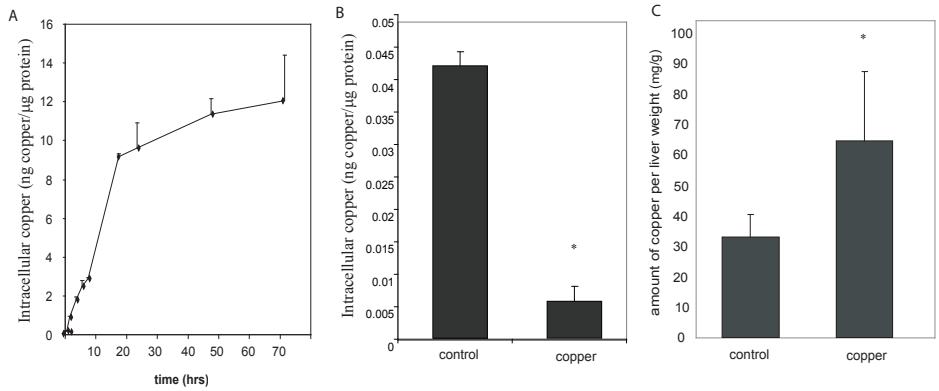

Figure 1. Copper status in HepG2 cells incubated with copper or BCS and livers of mice exposed to a copper rich diet.

(A) HepG2 cells were incubated for 0, 0.5, 1, 2, 4, 6, 8, 18, 24, 48 and 72 hrs with 100 µM $CuCl_2$, or (B) for 72 hrs with 100 µM BCS. The intracellular amounts of copper were subsequently measured by FAAS and corrected for the total amounts of intracellular protein. The data represent the mean of three biological replicates (error bars indicate standard deviation) and * indicates significant differences from the control cells (T-test, $p<0.05$). (C) The amounts of accumulated hepatic copper in mice treated for one month with 6 mM $CuCl_2$ in their drinking water was determined by FAAS. Copper values were corrected for liver wet weight and are averages of two independent measurements in seven control mice and eight copper-treated mice. Error bars indicate the standard deviation and * indicates statistical significance ($p< 0.05$).

100 µM $CuCl_2$, accumulated copper in a time dependent manner, reaching a plateau of about 12 ng copper per µg protein at around 48 hrs of incubation, which represents a 275-fold increase in intracellular copper content as compared to t = 0 (0.043 ng copper per µg protein) (figure 1A). After 72 hrs of copper chelation with 100 µM BCS the intracellular copper levels significantly decreased 6-fold as indicated in figure 1B. Longer incubation with BCS resulted in intracellular copper levels below FAAS detection limit.

Mice were given 6 mM $CuCl_2$ in drinking water for the duration of one month and suffered from chronic mild copper overload as they accumulated twice as much copper than non-treated mice in their livers (figure 1C). Livers of all mice appeared normal on macroscopic and histopathological level (data not shown) and these mice did not experience any visible discomfort of the high-copper diet.

Microarray analysis of HepG2 cells and mice livers upon copper exposure.

Based on the total amount of intracellular copper, nine time points (0-24 hrs) were included for cDNA microarray analysis to study both early and late responses in copper homeostasis upon copper overload. All cells were incubated in medium without fetal calf serum and harvested at the same confluence to prevent differential expression due to growth differences. All biological replicate copper-treated samples were hybridized using non-stimulated samples as a reference (figure 2A).

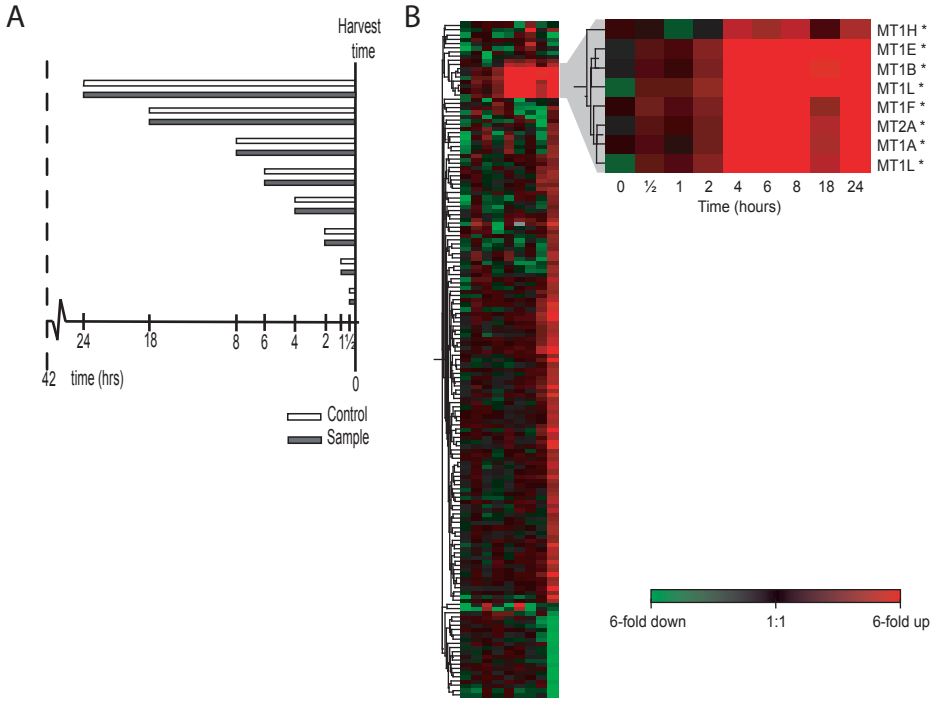

Figure 2. cDNA microarray analysis in HepG2 cells incubated with copper.
(A) HepG2 cells were incubated with 100 μM $CuCl_2$ during indicated periods and harvested at a similar confluence state as drawn schematically. (B) cDNA microarray analysis was performed as described in the materials and methods section and significantly differentially expressed genes are shown in a cluster diagram using a standard correlation coefficient. In the right part of the figure, genes corresponding to the "early" clusters are highlighted.

MAANOVA analysis of expression of all genes in time resulted in a list of 157 genes showing differential expression during copper overload ($p<0.05$; figure 2B, table 2 and supplementary table S1). Metallothioneins are known to be metal-induced proteins that can sequester copper in order to detoxify cells [52]. After 2 to 4 hrs, the expression of metallothioneins was markedly induced indicating that intracellular copper levels were increased (figure 2 B, right). Surprisingly, we could not detect early transcription responses such as previously detected in yeast [36] other than these metallothioneins.

After 18 to 24 hrs of copper overload, several other genes were upregulated (figure 2B). Most of these comprised genes that are upregulated in a direct or indirect response to oxidative stress. Table 2 lists all genes with a 3-fold or higher expression after 24 hrs of copper incubation as compared to untreated cells. As a direct response against the formation of free radicals, liver cells increase the expression of anti-oxidant proteins and heme oxygenase via the transcription factor Nrf2 [53] to protect themselves [54, 55]. Consistent with this, we detected increased expression of genes involved in the formation of glutathione (GCLM, 4.9-fold; GCLC, 3.8-fold) and HMOX1 (Heme Oxygenase

Table 2. Differential expression of >3-fold significantly upregulated genes after 24 hrs of copper incubation in HepG2 cells.

Process	Common name	Genbank	Description	F.I. 24 hrs
heavy metal detoxification	*MT1L*		metallothionein 1L	42.85
	MT1E		metallothionein 1E	30.29
	MT1L	NM_002450	metallothionein 1L	29.05
	MT1B		metallothionein 1B	22.84
	MT2A		metallothionein 2A	20.42
	MT1A		metallothionein 1A	15.71
	MT1F	NM_005951; NM_005950	metallothionein 1F	12.59
			Homo sapiens metallothionein 1H-like protein mRNA	3.144
oxidative stress	*HMOX1*	NM_002133	heme oxygenase 1	19.2
	IER5	NM_016545	immediate early response 5	7.041
	DUSP1	NM_004417	dual specificity phosphatase 1	6.161
	TALDO1		transaldolase 1	5.382
protein modification/ renaturation/ ubiquitination	*HSPA1B*		heat shock 70kD protein 1	19.4
	HSPA6	NM_002155	heat shock 70kDa protein 6	15.53
	BAG3	NM_004281	BCL2-associated athanogene 3	9.047
	HSPCA		heat shock 90kD protein 1, alpha	6.657
	CRYAB	NM_001885	crystallin, alpha B	6.141
	DNAJB1	NM_006145	DnaJ homolog, subfmaily B, member 1	4.923
	UBC	NM_021009	ubiquitin C	4.032
	HSPCA	NM_005348	heat shock 90kDa protein 1, alpha	4.007
	PSMC1	NM_002802	proteasome 26S subunit, ATPase, 1	3.587
	UFD1L	NM_005659	ubiquitin fusion degradation 1-like	3.508
	SPTREMBL:O00487	NM_005805	26S PROTEASOME-ASSOCIATED PAD1 HOMOLOG.	3.391
	PSMC4	NM_006503	proteasome 26S subunit, ATPase, 4	3
Electron transport	*TXNRD1*	NM_003330	thioredoxin reductase 1	5.726
	TXNL	NM_004786	thioredoxin-like, 32kDa	3.241
signaling	*SQSTM1*		sequestosome 1	6.387
	COPEB	NM_001300	core promoter element binding protein	4.863
	IL8	NM_000584	interleukin 8	4.691
	JUN		v-jun avian sarcoma virus 17 oncogene homolog	3.687
	RRAD	NM_004165	Ras-related associated with diabetes	3.62
	NCF2	NM_000433	neutrophil cytosolic factor 2	3.541
	MAFG		v-maf musculoaponeurotic fibrosarcoma oncogene family, protein G	3.37
	CYR61	NM_001554	cysteine-rich, angiogenic inducer, 61	3.361
	CKS2	NM_001827	CDC28 protein kinase regulatory subunit 2	3.356
glutathion biosynthesis	*GCLM*	NM_002061	glutamate-cysteine ligase, modifier subunit	4.853
	GCLC	NM_001498	glutamate-cysteine ligase, catalytic subunit	3.76

Table 2. (Continued)

Process	Common name	Genbank	Description	F.I. 24 hrs
other	*SPTREMBL:Q9P0K0*	NM_018433	ZINC FINGER PROTEIN; TESTIS-SPECIFIC PROTEIN A.	4.957
	CHORDC1	NM_012124	cysteine and histidine-rich domain -containing, zinc binding protein 1	4.464
	SPTREMBL:Q9H9E0	NM_022060	Hypothetical protein FLJ12816	4.344
			Homo sapiens dmd gene	3.96
	SPTREMBL:Q8TAZ8		SIMILAR TO PUTATIVE .	3.712
	GLA	NM_000169	galactosidase, alpha	3.604
			Homo sapiens lymphocyte-predominant Hodgkin's disease case #4 immunoglobulin heavy chain gene	3.499
	MRPL4	NM_015956	mitochondrial ribosomal protein L4	3.178
	HSPC027		hypothetical protein	3.161
	MAGEA2	NM_005361	melanoma antigen, family A, 2	3.156
	SPTREMBL:Q9Y3E9	NM_016081	PALLADIN; CGI-151 PROTEIN.	3.106

Genes that were significantly upregulated 3-fold or more as compared to non-treated cells are grouped corresponding to the process in which these genes are involved according to the GO annotation database. F.I. = fold induction of copper-treated samples as compared to non-treated samples.

1, 19.2-fold). Another mechanism to control oxidative stress damage in cells is exerted by increase of heat shock protein expression to renature damaged proteins and to increase the expression of genes involved in ubiquitination to degrade damaged proteins [56]. Here, we detected upregulation of several heat shock proteins (HSPCA, 6.7-fold; HSPA6, 15.5-fold; HSPA1B, 19.4-fold and HSPCA, 4-fold) and a remarkably high number of genes involved in ubiquitination and proteasomal degradation (table 3). Other genes that were upregulated, represented genes involved in electron transport, signaling and various others (table 2).

In order to study the physiological consequences of a high-copper diet on hepatic gene expression levels *in vivo* and to compare this with the *in vitro* profiles, livers of seven controls and eight copper-treated mice were subjected to microarray analysis.

MAANOVA analysis resulted in a differential expression of 22 genes that were all upregulated in response to copper (figure 3). Among these, we identified two genes involved in drug metabolism (*Cyp2d26, Cyp2c38)*, members of the P450 CYP family. Various other members of the CYP2 family have been shown to be induced in response to hepatic copper accumulation [57]. Sustained copper overload might therefore alter the expression of CYP2 family members and thereby affect the metabolism of specific drugs, which is relevant for individuals that ingest high amounts of copper. This set of genes further comprised genes involved in cholesterol metabolism *(Cyp27a1, Apom, Clu* and *Lcat),* innate immunity *(H2-K1, H2-Q10, H2-L),* and iron metabolism *(Hamp)*. Hepcidin (*Hamp*) is secreted from the liver into the serum to regulate the dietary intake of iron in

Table 3. Upregulated expression of genes involved in the ubiquitin pathway upon copper incubation in HepG2 cells.

			fold induction during various time points			
common name	**genbank**	**description**	0 hrs	8 hrs	18 hrs	24 hrs
PSMB2	NM_002794	proteasome subunit, beta type, 2	1.025	1.131	1.21	2.359
PSMD13	NM_002817	proteasome 26S subunit, non-ATPase, 13	0.994	1.098	1.224	2.561
PSMC4	NM_006503	proteasome 26S subunit, ATPase, 4	1.006	1.11	1.305	3
SPTREMBL:Q9H5K0	NM_023076	Human DNA sequence from clone 316G12 on chromosome 16. Contains the gene for C2 domain protein KIAA0	0.963	1.249	1.135	2.311
PSMB3	NM_002795	proteasome subunit, beta type, 3	0.981	0.966	0.913	2.854
PSMC1	NM_002802	proteasome 26S subunit, ATPase, 1	0.975	1.196	1.205	3.587
UFD1L	NM_005659	ubiquitin fusion degradation 1-like	1.069	1.095	1.065	3.508
PSMB7	NM_002799	proteasome subunit, beta type, 7	1.061	1.038	1.098	2.483
SPTREMBL:O00487	NM_005805	26S PROTEASOME-ASSOCIATED PAD1 HOMOLOG.	0.929	1.043	1.16	3.391
DNAJB1	NM_006145	DnaJ homolog, subfmaily B, member 1	0.964	1.125	1.643	4.923
SWISSPROT:MPL3_HUMAN	NM_022818	MICROTUBULE-ASSOCIATED PROTEINS 1A/1B LIGHT CHAIN 3	0.938	0.997	1.356	2.499
UBC	NM_021009	ubiquitin C	1.027	1.122	1.781	4.032
PSMD1		proteasome 26S subunit, non-ATPase, 1	0.911	1.059	1.547	2.711
PSMD11	NM_002815	proteasome 26S subunit, non-ATPase, 11	0.967	1.19	1.533	2.972
PSMD2	NM_002808	proteasome 26S subunit, non-ATPase, 2	1.042	0.996	1.507	2.307
SPTREMBL:Q9P0P0	NM_016494	hypothetical protein	0.824	1.073	0.652	2.038
SWISSPROT:EDD_HUMAN	NM_015902	UBIQUITIN--PROTEIN LIGASE EDD	0.876	0.982	1.645	1.693
FBXL11	NM_012308	F-box and leucine-rich repeat protein 11	1.31	1.103	1.646	2.726
CDC34	NM_004359	cell division cycle 34	0.978	0.563	0.545	2.051
TRAF5	NM_145759	TNF receptor-associated factor 5	0.822	6.72	0.979	2.289

Genes that are significantly upregulated and involved in the ubiquitin pathway, as annotated by the Gene Ontology consortium, are depicted in this table.

the intestine [58]. High hepatic copper levels might affect intestinal absorption of iron in this way.

Gene expression analysis in copper depleted HepG2 cells

HepG2 cells, subjected to copper depletion by BCS, were profiled after 72 hrs since significantly lower intracellular copper levels were measured at this time point (figure 1B). After BCS incubation, no significant changes in gene expression were identified compared to untreated HepG2 cells (data not shown). This is important because a similar chelation strategy is employed therapeutically in Wilson disease patients. Our data

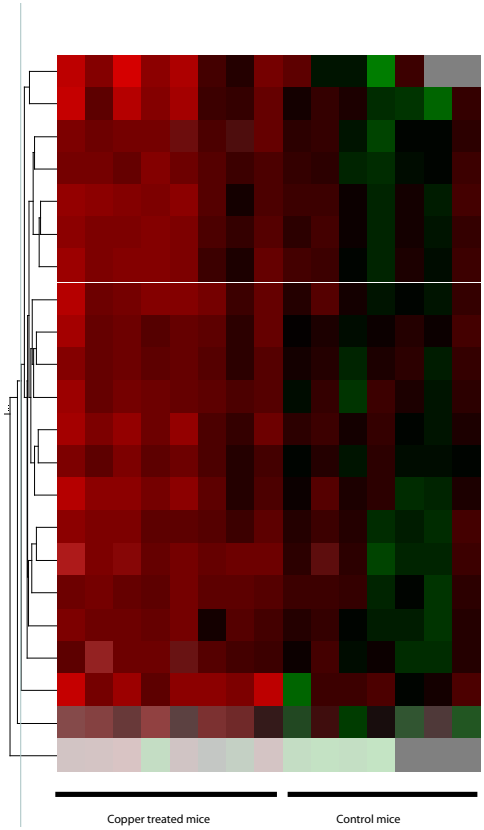

Common Name	F.I.	Short description	Genbank
Cyp2C38	2.5	Cytochrome p450, family 2, C, 38	NM_010002
KNG1	2.3	kininogen 1	NM_023125
H2-L	2.0	histocompatibility 2, D region locus 1	NM_010380
H2-Q10	1.8	histocompatibility 2, Q region locus 10	NM_010391
ALDN1L1	1.7	aldehyde dehydrogenase 1 family, member 1	NM_027406
H2-K1	1.8	histocompatibility 2, K1, K region	NM_019909
H2-K1	1.9	histocompatibility 2,K1, K region	NM_019909
CYP2D26	2.1	cytochrome p450, family 2, D, 26	NM_0029562
F2	1.8	coagulation factor II	NM_010168
CYP27A1	1.7	cytochrome p450, family 27, A, 1	NM_024264
CLU	1.8	Clusterin	NM_013492
SERPINF1	2.0	serine (or cysteine) peptidase inhibitor, D, 1	NM_0110340
SLC22A18	1.7	slute carrier family 22 (organic cation transporter), 18	NM_008767
FETUB	2.1	Fetuin beta	NM_021564
KNG2	2.3	kininogen 2	NM_201375
LY6E	2.1	lymphocyte antigen 6 complex, locus E	NM_008529
APOM	1.8	apolipoprotein M	NM_018816
IGF-1	1.7	Insulin-like growth factor 1	NM_010512
LCAT	1.7	Lecithin cholesterol acetyltransferase	NM_008490
HAMP1	2.6	Hepcidin antomicrobial peptide 1	NM_032541
C1qtn54	1.5	C1q and TNF-related protein 4	NM_026161
17D017D01 RIK	2.0	PREDICTED: hypothetical protein LOC69369	XM_484775

Figure 3 Cluster analysis of differentially expressed genes in livers of copper-treated mice
Microarray analysis was performed on livers of copper-treated and control mice. The 22 differentially expressed genes identified by MAANOVA analysis ($p<0.05$) are shown in a cluster diagram together with their common names, short descriptions, the Genbank identifiers and the fold induction of these genes. The fold induction represents the mean expression of the genes in copper-treated mice compared to the mean expression of the controls.

therefore suggest that copper chelation does not have adverse effects on transcriptional level.

Validation of the microarray analysis in HepG2 cells by quantitative RT-PCR analysis

We first validated the gene expression responses of HepG2 cells in the microarray analysis by analyzing the expression three members of the metallothionein family (1X, 1F and 2A). This revealed that all three genes were upregulated in a similar pattern compared to the microarray analysis during copper overload. Metallothionein expression increased during the initial 4 hrs of copper treatment, reaching its highest expression, followed by a gradual decrease in expression (figure 4A). After copper depletion, qRT-PCR analysis revealed that metallothioneins 1X and 1F were significantly downregulated two-fold,

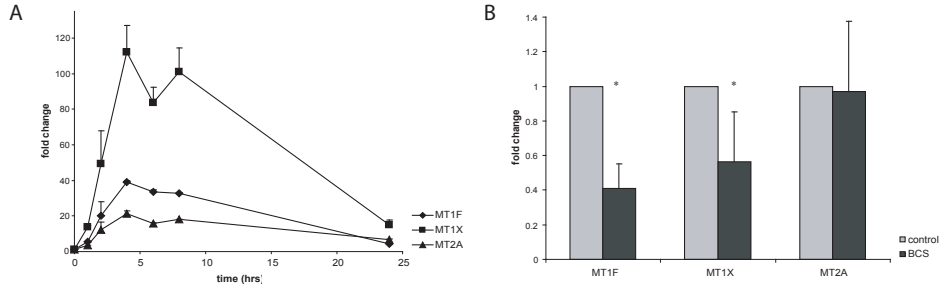

Figure 4. Validation of metallothionein gene expression upon copper overload or depletion in HepG2 cells. HepG2 cells were incubated as in figure 1 and the mRNA expression of metallothioneins (MT1F, MT1X and MT2a, indicated in the figure legend) was determined by qRT-PCR analysis upon copper overload (A) and copper depletion (B). Relative expression was normalized to relative expression on time point zero and shown as the mean ± SEM of four biological replicates and * indicates significant differences from the control cells ($p < 0.05$).

while the expression of metallothionein 2A did not change (figure 4B). This might be explained by the fact that qRT-PCR analysis is more sensitive than microarray analysis.

Furthermore, we determined the mRNA expression of the copper influx protein CTR1 and the putative copper transporter CTR2, the three copper chaperones CCS1, COX17 and ATOX1, and the hepatic copper efflux P-type ATPase ATP7B. The expression of these genes did not significantly change as a result of copper overload in time or copper depletion in HepG2 cells in either in the microarray or in the qRT-PCR analysis (data not shown).

The expression of COMMD1 and family members in response to prolonged copper incubation

COMMD1, another gene that was previously implicated in copper metabolism and was identified as the gene mutated in Bedlington terriers affected by copper toxicosis [8], was not present as a printed oligo on the microarray glass slide and we therefore examined the mRNA expression by qRT PCR analyis. In copper treated HepG2 cells, *COMMD1* expression was downregulated after approximately 8 hrs, concomitant with the moment the stress response appeared (figure 5A).Recently, nine other proteins have been identified that share a homologous COMM domain with COMMD1 and these were subsequently annotated as COMMD2-10 [11]. Some of the encoded COMMD proteins can interact with ATP7B similarly as COMMD1 [9], de Bie *et al*., manuscript submitted) suggesting a role in copper metabolism. It thus appeared relevant to analyze the specific expression of all *COMMD* genes in response to copper overload. Using qRT-PCR, most of these COMMD genes were significantly downregulated after 18 and 24 hrs of copper treatment, but to a lesser extent than *COMMD1,* whereas the expression of *COMMD9* was unchanged (figure 5B). To investigate whether the decreased mRNA levels of COMMD genes resulted in lower protein levels, we examined the COMMD1 protein levels in im-

munoblot analysis (figure 4C). COMMD1 protein expression was decreased concomitant with a marked increase in HMOX1 protein levels (figure 5C) similarly as COMMD1 mRNA levels dropped when HMOX1 mRNA levels increased..

NF-κB activity in cells overexpressing COMMD1 and challenged with high levels of copper

COMMD1 and other COMMD members have recently been identified as inhibitors of NF-κB activity [11]. As metal-induced oxidative stress is known to increase NF-κB activity [59], we speculated that COMMD levels might modulate the continuation of NF-κB activity upon metal stress. Previously, COMMD1 was shown to inhibit NF-κB dependent promoter activity in reporter assays. Therefore, we examined whether increased COMMD1

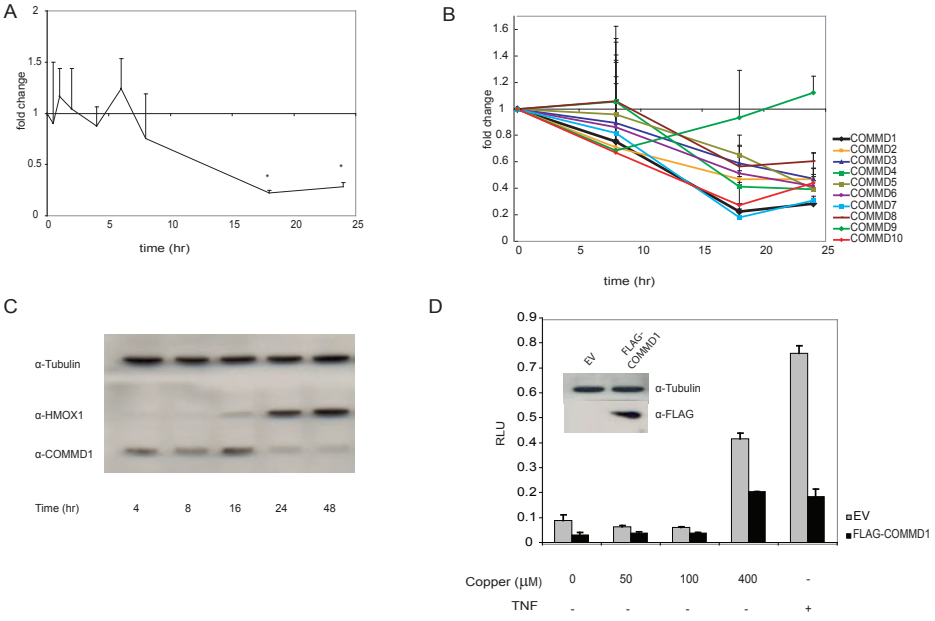

Figure 5. mRNA expression of *COMMD1* and *COMMD* family members after 24 hrs of copper overload in HepG2 cells.

(A) COMMD1 mRNA expression, and (B) COMMD family members mRNA expression were determined after copper overload in HepG2 cells by qRT-PCR analysis. mRNA expression was normalized to expression on time point zero and shown as the mean fold induction ± SEM of four biological replicates and * indicates significant differences from the control cells ($p < 0.05$). (C) HEK 293T cells were incubated with 100 μM copper for 0, 4, 8, 16 or 24 hrs or with TNF (500 U/ μl) for 12 hrs, where after COMMD1 protein levels were determined by immunoblot analysis. On the same blot, expression of Tubulin (loading control) and HMOX1 (a marker for oxidative stress) were determined. (D) NF-κB activity in HEK 293T cells was measured by examining luciferase reporter activity of a transfected κB-luciferase construct as a function of varying copper levels (0, 50, 100 and 400 μM) for 16 hrs or TNF (500 U/ μl) for 12 hrs. The effects of COMMD1 on luciferase activity were measured by co-transfection of a pEBB-FLAG-COMMD1 or pEBB alone (ev). The insert in this figure indicates COMMD1 overexpression levels compared to tubulin levels as determined by immunoblot analysis for FLAG expression.

levels were able to inhibit luciferase expression upon increasing copper levels (figure 5D). TNF and high-copper levels induced luciferase activity 7-fold or 5–fold, respectively. Overexpression of COMMD1 as confirmed by immunoblot analysis in the insert in figure 5D, resulted in a decreased reporter activity under normal conditions as well as upon TNF or copper incubation. Consistent with this conclusion, decreased COMMD levels as a results of a stable overexpression of a pSUPER vector with shRNA targeting COMMD1, affected reporter activity in an opposite manner, though to a lesser extent (data not shown).

Discussion

We examined the time-dependent changes in genome-wide gene expression profiles of HepG2 cells incubated with excess amounts of copper and of mouse livers exposed to a chronic elevated copper diet. This work revealed that the transcriptional response to copper overload in mice livers *in vivo* is quite different from the response of cells grown *in vitro* and cannot be compared to responses seen in yeast. Furthermore, our data in HepG2 cells revealed a novel set of copper-regulated genes that represent a delayed response to copper overload including the COMMD-family.

Upon increasing copper levels, all organisms respond by upregulating the expression of genes that are either directly regulated by copper, such as metallothioneins, or are regulated in response to oxidative stress, such as HMOX1 [55]. The expression of many individual genes in response to copper has been investigated, but the precise effects of copper on the complete transcriptome remain poorly understood. Although others have performed microarray analysis in mammalian cells upon copper treatment [16, 43, 60], we have for the first time examined the complete genome-wide gene expression profile of HepG2 cells during a time course experiment. This study identified an 'early' cluster comprising induced metallothionein genes and a 'late' cluster of 157 upregulated genes. This latter cluster comprised genes that are directly or indirectly involved in oxidative stress, such as genes involved in glutathione biosynthesis, protein renaturation and protein degradation. In response to oxidative stress in general, the transcription factors NRF2 and PPAR-α induce the expression of proteasome maintenance genes [61, 62]. Our study, for the first time, identified that proteasome maintenance genes are significantly upregulated in response to copper-induced oxidative stress (20 of the 157 differentially expressed genes, table 3). Other studies, in which microarrays were performed in LEC rat livers [57], ATP7A mutant fibroblasts [16], HepG2 cells [43] and metallothionein mutant fibroblasts [60] that either naturally or artificially acquired excess intracellular copper levels did not reveal upregulated proteasome maintenance genes, although other oxidative stress markers were clearly induced. This discrepancy might be explained by our

time-dependent analysis that allowed for statistical analysis of relatively small changes in gene expression. Furthermore, in comparison with the fibroblasts and the LEC livers, our oxidative stress response identified far less and only moderate upregulation of DNA damage genes suggesting that we possibly examined the early stages of copper-induced oxidative stress.

Concomitant with the 'late' cluster in HepG2 cells, we detected a novel set of genes that were downregulated upon high copper levels. This set of genes, the *COMMD* family, was recently implicated in the regulation of both copper homeostasis and NF-κB activity. Previous studies failed to detect a change in COMMD1 protein expression upon relatively short copper incubation [46], but the current study suggests that COMMD1 levels decrease as a result of prolonged high copper levels, probably in an indirect fashion by induction of oxidative stress related transcription factors. Metal-induced oxidative stress is known to activate NF-κB that enhances the transcription of a variety of genes including growth factors, cytokines and acute phase response proteins [59]. Some of these NF-κB targets, including Il-8, HMOX1 and ferritin, were indeed identified in the 'late' cluster. Our finding that *COMMD1* and all COMMD family members except *COMMD9,* were significantly down-regulated as a late response to copper overload, opens the exciting possibility that prolonged activation of NF-κB during metal-induced oxidative stress is in part mediated by a reduced expression of COMMD proteins. This idea is further supported by the fact that increased COMMD levels inhibited the activity of an NF-κB reporter construct upon oxidative stress. It will therefore be interesting to study the mechanisms that regulate the expression of COMMD proteins and explore the precise role for these proteins in inhibiting the NF-κB pathway and their putative protective roles in the oxidative stress response.

Our data in HepG2 cells clearly indicate that known copper transporters and copper chaperones are not regulated at the transcriptional level. Despite a high conservation in copper metabolism between yeast and higher eukaryotes, transcriptional regulation of copper homeostasis genes in mammals appears to be limited. This conclusion is further supported by the limited set of genes, differentially expressed in the livers of our mice exposed to a copper overload diet that was not comparable to the list of differentially expressed genes in copper-exposed HepG2 cells. Possibly, different responses of liver cells to copper *in vitro* and *in vitro* are due to differences of effective copper doses or exposure times. Our healthy control mice accumulated approximately twice as much copper upon chronic copper exposure, resulting in 22 differentially expressed genes involved in drug metabolism, innate immunity, cholesterol metabolism and iron metabolism. Previous studies identified a link between copper metabolism and cholesterol metabolism. Macrophages exposed to copper increased the expression of cholesterogenic genes [15], [41]Although it seems evident from this study and our study that copper affects expres-

sion of genes involved in cholesterol synthesis, the precise link between copper and cholesterol metabolism remains unknown.

Genes differentially expressed in livers of mice receiving a high-copper diet in this study cannot explain the relatively low hepatic copper accumulation. Thus, although efficient adaptive mechanisms preventing hepatic copper overload in our healthy mice are active, they do not represent transcriptional changes. The increased biliary copper output probably only results from differences in posttranslational mechanisms, including copper-dependent protein-protein interactions, protein internalization, degradation and translocation [7].

Together, these data suggest that direct transcriptional regulation of copper import, intracellular redistribution, and export does not represent an important general mechanism for regulation of intracellular copper levels in eukaryotes. However, copper-induced oxidative stress regulates the expression of many different target genes enabling cells to survive these extreme conditions. In addition, we here report decreased expression of a novel gene family, the COMMD family, during oxidative stress that could induce the expression of NF-κB responsive genes and thereby induce cell survival.

Acknowledgements

We are grateful to Mr. S. Bos (Pharmaceutical Department, University Medical Centre Utrecht, the Netherlands) for the use and support of the Flame Atomic Absorption Spectrometer.

Grant Support:

This study was supported by grants from the WKZ Fund and the Dutch Organization for Scientific Research Zon-MW (40-00812-98-03106 and 901-04-219)

Electronic supplementary material

The online version of this article (doi:10.1007/s00775-006-0201) contains supplementary material which is available to authorized users.

Chapter 3

Novel insights in the pathophysiology of Wilson disease and Hereditary hemochromatosis by a transcriptomics meta-analysis

Patricia A.J. Muller[1, 2], Prim de Bie[1, 2], Cisca Wijmenga[2, 3], Leo W.J. Klomp[1]

[1]Laboratory for Metabolic and Endocrine Diseases, UMC Utrecht, the Netherlands;
[2]Complex Genetics Section, DBG-Department of Medical Genetics, UMC Utrecht, the Netherlands; [3]Department of Genetics, UMC Groningen, University of Groningen, the Netherlands

submitted

Abstract

Copper and iron are essential transition metals, which are involved in many cellular processes. In excess, these metals are toxic as is illustrated by Wilson disease and hereditary hemochromatosis . These disorders are characterized by metal accumulation in the liver due to inherited mutations in genes that regulate the amount of body copper or iron.

Phenotypically, the progression of liver damage in Wislon Disease and hereditary hemochromatosis shares many characteristics, but the causative underlying transcriptional events are not completely understood. The pathogenesis of these disorders may be viewed as adaptive molecular events, characterized by tissue remodeling and transcriptional reprogramming secondary to toxic metal overload. Comparison of the differences and similarities between gene expression profiles in response to copper or iron overload could help to elucidate these pathogenic mechanisms. In the present work, we have reanalyzed all publicly-available hepatic gene expression data after copper or iron overload. This analysis identified a total of 1316 genes that were differentially expressed by iron or copper overload, including 84 overlapping genes. This transcriptomics meta-analysis permitted us to identify a series of biological processes involved in disease progression that would have remained unnoticed in individual studies Together, these data identify molecular pathways involved in the progression of metal overload disorders and illustrate that meta-analyses yield valuable knowledge that could be applied on a much broader scale in other liver diseases.

Introduction

Copper and iron are trace metals that play important roles in several biological processes. Free iron and copper catalyze the formation of toxic hydroxyl radicals from hydrogen peroxide in the Fenton reaction [63]. Dietary absorption and/or excretion of these metals are therefore tightly regulated and the consequences of abnormal metal homeostasis are illustrated by hereditary hemochromatosis (HH) and Wilson disease (WD). If untreated, both diseases result in liver failure or liver cirrhosis and can eventually progress into hepatocellular carcinoma (HHC) [64-68].

In trying to understand the progression of liver diseases and to identify potential diagnostic or prognostic biomarkers, transcriptomics has proven valuable [69]. Several studies have been employed to characterize the genes that are differentially expressed in response to changing metal levels both *in vivo* and *in vitro*. These studies included candidate gene approaches, but also more unbiased genome-wide approaches.

Here, we provide an extensive overview of the differential gene expression patterns in response to changing iron and copper levels in liver cells. Both HH and WD have a comparable pathophysiology, but the precise molecular mechanisms through which these events occur remain unknown. We have performed a transcriptomics meta-analysis in which we have followed the guidelines of HuGENet for genetic meta-analyses for as far as these guidelines are applicable to transcriptomics studies. This transcriptomics meta-analysis permitted us to identify similarities between copper and iron overload and can help us to understand pathophysiological mechanisms.

Iron overload disorders

Hereditary hemochromatosis (HH) is an autosomal recessive iron overload disorder that frequently arises from mutations in the *HFE* gene. *HFE*-related hemochromatosis is characterized by a progressive iron deposition in several organs due to uncontrolled intestinal iron absorption. Clinical symptoms present around the age of 40-50 years and comprise chronic fatigue, lethargy and hepatomegaly.

Non-HFE related hemochromatosis arises from mutations in *TFR2*, *FPN1*, *HJV* and *HAMP* (table 1) and is phenotypically similar to HFE-associated hemochromatosis, although specific differences between these genetic isoforms exist [70-72]. *HJV* and *HAMP*-mediated HH are juvenile forms of hemochromatosis with a disease onset before the age of 30 [73-75]. Classical HH and juvenile HH are characterized by high liver iron content, high serum ferritin levels and high transferrin saturation. In *TFR2*-related HH, transferrin saturation and serum ferritin levels are normal, while in *FPN1*-related HH no aberrant total body iron levels are detected. Symptomatic hemochromatosis

Table 1. Iron and copper overload disorders in humans and animals

Human (iron overload)				
Name	Subclass	Affected gene	Genetic inheritance	Reference
HFE-HH	Type 1	*HFE*	Autosomal recessive	61
None-HFE HH	Type 2A	*HJV*	Autosomal recessive	11, 12
None-HFE HH	Type 2B	*HAMP*	Autosomal recessive	13
None-HFE HH	Type 3	*TFR2*	Autosomal recessive	62
None-HFE HH	Type 4	*FP*	Autosomal dominant	63
Aceruloplasminemia		*CP*	Autosomal recessive	64
Hypotransferrinemia		*TF*	Autosomal recessive	65
Mouse (iron overload)				
Name		Affected gene		Reference
hfe -/- mouse		*HFE*		66, 67
Hfe (C282Y) mutant mouse		*HFE*		67
Hjv -/- mouse		*Hjv*		68
TFR2 (Y245X) mutant mouse		*Tfr2*		69
TFR2-/- mouse		*Tfr2*		70
Hepc1-/- mouse		*Hamp*		71
$Fpn^{flx/flx}$ mouse		*Fpn/ Slc40a1*		72
Usf2 -/- mouse		*Usf2*		73
Beta2m -/-mouse		*B2M*		74
Cp-/- mouse		*Cp*		75
Human (copper overload)				
Name		Affected gene	Genetic inheritance	Reference
Wilson disease		*ATP7B*	Autosomal recessive	76, 77
Indian childhood cirrhosis		*?*	Autosomal recessive	20
Idiopathic copper toxicosis		*?*	Autosomal recessive ?	21
Endemic Tyrolean infantile cirrhosis		*?*	Autosomal recessive	22
Animals (copper overload)				
Name		Affected gene	Species	Reference
LEC rat		*Atp7B*	Rat	78
Atp7b-/-		*Atp7B*	Mouse	79
Toxic milk mouse		*Atp7B*	Mouse	80
Canine copper toxicosis		*Commd1*	Dog	81

is generally treated by phlebotomy and sometimes iron chelation therapy is used [76, 77]. An overview of iron overload disorders in humans and animals is given in table 1.

Copper overload disorders

Wilson disease (WD) is an autosomal, recessively inherited copper overload disorder resulting from mutations in the gene *ATP7B* [78, 79]. *ATP7B* mutations result in decreased

biliary copper excretion and a copper deposition in the liver and some extra-hepatic organs. Patients present with a broad spectrum of clinical manifestations, comprising hepatic and/or neurological problems. Diagnosis is typically based on low serum ceruloplasmin levels, the presence of Kayser-Fleisher rings, liver copper content from biopsies and increased urinary copper excretion. Early diagnosis permits a therapy of a dietary copper reduction and/or an increase in copper excretion from the body [80]. Copper intake can be inhibited by zinc supplementation, and ammonium tetrathiomolybdate can be used to prevent copper absorption and to promote exhaustion of existing copper stores. Other genetic human copper overload disorders are listed in table 1 and phenotypically resemble WD patients without neurological defects. These disorders and those in seen in animal species that develop copper overload due to inherited genetic defects are listed in table 1.

Gene expression analysis in liver disease

Technical aspects of gene expression analysis

The possibility of surveying complete genomes of several species by cDNA microarray analysis renders this technology a powerful tool to acquire high-throughput gene expression data in various conditions. However, a significant propensity to detect false-positively regulated genes is intrinsic to high-throughput approaches. Appropriate statistics and well-designed experimental set-ups are pivotal to acquiring reliable results. Most journals currently require authors to deposit microarray data, experimental set-ups and technical procedures in public databases, including Minimal Information About a Microarray Experiment (MIAME), Gene Expression Omnibus (GEO) and Arrayexpress [81-83]. This standardization, in combination with gene ontology (GO) enrichment analysis, greatly enhances the reproducibility and comparison of transcription studies between laboratories [84].

The value of gene expression profiling in liver disease

The possibility to determine genome-wide gene expression have greatly increased the knowledge in liver diseases [69, 85]. These studies help to identify subsets of genes that are specifically differentially expressed in a certain disease or disease state to assist in diagnosis, prognosis or intervention [86-90]. Several liver disorders manifest in a similar fashion as WD and HH. Gene expression comparison analysis in liver diseases at the cirrhotic stadium revealed that the profiles of WD and HH and viral-induced hepatitis were comparable, but clearly different from the gene signature in alcoholic liver disease, autoimmune hepatitis or primary biliary cirrhosis [91]. Data from all these studies

illustrate the great potential of cDNA microarray analysis to help identify biomarkers for diagnosis, prognosis and therapy in liver disease.

Comparative transcriptomics in iron and copper overload

Literature-based transcriptomics meta-analysis of copper and iron overload

Since both copper and iron overload result in liver disease, we hypothesized that the overlap in differentially expressed genes between copper and iron overload might help to elucidate the pathophysiological transcriptional events. Ideally, genome-wide gene expression profiles of several stages of HH and WD, including pre-symptomatic stages of disease, should be compared to those of normal livers to determine overlap between these profiles. Previous cDNA microarray analysis studies compared livers of WD and HH patients at only the cirrhotic stage [91], while others only determined differential gene expression in a rat or mouse model for WD at specific stages [57, 92]. Each of these studies therefore provides important, but limited information. By listing and categorizing all the genes differentially expressed in response to changing iron or copper and reported between 1990 and 2007, we aimed to gain more knowledge on the processes involved in the pathogenesis in either of these disorders. For this purpose, we collected data of >50 gene expression studies that were deposited in MIAME, GEO or Pubmed, including supplemental material (figure S1). The inclusion criteria consisted of differential expression of >1.5-fold in response to primary or secondary copper or iron overload *in vivo* and *in vitro*, according to the statistics applied in the individual experiments. Comparisons between studies were made using NCBI RNA Refseq gene identifiers and interspecies differences were taken into account. Data on metal chelation or metal depletion from liver cells were excluded from this analysis.

We retrieved a total sum of 1316 annotated unique genes from our search (NCBI annotation and the Gene Ontology annotation of genes; www.ncbi.nih.gov and www.geneontology.org) of which 410 were differentially regulated by copper (copper list) and 906 were regulated by iron (iron list) (Figure 1). The majority (66%) of the genes in the copper list were upregulated. By contrast, only 45% of the genes in the iron list were upregulated. Permutation analysis revealed that we identified significantly more (84) genes that were common between the two lists (common list) than we would have expected to overlap by chance. Such a similarity is indicative for common dominators of gene expression differences in response to iron and copper overload. To speculate on the function of these 84 genes, we performed a gene-enrichment analysis, based on the GO (gene ontology) functional classifications. Using this analysis, we determined whether the functional classification of genes in this list was different from the functional classification in the total list of all annotated genes, using the program GeneTrail [93]. A

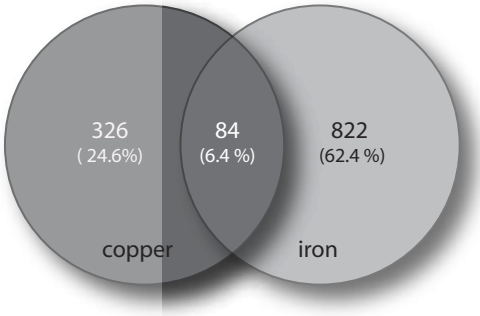

Figure 1. Overlap between the amount of differentially expressed genes as a result of iron or copper overload
Venn diagram indicating the overlap in the number of genes that are differentially expressed after copper or iron overload. Percentages of the number of genes per condition compared to all differentially expressed genes are depicted between brackets.

hypergeometric test in combination with FDR (false discovery rate) adjustment (Benjamini-Hochberg correction) and a significance threshold of 0.05 were used to determine significant enrichment of GO biological processes. Only significant GO processes and subprocesses containing four genes were included in the final results (table 2, table S1). Combining all well-defined literature data in such a meta-analysis minimizes the risk of selection bias. Furthermore, large numbers of genes allowed for more reliable statistics resulting in a more reliable functional enrichment classification in response to copper or iron overload compared to individual (genome-wide) gene expression experiments.

Most of the genes present in this common list of 84 genes were involved in the biological processes 'lipid metabolic process' (19%), 'generation of precursor metabolites and energy' (14%), 'cell cycle' (13%) and 'organic acid metabolic process' (13%) (table 2, table S2). We also compared the functional classification of the genes in the iron and copper lists to the functional classification of all annotated genes (table 3, supplemental table S3/ S4). The differences and similarities are discussed below in the context of WD or HH pathology.

Metal metabolism

In our enrichment analysis, we identified that genes involved in metal homeostasis were moderately, but significantly enriched in the iron and copper list compared to the total list of all annotated genes. In mammals, the expression of *FT* (ferritin) genes and *MT* (metallothionein) genes is induced to sequester iron and copper, respectively, and to prevent metal toxicity to a certain extent. Induction of *MT* genes and *FT* genes was encountered in many of the studies analyzed here. The fact that presymptomic mouse models of WD and HH have increased expression levels of these genes, illustrated the protective properties of the transcribed proteins [94-96]. In iron homeostasis, increased *HAMP* (hepcidin) expression is important in decreasing intestinal iron uptake [97]. Fur-

Table 2. Enrichment in biological processes in the common list regulated by iron and copper.

Biological process	A	E	%
Lipid metabolic process	16	3	19.3
Cellular lipid metabolic process	12	3	14.5
Lipid biosynthetic process	7	1	8.4
Sterol metabolic process	4	0	4.8
Steroid biosynthetic process	5	0	6.0
Steroid metabolic process	6	1	7.2
Sterol metabolic process	4	0	4.8
Steroid biosynthetic process	5	0	6.0
Generation of precursor metabolites and energy	12	3	14.4
Electron transport	12	2	14.4
Cell cycle	11	4	13.3
Regulation of cell cycle	9	2	10.8
Cell cycle phase	6	1	7.2
interphase	4	0	4.8
Regulation of progression through cell cycle	9	2	10.8
Organic acid metabolic process	11	2	13.3
Carboxylic acid metabolic process	11	2	13.3
Mono-carboxylic metabolic process	7	1	8.4
Oxygen and reactive oxygen species metabolic process	6	0	7.2
Response to oxidative stress	4	0	4.8
Cation homeostasis	4	1	4.8
Metal ion homeostasis	4	1	4.8
Di, tri-valent inorganic cation homeostasis	4	1	4.8
Transition metal ion homeostasis	4	0	4.8

Enrichment of genes involved in biological processes in response to both copper and iron overload compared to all annotated genes. The numbers at the right of the table indicate the actual number of genes identified in the enriched biological process (column A) in the set of copper- or iron-regulated genes, and the expected number in the set of copper- or iron-regulated genes, based on the normal distributions of the biological processes in all annotated genes (column E). The percentages indicate the relative number of genes present in the biological process compared to all genes regulated by copper or iron.

thermore, *TF* (transferrin) is downregulated to limit cellular iron uptake [98-100] Our enrichment analysis indicated that to a certain extent, copper was able to regulate genes involved in 'copper ion homeostasis'. These genes included *PRNP* (prion protein), *CP* (ceruloplasmin), *ATP7B* (Wilson disease protein) and *HAMP* (hepcidin). Notably, these genes are also differentially expressed in response to iron. These data suggest that increased iron might affect intracellular copper levels, or that iron and copper induce a common pathway involved in the upregulation of these genes.

The expression of ferritin and transferrin, that were respectively up and downregulated in response to iron in our analysis, are also known to be regulated on the post-transcriptional level via IRPs (Iron response proteins) [101, 102]. Similar post-transcriptional

Table 3. Summary of enrichment in main biological processes in the copper and iron list compared to all annotated genes.

GO biological processes	Cu (410)	Fe (906)	Both (83)
Transport	-	19 (172)	-
Lipid metabolic process	13 (53)	10 (91)	15 (13)
Electron transport	6 (25)	5 (45)	14 (12)
Organic acid metabolic process	7 (29)	10 (91)	13 (11)
Regulation of cell cycle	9 (37)	5 (45)	11 (9)
Oxygen and reactive oxygen species metabolic process	3 (12)	1 (9)	7 (6)
Cation homeostasis	2 (8)	2 (18)	5 (4)
Cell death	12 (49)	7 (63)	-
Inflammatory response	4 (16)	3 (27)	-
Protein kinase cascade	4 (16)	3 (29)	-
Enzyme linked receptor protein signaling pathway	4 (17)	-	-
Vasculature development	3 (12)	-	-
Modification dependant protein catabolic process	2 (9)	-	-
Nitric oxide metabolic process	1 (5)	-	-
Response to hypoxia	1 (4)	-	-
Transition metal ion transport	-	2 (18)	-

Enrichment of genes involved in the main biological processes in response to copper overload, iron overload or overload of both metals, compared to all annotated genes. The numbers indicate the percentage of genes involved in the depicted process compared to all genes differentially expressed as a result of copper overload, iron overload or overload of both metals. Between brackets, the actual number of genes in the indicated conditions is depicted.

regulation mechanisms have not been described for copper overload, but the existence of other or similar mechanisms in iron and copper regulation cannot be excluded.

Oxidative stress and cell fate

Oxidative stress is generated as a result of intracellular metal accumulation and can cause damage to lipids, proteins and nucleic acids. Oxidative stress can influence the expression of genes in various pathways (figure 2) [63]. In an apparent response to prevent damage, the expression of cell cycle regulators, apoptosis enhancers and genes that neutralize the damage caused by reactive oxygen species are differentially expressed. Important signaling molecules that are formed by the peroxidation of lipids are aldehydes; these can eventually induce AP-1 mediated transcription to increase cell proliferation. The total profile of gene expression variations in response to iron and copper is therefore the result of several cytosolic and nuclear events that are probably intimately linked. In an apparent attempt to prevent these toxic events, cells rapidly increase the expression of *GST* (glutathione-S-transferase) and *HO1* (heme oxygenase 1); both identified in the common list (table 2). GSTM1 conjugates toxic compounds to glutathione to enable subsequent excretion via the bile. HO-1 mediates the conversion of heme into biliverdin, which has anti-oxidant properties. When metal levels exceed a

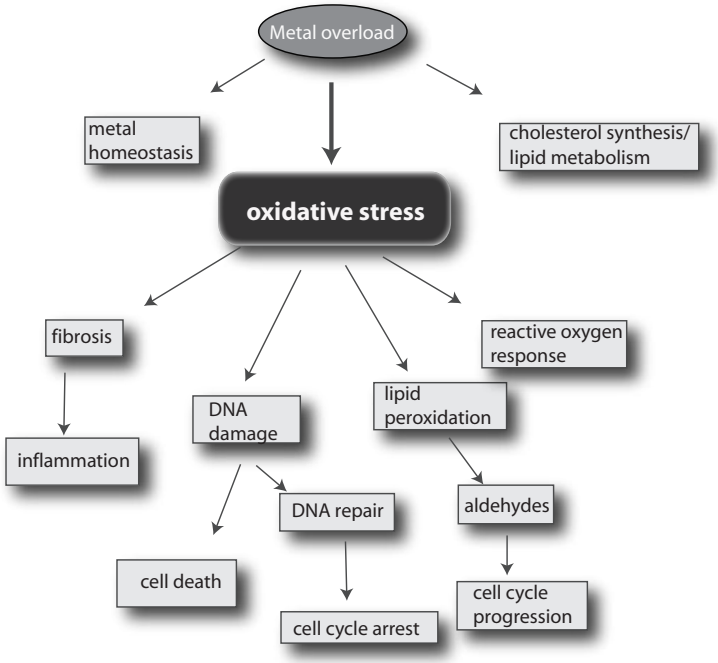

Figure 2. Flow chart indicating the oxidative stress-mediated transcriptional responses of metal-overload.

certain threshold, DNA damage occurs and initiates a cascade of signaling events that determine cell fate. Depending on the degree of DNA damage, cells are reprogrammed to attempt DNA repair and a concomitant cell cycle arrest, or they are directed to apoptosis [103, 104]. Copper and iron overload resulted in enrichment of genes involved in 'cell death' and 'regulation of cell cycle' in the copper and iron lists compared to the total list of all annotated genes (tables 2 and 3). Genes involved in the subprocesses 'negative regulation of programmed cell death' and 'negative regulation of progression through the cell cycle' of the biological, , were mostly upregulated by both iron and copper. These data suggest that, in response to copper and iron overload, the main response is to inhibit cell cycle progression and to prevent cell death in order to enhance cell survival. Remarkably, in the common list of 84 genes we detected no enrichment in 'cell death'. indicating that the individual genes involved in cell death are different after copper or iron overload. This suggests that iron and copper exposure might have similar results on the liver, but via different signaling cascades. More importantly, these findings provide a molecular "barcode" to these pathophysiological processes that will help to dissect the precise molecular events eventually leading to liver failure in WD and HH and identified potential biomarker genes (table S5).

Inflammatory response and fibrosis

A late manifestation of both WD and HH is liver fibrosis, a process that is characterized by the deposition of excessive amounts of extracellular matrix by activated stellate cells in response to liver injury [105]. Several cell types, growth factors and cytokines contribute to the process of fibrinogenesis. Both copper and iron induced the expression of collagen genes (table S1); *COL27A1* (collagen 27a1) and *COL5A2* (collagen 5a2) [57, 106-111]. The biological process 'inflammatory response' was enriched in the copper and iron lists compared to the total list of all annotated genes. The most potent fibrosis-inducing cytokine, *TGF-beta* (transforming growth factor beta) was present in the common list (table 3), indicating that both iron and copper regulate the expression of *TGF-beta*. Most remarkably, apart from *TGF-beta* expression, the biological process 'inflammatory response' was not detected in the functional enrichment classification of the common list, indicating a possible specificity in the inflammatory response profile by iron or copper. As the many cytokines present in this process are secreted into the blood, they could serve as novel biomarkers for discriminating between WD and HH (table S5).

Lipid metabolism

Of all genes regulated by iron and copper, a surprisingly high proportion was involved in 'cellular lipid metabolic process': 13% of the copper list, 10% of the iron list and 15% of the common list. Remarkably, some specific subprocesses of 'cellular lipid metabolic processes' were enriched either in the copper list or in the iron list, compared to the total list of all annotated genes (table 4, table S5). Approximately 6% of all genes that were downregulated by iron overload (32 genes) were involved in fatty acid metabolism. Especially genes involved in 'fatty acid oxidation' were downregulated in response to iron exposure. Notably, the protein levels of two of the identified genes involved in 'fatty acid oxidation', *ACTH1* (Acyl-CoA thioester hydrolase 1) and *ECAH1* (Enoyl coenzyme A hydratase 1, peroxisomal), were also decreased in response to iron exposure [112]. Rats that were chronically administered a high-iron diet revealed a disturbed plasma lipid profile [113].

Copper overload decreased the expression of genes involved in the subprocess 'steroid metabolic process' (table 4, table S5). Of these 17 genes, six were involved in cholesterol biosynthesis, including the rate-limiting enzyme *HMGCR* (3-hydroxy 3-methylglutaryl CoA reductase). Examination of lipid profiles in Wilson disease patients revealed low total cholesterol levels [114]. An inverse correlation between dietary copper intake and serum cholesterol levels in healthy men was described by Klevay [115]. LEC rats also experience an overall hypocholesterolemia that is accompanied by an abnormal lipoprotein particle composition, and decreased activity of enzymes involved in cholesterol synthesis and cholesterol conversion into bile acids [116]. These studies suggest that increased hepatic copper reduces cholesterol synthesis and that iron decreases fatty acid

Table 4. Enrichment of subprocesses of the biological 'lipid metabolic process' in the up- and down-regulated groups of genes of the copper and iron list compared to all annotated genes.

Biological process	Cu (410)		Fe (906)	
	Up (268)	**Down (142)**	**Up (408)**	**Down (498)**
Lipid metabolic process	7 (20)	21 (32)	8 (32)	12 (60)
Cellular lipid metabolic process	6 (15)	17 (26)	7 (27)	9 (47)
Fatty acid metabolic process	-	3 (6)	3 (12)	6 (32)
Fatty acid oxidation	-	-	-	2 (9)
Fatty acid beta oxidation	-	-	-	2 (9)
Acyl CoA metabolic process	-	-	-	1 (7)
Very-long-chain fatty acid metabolic process	-	-	-	1 (4)
Steroid metabolic process	-	11 (17)	3 (12)	2 (12)
Sterol biosynthetic process	-	8 (12)	1 (6)	2 (8)
Cholesterol metabolic process	-	7 (10)	-	1 (7)
Cholesterol biosynthetic process	-	4 (6)	-	-

The numbers at the right of the table indicate the actual number of genes identified in the enriched biological process (column A) in the set of copper- or iron-regulated genes, and the expected number in the set of copper- or iron-regulated genes, based on the normal distributions of the biological processes in all annotated genes (column E). The percentages indicate the relative number of genes present in the given biological process compared to all genes regulated by copper or iron.

oxidation. Oxidative stress is known to affect lipid metabolism by lipid peroxidation. However, the fact that copper and iron decrease the expression of distinct subgroups of genes involved in lipid metabolism suggests distinct roles for copper and iron in these processes.

HH versus WD

A meta-analysis as performed here allows us to determine the differences and similarities between HH and WD on the transcriptional level. By comparing differential expression as a result of copper or iron overload, we were able to identify that both copper and iron exposure similarly activated genes involved in cell proliferation, electron transport, organic acid metabolic process, oxygen and reactive oxygen species metabolic process, and cation homeostasis. These data thus define an adaptive transcriptional liver tissue remodeling program in response to metal overload. Not surprisingly, oxidative stress has a prominent role in many of these processes (figure 2).

Determination of the differences between iron and copper overload revealed that particularly the individual genes involved in cell death, inflammation and lipid metabolism were distinct. Careful gene expression studies on a limited subset of the presented genes at different stages of disease progression is feasible and may yield valuable insight into the sequence of events that occur in the metal-overloaded liver. In addition,

these differences may also identify biomarkers or biomarker profiles that are unique and specifically associated with disease initiation or progression. Genes involved in the processes of cell death, inflammation and lipid metabolism that are differentially expressed in response to either copper or iron are therefore potential biomarkers, (table S5).

Conclusions and perspectives

We have analyzed all the genes that are differentially expressed as a result of hepatic iron or copper overload revealing an overlap of 84 genes regulated by both iron and copper. Such large numbers of genes are indicative for common dominators of iron and copper overload that are responsible for gene expression differences. In addition, we determined which biological processes were transcriptionally regulated to a higher extent due to copper or iron exposure than the levels expected based on the total distribution of biological processes in all annotated genes. Remarkably, iron exposure uniquely resulted in the repression of genes involved in fatty acid oxidation and copper exposure resulted in an inhibition of the expression of genes involved in cholesterol biosynthesis. Finally, these data indicate that a literature and database survey, can yield valuable data that might otherwise remain unnoticed. Similar strategies to study other liver diseases, such as hepatitis and alcoholic liver disease, could contribute to the knowledge of how various transcriptional events are involved in the progression of liver damage to liver cirrhosis and HCC.

Supplemental material is deposited at http://www.umcutrecht.nl/subsite/metabool/Onderwijs-Onderzoek/Research-Projects/P.Muller-thesis-supplement.htm

Chapter 4

Increased activity of hypoxia-inducible factor 1 is associated with early embryonic lethality in COMMD1 null mice

Bart van de Sluis[1, 2], Patricia A.J. Muller[1, 2], Karen Duran[1], Amy Chen[3], Arjan J. Groot[4], Leo W. Klomp[2], Paul P. Liu[5], Cisca Wijmenga[1,6].

[1]Complex Genetics Section, DBG-Department of Medical Genetics, University Medical Center Utrecht, the Netherlands; [2]Laboratory for Metabolic and Endocrine Diseases, UMCU, Utrecht, The Netherlands; [3]Genetic Disease Research Branch, NHGRI, National Institutes of Health, Bethesda, USA; [4]Department of Pathology, University Medical Center Utrecht, the Netherlands; [5]Oncogenesis and Development Section, NHGRI, National Institutes of Health, Bethesda, USA. [6]Department of Genetics, University Medical Center Groningen, Groningen, the Netherlands

Molecular cell biology, 2007 Jun;27(11):4142-56

Abstract

COMMD1 (previously known as MURR1) belongs to a novel family of proteins termed the Copper Metabolism gene MURR1 Domain (COMMD) family. The ten COMMD family members are well conserved between vertebrates but the functions of most of the COMMD proteins are unknown. We recently established that COMMD1 is associated with the hepatic copper overload disorder copper toxicosis in Bedlington terriers.

Recent *in vitro* studies indicate that COMMD1 has multiple functions including sodium transport and NF-κB signaling. To elucidate the function of Commd1 *in vivo* we generated homozygous *Commd1* null (*Commd1-/-*) mice. *Commd1-/-* embryos die in utero between 9.5 and 10.5 days post coitum and their development was generally retarded and placenta vascularization was absent. Microarray analysis identified transcriptional upregulation of hypoxia-inducible factor 1 target genes in 9.5 dpc *Commd1-/-* embryos compared to normal embryos, which was associated with increased Hif-1α stability. Consistent with these observations, COMMD1 physically associates with HIF-1α and inhibits HIF-1α stability and HIF-1 transactivation *in vitro*. Thus, this study identifies COMMD1 as a novel regulator of HIF-1 activity and shows that *Commd1* deficiency in mice leads to embryonic lethality associated with dysregulated placenta vascularization.

Introduction

COMMD1 (previously known as *MURR1*) is the prototype of a recently defined protein family the Copper Metabolism gene MURR1 Domain (COMMD) protein family [11]. So far, ten family members of largely unknown function have been identified in man and they share the unique COMM domain of 70-85 amino acids. This domain appears to have an important role in protein-protein interactions and represents a novel protein-protein interaction motif. The COMMD proteins are well conserved between vertebrates and COMMD orthologs have been found in lower organisms [11]. Recent data have implicated COMMD1 in various cellular processes.

We established that a loss-of-function of the COMMD1 protein, due to a homozygous deletion encompassing exon 2 of the *COMMD1* gene, is associated with the autosomal recessive copper toxicosis in Bedlington terriers [8, 46, 117]. This autosomal recessive disorder is characterized by an inefficient excretion of copper via the bile, resulting in progressive accumulation of hepatic copper, which leads to chronic hepatitis and ultimately liver cirrhosis [118-120]. COMMD1 interacts with ATP7B, the copper transporting P-type ATPase mutated in Wilson disease, a hepatic copper overload disease in man very similar to canine copper toxicosis [9]. In addition, downregulation of COMMD1 expression by siRNA increases the cellular copper levels [121]. A protein-protein interaction has also been identified between COMMD1 and the X-linked inhibitor of apoptosis (XIAP) [121]. The E3 ubiquitin ligase activity of XIAP regulates the ubiquitination and proteasomal degradation of COMMD1, which subsequently influences cellular copper levels [121]. Biasio *et al.* established that COMMD1 can also interact with several subunits of the epithelial sodium channel (ENaC), resulting in inhibition of the ameloride-induced sodium current [122]. Recent studies identified an association between COMMD1 and several components of the NF-κB signaling pathway [11, 123]. COMMD1 inhibits the NF-κB transcriptional activity that induces human immunodeficiency virus-1 (HIV-1) replication in resting $CD4^+$ lymphocytes. Interestingly, all COMMD proteins can regulate NF-κB transcriptional activity, which suggests that the COMMD family members are not only structurally related but also have some functional redundancy [11, 124]. These data indicate that COMMD1 is a regulator of multiple, important cellular processes, but its exact biochemical function and physiological role *in vivo* remain elusive.

To explore the *in vivo* function of COMMD1, we generated and characterized a *Commd1* knockout mouse (*Commd1-/-*). Our data clearly demonstrate that Commd1 has an essential role in regulating HIF-1 activity during early mouse embryogenesis.

Materials and methods

Generation of the target vector and the transgenic mice

The genomic sequences that flank *Commd1* exon 2 of the 5′ and 3′ ends were amplified with the sense primer 5′-TCTAGACCCCAGATCAAGATACTGATTG -3′ and antisense primer 5′-TCTAGAGAGCCAGCTCTTCAGTGATCAG-3′ and with the sense primer 5′-GGATCCTCTA-GAGCTACATGTCTTTGCAGTTGTC-3′ and antisense primer 5′-CTCGA*G*CAGAACTATTCT-TCACAATTGGAG-3′, respectively. The amplified products were separately cloned into the pCR2.1 TA cloning vector (Invitrogen, Breda, the Netherlands). The 5′ target sequence (1.8 kb) and the 3′ target sequence (2.1 kb) were subcloned into the target vector (pM-Cneo) using the restriction sites *Xba*I for the 5′ target sequence, *Bam*HI and *Xho*I for the 3′target sequence (Fig. 1A). The target vector contained the neomycin (*neo*) gene and thymidine kinase (*tk*) gene for positive and negative selection, respectively. The *Xho*I-linearized targeting vector was electroporated into the 129Sv/Ev embryonic stem (ES) cell line [125]. Neomycin resistance and thymidine kinase selection was carried out and two correctly-targeted ES cell lines, #7 and #62, were injected into blastocysts collected from C57BL/6J mice according to standard procedures to generate two independent mouse lines. Genotyping of ES cells and F1 animals was performed by PCR using primers

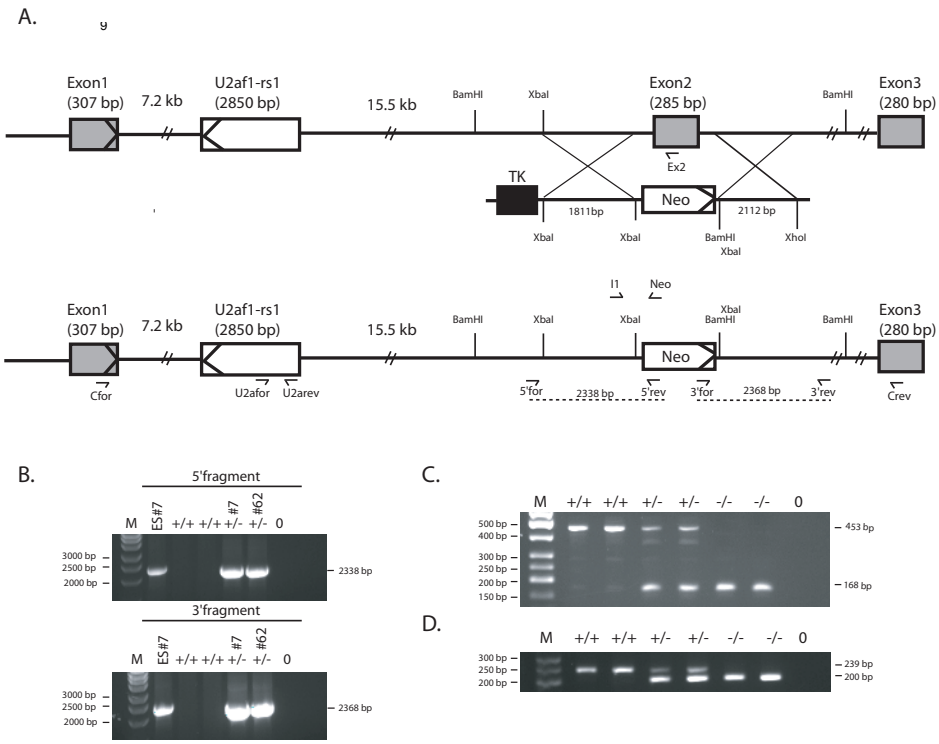

localized outside the target sequences and primers localized inside the *neo* gene. A 5′ fragment (2.3 kb) was amplified using the sense primer 5′for 5′-CTGGTATTAAATGAGAAT-GCATG-3′ and antisense primer 5′rev 5′-CCTGCGGCAATCCATCTTG-3′, a 3′ fragment (2.4 kb) was amplified using the sense primer 3′for 5′-CCTCGTGCTTTACGGTATCG-3′ and the antisense primer 3′rev 5′-GAGTGGTCCATTTCAATTGCTG-3′ (Fig. 1A, B). Genomic DNA isolated from tail [126], embryos or yolk-sac [127] was used for genotyping by duplex PCR using the sense primers Ex2 (5′-CAG ATA CAC AGC CCT GTT GC-3′), Neo (5′-CCT CGT

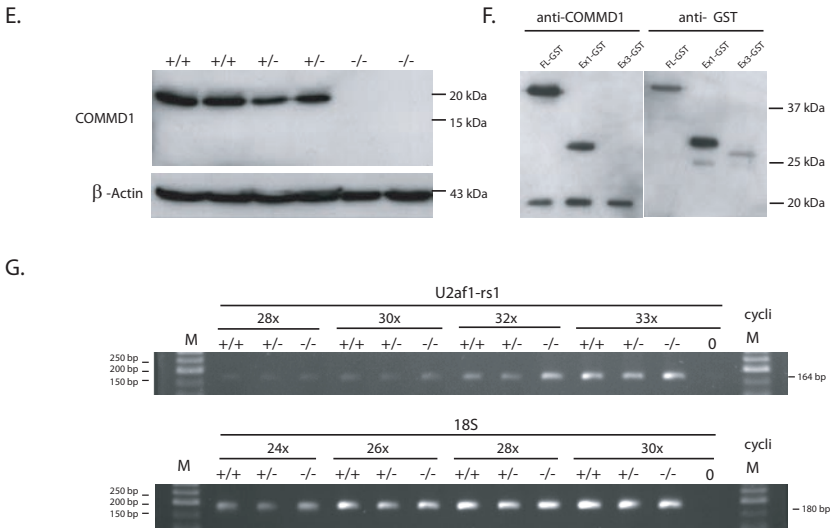

Figure 1 Targeted disruption of the *Commd1* gene by homologous recombination.
(A) Maps of the wild-type *Commd1* allele, the targeting vector, and the targeted *Commd1* allele. The three exons of the *Commd1* gene are indicated by gray boxes. The intronic gene *U2af1-rs1* is denoted by a white box. The orientation of the transcription of Commd1 and *U2af1-rs1* are indicated by arrowheads within the first exons of the genes. The targeting vector contains the flanking genomic sequences, a neomycin gene (neo) and a thymidine kinase gene (tk). Homologous recombination is indicated by X and should result in the predicted targeted allele. Primers used for genotyping and RT-PCR are indicated by arrows. (B) PCR primers located outside the target sequences and primers localized inside the *neo* gene were used for PCR analysis to verify the correctly targeted ES cell clones. Genomic DNA was isolated from the ES cell clone #7 and F1 progeny from the independent lines #7 and #62. A 5′ fragment (2.3 kb) was amplified using the sense primer 5′for and antisense primer 5′rev, a 3′ fragment (2.4 kb) was amplified using the sense primer 3′for and the antisense primer 3′rev. (C) RT-PCR of wild-type, heterozygous and homozygous *Commd1* null embryos using primers Cfor and Crev. (D) PCR analysis of wild type (+/+), heterozygous (+/-) and homozygous *Commd1* null (-/-) embryos using a duplex PCR. (E) Immunoblot analysis of Commd1 and β-actin in 9.5 dpc embryos. (F) Immunoblot analysis of *Commd1*-GST (FL-GST), *Commd1* exon 1-GST (Ex1-GST), *Commd1* exon 3-GST (Ex3-GST) in transfected HEK 293T cells using anti-Commd1 antiserum or anti-GST antibodies. (G) Semi-quantitative RT-PCR analysis to determine the expression of *U2af1-rs1* in relation to the expression of 18S in wildtype (+/+), heterozygous *Commd1* null (+/-) and homozygous *Commd1* null (-/-) 9.5 dpc embryos. The number of cycles used in this PCR is indicated. Demineralized water was used as a negative control, indicated by 0, and the size marker indicated by M is a 50-bp ladder.

GCT TTA CGG TAT CG-3′) and I1 (5′-GAG ACA ACT GCA AAG ACA TGT AGC-3′), yielding a 239-bp product for the wild-type allele and a 200-bp product for the targeted allele.

RNA isolation and RT-PCR

Total RNA was isolated from 9.5-dpc old embryos using RNAstat60 (Tel-Test Inc, Texas, USA), according to the manufacturer's specification. Total RNA was treated with Dnase I (Invitrogen) and approximately 1 µg of total RNA was used to generate first strand cDNA using oligodT primers and Superscript SVII (Invitrogen, Breda, the Netherlands). DNase treatment and reverse transcriptase reactions were performed according to manufacturer's specification. Successful DNase treatment was verified by using PCR specific for genomic DNA. RT-PCR was used to genotype the embryos using the sense primer Cfor (5′-CGCAGAACGCCTTTCACGG-3′) and the antisense primer Crev (5′-TTTGCTTGACTT-TAACTTCATC-3′), yielding a 453-bp product for the wild-type transcript and a 169-bp product for the mutant transcript. The expression of *U2af1-rs1* in wild-type, heterozygous and homozygous *Commd1* null embryos was determined by semi-quantitative PCR using the sense primer U2afor (5′-TCTAATTCCCAACCAAGTTAC-3′) and antisense primer U2arev (5′-AAAACAACATGGGAAGCCAC-3′) (Fig. 1A). As an endogenous reference, the expression of ribosomal 18S was determined using the sense primer 18Sfor (5′-CCACATC-CAAGGAAGGCAG-3′) and antisense primer 18Srev (5′-GCTGGAATTACCGCGGCTG-3′).

Copper supplementation

Drinking water containing 6 mM $CuCl_2$ was provided to female *Commd1*$^{+/-}$ mice starting 3 weeks before intercrossing and copper supplementation continued through gestation and lactation. As described previously, these mice ingested approximately 50-100 times more copper than mice on a control diet [128].

Expression constructs, cell culture, transfections and immunoblotting

Sequences representing full-length mouse *Commd1*, or exons 1 and 3 of mouse *Commd1* were amplified from mouse liver cDNA using the primers ex1for 5′-GGATCCGCCACCAT-GGCGGG CGATCTGGAGG-3′, ex1rev 5′-GCGGCCGCCTTGAGAAGTCCTCTCATC-3′, ex3for 5′-GGATCCGCCACCATGGAATCTGAATTTTTGTGTC-3′ and ex3rev 5′-GCGGCCGCGGCTGC-CTGCATCAGCCTG-3′. PCR products were subcloned in pEBB-GST using the restriction sites *Bam*HI *and Not*I. The sequences of the constructs were verified by sequence analysis. Human embryonic kidney (HEK) HEK 293T cells were cultured in DMEM supplemented with 10% FBS and L-glutamine and penicillin/streptomycin. Calcium phosphate precipitation was used to transfect HEK 293T cells as described previously [45]. After transfection, cells were lysed in lysis buffer (1% Triton X-100, 25 mM HEPES, 100 mM NaCl, 1 mM EDTA, 10% glycerol) supplemented with 1 mM Na_3VO_4, 1 mM PMSF, protease inhibitors (Roche, Basle, Switzerland) and 10 mM DTT. Cell line extracts representing 60 µg protein were

electrophoresed and then transferred to Hybond-P membranes. (These techniques are described in [46]). Immunoblots were probed with anti-COMMD1 antiserum (1:2000), anti-GST antiserum (Santa Cruz, Santa Cruz, CA, USA) or anti-β-actin monoclonal antibodies (clone AC-74, Sigma-Aldrich, Zweindrecht, the Netherlands). 9.5 dpc normal and *Commd1-/-* embryos were used for the preparation of total homogenates using the lysis buffer containing 0.4 M NaCl, 0.1% Nonidet P-40 (NP-40), 10 mM Tris-HCl (pH 8.0), 1 mM EDTA, 400 nM NaCl. Equal amounts of protein from the embryos were transferred to Hybond-P membranes and were probed with anti-HIF-1α (NB 100-449, Novus, Huissen, the Netherlands) or anti-α-Tubulin (clone DM 1A, Sigma). HIF-1α protein expression in HEK 293T cells was detected with anti-HIF-1α (clone 54, BD Bioscience, Alphen aan den Rijn, the Netherlands)

Generation of stable COMMD1 knockdown HEK 293T cells.

Plasmids encoding short hairpin RNAs (shRNAs) were generated by cloning a target sequences specific for COMMD1 (GTCTATTGCGTCTGCAGAC) in pRETRO-SUPER as previously described [129, 130]. To produce amphotropic retrovirus supernatants, Phoenix packaging cells were transfected with empty pRETRO-SUPER, or pRETRO-SUPER construct targeting COMMD1, using Fugene-6 (Roche, Woerden, the Netherlands) according to the manufacturer's instructions. Upon adding 4 μg/ml polybrene, HEK 293T cells were infected with the retrovirus supernatants and grown on media supplemented with 1 μg/ml puromycin (Sigma-Aldrich) to allow for monoclonal selection. Western blot analysis with anti-COMMD1 antibody was used to quantitative the excess of knockdown; typically ≥ 90% (de Bie et al submitted).

Histology and immunohistochemistry

Embryos at 7.5-10.5 dpc were dissected from the decidua, and the yolk-sac was removed for genotyping. The embryos were photographed and fixed for 12h in 4% paraformaldehyde in PBS at 4°C. Embryos were dehydrated in ethanol, embedded in paraffin; and serial sections of 4 μm were prepared. Sections were stained with hematoxylin and eosin. Apoptosis was detected by TUNEL staining using DeadEnd^{TM} colorimetric TUNEL system (Promega, Leiden, the Netherlands). Incorporation of 5-bromo-2'-deoxy-uridine (BrdU) was used to evaluate DNA synthesis during cell proliferation. Pregnant females received 50 mg/kg body weight of BrdU (Sigma), by intraperitoneal injection. After 2 hours, embryos were dissected, genotyped and fixed as described above.

For the immunohistochemistry study, sections were deparaffinized and primary antibodies against the mitosis marker phospho-Histone H3 (Ser10) (06-570, Upstate, Veenendaal, the Netherlands) or anti-BrdU (ab6326, Abcam, Huissen, the Netherlands) were used to study cell proliferation. Immunoreactivity was visualized with the appropri-

ate species-specific FITC- or HRP-conjugated antibodies. Histochemical copper staining was performed using rhodanine.

Whole mount* in situ *hybridization

Wild type embryos from different embryonic stages were dissected from the decidua and were fixed for 12 h in 4% paraformaldehyde in PBS, washed with PBS-0.1% Tween 20, and dehydrated in methanol. Whole mount *in situ* hybridization was performed as described previously [131]. *Commd1* antisense and sense probes were generated as described previously [132].

Microarray analysis and quantitative RT-PCR

The microarray data and the complete protocols used in this study have been deposited in the MIAME (Minimal Information About a Microarray Experiment) database (is in progress) at http://www.ebi.ac.uk/arrayexpress with the following accession numbers: Microarray layout, A-UMCU-7; data, E-MEXP-832; protocols for embryos dissection P-MEXP-30783; RNA isolation, P-MEXP-30781; mRNA amplification, P-MEXP-30781; cRNA labeling, P-MEXP-28902/3; generating reference pool, P-MEXP-28722; hybridization and washing of slides, P-MEXP-28890; scanning of slides, P-MEXP-28893; Data normalization, P-MEXP-28894.

mRNA expression of *BNIP3* in HEK 293T knockdown and HEK 293T control cell lines was determined in by a quantitative RT-PCR (qRT-PCR) on the ABI-7900 (Applied Biosystems, Nieuwerkerk a/d IJsel,the Netherlands) using SYBR PCR master mix (Applied Biosystems). Total RNA was isolated from HEK 293T cells using Trizol (Invitrogen) according to the manufacturer's specifications. The high capacity cDNA archive kit (Applied Biosystems) was used to generate single stranded cDNA from one microgram of total RNA. We used the primers 5'-AATATTCCCCCCAAGGAGTTCC-3' and 5'-CTGCAGAGAATATGCCCCCTTT-3' to amplify *BNIP3*. *β-Actin* was used to normalize our data and was amplified using the primers 5'-CATGTACGTTGCTATCCA GGC-3' and 5'- CTCCTTAATGTCACGCACGAT-'3. PCR reaction was initiated by heating for 2 min at 50°C and by a denaturing step at 94°C for 10 min, followed by 40 cylces of 94°C for 15 s, annealing and elongation for 1 min at 60°C. The results were expressed as fold changes in mRNA expression level and as means plus/minus the standard error of the mean.

Luciferase reporter assay, GST-pull down assay and co-immunoprecipitation.

For luciferase assays, HEK 293T cells were seeded in 24-well plates in triplicate for each treatment group. Cells were cotransfected with HIF-1-dependent 5xHRE-luciferase reporter plasmid [133] and expression vectors encoding TK-renilla, COMMD1-flag [124] and/or HIF-1α. 24 hours after transfection, cells were exposed to normoxic or hypoxic conditions (1% O_2) for 24 hours. A microplate luminometer (Berthold, Regensdorf, Swit-

zerland) has been used to determine the luciferase reporter activity as described by the manufacturer (Promega Dual-Luciferase Reporter Assay System). Luciferase activity was normalized for Renilla luciferase activity to correct for transfection efficiency.

HEK 293T cells were cotransfected with HIF-1α-Flag and COMMD-GST or HIF-1α-Flag and GST or cotransfected with HIF-1α-Flag and COMMD1. Precipitations with GSH-sepharose were performed as previously described [124]. HIF-1α-Flag immunoprecipitation was performed using FLAG M2 agarose beads (Sigma-Aldrich) according to the manufacturer instructions. Anti-COMMD1 antiserum was added to HEK 293T cell lysates to immunoprecipitate COMMD1, which was performed as described previously with minor changes [124]. Instead of using protein G agarose beads, protein A/G agarose (Santa Cruz, Heidelberg, Germany) were used. Protein detection was performed by immunoblotting for GST, HIF-1α (clone 54, BD Bioscience), COMMD1 or Flag (A8592, Sigma).

Results

Generation and initial characterization of Commd1 deficient mice

To study the function of Commd1 *in vivo*, we generated Commd1 deficient mice by replacing exon 2 with a *neo* gene. Like in humans and dogs, the mouse *Commd1* gene consists of three exons (Fig. 1A) so this strategy mimics the in-frame exon 2 deletion observed in Bedlington terriers affected with copper toxicosis. Three out of 132 ES clones were correctly targeted and two of these clones (#7 and #62) (Fig. 1B) were used to generate two independent transgenic mouse lines. F1 heterozygous mice were generated by crossing the male chimeras with 129Sv/Ev females (Fig. 1B and 1D). Heterozygous mice were born healthy and were fertile; no apparent phenotype has been observed.

We confirmed that exon 2 was correctly targeted by genomic PCR (Fig. 1B), RT-PCR and immunoblotting (Figs. 1C and 1E). Analysis of 9.5 dpc embryos indicated that replacing exon 2 with the *neo* gene resulted in a truncated *Commd1* transcript (Fig. 1C). After we had confirmed that *Commd1* exon 2 was correctly targeted, we genotyped the mice by using a duplex genomic PCR with primers corresponding to exon 2, the *neo* gene and a primer within intron 1 of the *Commd1* gene (Fig. 1D). This in frame deletion leads to a *Commd1* null allele as no Commd1 protein could be detected in *Commd1-/-* embryos, whereas Commd1 protein was readily detected in wild-type and heterozygous embryos (Fig. 1E). We confirmed that the anti-COMMD1 antisera [46] would recognize the putative in-frame deleted protein encoded by the truncated transcript (exon1-exon3 predicted protein product of 11 kDa) by immunoblotting. As shown in Fig. 1F, anti-COMMD1 antisera detected the part of the Commd1 protein encoded by *Commd1* exon 1 but failed to detect the amino acids 154-188 encoded by *Commd1* exon 3. Hence, a shortened in-frame protein product, if expressed, would have been detected. These

combined analyses clearly demonstrated that replacing exon 2 with a *neo* gene leads to a complete loss-of-function of the Commd1 protein, similar to that observed in Bedlington terriers affected with copper toxicosis [8, 46].

Intron 1 of the mouse *Commd1* locus contains the imprinted gene *U2af1-rs1* (Fig. 1A) [134]. The single-exon *U2af1-rs1* gene is not located within either the human or dog *COMMD1* loci. In mice, it has been shown that *U2af1-rs1* is mainly transcribed from the paternal allele in the adult brain and the liver and may interfere with transcription of the paternal *Commd1* allele [132, 135]. We addressed the possibility that our targeting strategy had interfered with *U2af1-rs1* expression by analyzing the expression of the intronic gene *U2af1-rs1* in 9.5 dpc embryos. This analysis indicated that the *U2af1-rs1* mRNA expression was not affected by targeting the *Commd1* allele as no difference in *U2af1-rs1* expression were observed between *Commd1-/-* and *Commd1+/+* embryos (Fig. 1G). Recently, a novel transcript, *U2mu*, which is transcribed from a part of *U2af1-rs1* and exons 2 and 3 of *Commd1*, has been described [136]. The transcript of *U2mu* was also truncated after replacing exon 2 of the *Commd1* gene. The *U2mu* transcript is confined to the mouse transcriptome, is in-frame with exons 2 and 3 of *Commd1* and encodes a predicted protein of approximately 26 kDa [136]. We and others [136] performed extensive RNA expression analysis in different mouse tissues during development, which revealed that the expression of *U2mu* is extremely low compared to *Commd1*. Finally, although our anti-COMMD1 antisera recognize the protein encoded by *Commd1* exon 2 (data not shown), a protein of 26 kDa could not be detected by anti-COMMD1 antisera in normal mice. These observations strongly imply that the *U2mu* transcript does not encode an expressed functionally protein. Together, these data therefore suggest that our targeting of *Commd1* exon 2 only affects the specific function of the *Commd1* gene.

The *Commd1+/-* mice were intercrossed in order to produce *Commd1-/-* mice. Surprisingly, loss of *Commd1* results in a recessive embryonic lethal phenotype since no homozygous null mice were detected among 259 offspring (Table 1). Embryonic lethality was also observed on a C57BL/6J genetic background, indicating that this lethal phenotype is independent of the genetic background of the mouse strain (E. Burstein, Univ. Michigan, pers. comm.). To characterize the timing of the embryonic lethality we

Table 1 Genotype analysis of offspring of Commd1 +/- matings

	Genotype			
Age	+/+	+/-	-/-	total
Weanling	29	54	0	83
12.5 dpc	2	6	0	8
11.5 dpc	7	13	1	21
10.5 dpc	15	21	8	44
9.5 dpc	12	30	13	55
8.5 dpc	15	21	12	48

collected embryos from timed *Commd1+/-* intercrosses at different stages of gestation. *Commd1-/-*, *Commd1+/-* and *Commd1+/+* embryos with the expected Mendelian ratio were recovered up to 9.5 dpc (Table 1). Only a few 10.5-dpc embryos and one *Commd1-/-* embryo at 11.5 dpc were recovered, but these were starting to be resorbed (Table 1, Fig. 2A), implying that *Commd1-/-* embryos die between 9.5 and 10.5 dpc.

Phenotypes of the Commd1 null embryos

To characterize the nature of the embryonic lethality, we studied the morphology of embryos from timed *Commd1+/-* intercrosses at different stages of gestation. *Commd1-/-* embryos were atypically small in size and were markedly delayed in development at 8.5 and 9.5 dpc (Fig. 2A). In spite of the developmental delay, no gross morphological abnormalities could be seen in *Commd1-/-* embryos at 9.5 dpc and they were comparable in size to normal embryos at 8.5 dpc (Fig. 2A). Heart beating was observed in 9.5 dpc *Commd-/-* embryos as well as in normal embryos (both *Commd1+/+ and Commd1+/-*) at this embryonic stage, indicating that *Commd1-/-* embryos are still alive at 9.5 dpc. At 9.5 dpc of embryonic development, the wild-type and the heterozygous embryos had undergone axial rotation but this was not seen in *Commd1-/-* embryos (Fig. 2A).

The *Commd1-/-* embryos were further characterized by histochemical staining of transverse and sagittal serial sections of 9.5 dpc old embryos. Although the development was markedly delayed, no gross abnormalities of the primitive organs could be seen in the *Commd1-/-* embryos compared to 8.5 dpc wild-type and heterozygous embryos. This was confirmed by studying the expression of the mesodermal marker *Fgf8* and the somitic marker *Meox1* with whole mount *in situ* hybridization. No clear differences in mRNA expression of these genes were observed between 9.5 dpc *Commd1-/-* embryos and 8.5 dpc wild-type and heterozygous embryos (data not shown). Primitive nucleated red blood cells were seen throughout the whole *Commd1-/-* embryos indicating that primitive hematopoiesis was not affected in *Commd1-/-* embryos (Fig. 2B). Although allantochorion fusion was observed at 9.5 dpc, the labyrinth formation was retarded and the vascularization of the placenta had not started in the *Commd1-/-* embryos whereas this was seen in both wild-type and heterozygous embryos (Fig. 2B). In addition, an increased number of maternal erythrocytes were seen in the placenta compared to both wild-type and heterozygous embryos (Fig. 2B).

Expression of Commd1 during normal mouse embryogenesis

The essential role of *Commd1* in mouse embryogenesis demanded a thorough analysis of the developmental expression of *Commd1*. We studied the expression of mouse *Commd1* at different stages (8.5-13.5 dpc) of the embryonic development by whole mount RNA *in situ* hybridization (Fig. 3). At 8.5 dpc, *Commd1* expression was detected throughout the embryo with the highest expression in the headfold, allantois and the

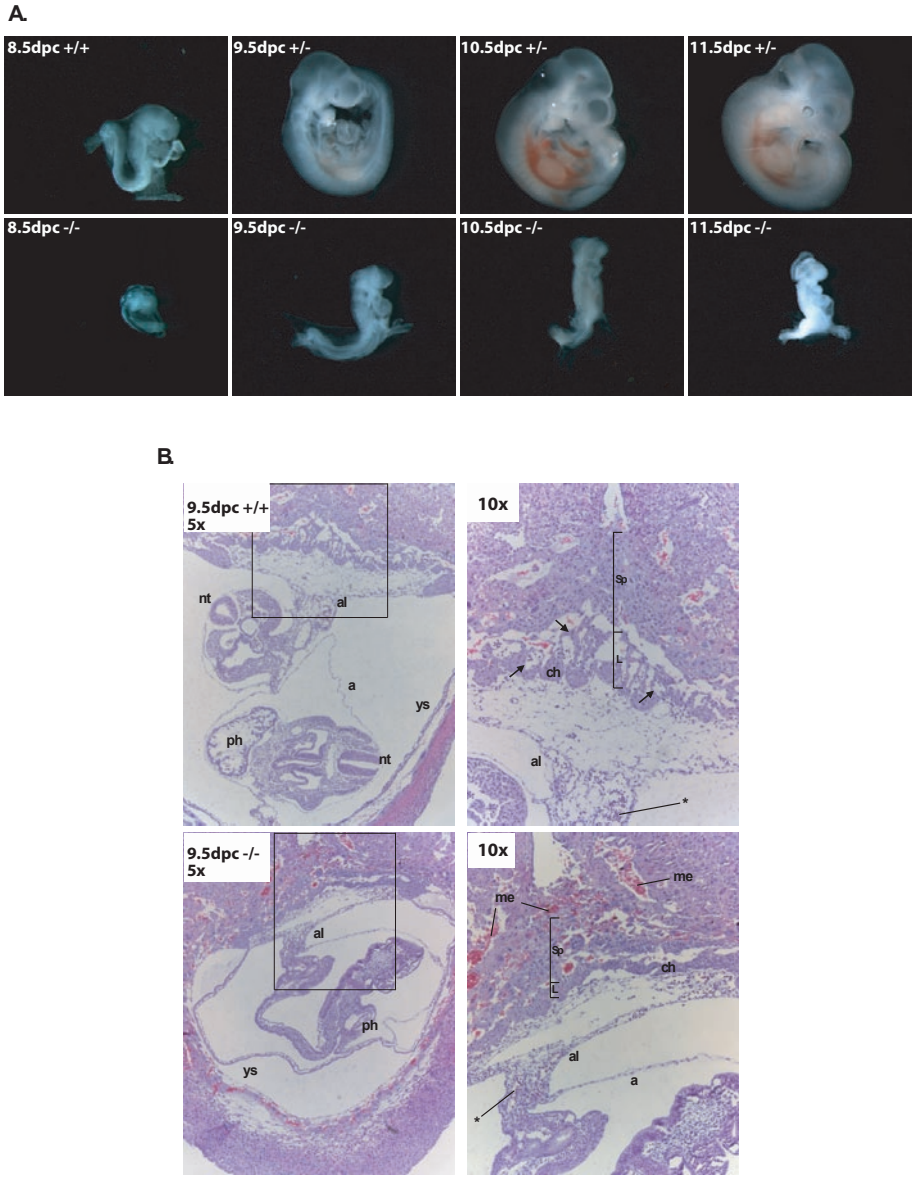

Figure 2 Morphological and histological analysis of wild-type and mutant embryos.
(A) Different developmental stages (8.5-11.5 dpc) of a wildtype (+/+), heterozygous *Commd1* null embryos (+/-), and homozygous *Commd1* null (-/-) littermates. Embryonic development of *Commd1-/-* mice was delayed and the embryonic development was arrested at 9.5 dpc compared to their littermates. No axial rotation was observed in *Commd1-/-* embryos. (B) Hematoxylin and eosin staining of saggital sections of a 9.5 dpc wild-type and *Commd1-/-* embryos in the decidua at 9.5 dpc (inset enlarged in right panel). Besides the developmental delay, no vascularization in the placenta and increased number of maternal erythrocytes were observed in *Commd1-/-* embryos. Allantois (al) is fused with the chorionic plate (ch). Primitive embryonic blood cells are present throughout the *Commd1-/-* embryo as indicated by asterisks. a, amnion; al, allantois; ch, chorionic plate; L, labyrinth; me, maternal erythrocytes; nt, neural tube; ph, primitive heart; Sp; spongiotrophoblast; ys, yolk sac.

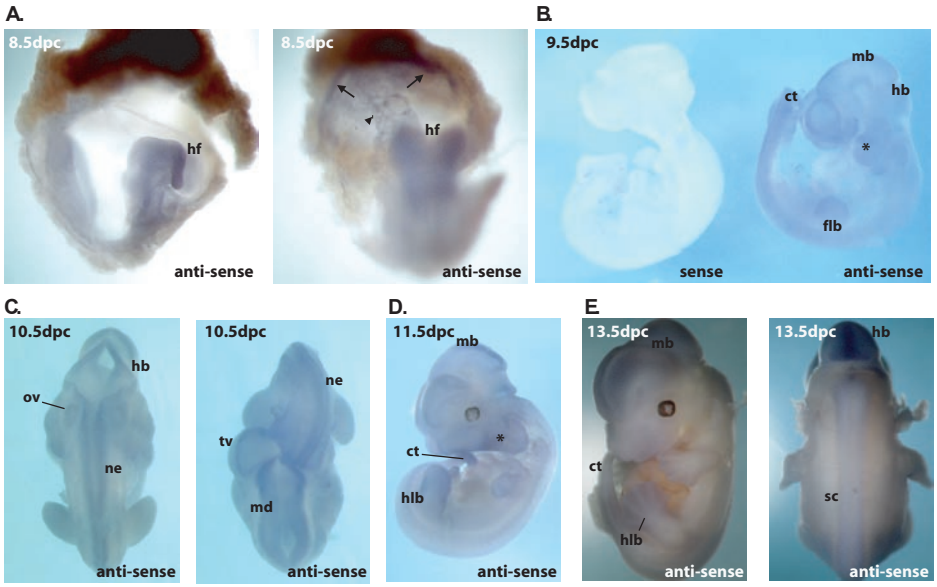

Figure 3 Expression of *Commd1* during the embryonic stages 8.5-12.5dpc.
Whole mount *in situ* hybridization was performed using an anti-sense probe to detect *Commd1* expression and a sense probe was used as a negative control. (A) Expression of *Commd1* at 8.5 dpc was observed throughout the embryo. Higher expression was seen in the headfold (hf) and in the allantois and choronic plate, indicated by an arrowhead and arrows, respectively. (B-E) Diffuse expression of *Commd1* was also seen at 9.5, 10.5, 11.5 and 13.5 dpc but was more distinct at the neural tube (nt), limb buds, caudal region of the tail (ct), neuroepithelium (ne) and branchial arches (*). Hf, headfold; flb, forelimb bud; hlb, hindlimb bud; ne, neuroepithelium; md, midbrain; hb, hindbrain; tv, telencephalic vesicle; ov, otic vesicle; sc, spinal cord; ct, caudal region of the tail; *, branchial arches.

chorionic plate, but no clear expression was seen in the yolk sac (Fig. 3A). Diffuse expression of *Commd1* continued during embryogenesis at stages 9.5 dpc, 10.5 dpc and 11.5 dpc, but no expression was observed in the primitive heart (Fig. 3B-D). At later stages during the development, *Commd1* expression was relatively high in the neuroepithelium of the brain, the neural tube and the epithelium of the otic vesicle (Fig. 3C-D). The expression was also clearly discernable in the caudal extremity of the tail, limb buds and the branchial arches. The same expression pattern was observed in 13.5 dpc embryos (Fig. 3D) but at this stage *Commd1* expression was more pronounced in the interdigital regions of the hindlimb bud, the spinal cord, the caudal extremity of the tail, developing brain, and the nose. Thus, *Commd1* is ubiquitously expressed in the embryo and in the primitive placenta at 8.5-11.5 dpc but more distinctively at 13.5 dpc. In addition, these data clearly show that *Commd1* expression is vital during the early embryonic stages of the mouse development.

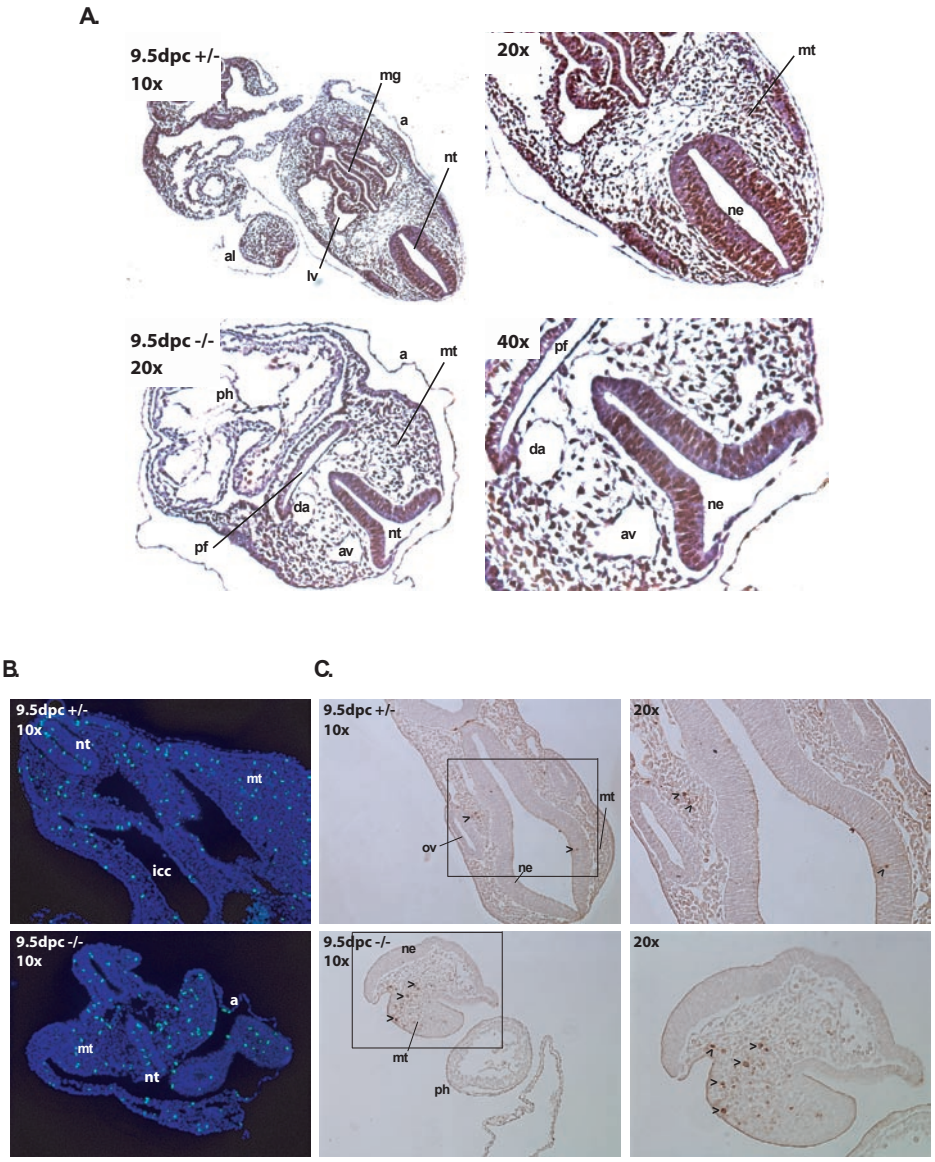

Figure 4. Analysis of cell proliferation and apoptosis.
Analysis of BrdU incorporation anti-phospho-Histone H3 immunohistochemistry, and TUNEL assay in transverse section of *Commd1*+/- and *Commd1*-/- embryos at 9.5 dpc. (A) BrdU staining (B) anti-phospho-Histone H3 staining (C) TUNEL assay (inset enlarged in right panel). Apoptotic cells are indicated with arrowheads; a, amnion; al, allantois; ph, primitive heart; mt, mesenchyme tissue; nt, neural tube; ne, neural epithelium; av, anterior cardinal vein;da, dorsal aorta ;pf, pharyngeal region; icc, intra-embryonic coelomic cavity; mg, midgut; ov, otic vesicle.

Analysis of cell proliferation and apoptosis in Commd1$^{-/-}$ embryos

Since controlled cell proliferation and apoptosis are essential for the development of multicellular organisms, we investigated whether affected cell proliferation or in-

creased cell death could explain the developmental delay and ultimately the arrest of *Commd1-/-* embryos. DNA replication in 9.5 dpc embryos was studied by determining the BrdU incorporation in DNA. We observed no detectable difference by BrdU incorporation between Commd1 deficient embryos and both wild-type and heterozygous embryos (Fig. 4A). Cells in the G2 phase of the cell cycle were studied by determining the phosphorylation status of histone H3. At 9.5 dpc phosphohistone H3-positive cells were clearly discerned in *Commd1-/-* embryos (Fig. 4B). The localization of the phosphohistone H3-positive cells (mesenchymal and epithelial cells), as well as the approximate ratios of phosphohistone H3-positive versus negative cells, did not differ between heterozygous and wild-type embryos (Fig. 4B). Detection of TUNEL labeling was used to study cell death in 9.5 dpc embryos. An increase in the number of TUNEL-positive mesenchymal cells in the developing brain was seen in 9.5 dpc *Commd1-/-* embryos compared to both wild-type and heterozygous embryos (Fig 4C), whereas no clear difference in the number of TUNEL-positive cells could be identified elsewhere in the embryos. Immunohistochemical analysis revealed almost no cleaved capsase-3 positive cells in 9.5-dpc *Commd1-/-* embryos nor in wild-type and heterozygous embryos (data not shown). These combined data indicate that cell proliferation is not appreciably affected in 9.5 dpc *Commd1-/-* embryos, but the increase of apoptotic cells indicates that 9.5 dpc *Commd1-/-* embryos are in poor vigor.

Copper homeostasis in Commd1$^{-/-}$ embryos

Since COMMD1 plays an essential role in copper homeostasis in dogs, we investigated whether embryonic copper overload could explain the lethal phenotype of Commd1$^{-/-}$ mice. The possibility of copper overload in Commd1$^{-/-}$ embryos or in the primitive placenta was analyzed using rhodanine staining of embryonic sections. This specific histochemical copper staining was used to identify copper overload in the livers of Bedlington terriers affected with copper toxicosis [137] but it did not show granular copper in 9.5 dpc Commd1$^{-/-}$ embryos nor in the primitive placenta (data not shown). These data imply that Commd1$^{-/-}$ embryos do not have detectably elevated copper levels.

Previous studies have shown that severe copper deficiency leads to early embryonic death [128, 138-141]. In line with these observations, we hypothesized that inefficient copper transport from the mothers to their offspring due to the loss of Commd1 could explain the embryonic lethality of *Commd1-/-* embryos. In an attempt to circumvent this potential copper deficiency, heterozygous females were provided with a high-copper diet (6 mM $CuCl_2$ supplied via the drinking water [128]) starting at 3 weeks before intercrossing and lasting through gestation and lactation. This intervention did not rescue the lethal phenotype of the *Commd1-/-* embryos, suggesting that copper deficiency is not the main cause for this phenotype. Alternatively, Commd1 might not be essential for copper uptake even under conditions of excessive copper intake.

Genome-wide gene expression analysis of whole embryos

A gene expression study using microarray analysis was performed to elucidate the underlying mechanism leading to embryonic lethality in *Commd1-/-* embryos. Since 9.5 dpc *Commd1-/-* embryos are morphologically more similar to 8.5 dpc normal embryos than 9.5 dpc normal embryos, we compared the gene expression profile of 9.5 dpc *Commd1-/-* embryos with 8.5 dpc as well as 9.5 dpc wild-type and heterozygous embryos. MAANOVA analysis resulted in a total of 236 genes with significantly different levels of mRNA expression (p-value < 0.05) in 9.5 dpc *Commd1-/-* embryos compared to 8.5 dpc and 9.5 dpc wild-type and heterozygous embryos (Fig.5). As shown in these Venn diagrams, the number of differentially expressed genes in 9.5 dpc *Commd1-/-* embryos compared to 8.5 dpc wild-type and heterozygous embryos was lower than in 9.5 dpc *Commd1-/-* embryos compared to 9.5 dpc wild-type and heterozygous embryos (red area) (Fig. 5A). Many differentially expressed genes were in common (20%), between 9.5 dpc *Commd1-/-* - 9.5 dpc wild-type comparison and 8.5 dpc wild-type - 9.5 dpc wild-type comparison (light blue area, Fig. 5A). These demonstrate that the gene expression profiles of 9.5 dpc *Commd1-/-* embryos reflect their delay in embryonic development. Next, we reasoned that most information on the mechanisms of embryonic lethality would be provided by genes that were differentially expressed in *Commd1-/-* embryos compared with wild-type and heterozygous embryos of both 8.5 and 9.5 dpc. We identified an overlap of only 16 upregulated and two downregulated genes between 9.5 dpc *Commd1-/-* - 9.5 dpc wild-type and heterozygous embryos comparison and 9.5 dpc *Commd1-/-* - 8.5 dpc wild-type and heterozygous embryos comparison (yellow area, Fig. 5A). Most interestingly, 8 of the 16 upregulated genes appeared to be targets of hypoxia-inducible factor 1 (HIF-1) (Fig. 5A and B, supplementary data). The mRNA expression of eight additional HIF-1 target genes were significantly increased in 9.5 dpc *Commd1-/-* embryos compared to 9.5 dpc wild-type and heterozygous embryos and two additional genes compared to 8.5 dpc wild-type and heterozygous embryos (Fig. 5A and B, supplemental data). Almost 10% of the significantly differentially expressed

Figure 5. Genome-wide gene expression analysis of 9.5 dpc *Commd1-/-* embryos compared to 8.5 and 9.5 dpc normal embryos.
(A) The number of the significantly differentially expressed genes between the indicated groups 9.5 dpc *Commd1-/-* versus 8.5 dpc wild type embryos, 9.5 dpc *Commd1-/-* versus 9.5 dpc wild type embryos, 8.5 dpc wild type embryos versus 9.5 dpc wild type embryos are depicted in the Venn diagrams; upregulated and downregulated genes are shown in the left and right panels, respectively. (B) Genes significantly upregulated in 9.5 dpc *Commd1-/-* embryos compared to each wild type group are shown in a cluster diagram. The cluster of genes with increased mRNA expression in 9.5 dpc *Commd1-/-* embryos compared to both 8.5 and 9.5 dpc normal embryos is enlarged and is illustrated together with their fold induction (F.I.) and gene names. The fold induction represents the mean expression of the genes in 9.5 dpc *Commd1-/-* embryos compared to the average expression of 8.5 dpc and 9.5 dpc normal embryos. The color bars correspond with the colors used in the Venn diagrams and the HIF-1 target genes based on literature are indicated by asterisks.

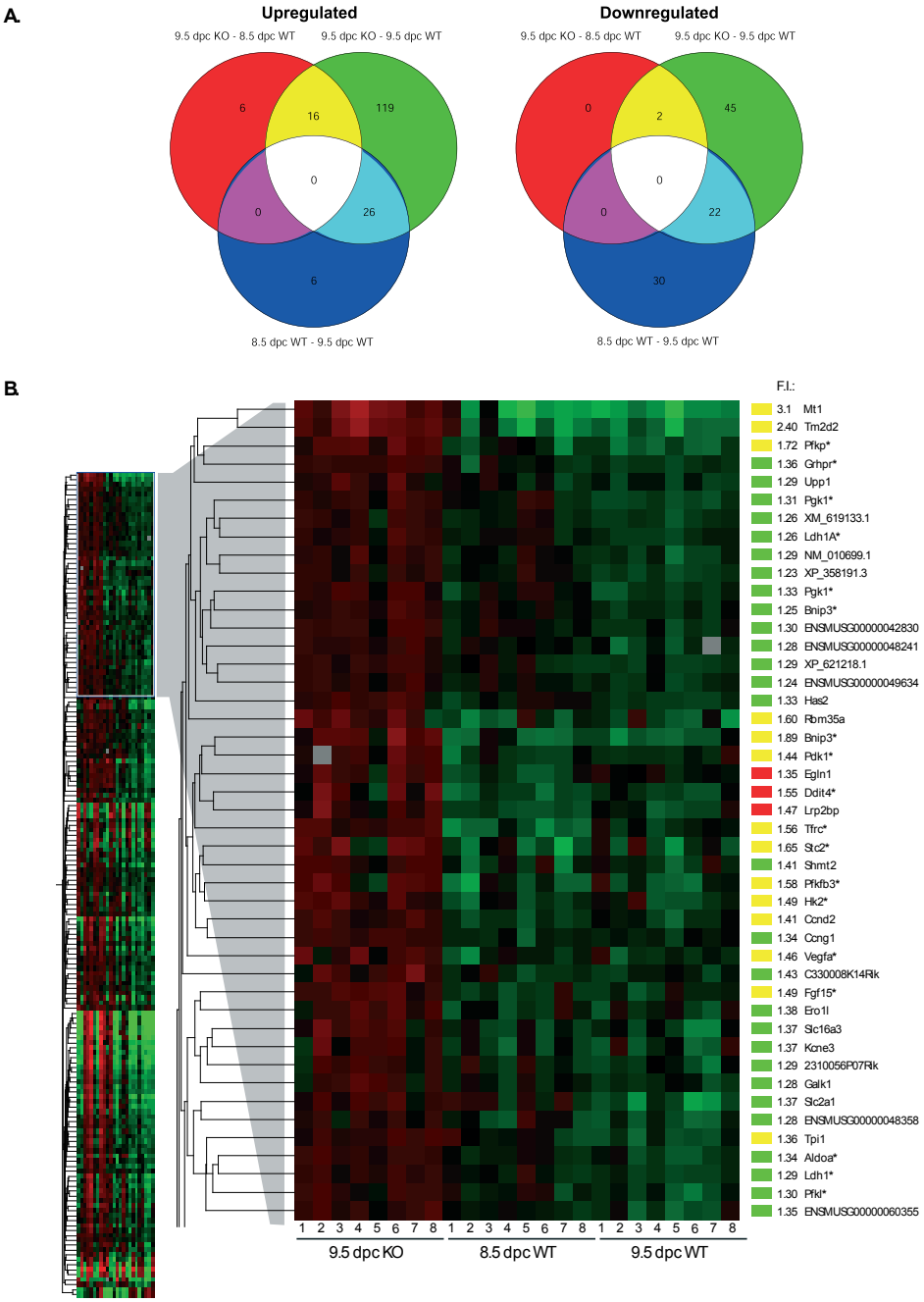
A.
Upregulated
9.5 dpc KO - 8.5 dpc WT
9.5 dpc KO - 9.5 dpc WT
8.5 dpc WT - 9.5 dpc WT
6
16
119
0
0
26
6
Downregulated
9.5 dpc KO - 8.5 dpc WT
9.5 dpc KO - 9.5 dpc WT
8.5 dpc WT - 9.5 dpc WT
0
2
45
0
0
22
30
B.
F.I.:
3.1 Mt1
2.40 Tm2d2
1.72 Pfkp*
1.36 Grhpr*
1.29 Upp1
1.31 Pgk1*
1.26 XM_619133.1
1.26 Ldh1A*
1.29 NM_010699.1
1.23 XP_358191.3
1.33 Pgk1*
1.25 Bnip3*
1.30 ENSMUSG00000042830
1.28 ENSMUSG00000048241
1.29 XP_621218.1
1.24 ENSMUSG00000049634
1.33 Has2
1.60 Rbm35a
1.89 Bnip3*
1.44 Pdk1*
1.35 Egln1
1.55 Ddit4*
1.47 Lrp2bp
1.56 Tfrc*
1.65 Slc2*
1.41 Shmt2
1.58 Pfkfb3*
1.49 Hk2*
1.41 Ccnd2
1.34 Ccng1
1.46 Vegfa*
1.43 C330008K14Rik
1.49 Fgf15*
1.38 Ero1l
1.37 Slc16a3
1.37 Kcne3
1.29 2310056P07Rik
1.28 Galk1
1.37 Slc2a1
1.28 ENSMUSG00000048358
1.36 Tpi1
1.34 Aldoa*
1.29 Ldh1*
1.30 Pfkl*
1.35 ENSMUSG00000060355
1 2 3 4 5 6 7 8 1 2 3 4 5 6 7 8 1 2 3 4 5 6 7 8
9.5 dpc KO
8.5 dpc WT
9.5 dpc WT

Table 2 Hypoxia associated genes which are upregulated in 9.5 dpc Commd1 -/- embryos compared to 8.5 dpc and 9.5 pc normal embryos

function	Gene name	
glycolysis	Pfkfb3	6-phosphofructo-2-kinase/fructose-2,6-biphosphatease 3
	Pfkp	Phosphofructokinase, platelet
	Pdk1	Pyruvate dehydrogenase kinase, isoenzyme
	Pgk1	Phosphoglycerate kinase 1
	Hk2	Hexokinase 2
	ldhA	Lactate dehydrogenase 1, A chain
	AldoA	Aldolase 1, A isoform
Angiogenesis	Vegfa	Vascular endothelial growth factor A
Metabolism	Grhpr	Glyoxylate reductase/ hydroxypyruvate reductase
	Tf	Transferrin
	Tfrc	Transferrin receptor
Prolyl hydroxylase	Phd2	EGL nine homolog 1 (C. elegans)
	Phd3	EGL nine homolog 3 (C. elegans)
apoptosis	Ddit4	DNA-damage-inducible transcript 4
	Bnip3	BCL2/adenovirus E1B 19kDa-interacting protein 1, NIP3
cytoskeleton	Krt19	Keratin complex 1, acidic, gene 19
Calcium/phosphate homeostasis	Stc2	Stanniocalcin 2
Cell-cell interaction	Lgals2	Lectin, galactose-binding, soluble 2

genes in 9.5 dpc *Commd1-/-* embryos have previously been shown to be induced by the transcription factor HIF-1 [142-146] (Table 2). These genes are involved in different cellular processes, including angiogenesis and glycolysis (Table 2). These data indicate that transcriptional regulation by HIF-1 is markedly affected in *Commd1-/-* embryos, which provided a possible mechanism for the embryonic lethality associated with Commd1 deficiency in mice.

HIF-1α protein expression, activity and COMMD1 interaction

HIF-1 is a heterodimeric basic helix-loop-helix transcription factor composed of HIF-1α and HIF-1β. HIF-1α is constitutively expressed, but rapidly degraded under normoxic conditions, which involves oxygen-dependent prolyl-hydroxylation and ubiquitination. Given the observation that Hif-1 target genes were transcriptionally upregulated in *Commd1-/-* embryos, we investigated whether this was the result of increased Hif-1α protein levels in *Commd1-/-* embryos compared to wild-type and heterozygous embryos. Hif-1α protein expression in 9.5 dpc normal and *Commd1-/-* embryos was determined by immunoblot analysis. As a control for distinguishing active Hif-1α, NIH3T3 cells were treated with the iron-chelator desferrioxamine (DFO). DFO mimics hypoxia by reducing the hydroxylation of HIF-1α via the prolyl-hydroxylases [147], resulting in a clear accu-

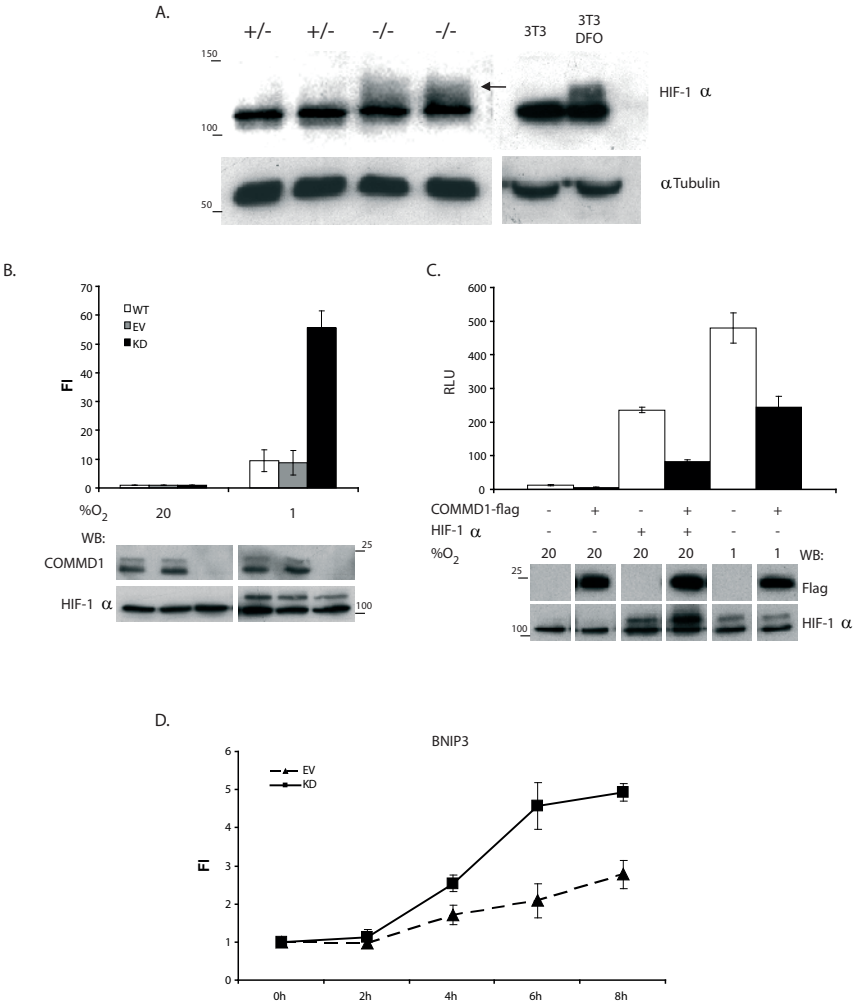

Figure 6 Increased HIF-1α expression in *Commd1-/-* embryos and COMMD1 regulates HIF-1-mediated transcription (A) Immunoblot analysis of HIF-1α, indicated with an arrow, and tubulin in 9.5 dpc embryos and in NIH3T3 cells either treated or untreated with DFO; the latter served as a control for distinguishing active Hif-1α (B) HEK 293T cells with a stable knockdown of COMMD1 (KD) were cotransfected with 5xHRE-firefly luciferase reporter and renilla luciferase control plasmids. HEK 293T cells (WT) and HEK 293T cells stably transfected with an empty siRNA vector (EV) were used as negative controls. Cells were incubated under normoxia or hypoxia. Firefly luciferase activities in the lysates were measured, corrected for renilla luciferase activities and expressed as fold induction (FI) relative to normoxic conditions. (C) HEK 293T cells were cotransfected with a luciferase reporter plasmids as described in (B), COMMD1-Flag and/or HIF-1α and were incubated under normoxia or hypoxia. Luciferase activities in the lysates were measured and expressed as relative light units (RLU). All luciferase experiments were performed in triplicate. Error bars represent standard deviations. Immunoblot analyses of HIF-1α and COMMD1 and of COMMD-flag protein expression are shown in the lower panels. The molecular size markers are indicated in kDa on the left. (D) *BNIP3* mRNA expression was determined in COMMD1 knockdown HEK 293T cells (KD) and control HEK 293T cells (EV) at different time points during hypoxic exposure (3% O_2) by qRT-PCR analysis. mRNA expression was normalized to the expression at time point zero and is shown as the mean fold induction ±SEM of tree biological replicates.

mulation of active Hif-1α which was visible as a smear, similarly to previous experiments using this antiserum (Fig. 6A) [148]. Increased active Hif-1α protein levels were also readily detected in 9.5 dpc *Commd1-/-* embryos compared to 9.5 dpc wild-type embryos (Fig. 6A). Next, we set out to investigate the relation between COMMD1 and HIF-1 activity in independent *in vitro* studies. To investigate whether COMMD1 deficiency leads to increased HIF-1 activity in cultured cells, reporter assays were performed in normal HEK 293T and in HEK 293T cells, in which the expression of COMMD1 was stably knocked down to undetectable levels by RNAi (Fig. 6B). These cells were transfected with a HIF-1-dependent reporter plasmid and were grown under normoxic or hypoxic conditions. As shown in Fig. 6B, reporter gene activity was induced by hypoxia. Consistent with our observations in Commd1 deficient embryos, COMMD1 knockdown in HEK 293T cells resulted in 6-fold higher induction of HIF-1 reporter gene activity compared to normal HEK 293T cells. To further corroborate these findings, overexpression of COMMD1 in HEK 293T cells resulted in marked inhibition of reporter induction, both under hypoxic and normoxic conditions (Fig. 6C). To study the affect of COMMD1 deficiency on endogenous HIF-1 activity, we examined the mRNA expression of the HIF-1 target gene *BNIP3* following hypoxic exposure (3% O_2). *BNIP3* was one of the HIF-1 target genes, which was transcriptionally induced in *Commd1-/-* embryos compared to wild-type embryos (Fig. 5B). In both cell lines, hypoxic exposure resulted in time-dependent increases in *BNIP3* mRNA expression (Fig. 6D). Consistent with our previous observation, the level of *BNIP3* mRNA expression was induced in COMMD1 knockdown HEK 293T cells compared to control HEK 293T cells.

Although increased Hif-1α protein expression was observed in *Commd1-/-* embryos no aberrant HIF-1α expression was seen in COMMD1 knockdown HEK 293T cells under normoxic conditions. To further investigate if COMMD1 mediates HIF-1α protein levels we studied the stability of hypoxia-stabilized HIF-1α in COMMD1 knockdown HEK 293T cells and control HEK 293T cells. These cells were cultured for 18 hours under hypoxia (1% O_2) and subsequently exposed to 20% O_2 for different periods of time. Under hypoxia (time point zero) both cell lines showed high HIF-1α expression but this decreased as soon the cell were exposed to 20% O_2. Interestingly, HIF-1α expression was almost absent in control cells after 10 minutes exposure to 20% O_2, whereas HIF-1α protein was still clearly observed in COMMD1 knockdown cells (Fig.7A). Remarkably, after the cells were exposed to 20% O_2 for 2 minutes, HIF-1α protein of increasingly higher molecular mass were detected in both cell lines (Fig.7A). These higher molecular weight proteins most probably represent ubiquitinated HIF-1α, since high oxygen levels promote the ubiquitination of HIF-1α. These data support the *in vivo* data that COMMD1 deficiency is associated with increased HIF-1α protein stability.

Next, we investigated whether the role of COMMD1 in mediating HIF-1 activity and HIF-1α stability was regulated by a physical association between COMMD1 and HIF-1α.

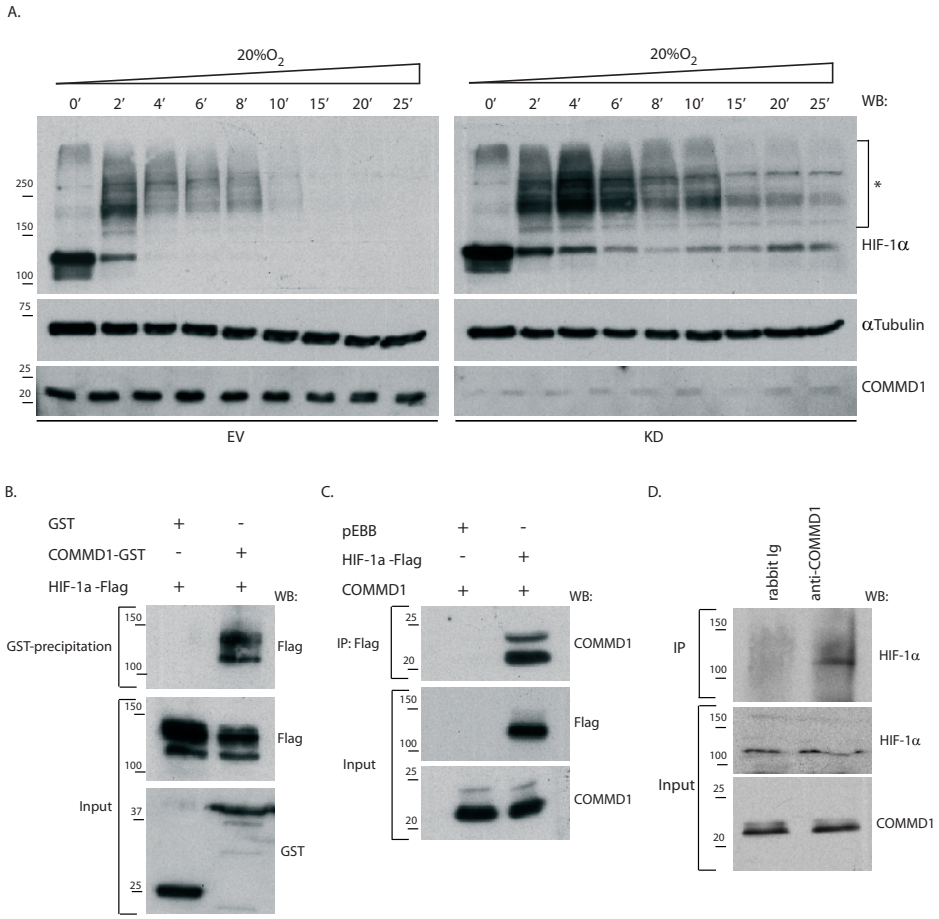

Figure 7. Increased HIF-1α protein stability in COMMD1 knockdown cells and association of COMMD1 with HIF-1α (A) Stability of HIF-1α protein was determined in COMMD1 knockdown HEK 293T cells (KD) and control HEK 293T cells (EV) by immunoblot analysis. After the cells were cultured under hypoxic conditions (1% 0_2) cells were exposed to 20% O_2 for the indicated time periods. Proteins with high moleculair mass detected by anti-HIF-1 α is indicated by *. α Tubulin expression was used as a loading control. (B) Glutathione-sepharose precipitations using cell lysates of HEK 293T cells expressing HIF-1α-Flag, GST or COMMD1-GST. (C) Flag immunoprecipitation using cell lysates of HEK 293T cells cotransfected with HIF-1α-Flag, or pEBB-flag and COMMD1. (D) Endogenous COMMD1 immunoprecipitation using HEK 293T cell lysates. All precipitates were washed and separated by SDS-PAGE and immunoblotted as indicated. Input indicates direct analysis of cell lysates. The molecular size markers are indicated in kDa on the left.

GST-pull down studies were performed using lysates from HEK 293T cells coexpressing COMMD1-GST and HIF-1α-Flag. HIF-1α was clearly detected in COMMD1-GST samples precipitated by glutathione sepharose but not in GST precipitates, indicating a specific interaction between COMMD1 and HIF-1α (Fig. 7B). Coimmoprecipitation studies were performed using cell lysates from HEK 293T cells coexpressing COMMD1 and HIF-1α-Flag or untransfected cells to confirm the physical association between HIF-1α and COMMD1.

COMMD1 was clearly detected in HIF-1α-Flag immunoprecipitates but not in immunoprecipitates from cells transfected with empty vector (Fig 7C). HIF-1α was also observed in COMMD1 immunoprecipitates but not in control immunoprecipitates demonstrating the specificity of the interaction between COMMD1 and HIF-1α (Fig 7D). Taken together, these *in vitro* data indicate that COMMD1 modulates the protein level of HIF-1α and HIF-1 activity, possibly via a COMMD1- HIF-1α protein interaction.

Discussion

We and others have shown that COMMD1 is associated with copper homeostasis [8, 9, 46, 117] but recent studies have revealed that COMMD1 also has a role in NF-κB signaling, sodium transport and XIAP-signaling [11, 121-123, 149]. To further investigate the pleiotropic function of COMMD1 *in vivo* we targeted exon 2 of the murine *Commd1* gene by homologous recombination.

Extensive analyses of the targeted Commd1 locus showed that loss of *Commd1* exon 2 specifically leads to Commd1 deficiency, comparable to the situation in copper toxicosis affected Bedlington terriers. To our surprise, *Commd1*$^{-/-}$ mice are embryonically lethal, whereas COMMD1-deficient Bedlington terriers pups are born healthy but gradually accumulate copper in their liver, leading to liver cirrhosis between 2 and 6 years of age [118]. Although the reason for the phenotypic discrepancy between dog and mice is currently unknown, one can speculate that there is some functional redundancy of the COMMD protein family that is species-dependent. We were unable to detect any obvious copper accumulation in *Commd1-/-* embryos or in their placentas at 9.5 dpc. Embryonic lethality has previously been described in mice deficient for the copper transporters Ctr1 and Atp7a [128, 138, 140]. The phenotypes of *Commd1-/-* mice differ markedly from the phenotypes of *Ctr1*$^{-/-}$ and *Atp7a-/-* mice and we were unable to rescue the *Commd1-/-* embryonic lethality by providing a high-copper diet to the pregnant and lactating mothers. We therefore conclude that the embryonic lethal phenotype cannot be explained by a prominent role of Commd1 in copper homeostasis during mouse embryogenesis.

In this study we have uncovered a previously unidentified role of Commd1 as a mediator of HIF-1 activity during mouse embryogenesis. Gene expression profiling showed that HIF-1 target genes were induced in 9.5 dpc *Commd1-/-* embryos compared to 8.5 dpc and 9.5 dpc normal embryos. Interestingly, Murphy *et. al.* suggested that hypoxia recruits metal transcription factor 1 (MTF-1) and HIF-1 to the promoter of the mouse *Mt-1* gene and this phenomenon might therefore also explain the induction of *Mt-I* (Fig. 5B) in 9.5 dpc *Commd1-/-* embryos [150]. The transcriptional induction of HIF-1 target genes is associated with elevated Hif-1α protein levels in 9.5 dpc *Commd1-/-* embryos

(Fig. 6A). HIF-1 is the master transcriptional regulator of adaptive responses to hypoxia and previous studies have established that a proper HIF-1 activity is essential for normal embryogenesis. Loss of Hif-1α leads to embryonic arrest at 9 dpc and these embryos die at 10.5 dpc. *Hif-1α -/-* embryos show defects in the vascularization of the placenta, cardiovascular and neural tube development and an increased cell death within cephalic mesenchyme [151]. More importantly, also increased HIF-1 activity has been shown to lead to embryonic lethality during midgestation. This is illustrated by the phenotypes of the von Hippel-Lindau knockout mouse (*Vhl-/-*), a HIF-1α inhibitor protein [152, 153] and the PHD2 knockout mouse [148]. The embryonic lethality of both mouse models is caused by abnormalities of placental vasculogenesis due to upregulated HIF-1-mediated transcription [152]. The importance of balanced HIF-1 activity for proper placental development between 8 dpc and 10 dpc was further demonstrated by others [148, 154]. They established that HIF-1 mediates the differentiation of trophoblast cells into spongiotrophoblast cells and inhibits the differentiation into labyrinthine trophoblast cells. Absence of vasculogenesis and an increased amount of non-nucleated maternal erythrocytes was also observed in the placentas of *Commd1-/-* embryos (Fig.2B), very similar to what has been seen in *Vhl-/-* embryos. Our observation of high levels of *Commd1* mRNA expression in the allantois and the chorionic plate at 8.5 dpc and recent data establishing the expression of COMMD1 in human placental villi [155] further supports an essential role for *Commd1* in the development of the chorioallantoic placenta. In this context it is important to realize that vascularization of the placenta starts at 9.0 dpc [156] and since 9.5 dpc *Commd1-/-* embryos resemble the developmental stage of 8.5 dpc normal embryos, placental development in *Commd1-/-* embryos could be retarded rather than completely prevented. Finally, our data cannot rule out the possibility that Commd1 regulation of Hif-1 activity during mouse embryogenesis is indirect.

More evidence for the conclusion that COMMD1 mediates HIF-1 activity was provided by several independent *in vitro* experiments. HIF-1 luciferase reporter assays and quantitative RT-PCR indicated that endogenous and overexpressed COMMD1 directly mediate HIF-1 activity. The involvement of COMMD1 in HIF-1-mediated transcriptional regulation is corroborated by the observed protein-protein interaction between COMMD1 and HIF-1α. Interestingly, the increased HIF-1 activity in COMMD1 deficient cells compared to wild-type cells was only detectable under hypoxic conditions and not under normoxic conditions. This observation appears to be in accordance with the increased Hif-1 activity in Commd1 null embryos, since the physiological oxygen levels at 9.5 dpc is low, approximately 3% [154], suggesting that COMMD1 mediates HIF-1 activity under specific physiological conditions.

Elevated Hif-1α levels in *Commd1-/-* embryos and increased HIF-1α stability in COMMD1 knockdown cells suggest that COMMD1 regulates HIF-1 activity through controlling HIF-1α protein stability. The role of COMMD1 in stabilizing transcription factors

has recently also been reported by others [11, 157]. They demonstrated that COMMD1 mediates protein stability of NF-κB subunits via the ubiquitin ligase complex ECS^{SOCS1}, thereby regulating κB-mediated transcription. This may suggest that COMMD1 regulates HIF-1 activity in similar fashion as its controls κB-mediated transcription, since HIF-1α protein stability is also regulated via an E3 ubiquitin ligase complex very similar to ECS^{SOCS1} [158].

Taken together, this study identified COMMD1 as a novel interactor and regulator of HIF-1 activity and indicates that loss of Commd1 leads to aberrant Hif-1α expression during early embryogenesis, resulting in increased mRNA expression of HIF-1 target genes. Apparently, dysregulated energy metabolism and lack of placental vascularization might explain the delay and eventual arrest of embryonic development of *Commd1-/-* mice, but additional studies are needed to further delineate the role of Commd1 in regulation Hif-1 activity in the developing mouse embryo. Phenotypic discrepancy between COMMD1 deficiency in dog and mouse might be explained by differences in the development of the mouse placenta and the placentas of other mammals, even though substantial similarities exist [156]. These data demonstrate for the first time that Commd1 regulates HIF-1 activity and is essential for normal mouse embryogenesis. Increased HIF-1 activity has also been associated with different diseases such as preeclampsia and cancer (reviewed by [159]). Therefore, it will be interesting to further define the molecular mechanism by which COMMD1 regulates HIF-1 activity in different biological processes.

Acknowledgements

We thank Dr. F. Meijlink and Dr. J. Deschamps for their valuable discussions and Jackie Senior for improving the manuscript. We thank Marc Vooijs (Dept. of Pathology, UMCU Utrecht) for reagents, advice on HIF-1α and the use of the Ruskin INVIVO2 1000 hypoxic working station, which was financially supported by the Maurits and Anna de Kock Foundation. We acknowledge Dr. T.B. O'Brien for providing the Meox1 construct. This work was financially supported partly by grant 40-00812-98-03106 to LWK and CW from the Dutch Organization for Scientific Research (NWO), and partly by the Intramural Research Program of The National Human Genome Research Institute, National Institutes of Health, USA (to BS, AC and PL).

Chapter 5

Distinct COMMD proteins regulate the expression of specific subsets of NF-κB target genes

Patricia A.J. Muller[1,2,*], Aparna Repaka[3,*], Xicheng Mao[3], Gabriel Maine[3], Bart van de Sluis[1,2], Cisca Wijmenga[2,4] Leo W.J. Klomp[1,#], Ezra Burstein[3,#]

[1]Department of Metabolic and Endocrine Diseases, UMC Utrecht, and Netherlands Metabolomics Centre, the Netherlands; [2]Complex Genetics Section, DBG-Department of Medical Genetics, UMC Utrecht, the Netherlands; [3]Department of Internal Medicine, University of Michigan Medical School, Ann Arbor, MI, USA; [4]Department of human genetics, UMC Groningen and University of Groningen, Groningen, the Netherlands

* Shared first author

Shared last author

Manuscript in preparation

Abstract

The NF-κB/ rel family of transcription factors regulates the expression of several hundreds of genes involved in biomedically relevant processes such as cell survival and inflammation. The precise mechanisms determining the specificity in the regulation of these genes is dependent on the cell type, stimulus and the duration of the stimulus, but have not been established in molecular detail yet.

Recent studies have revealed that the newly identified COMMD family of proteins plays a role in NF-κB signaling. *In vitro*, all COMMD proteins could inhibit NF-κB activity. As specific COMMD proteins interact with distinct NF-κB subunits, we hypothesized that COMMD proteins might determine NF-κB-mediated transcription specificity. In order to investigate this possibility, we used RNA interference to knock down the expression of COMMD1, COMMD6 or COMMD9 in HT29 cells and investigated the genome-wide gene expression profiles after culturing cells in the absence or presence of TNF, a well-known inducer of NF-κB signaling. From these analyses, we could identify specific TNF-target genes that were uniquely regulated by the individual COMMD proteins. Collectively, these data indicate that the COMMD family of proteins might serve as modulators of NF-κB target gene expression and define transcriptional specificity within NF-κB signaling.

Introduction

The nuclear factor kappa B (NF-κB)/ Rel family of transcription factors regulate the expression of a multitude of genes involved in cell growth, cell survival, apoptosis, inflammation and immunity. This protein family consists of the five subunits RelA (p65), c-Rel, v-Rel, p50 (NF-κB2) and p52 (NF-κB1), which form heterodimers or homodimers that are denoted as NF-κB. The interplay between all the proteins involved in NF-κB regulation is termed the NF-κB signaling module. Two NF-κB signaling patways can be distinguished: the canonical pathway and the non-canonical pathway. Within the canonical pathway, regulation of NF-κB transcriptional activity is mainly achieved by the inhibitor of κB (IκB) family of proteins that comprises IκBα, IκBβ and IκBε. IκB proteins keep the NF-κB subunits sequestered in the cytoplasm. In response to external stimuli, including various sources of stress, pathogens and cytokines, IκB proteins are phosphorylated by IKK proteins, ubiquitinated and subsequently degraded. This process results in the dissociation of the IκB protein from NF-κB, allowing translocation of NF-κB into the nucleus to initiate the transcription of NF-κB target genes. In the non-canonical pathway, the C-terminal part of the p52 precursor protein p100 works similar to IκB protein in sequestering the NF-κB subunits in the cytoplasm.

Much effort has been made in elucidating the specificity of the NF-κB signaling module in transcriptional regulation (reviewed in [160]). Cell lines in which expression of specific NF-κB subunits was abolished, displayed distinct gene expression profiles [161, 162], indicating subunit specificity. Furthermore, distinct NF-κB dimers display a higher DNA sequence affinity although an extended overlap in DNA sequence recognition exists among the dimers [163, 164]. In addition to subunit and dimer specificity, NF-κB-mediated gene expression is also tissue-dependent, stimulus-dependent, dependent on the activity of other transcription factors and subject to dynamic control [160]. All these mechanisms are illustrative for the highly complex manner in which the hundreds of NF-κB target genes are regulated, but the precise way in which these mechanisms cooperate to induce the expression of specific sets of genes, is largely unknown.

COMMD1 is a ubiquitously expressed protein which is highly conserved among higher eukaryotes, but its precise functions remain elusive. Various protein-protein interaction studies have identified COMMD1 as a protein involved in several biological processes including NF-κB activity [8, 9, 122, 165-167]. COMMD1 interacts with all NF-κB subunits, IκB-α and the Cullin complexes that mediate ubiquitination of IκB-α or NF-κB [11, 123, 168]. Increased expression of COMMD1 results in stabilization of IκB-α. Furthermore, COMMD1 can also promote the proteasomal degradation of DNA-bound NF-κB subunits by recruiting a ubiquitin ligase complex. Both of these events ultimately result in the repression of NF-κB activity and, subsequently, reduced expression of NF-κB target genes.

COMMD1 is the first identified protein in a family of ten COMMD proteins that all share a homologous COMM domain. Similar to COMMD1, all these nine COMMD proteins are ubiquitously expressed and can inhibit NF-κB activity *in vitro* [11]. Interaction studies revealed that not all COMMD proteins interact with all NF-κB subunits. For example, c-Rel specifically interacts with COMMD1; COMMD6 interacts with only NF-κB1 and RelA; and COMMD9 interacts with only NF-κB1 and RelB [11, 166]. These data suggest that the COMMD proteins do not simply have redundant physiological roles in NF-κB signaling. Furthermore, the distinct binding affinities of the COMMD proteins to the NF-κB subunits are possibly indicative for yet another level of regulation of NF-κB transcriptional specificity. From these data we hypothesized that different COMMD proteins could regulate the expression of distinct subsets of NF-κB target genes. In this study, we aimed to determine the role of COMMD1, COMMD6 and COMMD9 in NF-κB mediated transcriptional regulation in HT29 cells in the presence and in the absence of the NF-κB stimulus TNF. We were particularly interested in COMMD1 as COMMD1 knockout mice are embryonically lethal, excluding redundant functions of other COMMD proteins for COMMD1 function. To specifically investigate the effect of the COMM domain, COMMD6 was included as this is the shortest COMMD protein that almost only comprises the COMM domain. Hence, COMMD6-mediated gene expression changes could be attributed to its COMM domain alone. To further investigate if different COMMD members exhibit NF-κB target gene specificity, COMMD9 was included as this protein is highly expressed in HT29 cells.

Materials and methods

Cell culture and constructs

HT29 cells and HEK293T cells were cultured in DMEM supplemented with 10% heat-inactivated fetal calf serum and 1% penicillin/streptomycin (37˚C in 5% CO_2/air). If indicated, HT29 cells or HEK293T cells were incubated with 1000 U/ml TNF (Roche Applied Science, Manheim, Germany) for 10 min followed by 1 hr recovery.

Transfections, RNA isolation and Illumina cRNA preparation

HT29 cells were seeded one day prior to transfection in 10 cm dishes. Cells were transfected with shRNAs targeted against CAT, COMMD1, COMMD6 or COMMD9 using a standard calcium phosphate procedure [45] and were harvested at 70-90% confluence the next day. Total RNA was isolated using Trizol reagent (Invitrogen, Leek, the Netherlands) according to the manufacturer's protocol. High-quality total RNA (500 ng), as determined by a 28S/18S ribosomal RNA ratio >1.8 in a bioanalyzer (2100; Agilent, Amstelveen, the Netherlands) was used for cDNA synthesis and amplification by an *in*

vitro transcription reaction of 5 hrs according to the manufacturer's protocol. (Ambion, Sanbio B.V., Uden, the Netherlands). Biotin-16-UTP (Ambion) was added in the *in vitro* transcription reaction.

Quantitative RT-PCR analysis

Total RNA was extracted from HT29 and HEK293 cells using the Trizol method (Invitrogen) according to the manufacturer's protocol. The yield and the purity were verified by measurement of OD260/280. Quantitative real time polymerase chain reaction (q RT PCR) was performed using Sybr-Green detection.

Gene expression analysis and statistics

Biological quadruplicate samples were used to hybridize on Illumina sentrix-8-bead chips, containing 24.000 specific oligonucleotide beads. In total, 44 samples were hybridized on six sentrix-8-bead chips in three rounds of hybridization. In each of these rounds a standard cRNA sample of unstimulated control cells was used to correct for hybridization-differences in gene expression. Hybridization of the cRNA was performed according to the manufacturer's protocol. Briefly, 800 ng of cRNA was hybridized for 18 hrs at 58°C, and the slides were subsequently washed and scanned using the beadstation 500 (Illumina, San Diego, CA, USA). Using the Illumina beadstudio software, the data was normalized by a rank invariant analysis and corrected for inter-chip variations. Statistical significance in differential gene expression was determined by using the Illumina custom method supplied in this software, which is based on the analysis of variance. Genes with a differential score lower than -10 or higher than 10 were considered to be differentially expressed. In the list of differentially expressed genes, overrepresentation of genes involved in specific biological processes (according to the gene ontology annotation (GO); www.go.com) compared to the distribution of all the genes present on the Illumina slides involved in these biological processes was determined by the web based program Genetrail (http://genetrail.bioinf.uni-sb.de/index.php) and by the web based program Babelomics (http://babelomics.bioinfo.cipf.es/index.html). A hypergeometric test in combination with FDR (false discovery rate) adjustment (Benjamini-Hochberg correction) and a significance threshold of 0.05 were used to determine significant enrichment of GO biological processes. Only significant GO processes and sub processes containing 4 genes or more were included in the final results.

Results

Verification of COMMD1, COMMD6 and COMMD9 knockdown

To investigate the possibility that distinct COMMD proteins could regulate the expression of specific NF-κB target genes, we used RNA interference to knock down the expression of three COMMD proteins in HT29 cells. Examination of the expression of all COMMD proteins in HT29 cells revealed a very low expression of COMMD5 and a high expression of COMMD6 and COMMD9 (figure 1A). We therefore decided to knockdown the expression of COMMD1, COMMD6 and COMMD9 and we determined whether COMMD1, COMMD6 and COMMD9 were effectively knocked down. Compared to the expression of the COMMD proteins under normal conditions, COMMD1 (figure 1B), COMMD6 (figure 1C) and COMMD9 (figure 1D) mRNA levels were reduced 10-fold, 3-fold and 4-fold respectively after the use of RNA interference. In addition, we determined whether decreased COMMD1, COMMD6 and COMMD9 expression could (indirectly) affect the expression of other COMMD proteins. A knockdown of any of these three COMMD proteins did not result in major, more than 2-fold, differences in the mRNA expression of other COMMD proteins. This indicated that the RNA interference resulted in specific knockdown of

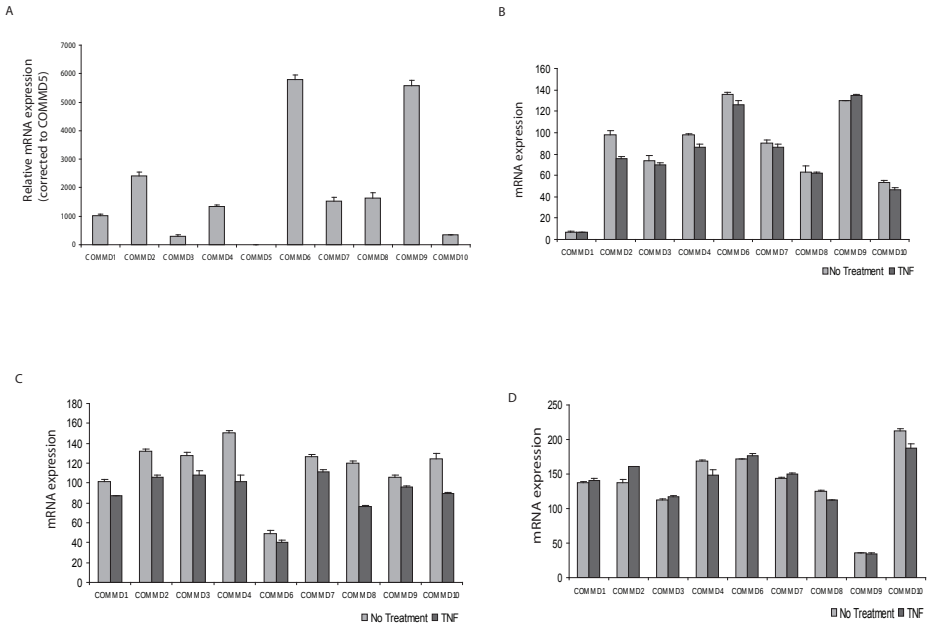

Figure 1 COMMD family gene expression in HT29 cells

A. The mRNA expression of COMMD1-10 was determined in HT29 cells and related to COMMD5 expression (The COMMD member with the lowest expression) using qRT PCR. B/C/D. The mRNA expression of COMMD1-10 was determined in HT29 cells in which COMMD1 (B), COMMD6 (C) and COMMD9 (D) expression was decreased through the use of short hairpin RNA targeted against these COMMD members using qRT PCR.

COMMD1, COMMD6 or COMMD9, and also suggested that COMMD proteins do not constitute important transcriptional regulators of other COMMD proteins.

Knockdown of COMMD1, COMMD6 and COMMD9 results in differential gene expression

Differential gene expression as a result of decreased COMMD1, COMMD6 and COMMD9 expression was determined by Illumina technology. In total, we detected 331 genes that were significantly differentially expressed in COMMD1 knockdown cells. Of these genes, 144 were exclusively expressed in COMMD1 knockdown cells and not in COMMD6 or COMMD9 knockdown cells (figure 2A). Furthermore, 64 genes were more than 2-fold differentially expressed, of which 8 were induced and 56 were repressed (figure 3A). In COMMD6 knockdown cells, 468 genes were differentially expressed, of which 243 genes were unique for COMMD6 deficiency (figure 2A). In COMMD6 knockdown cells, 80 genes were differentially expressed more than 2-fold, of which 56 were induced and 24 were repressed (figure 3B). In COMMD9 knockdown cells, 242 genes in total were differentially expressed, of which 112 genes were exclusive for COMMD9 deficiency cells (figure 2A). In COMMD9 knockdown cells, 44 genes were differentially expressed more than 2-fold, of which 25 were induced and 19 were repressed (Figure 3C). As a control, we noted decreased expression of COMMD1, COMMD6 and COMMD9 in the corresponding knockdown cell lines using the Illumina technology (figure 3 A, B, C). The numbers of differentially expressed genes in any of the three knockdown cell lines that overlap are depicted in figure 3A. A marked overlap of 58 differentially expressed genes in all the three knockdown cells was observed (figures 3A and 3B). These results suggest that regulation of some genes might be COMMD specific, whereas other genes can be regulated by more than one COMMD protein.

Genes involved in distinct biological processes were overrepresented in the knockdown- induced lists of differentially expressed genes

In order to understand the physiological implications of the observed gene expression changes, we performed enrichment analyses. In this analysis, we asked whether sets of genes involved in defined biological processes, according to the GO database, were overrepresented in the specific lists of all genes differentially expressed in COMMD1, COMMD6 or COMMD9 knockdown cells. These genes were compared to the distribution of all genes present on the chip in these biological processes. To determine the way in which COMMD1 regulated these responses we separated the differentially expressed genes in those that were induced and those that were repressed and determined enrichment of biological processes in these separate lists. In table 1, we depicted the observed number of genes in the indicated list of genes for each enriched biological process and the number of genes we would have expected based on the distribution of all genes

A

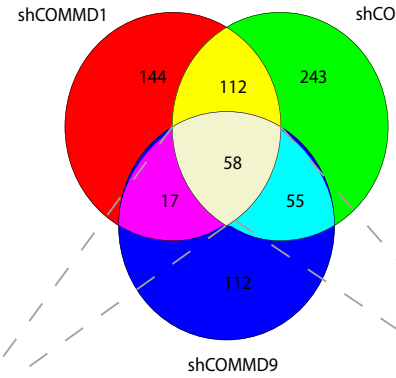
shCOMMD1
shCOMMD6
shCOMMD9
144
112
243
58
17
55
112

B

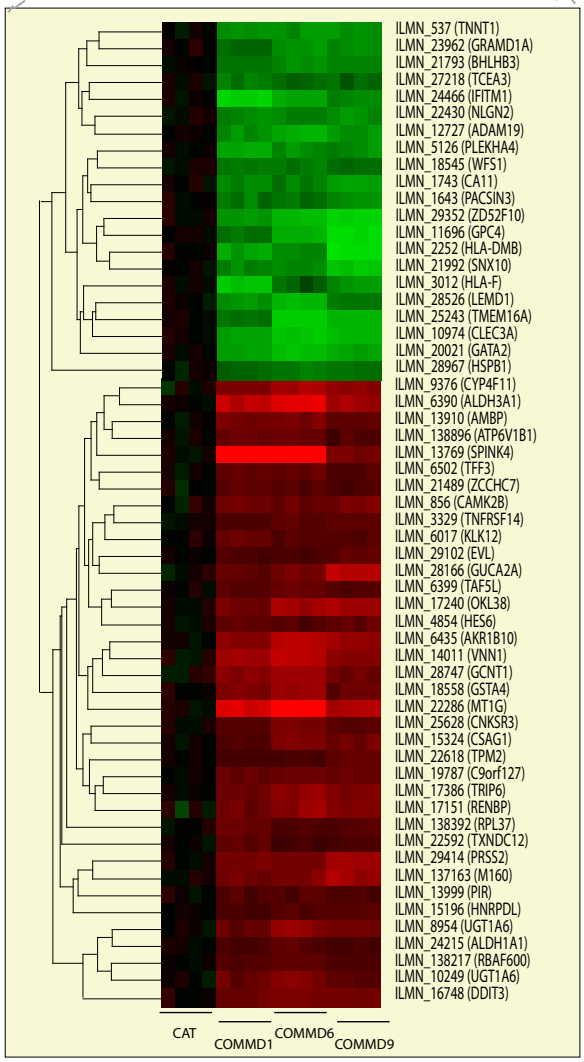
ILMN_537 (TNNT1)
ILMN_23962 (GRAMD1A)
ILMN_21793 (BHLHB3)
ILMN_27218 (TCEA3)
ILMN_24466 (IFITM1)
ILMN_22430 (NLGN2)
ILMN_12727 (ADAM19)
ILMN_5126 (PLEKHA4)
ILMN_18545 (WFS1)
ILMN_1743 (CA11)
ILMN_1643 (PACSIN3)
ILMN_29352 (ZD52F10)
ILMN_11696 (GPC4)
ILMN_2252 (HLA-DMB)
ILMN_21992 (SNX10)
ILMN_3012 (HLA-F)
ILMN_28526 (LEMD1)
ILMN_25243 (TMEM16A)
ILMN_10974 (CLEC3A)
ILMN_20021 (GATA2)
ILMN_28967 (HSPB1)
ILMN_9376 (CYP4F11)
ILMN_6390 (ALDH3A1)
ILMN_13910 (AMBP)
ILMN_138896 (ATP6V1B1)
ILMN_13769 (SPINK4)
ILMN_6502 (TFF3)
ILMN_21489 (ZCCHC7)
ILMN_856 (CAMK2B)
ILMN_3329 (TNFRSF14)
ILMN_6017 (KLK12)
ILMN_29102 (EVL)
ILMN_28166 (GUCA2A)
ILMN_6399 (TAF5L)
ILMN_17240 (OKL38)
ILMN_4854 (HES6)
ILMN_6435 (AKR1B10)
ILMN_14011 (VNN1)
ILMN_28747 (GCNT1)
ILMN_18558 (GSTA4)
ILMN_22286 (MT1G)
ILMN_25628 (CNKSR3)
ILMN_15324 (CSAG1)
ILMN_22618 (TPM2)
ILMN_19787 (C9orf127)
ILMN_17386 (TRIP6)
ILMN_17151 (RENBP)
ILMN_138392 (RPL37)
ILMN_22592 (TXNDC12)
ILMN_29414 (PRSS2)
ILMN_137163 (M160)
ILMN_13999 (PIR)
ILMN_15196 (HNRPDL)
ILMN_8954 (UGT1A6)
ILMN_24215 (ALDH1A1)
ILMN_138217 (RBAF600)
ILMN_10249 (UGT1A6)
ILMN_16748 (DDIT3)
CAT
COMMD1
COMMD6
COMMD9

present on the chip in these biological processes. We observed that genes involved in the immune response process were significantly overrepresented in the list of repressed genes in COMMD1 knockdown cells ($p = 1.05x10^{-17}$) (table 1). Furthermore, an increased expression of genes involved in cholesterol biosynthesis was noted ($p = 8.52x10^{-3}$). A knockdown of COMMD6 mainly resulted in an increased expression of genes involved in organic acid metabolic processes ($p = 3.47x10^{-4}$) (table 1). Within the lists of differentially expressed genes as a result of COMMD9 knockdown, we did not detect a statistically significant overrepresentation of specific biological processes. Due to the limited number of overlapping genes, we could not detect significant enrichment of genes involved in specific biological processes in the common list of differentially expressed genes compared to all the genes present on the chip. These data suggest that COMMD1 and COMMD6 specifically regulate the expression of genes involved in distinct pathways.

Distinct COMMD proteins affect the expression of TNF target genes

As the COMMD proteins were previously implicated in NF-κB signaling, we specifically monitored for known NF-κB target genes in the lists of differentially expressed genes in the knockdown cell lines as compared to control cells. Under basal conditions, the NF-κB pathway is kept in an inactive state, predominantly by retaining the NF-κB subunits to the cytoplasm. As a consequence, the expression of NF-κB target genes is very low [160, 169], which probably accounts for our inability to detect overrepresentation of NF-κB target genes in these lists. We therefore activated the NF-κB pathway using TNF. Genome-wide gene expression analysis was performed in control cells and in knockdown cells after TNF exposure and the results were analyzed as schematically depicted in figure 4A.

In the control shCAT transfected cell line, we identified 335 differentially expressed genes, of which 107 were repressed and 228 were induced after TNF exposure. The latter

Figure 2 Decreased expression of COMMD1, COMMD6 or COMMD9 in HT29 cells results in differential gene expression

A Endogenous COMMD1, COMMD6 or COMMD9 levels in HT29 cells were decreased using short hairpin RNA targeted against these COMMD members. RNA was isolated and differential gene expression analysis was performed using the Illumina bead station technology and compared to HT29 cells that were transfected with short hairpin RNA targeted against *CAT* as control,. In the VENN diagram, the overlap of differential gene expression as a result of decreased COMMD1, COMMD6 or COMMD9 levels is depicted. In contract to figure 2, no cutoff for raw expression or fold induction was set. The numbers in this VENN diagram indicate the number of genes differentially expressed in the corresponding conditions, indicated by colors. Red; number of genes regulated specifically by COMMD1. Green; number of genes regulated specifically by COMMD6. Dark blue; number of genes regulated specifically by COMMD9. Yellow; number of genes regulated specifically by COMMD1 and COMMD6. Light Blue; number of genes regulated specifically by COMMD6 and COMMD9. Purple; number of genes regulated specifically by COMMD1 and COMMD9. White; number of genes regulated by COMMD1, COMMD6 and COMMD9. B. Cluster diagram of the genes that were regulated by COMMD1, COMMD6 and COMMD9 (white condition of the VENN diagram). Green indicates downregulation, black indicates no differential expression and red indicates upregulation. The intensity of the colors is indicative for the rate of up regulation or downregulation.

Table 1 Enrichment of genes involved in the indicated biological processes in COMMD1 and COMMD6 knockdown cells compared to control cells under normal conditions.

Gene Ontology	p-value	expected number of genes	observed number of genes
shCOMMD1 induced			
lipid biosynthetic process	3.21E-02	2	9
steroid metabolic process	1.24E-03	2	10
steroid biosynthetic process	1.24E-03	1	7
sterol metabolic process	4.07E-02	1	5
sterol biosynthetic process	1.38E-02	0	4
cholesterol metabolic process	3.21E-02	1	5
cholesterol biosynthetic process	8.52E-03	0	4
aldehyde metabolic process	1.53E-02	0	3
shCOMMD1 repressed			
response to stimulus	5.16E-10	18	50
response to biotic stimulus	2.23E-13	2	20
response to other organism	5.16E-10	1	15
response to virus	1.48E-12	1	14
immune system process	3.33E-17	6	37
immune response	1.05E-17	4	34
defense response	5.00E-03	4	13
innate immune response	1.14E-03	1	6
acute inflammatory response	2.53E-02	1	4
humoral immune response	2.60E-02	1	4
antigen processing and presentation	2.36E-05	0	7
antigen processing and presentation of peptide antigen	6.57E-05	0	5
antigen processing and presentation of peptide antigen via MHC class I	3.23E-05	0	5
amine biosynthetic process	2.53E-02	1	4
amino acid biosynthetic process	6.72E-03	0	4
sh COMMD6 induced			
organic acid metabolic process	3.47E-04	8	25
carboxylic acid metabolic process	3.47E-04	8	25
nitrogen compound metabolic process	8.05E-04	7	22
amino acid metabolic process	1.98E-03	4	15
generation of precursor metabolites and energy	4.31E-02	9	18
transcription, DNA-dependent	7.72E-03	38	19
aldehyde metabolic process	8.05E-04	0	5

The differentially expressed genes as a result of COMMD1 and COMMD6 decreased expression compared to control cells were separated in induced and repressed genes. Enrichment in biological processes in these lists of genes was determined, compared to the distribution of these processes in all genes present on the chip. Significant overrepresented biological processes are indicated in this table. A p-value for the statistical change that a biological

process is overrepresented was calculated by a hypergeometric test as described in the materials and methods section. The observed number of genes indicate the number of genes that we detected in the lists of induced or repressed genes in COMMD1 or COMMD6 deficient cells for the indicated biological process. The expected number of genes represent the amount of genes we would have expected to be differentially expressed in the indicated biological process, based on the distribution of all genes present on the chip involved in this biological process.

list included several well-known TNF-induced genes; *IL8*, *CXCL1* and *NF-κB1A* [170]. This total set of differentially expressed genes will further be referred to as TNF target genes. In order to determine whether TNF exposure in cells with low COMMD1, COMMD6 or COMMD9 expression provoked an aberrant gene expression pattern, we compared differential gene expression patterns in the knockdown cells stimulated by TNF, to control cells stimulated by TNF. In COMMD1 knockdown cells stimulated by TNF, we identified 678 differentially expressed genes (figure 4B). Remarkably, 53 of these genes were present in our TNF target gene list (figure 4C). Our calculations revealed that analysis of a randomly chosen group of 335 genes (as the TNF target gene list contained 335 genes), would have identified only 11 genes. Permutation analysis revealed that the chance that one would randomly identify 53 genes, is less than 0.0001, indicating that TNF target genes were indeed significantly aberrantly expressed in COMMD1 knockdown cells after TNF exposure. Similarly, approximately 4-5 times more TNF target genes were identified in COMMD6 and COMMD9 knockdown cells stimulated by TNF than we would have expected based on random calculations. In COMMD6 knockdown cells, 1297 genes were differentially expressed after TNF exposure compared to control cells after TNF exposure (figure 4B), including 82 TNF target genes (figure 4C). In COMMD9 knockdown cells, 216 genes were differentially expressed (figure 4B), including 19 TNF target genes (figure 4C). These results indicate that the expression of TNF target genes can be regulated by COMMD1, COMMD6 and COMMD9 after TNF exposure. The overlap in the number of differentially expressed TNF target genes between each of the knockdown cells is depicted in figure 4C. A marked overlap in differentially expressed TNF target genes between knockdown cells lines was detected, but each knockdown cell line also affected the expression of a unique set of TNF target genes.

To speculate on the function of these genes we reorganised all the overlapping 109 TNF-target genes. These 109 TNF genes represent the total number of TNF target genes that were differentially expressed in any of the knockdown cells after TNF exposure compared to control cells after TNF exposure (the total sum of figure 4C). From these 109 TNF target genes, 21 were repressed by TNF and 88 were induced. Cluster analysis of the 88 induced genes revealed that in any of the three knockdown cell lines 39 of these genes were statistically significantly further induced and 49 of these genes were statistically significantly repressed by TNF, compared to control cells incubated with TNF (figure 5A). The mRNA expression of two of these genes, *CX3CL1* and *TNFAIP3,* was verified by qRT

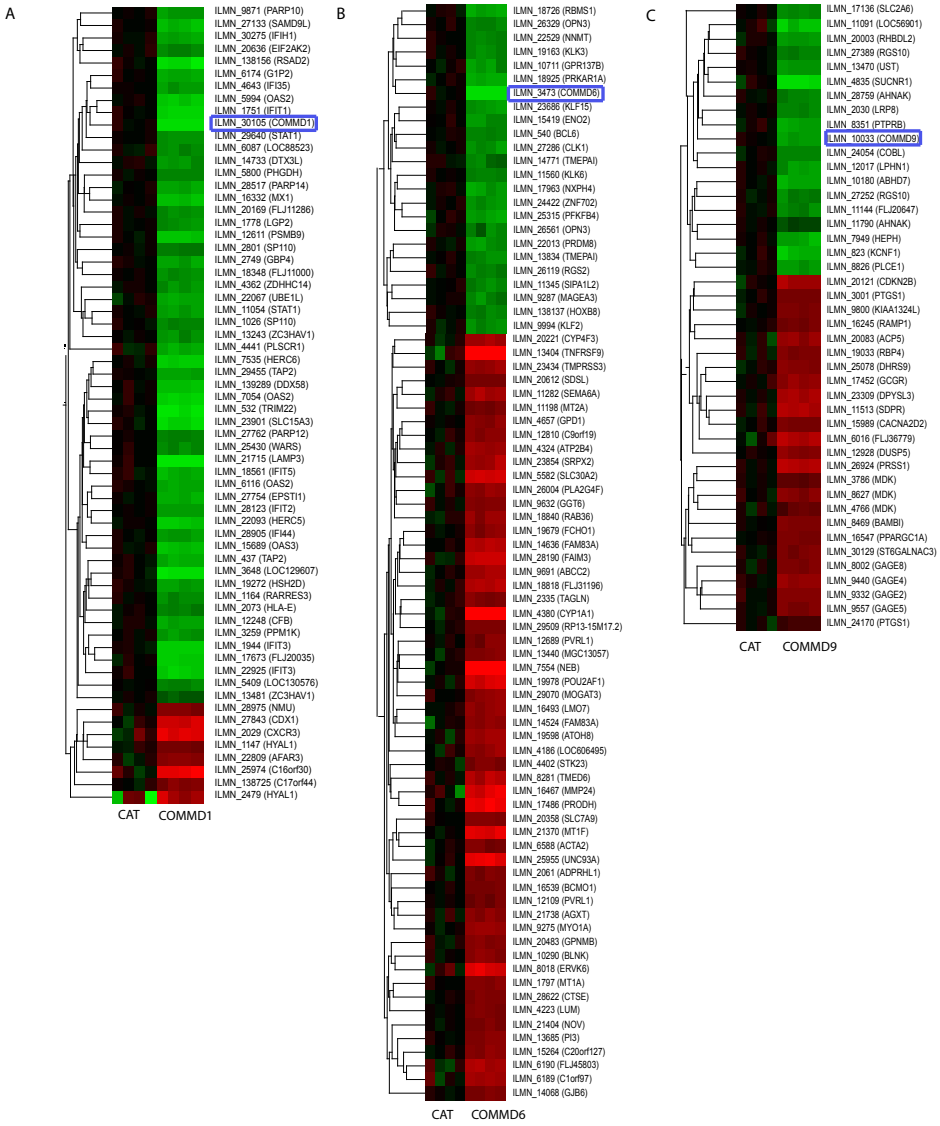

Figure 3 Gene expression of several genes is regulated by more than one COMMD protein

Endogenous COMMD1 (A), COMMD6 (B) or COMMD9 (C) levels in HT29 cells were decreased using short hairpin RNA targeted against these COMMD members. RNA was isolated and differential gene expression analysis was performed using the Illumina bead station technology and compared to HT29 cells that were transfected with short hairpin RNA targeted against *CAT* as control. Genes that were either induced or repressed more than 2-fold and had a raw expression of more than 15 were clustered in a standard cluster diagram using the Genespring 7.0 software. Mean gene expression levels in the control HT29 cells, transfected with shCAT, were set to 1. Overlapping differentially expressed genes between COMMD proteins were excluded. Green indicates downregulation, black indicates no differential expression and red indicates upregulation. The intensity of the colors is indicative for the rate of up regulation or downregulation. In blue boxes COMMD1, COMMD6 and COMMD9 are indicated.

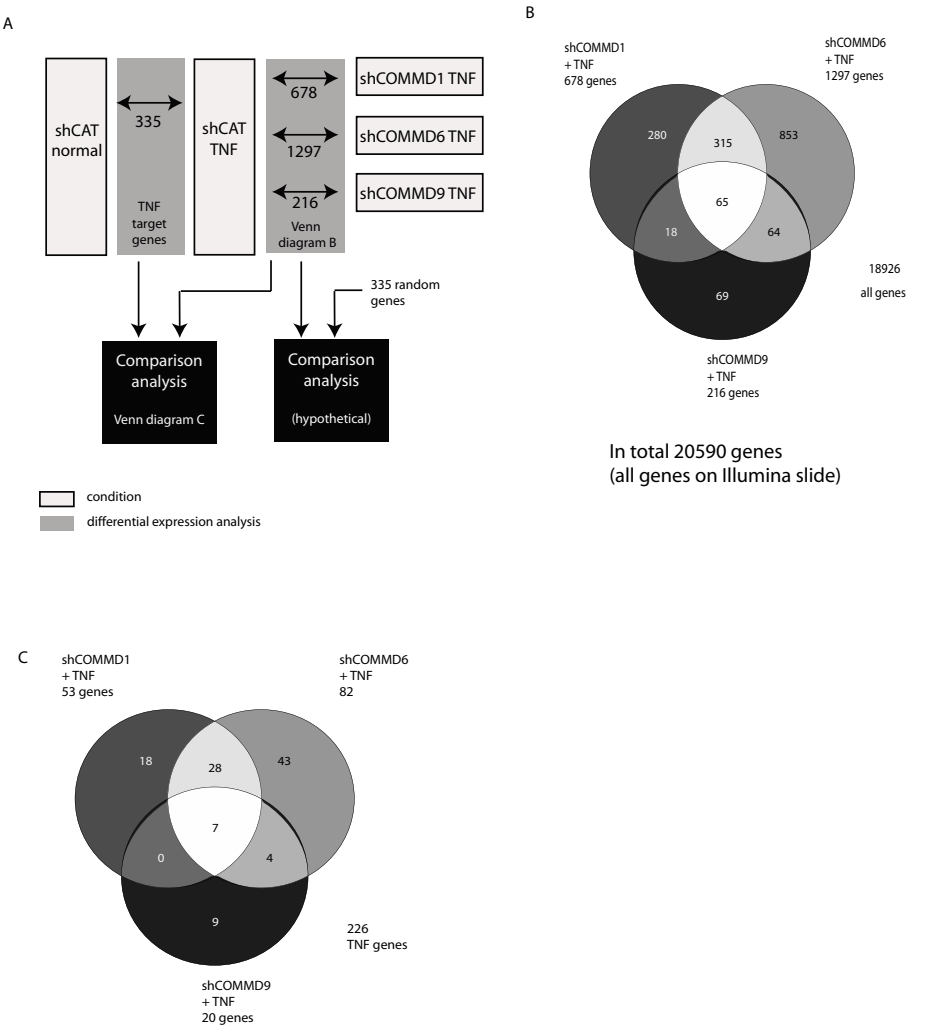

Figure 4 COMMD1, COMMD6 and COMMD9 regulate specific sets of NF-kB /TNF-α responsive genes.
A. Flow chart indicating the specific analyses used to identify which TNF-target genes could be regulated by specific COMMD proteins. We first determined which genes were differentially expressed as a result of TNF exposure in HT29 cells (referred to as 340 TNF-target genes). We next determined which genes were differentially expressed as a result of decreased expression of COMMD1 (678), COMMD6 (1297) or COMMD9 (216) in the presence of TNF. These genes and the overlap between the COMMD proteins is indicated in the VENN diagram in figure B. We next performed comparison analyses to determine the overlap among differentially expressed genes as a result of COMMD knockdown in the presence of TNF and the 340 TNF target genes. The overlap is visualized in the VENN diagram in figure C.

PCR analysis in biologically independent samples (figure 5B and figure 5C upper charts). These data were consistent with the Illumina results.

As the specificity in induction of distinct NF-κB target genes is specific to certain tissues and cell types, we wondered whether COMMD proteins would similarly affect the expression of TNF target genes in a cell line that originated from a different background, HEK293T cells. For this purpose COMMD1, COMMD6 and COMMD9 expression was effectively knocked down using RNA interference (data not shown). Examination of the gene expression of *CX3CL1* in control HEK293T cells revealed that *CX3CL1* was not induced by TNF (figure 5B and 5C). Remarkably, of the three investigated HEK293T COMMD knockdown cell lines, only COMMD1 knockdown induced the expression of *CX3CL1* in the presence and in the absence of TNF in HEK293T cells (figure 5B). In HT29 cells, the induced expression of *TNFAIP3* by TNF was significantly further increased in COMMD1 and COMMD6 deficient cells, but not COMMD9 deficient cells (figure 5C, upper panel). In contrast, in HEK293T cells, knockdown of any of the three COMMD proteins significantly further increased the expression of *TNFAIP3* (figure 5C, lower panel). In addition, the expression of two other well known TNF-target genes, *IL8* and *CXCL1* was investigated in both cell types. In our array analysis, in HT29 cells, *IL8* expression was induced 130-fold and *CXCL1* expression 34-fold by TNF (data not shown). However, no statistically significant aberrant TNF-induced expression of these genes was identified in any of the HT29 knockdown cell lines as compared to control HT29 cells after TNF incubation (data not shown). In HEK293T cells, *IL8* expression was induced 22-fold and *CXCL1* expression 20-fold by TNF. In contrast to HT29 cells, expression of *IL8* was markedly further induced by COMMD1 deficiency and the expression of *CXCL1* was further induced by both COMMD1 and COMMD9 deficiency, but not by COMMD6 deficiency in HEK293T cells. These data suggest that the specificity of COMMD proteins to regulate NF-κB target gene expression is cell-type specific.

To identify possible common processes in which the genes in these clusters could be involved in, we performed enrichment analysis on these 39 'further induced' and 49 'repressed' genes. In the 49 'repressed' genes, enrichment analysis indicated a significant overrepresentation of genes involved in chromatin binding; the histone genes (table

Figure 5. Specific groups of TNF-target genes are regulated by distinct COMMD proteins
A. Of the 109 TNF- target genes, that were also differentially expressed as a result of decreased COMMD expression in the presence of TNF, the expression of 88 genes was increased in the control cell after TNF treatment. The expression of these genes in control cells (shCAT transfected), in COMMD1 knockdown cells, in COMMD6 knockdown cells and in COMMD9 knockdown cells in the presence of TNF is depicted in the cluster diagram. Green indicates downregulation, black indicates no differential expression and red indicates upregulation compared to control cell after TNF treatment. The intensity of the colors is indicative for the rate of up regulation or downregulation.. In gray and yellow the distinguishable clusters are indicated. B/C. The expression of two of the genes of the cluster diagram of A were verified by qRT-PCR analysis; *CX3CL1* (B, upper chart) and *TNFAIP1* (C, upper chart). In the lower charts the mRNA expression of these genes under similar conditions in HEK293T cells was determined. The fold induction of these genes was determined by normalizing the expression of these genes in all conditions to the expression in the control cell line (shCAT) without TNF exposure.

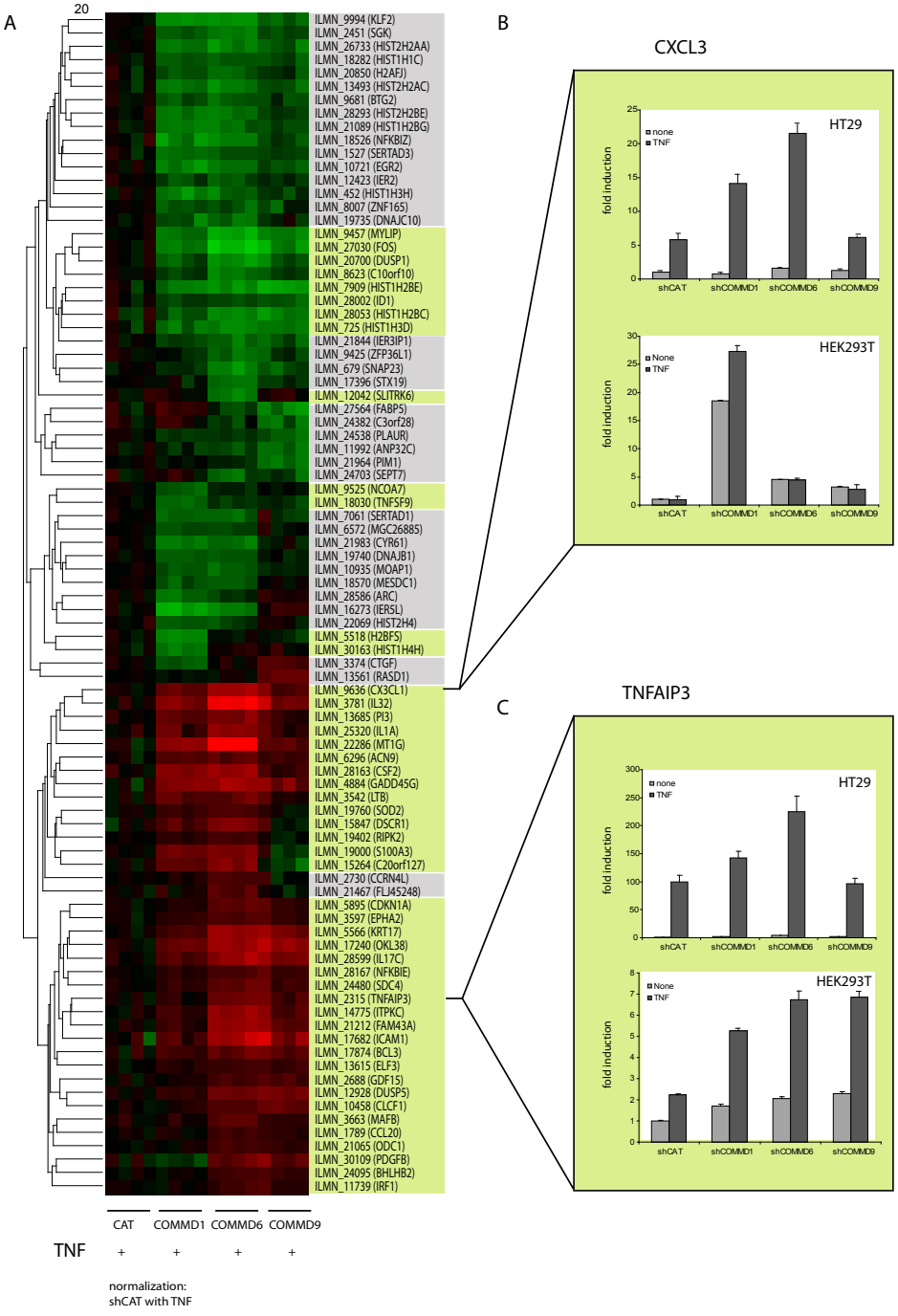
A
20
ILMN_9994 (KLF2)
ILMN_2451 (SGK)
ILMN_26733 (HIST2H2AA)
ILMN_18282 (HIST1H1C)
ILMN_20850 (H2AFJ)
ILMN_13493 (HIST2H2AC)
ILMN_9681 (BTG2)
ILMN_28293 (HIST2H2BE)
ILMN_21089 (HIST1H2BG)
ILMN_18526 (NFKBIZ)
ILMN_1527 (SERTAD3)
ILMN_10721 (EGR2)
ILMN_12423 (IER2)
ILMN_452 (HIST1H3H)
ILMN_8007 (ZNF165)
ILMN_19735 (DNAJC10)
ILMN_9457 (MYLIP)
ILMN_27030 (FOS)
ILMN_20700 (DUSP1)
ILMN_8623 (C10orf10)
ILMN_7909 (HIST1H2BE)
ILMN_28002 (ID1)
ILMN_28053 (HIST1H2BC)
ILMN_725 (HIST1H3D)
ILMN_21844 (IER3IP1)
ILMN_9425 (ZFP36L1)
ILMN_679 (SNAP23)
ILMN_17396 (STX19)
ILMN_12042 (SLITRK6)
ILMN_27564 (FABP5)
ILMN_24382 (C3orf28)
ILMN_24538 (PLAUR)
ILMN_11992 (ANP32C)
ILMN_21964 (PIM1)
ILMN_24703 (SEPT7)
ILMN_9525 (NCOA7)
ILMN_18030 (TNFSF9)
ILMN_7061 (SERTAD1)
ILMN_6572 (MGC26885)
ILMN_21983 (CYR61)
ILMN_19740 (DNAJB1)
ILMN_10935 (MOAP1)
ILMN_18570 (MESDC1)
ILMN_28586 (ARC)
ILMN_16273 (IER5L)
ILMN_22069 (HIST2H4)
ILMN_5518 (H2BFS)
ILMN_30163 (HIST1H4H)
ILMN_3374 (CTGF)
ILMN_13561 (RASD1)
ILMN_9636 (CX3CL1)
ILMN_3781 (IL32)
ILMN_13685 (PI3)
ILMN_25320 (IL1A)
ILMN_22286 (MT1G)
ILMN_6296 (ACN9)
ILMN_28163 (CSF2)
ILMN_4884 (GADD45G)
ILMN_3542 (LTB)
ILMN_19760 (SOD2)
ILMN_15847 (DSCR1)
ILMN_19402 (RIPK2)
ILMN_19000 (S100A3)
ILMN_15264 (C20orf127)
ILMN_2730 (CCRN4L)
ILMN_21467 (FLJ45248)
ILMN_5895 (CDKN1A)
ILMN_3597 (EPHA2)
ILMN_5566 (KRT17)
ILMN_17240 (OKL38)
ILMN_28599 (IL17C)
ILMN_28167 (NFKBIE)
ILMN_24480 (SDC4)
ILMN_2315 (TNFAIP3)
ILMN_14775 (ITPKC)
ILMN_21212 (FAM43A)
ILMN_17682 (ICAM1)
ILMN_17874 (BCL3)
ILMN_13615 (ELF3)
ILMN_2688 (GDF15)
ILMN_12928 (DUSP5)
ILMN_10458 (CLCF1)
ILMN_3663 (MAFB)
ILMN_1789 (CCL20)
ILMN_21065 (ODC1)
ILMN_30109 (PDGFB)
ILMN_24095 (BHLHB2)
ILMN_11739 (IRF1)
CAT
COMMD1
COMMD6
COMMD9
TNF
+
+
+
+
normalization:
shCAT with TNF
B
CXCL3
HT29
none
TNF
fold induction
shCAT
shCOMMD1
shCOMMD6
shCOMMD9
HEK293T
None
TNF
C
TNFAIP3
HT29
HEK293T

Table 2 The expression of histone genes in COMMD knockdown cells and control cells in the presence of TNF compared to control cells under normal conditions.

COMMD knockdown cell line	common name	genbank ID	Control + TNF	Sh COMMD1 + TNF	Sh COMMD6 + TNF	Sh COMMD9 + TNF
COMMD1	HIST1H1C	NM_005319	2.5	1.5	1.5	1.8
	HIST1H3H	NM_003536	1.7	0.9	1.1	1.4
	HIST1H4H	NM_003543	2.2	1.1	2.2	2.2
	HIST2H4	NM_003548	1.9	1.1	1.5	1.9
	H2BFS	NM_017445	1.6	0.8	1.6	1.4
COMMD6	HIST1H2BE	NM_003523	16.7	9.0	8.4	13.4
	HIST1H2BC	NM_003526	8.9	6.3	4.5	4.7
	HIST1H3D	NM_003530	3.6	2.2	2.0	2.2
COMMD1/COMMD6	HIST1H2BG	NM_003518	3.4	1.8	1.8	2.4
	HIST2H2BE	NM_003528	5.5	2.8	2.8	2.2
	HIST2H2AC	NM_003517	4.4	2.6	2.2	3.6
	H2AFJ	NM_177925	1.4	1.0	0.8	1.1
COMMD1/COMMD6/ COMMD9	HIST2H2AA	NM_003516	5.0	2.5	2.5	3.0

All histone genes that are TNF target genes and differentially regulated in COMMD knockdown cells compared to control cells in the presence of TNF are depicted in this table. The knockdown cell line in which these genes are statistically differentially expressed according to the differential expression analysis by Illumina bead station software is indicated in the left column. The numbers represent the fold induction of the histone genes in the indicated cell line compared to the expression of the gene in the control cell line under normal conditions.

2). Clearly, a pulsed TNF stimulation in HT29 cells resulted in an increased expression of these histone genes; a response that has not been described previously. These data suggest a possible link between NF-κB activity and histone gene expression that is modulated by COMMD proteins.

Discussion

NF-κB was identified over 20 years ago as a transcription factor in B-cells [171], but the regulation of specificity within the NF-κB pathway is still poorly understood. Ten novel proteins, the COMMD family of proteins, were recently implicated as ubiquitous inhibitors of NF-κB signaling. After knocking down COMMD1, COMMD6 and COMMD9 in HT29 cells, we identified many genes that were differentially regulated by these COMMD proteins. A marked overlap of 58 genes that are regulated by all three tested COMMD proteins suggested a common gene expression regulation pathway among COMMD proteins. These gene expression data therefore provide strong experimental support for the classification of COMMD proteins as transcriptional modulators. Interestingly, many more genes were uniquely regulated by knocking down distinct COMMD proteins. In

COMMD1 deficient cells, genes involved in cholesterol biosynthesis were induced and were overrepresented compared to control cells. In COMMD6 knockdown cells, genes involved in organic acid metabolic processes were mainly induced. Together, these results indicate that distinct COMMD proteins have non-redundant functions in modulation of gene expression in multiple biological processes.

To identify which genes are differentially expressed as a result of NF-κB activation, we compared the genome-wide gene expression profiles of control HT29 cells with and without exposure to the NF-κB stimulus, TNF. Many more TNF target genes were identified compared to other gene expression studies [172-175], which is most likely caused by the high sensitivity and accuracy of the Illumina technology. These genes comprised several well-known TNF-induced chemokine genes and inflammatory mediator genes, including many NF-κB dependent genes [170]. Surprisingly a marked number of genes revealed suppressed activity, possibly representing indirect effects of TNF. These TNF target genes were used to address the question whether COMMD proteins modulate NF-κB-mediated gene expression after NF-κB activation. We indeed detected a marked and statistically significant enrichment of TNF target genes in all three investigated COMMD deficient cell lines after TNF exposure, suggesting that COMMD proteins modulate NF-κB-mediated gene expression after NF-κB activation. In line with these observations, Burstein *et al.* demonstrated that COMMD1 deficiency resulted in aberrant expression of a number of well-established NF-κB target genes [168]. The other COMMD proteins were implicated in NF-κB signaling based on *in vitro* κB luciferase reporter assays and protein-protein interaction studies [11, 166]. Using an unbiased genome-wide approach, we now provide experimental evidence that all three different COMMD proteins modulate the expression of NF-κB target genes.

Although some overlap between transcriptional regulation by distinct COMMD proteins was noted, deficiency of the three tested COMMD proteins resulted in unique TNF target gene expression profiles. Our data therefore raise the possibility that the COMMD family of proteins serve as transcription regulator proteins that define transcriptional specificity within NF-κB signaling. Our data also indicate that the role of COMMD proteins in regulating NF-κB signaling is cell-type dependent, consistent with the known spatiotemporal- and tissue-dependent control of NF-κB target gene expression [160, 163, 174, 176, 177].

Notably, within the genes that were repressed in COMMD knockdown cells compared to control cells after TNF exposure, many histone genes were present. The expression of these genes is controlled by the protein SLBP (stem loop binding protein) [178, 179]. SLBP interacts with the histone mRNA 3′ end and facilitates the expression of histones during cell cycle progression [180]. To our knowledge, the induction of histone genes has not been identified in the many microarray studies in which the whole genome or extended sets of genes were examined after TNF exposure [170, 174, 181, 182]. In our

study, the expression of these genes was clearly and markedly induced by TNF (table 2). In HepG2 cells, the activation state of NF-κB regulated the expression of SLBP [183]. TNF exposure induced the expression of SLBP and resulted in an increased cell proliferation, suggesting that under these conditions the expression of histone genes was increased. Together, these data suggest a regulatory mechanism of COMMD proteins and NF-κB signaling in histone gene expression, possibly via the SLBP protein. Further experiments are necessary to test the physiological implications of this finding.

The data presented here clearly demonstrate that COMMD proteins have distinct effects on regulating NF-κB-dependent transcription. The exact molecular mechanisms how these COMMD proteins define transcriptional specificity remains to be further elucidated. Previous studies provide some mechanistic insight into the regulation of NF-κB activity by COMMD1. Maine *et al.* revealed that COMMD1 can associate with DNA-bound RelA and thereby recruit a ubiquitin ligase complex that mediates the ubiquitination and subsequent degradation of RelA [168]. As specific COMMD proteins interact with distinct NF-κB subunits [11], a possible explanation for transcriptional specificity could reside in the fact that specific COMMD proteins mediate the degradation of distinct NF-κB subunits. Another mechanistic possibility for generating specificity among COMMD proteins is provided by the fact that the regulatory function of COMMD1 itself can be regulated by nuclear export signals (NESs) in COMMD1. These NESs determine the localization and thereby the transcriptional function of COMMD1 (PM and LK, submitted manuscript). The NESs of COMMD1 are localized in the COMM domain and are conserved within COMMD6 and COMMD9. Together with the observation that COMMD1 and COMMD6 are detectable both in the nucleus and the cytoplasm under normal conditions [166], these data suggest that the localization of COMMD proteins is subject to nuclear cytoplasmic transport mechanisms. Distinct ways to regulate the localization of specific COMMD proteins could therefore perhaps provide a mechanistic way to control NF-κB mediated transcription.

In conclusion, we identified novel genes regulated by three members of the COMMD family of proteins; COMMD1, COMMD6 and COMMD9. These data together illustrate that the COMMD proteins are not redundant and modulate spatiotemporal- and tissue-dependent control of NF-κB target gene expression [160, 163, 174, 176, 177] signaling in distinct ways, providing the possibility to fine-tune NF-κB-dependent processes such as inflammation and cell survival.

Acknowledgements

We are grateful to Ir. Ruben van 't Slot for the use and support of the Illumina technology. This work is funded by the WKZ Fund (40-00812-98-03106)

Chapter 6

Nuclear-cytosolic transport of COMMD1 regulates NF-κB activity

Patricia A.J. Muller[1,2], Bart van de Sluis[1,2], Dineke Verbeek[3], Willianne I.M. Vonk[1,2], Ezra Burstein[4], Cisca Wijmenga[5], Eric Reits[3], Leo W.J. Klomp[1,*]

[1]Department of Metabolic and Endocrine Diseases, UMC Utrecht, and Netherlands Metabolomics Centre, the Netherlands [2]Complex Genetics Section, DBG-Department of Medical Genetics, UMC Utrecht, the Netherlands [3]Department of Cell Biology and Histology, Academic Medical Centre, University of Amsterdam, the Netherlands [4]Department of Internal Medicine, University of Michigan Medical School, Ann Arbor, MI, USA [5]Department of human genetics, University Medical Center Groningen and Groningen University, Groningen, the Netherlands

Submitted

Abstract

The NF-κB / Rel family of transcription factors regulates the expression of several genes involved in inflammation, cell survival and proliferation. Recent reports identified COMMD1 as a novel inhibitor of the NF-κB pathway by promoting nuclear ubiquitination and subsequent degradation of NF-κB subunits. Here, we identified two highly conserved nuclear export signals (NESs) in COMMD1 and revealed that these NESs were both necessary and sufficient to induce maximal nuclear export. Disruption of the NESs in COMMD1 led to enhanced repression of NF-κB signalling by COMMD1, underscoring the regulatory role of NESs in COMMD1 localization and activity. Pharmacological inhibition of CRM1-mediated nuclear export by Leptomycin B resulted in nuclear accumulation of COMMD1 and a concomitant decreased COMMD1 ubiquitination. Nuclear export of COMMD1 facilitated the formation of cytoplasmic COMMD1 and ubiquitin containing aggregates. In conclusion, these data indicate that COMMD1 undergoes constitutive nucleocytoplasmic transport as a novel mechanism to fine-tune the NF-κB pathway.

Introduction

Transcription of a wide variety of genes involved in inflammation, proliferation, immunity and cell survival are regulated by the nuclear factor kappa B (NF-κB) /Rel family of transcriptional activators [184-186]. Members of this family, including RelA (p65), c-Rel, v-Rel, RelB, p52 and p50 exist as homodimers or heterodimers to form active transcriptional complexes known as NF-κB. Under basal conditions, members of the IκB family, including IκB-α, inhibit transcriptional activity by retaining NF-κB in the cytoplasm in an inactive state [187, 188]. Most physiological inducers of NF-κB, such as cytokines, pathogens or various stress factors, operate by engaging the canonical NF-κB activation pathway. In response to activating stimuli, signalling cascades are activated to phosphorylate IκB-α via the IKK complex of proteins, resulting in ubiquitination and degradation of IκB-α by the 26S proteasome. The dissociation of IκB-α from NF-κB unmasks nuclear localization signals (NLSs) present in the Rel homology domains of NF-κB subunits and in IκB-α. This permits translocation of NF-κB to the nucleus and subsequent transcriptional activation of target genes. Thus, the spatiotemporal localization of the NF-κB subunits forms the rate-limiting and critical regulatory mechanism that determines the transcriptional activity of NF-κB target genes.

The export of NF-κB from the nucleus is also highly regulated. Active nucleocytoplasmic transport depends on the interaction of the nuclear export receptor CRM1 (named for 'required for region chromosome maintenance 1') with leucine-rich nuclear export signals (NESs) in proteins and is controlled by the small GTPase Ran. NESs have been identified in the protein sequences of IκB-α and NF-κB subunits [189, 190]. Inhibition of CRM1-dependent nuclear export under basal conditions resulted in accumulation of both IκB-α and NF-κB within the nucleus, indicating that NF-κB constitutively cycles between the cytosol and the nucleus even in resting cells [191]. These findings also suggest that IκB-α does not only function to sequester NF-κB in the cytosol, but also to prevent basal transcriptional activation of NF-κB target genes in the nucleus. Besides IκB-α and NF-κB, various other regulatory proteins of the NF-κB pathway undergo regulated nucleocytoplasmic shuttling. This allows for constitutive transcription of genes involved in essential processes [192, 193]. Together, these data suggest that the regulation of NF-κB is dynamic and highly dependent on the controlled nuclear import and export of important signalling molecules.

Recently, COMMD1 was identified as a novel inhibitor of NF-κB activity [11]. COMMD1 is the first characterized protein within a family of ten COMMD proteins that all share a homologous COMM domain. COMMD proteins are ubiquitously expressed and highly conserved among higher eukaryotes, but the precise functions of these proteins remain elusive. COMMD1 interacts with various other proteins involved in several biological processes including copper metabolism, hypoxia, sodium transport and NF-κB activity

[8, 9, 122, 165-167]. Consistent with this pleiotropic function, COMMD1 is predominantly localized in the cytoplasm, but is also present in the nucleus [11, 46, 166]. Within the NF-κB pathway, COMMD1 interacts with p52/p105, p50/p100, RelA, RelB, c-Rel, IκB-α and with the Cullin E3 ubiquitin ligase complexes that mediate ubiquitination of IκB-α and NF-κB [11, 123, 168]. Increased expression of COMMD1 results in stabilization of IκB-α, possibly via the interaction of COMMD1 with the E3 ubiquitin ligase complex responsible for IκB-α degradation [123]. However, overexpression of COMMD1 does not prevent nuclear import of NF-κB in response to NF-κB activating stimuli [11]. In the nucleus COMMD1 mediates the degradation of NF-κB subunits via the multimeric E3 ubiquitin ligase that contains Elongins, Cul2 and SOCS1 (ECS^{SOCS1}) [168]. This results in an enhanced dissociation of NF-κB from chromatin [11] and repression of κB responsive gene expression. These findings imply that COMMD1 can act as an NF-κB inhibitory molecule that operates both in the cytoplasm to stabilize IκB-α and in the nucleus to control NF-κB stability. In this study, we set out to investigate if nuclear import and export of COMMD1 are regulated processes involved in the modulation of NF-κB activity.

Materials and methods

Constructs

pEBB and pEBB-COMMD1-FLAG were described previously [11]. COMMD1 was subcloned in the pEGFP-N2 (Clontech, Woerden, the Netherlands), pEGFP-C (Clontech) and mCHERRY vector (kindly provided by Dr. R. Tsien). In these constructs COMMD1 NES mutants (Mut1, Mut2, Mut1/2) were generated by site-directed mutagenesis using the oligonucleotides depicted in table 1. The COMMD1 NES double mutant (Mut 1/2) was generated by sequential site-directed mutagenesis with the Mut1 and Mut2 primers.

GFP-NES1-COMMD1, GFP-NES2-COMMD1, GFP-NES-c-terminal-p53 and GFP-NLS-PTEN fusion constructs were generated by annealing the oligonucleotide sets depicted in table 1, which contained flanking restriction enzyme sequences.

For GFP-fusion constructs, 20 μg of sense and antisense oligonucleotides were annealed in 48 μl annealing buffer (100mM potassium acetate, 30 mM HEPES-KOH pH 7.4, 2 mM Mg-acetate) for 4 min at 95°C followed by 10 min 70°C. Annealed oligonucleotides were phosphorylated using PNK (Sigma, Zwijndrecht, the Netherlands), according to the manufacturer's protocol and subsequently ligated into pEGFP-N1 vector (Clontech). HIS-Ub was kindly provided by Dr. B. Burgering (department of physiological chemistry, UMC Utrecht, the Netherlands). The RFP-UB construct is described elsewhere [194].

Table 1 Oligo sequences

oligonucleotide	forward	reverse
Mut1	AAATACACACACCTGTTGCCATTGCAGAGGCG-GAAGCAGGCAAATATGGACAGGAATC	GATTCCTGTCCATATTTGCCTGCTTCCGCCTCTG-CAATGGCAACAGGTGTGTGTATTT
Mut2	GGAATTTGATGAGGTCAAAGTCAACCAAAT-TGCGAAGACGGCGTCAGAGGCAGAAGAAAG-TATCACACACTGA	TCAGTGTGCTGATACTTTCTTCTGCCTCTGACGC-CGTCTTCGCAATTTGGTTGACTTTGACCTCAT-CAAATTCCA
GFP-NES1-COMMD1	AATTCCCACCATGCCTGTTGCCATTATAGAGCT-GGAATTAGGCGCG	GATCCGCGCCTAATTCCAGCTCTATAATGGCAA-CAGGCATGGTGGG
GFP-NES2-COMMD1	AATTCCCACCATGGTCAACCAAATTCTGAA-GACGCTGTCAGAGGTAGAAGCG	GATCCGCTTCTACCTCTGACAGCGTCTTCA-GAATTTGGTTGACCATGGTGGG
GFP-NES-c-terminal-p53	AATTCCCACCATGATGTTCCGAGAGCTGAAT-GAGGCCTTGGAACTCAAGGCG	GATCCGCCTTGAGTTCCAAGGCCTCAT-TCAGCTCTCGGAACATCATGGTGGG
GFP-NLS-PTEN	AATTCCCACCATGCCAAAGAAGAAGAG-GAAGGTGGCG	GATCCGCCACCTTCCTCTTCTTCTTTGGCATG-GTGGG
MGAM	TACCACTCCTGTTTCTGCTGA	ACCAGGGAACACTTACAGCTC
ISG20	TCTACGACACGTCCACTGACA	CTGTTCTGGATGCTCTTGTGC
GAPDH	TCAACGGATTTGGTCGTATTG	TCTCGCTCCTGGAAGATGG

Cell culture, 2κB-firefly luciferase assay

Human embryonic kidney (HEK 293T) cells (ATCC, Rockville, MD, USA) were cultured in DMEM supplemented with 10% heat-inactivated fetal calf serum and 1% penicillin/streptomycin (37˚C in 5% CO_2/air).

For luciferase assays HEK 293T cells were seeded in 24 wells plates and transfected with 62.5 ng 2κB-firefly-luciferase construct (kindly provided by Dr. C. Duckett, University of Michican Medical School, Ann Arbor) and 12.5 ng TK-renilla luciferase construct in combination with either 0.5 µg COMMD1-FLAG pEBB or 0.5 µg pEBB (EV) using calcium phosphate transfection [44, 45]. After 24 hrs, cells were subjected to 500 U/ µl TNF for 12 hrs (Roche applied science, Penzberg, Germany). Cells were lysed and luciferase activity was measured in a luminometer (Berthold, LB 953, Woerden, The Netherlands). Firefly luciferase values were corrected for Renilla luciferase values and were expressed as relative light units (RLU). Statistical significance in luciferase assays was determined by a unpaired t-tests ($p<0.05$)

Quantitative RT-PCR analysis

Gene expression was determined by quantitative reverse transcriptase-polymerase chain reaction (qRT-PCR) with the MyIq cycler (Bio-Rad Laboratories BV, Veenendaal, the Netherlands), using a SYBR Green kit (Ambion, Nieuwekerk a./d IJssel). All qRT-PCR primers were designed to span intron-exon boundaries when possible and the expression levels of GAPDH were used to normalize the data in all conditions (table 1). Linear amplification ranges were determined for all primer sets. All reactions were performed using 1.5 µg total RNA to create cDNA with the superscript first strand synthesis system

(Invitrogen, Leek, the Netherlands) according to the manufacturer's protocol. cDNA was diluted 10-fold and 2 µl was used in each qRT-PCR reaction. Reaction conditions consisted of an initial denaturation step at 92˚C for 2 minutes, followed by 40 cycles of 30 s. denaturation at 92˚C, 1 min. annealing at 60˚C and 30 s. elongation at 72˚C. Specificity of all products was verified both by melting curve analysis and analysis on agarose gels. Results are expressed in relative arbitrary units as fold changes in mRNA expression level and as means ± SD. Differences between means were statistically assessed by a Student's t test in which the limit of statistical significance was set at $p< 0.05$.

Immunoblot analysis and cellular fractionation

HEK293T cells were seeded one day prior to transfection in 10 cm dishes. Cells were transfected with 1.5 µg DNA, using a standard calcium phosphate procedure [45] and were harvested at 70-90% confluence the next day.

For detection of the expression of COMMD1-WT and the COMMD1 NES mutants, cells were scraped in phosphate buffered saline (PBS), rinsed twice with PBS and lysed in lysis buffer, containing Triton X-100 [46]. Preparation of nuclear and cytosolic fractions was performed as described elsewhere [11].

Immunoblotting was performed using anti-Flag antibodies (Sigma), anti-Tubulin-alpha (Sigma), anti-COMMD1 [46] and anti-lamin A (Genetex, San Antonio, TX, USA) as previously described [46].

Direct Ubiquitination assay

HEK293T cells were seeded one day prior to transfection in 10 cm dishes. Cells were transfected with 3 µg DNA construct and 1.5 µg His-Ub cDNA using a standard calcium phosphate procedure [45]. 16 hrs post–transfection, cells were incubated with 5 µM MG132 (Calbiochem, Breda, the Netherlands) or 5 ng/µl leptomycin B (LB, Sigma) and harvested after 8 hrs in lysis buffer, containing urea [195]. Immunoprecipitation with Ni-NTA-beads (Qiagen, Leusden, the Netherlands) was used to identify ubiquitination as described elsewhere [195].

Immunofluorescence, live cell imaging

For detection of endogenous COMMD1 by indirect immunofluorescence, HEK293T cells were seeded in 24 wells plates on cover slips (Marienfield Bad Mergentheim, Germany), that were coated with 10 % poly-L-lysine (Sigma) for 30 min at 37°C and rinsed twice with PBS. After 24 hrs recovery, cells were incubated with 5 ng/µl LB, 500 U/µl Tumor necrosis factor (TNF, Sigma) for 4 hrs. Cells were fixed in 3.7 % paraformaldehyde [46] and incubated with anti-COMMD1 (1:400) [46] or anti-lamin A antibodies (GeneTex) (1:250). As secondary antibodies Alexa Fluor 488-conjugated donkey anti-rabbit-IgG (H+L) (Invitrogen) (1:500) for anti-COMMD1 and Alexa 563-conjugated donkey anti-mouse-IgG

(H+L) (Invitrogen) (1:500) for Lamin A was used. The cover slips were mounted with FluorSave reagent (Calbiochem) and images were analyzed on a confocal laserscanning microscope (Nicon Eclipse E600, Kawasaki, Japan).

The localization of overexpressed COMMD1 was determined by confocal immune fluorescence microscopy or live cell imaging in HEK293T cells. The cells were seeded one day prior to transfection in either 24 wells plates or 6 wells plates on coated coverslips. The next day, cells were incubated with 5 ng/µl LB or 500 U/µl TNF for 4 hrs. For immune fluorescence, cells were fixed in 3.7 % paraformaldehyde, incubated with the molecular probe TO-PRO 3 (1:1000, invitrogen) and analyzed for COMMD1 localization. For live cell imaging, the coverslips were attached in a heated chamber prior to the addition of LB to analyze COMMD1 localization in time. Images were optained using a confocal microscope (Leica TCS-SP2 confocal microscope with heated chamber for coverslips) using a 63X objective.

Results

COMMD1 contains nuclear export signals (NESs)

Many proteins involved in NF-κB signalling shuttle between the nucleus and the cytoplasm and thereby affect NF-κB activity [189-192]. The localization of these proteins is mainly determined by the presence of nuclear localization signals (NLSs) or nuclear export signals (NESs) in their amino acid sequences. As COMMD1 could be detected in the nucleus and in the cytosol [11, 46, 166], we searched the amino acid sequence of COMMD1 for potential NLSs or NESs. Based on the NES consensus sequence of $LX_{1-3}LX_{2-3}LX_{1-2}L$ in which L indicates the hydrophobic amino acids I, L, V, F or M (indicated by arrows) and X indicates any amino acid [196, 197], we identified two putative NESs (figure 1A) in the COMM domain of COMMD1. The N-terminal NES and the C-terminal NES were designated NES1 and NES2, respectively. The important hydrophobic amino acids in these domains were highly conserved among species (data not shown) and to a lesser extent in the COMM domains of other COMMD proteins (figure 1B) [11]. This high degree of conservation illustrates the importance of these amino acid residues in COMMD protein function. Nuclear export of NES containing proteins is dependent on the CRM1 nuclear export receptor, located on the nuclear envelope. We blocked CRM1 activity using leptomycin B (LB) and investigated the localization of endogenous COMMD1 by indirect immune fluorescence in HEK293T cells (figure 1C). COMMD1 was mainly detected in punctuate structures throughout the cytosol [11, 46, 166]. LB-treatment resulted in a marked and rapid accumulation of endogenous COMMD1 in the nucleus. To confirm these results, HEK293T cells were fractionated in nuclear and cytosolic fractions

and analyzed by anti-COMMD1 immunoblotting (figure 1D). In addition, GFP-COMMD1 localization was monitored by live cell imaging (figure 1E).

Although the localization of exogenously expressed COMMD1 appeared somewhat more diffuse compared to endogenous COMMD1 , in both of these experiments cells accumulated COMMD1 in the nucleus following LB-treatment. These data suggest that COMMD1 undergoes constitutive nucleocytoplasmic recycling. Although the degree of nuclear COMMD1 expression under normal conditions varied somewhat amongst different cell types, all tested cell lines (HEK293T, HepG2, CaCo2, Hep3B and MeLJuso cells) displayed nuclear accumulation of COMMD1 in response to LB-treatment (data not shown). Furthermore, LB-treatment resulted in nuclear accumulation of COMMD1 fused to the N-terminus or the C-terminus of GFP or to other epitope tags (FLAG and mCHERRY; data not shown).

NES2 is most important in nuclear export of COMMD1

To further establish the functionality of these NESs in COMMD1, we generated NES mutants in which critical hydrophobic amino acid residues were replaced by alanine residues (figure 2A). In this way we created constructs encoding COMMD1 in which NES1 and NES2 were individually mutated (Mut1; Mut2) and a construct in which both NESs were mutated (Mut1/2). The subcellular localization of GFP-tagged COMMD1 was determined by direct fluorescence microscopy (figure 2B) and the localization of FLAG-tagged COMMD1 was determined by cell fractionation and subsequent anti-FLAG immunoblotting (figure 2C). Compared to COMMD1- wildtype (WT), all three COMMD1-NES mutants exhibited a strongly increased nuclear localization, but were not completely retained within the nucleus. These data indicated that the identified NESs in COMMD1 indeed played functional and partly redundant roles in CRM1-mediated nuclear export.

To investigate if the NESs in COMMD1 were sufficient to induce nuclear export, we fused these domains to a heterologous protein (GFP) and examined the localization of these GFP-fusion proteins (figure 3). The normal localization of GFP was both nuclear and cytosolic and LB-treatment did not change this localization (figure 3A). Previously, a functional NLS was demonstrated in PTEN [198] and a functional NES in p53 [199]. A GFP fusion protein containing the NES of p53 was largely excluded from the nucleus in the absence of LB, but exhibited increased nuclear expression in the presence of LB (figure 3B). In contrast, GFP fused to the NLS of PTEN was predominantly localized in the nucleus irrespective of LB-treatment (figure 3C). These experiments revealed that the localization of GFP was modified by fusion to a known NES or NLS and thus established the validity of this approach (figure 3A-C). Compared to GFP-COMMD1 (figure 3D), GFP-NES 2-COMMD1 (data not shown), GFP-NES1/2-COMMD1 (figure 3E) and to a lesser extent GFP-NES1-COMMD1 (data not shown) were predominantly localized in the cytoplasm. In response to LB-treatment, GFP-COMMD1 and the GFP-COMMD1 NES fusion proteins

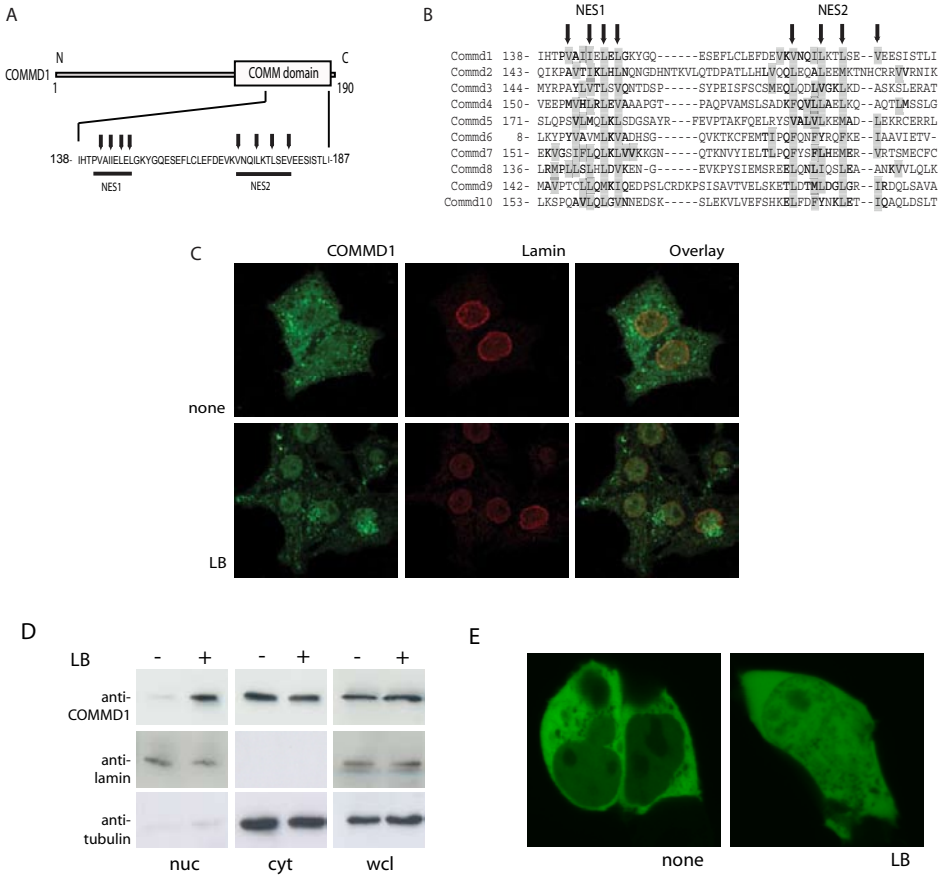

Figure 1 COMMD1 contains conserved NESs

A. In the COMM domain of COMMD1 two potential NESs were identified based on the consensus amino acid NES sequence of $LX_{1-3}LX_{2-3}LX_{1-2}L$ in which L indicates the hydrophobic amino acids I, L, V, F or M (indicated by arrows) and X indicates any amino acid. N indicates the aminoterminus and C indicates the carboxyterminus B. COMMD proteins were aligned and several hydrophobic amino acids were conserved among COMMD family members, indicated in gray in the alignment. C. In HEK293T cells, the localization of endogenous COMMD1 in the absence and in the presence of 4 hrs 5ng/μl LB (leptomycin B) incubation was determined by indirect immunofluorescence with antibodies directed against endogenous COMMD1. Antibodies directed against Lamin A were used as a control to locate the nuclear envelope (middle panel) and the overlay of COMMD1 and lamin staining is depicted in the right panel. D. In HEK293T cells, the localization of endogenous COMMD1 in the absence and in the presence of LB was determined by cell fractionation followed by immunoblotting with antibodies directed against endogenous COMMD1. The protein expression of lamin A and tubulin were used as loading controls and markers for nuclear and cytosolic fractions (D) nuc indicates nuclear fractions, cyt indicates cytosolic fractions and wcl indicates whole cell lysates. E. The localization of GFP-COMMD1 in 293T cells was determined 24 hrs post-transfection by live cell imaging in the presence and in the absence of a 4 hr-LB treatment.

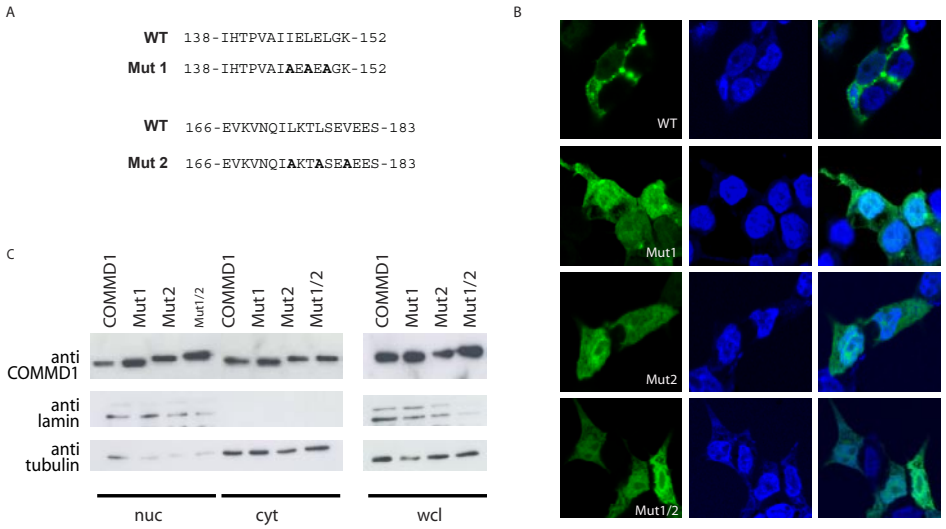

Figure 2 Two NESs in COMMD1 are involved in nuclear export

A. Using site directed mutagenesis, important amino acids in the NESs of COMMD1 were substituted by alanines, indicated in **Bold**. B. HEK293T cells were transfected with GFP-COMMD1 (WT), GFP-NES1-COMMD1 (Mut1), GFP-NES2-COMMD1 (Mut2), GFP-NES1/2-COMMD1 (Mut1/2). The localization of the NES mutants was determined by direct immunofluorescence in which the DNA was counterstained by TOPRO staining, indicating the nucleus. C. The localization of FLAG-COMMD1 (WT), FLAG- Mut1-COMMD1 (Mut1), FLAG-Mut2-COMMD1 (Mut2) and FLAG-Mut1/2 -COMMD1 (Mut1/2) was determined by cell fractionation and immunoblotting of nuclear, cytosolic and total cell lysates. Lamin A and Tubulin expression were used as markers and loading controls for the nuclear and cytosolic lysates, respectively.) nuc indicates nuclear fractions, cyt indicates cytosolic fractions and wcl indicates whole cell lysates

partially accumulated in the nucleus (figure 3B, D, E, F, G). The contribution of NES2 to nuclear export of COMMD1 was consistently higher than that of NES1.

Next, we simultaneously transfected cells with constructs encoding mCHERRY-COMMD1-WT and GFP-COMMD1-Mut1/2 to compare the localization of these fusion proteins within single cells. As a control, the expression of mCherry-COMMD1-WT was compared to GFP-COMMD1-WT. These latter fusion proteins perfectly colocalized in the absence and in the presence of LB (figure 4A). In the absence of LB, mCherry-COMMD1-WT predominantly localized within the cytosol, whereas GFP-COMMD1-MT1/2 was also expressed in the nucleus, as can be appreciated from the green nuclei in the overlay image (figure 4B, upper panel). In the presence of LB, colocalization between COMMD1-WT and the double mutant in the nucleus was almost completely restored (figure 4B lower panel). Together, these data indicate that within single cells, the absence of functional NESs lead to aberrant COMMD1 localization and reveal that the NESs of COMMD1 were necessary and sufficient to induce maximal nuclear export of COMMD1.

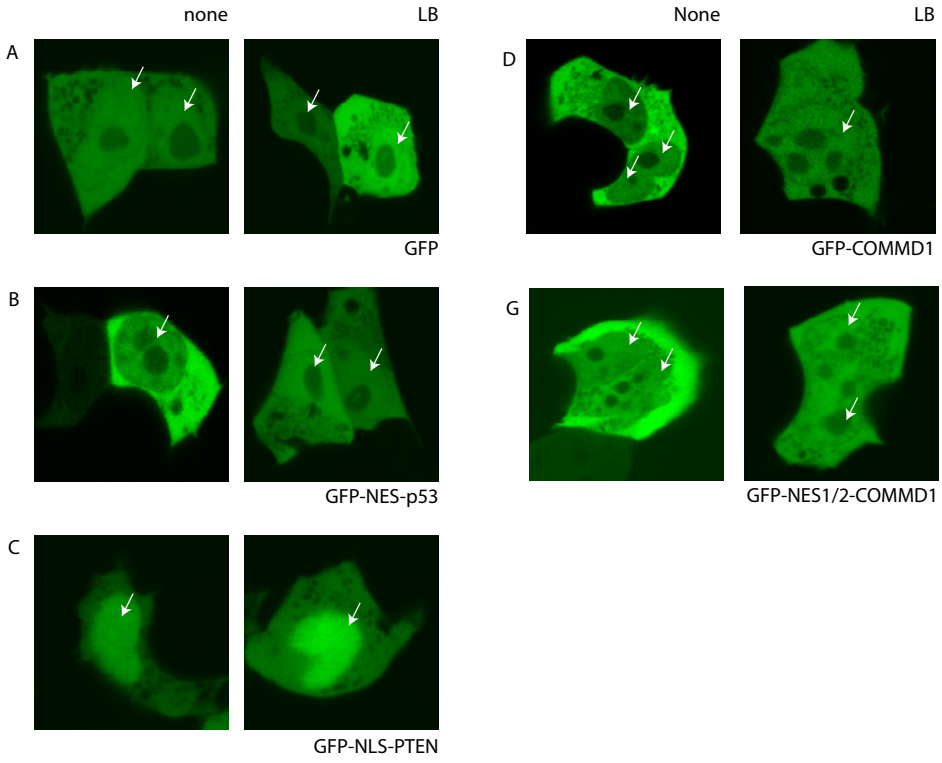

Figure 3 The second NES in COMMD1 is mainly important for nuclear export
HEK293T cells were transfected with GFP, COMMD1-WT fused to GFP (COMMD1-GFP), a combination of NES1 and NES2 fused to GFP (GFP-NES1/2-COMMD1), a NES of p53 fused to GFP (GFP-NES-p53) or a NLS of PTEN (GFP-NLS-PTEN). Cells were incubated with LB 24 hrs post-transfection and the localization was determined by live cell imaging. Arrows indicate the nucleus

The NF-κB inhibitory activity of COMMD1 is enhanced by increased nuclear expression of COMMD1 due to NES mutations

Next, we set out to investigate if the subcellular localization might affect the regulatory role of COMMD1 in NF-κB signalling. As COMMD1 is a rather small protein (21 kDa), we initially excluded the interference of an epitope tag on the inhibitory role of COMMD1 in the NF-κB pathway using 2κB-firefly-luciferase reporter assays. Untagged COMMD1 and COMMD1 tagged with different epitopes (FLAG, GFP, mCherry) inhibited NF-κB activity to a similar extent (Figure 5A) and therefore FLAG-tagged COMMD1 was used in experiments in which we determined NF-κB activity. To assess whether mutations in the NESs would affect the NF-κB inhibitory activity of COMMD1, FLAG-COMMD1 WT and the single and double NES mutants were expressed at equal levels (figure 5C). Cells were cultured in the presence or in the absence of TNF and 2κB-dependent luciferase activity was measured, In the absence of TNF, COMMD1-WT and all three NES mutants clearly inhibited NF-κB activity (figure 5B). In the presence of TNF, expression of COMMD1-WT

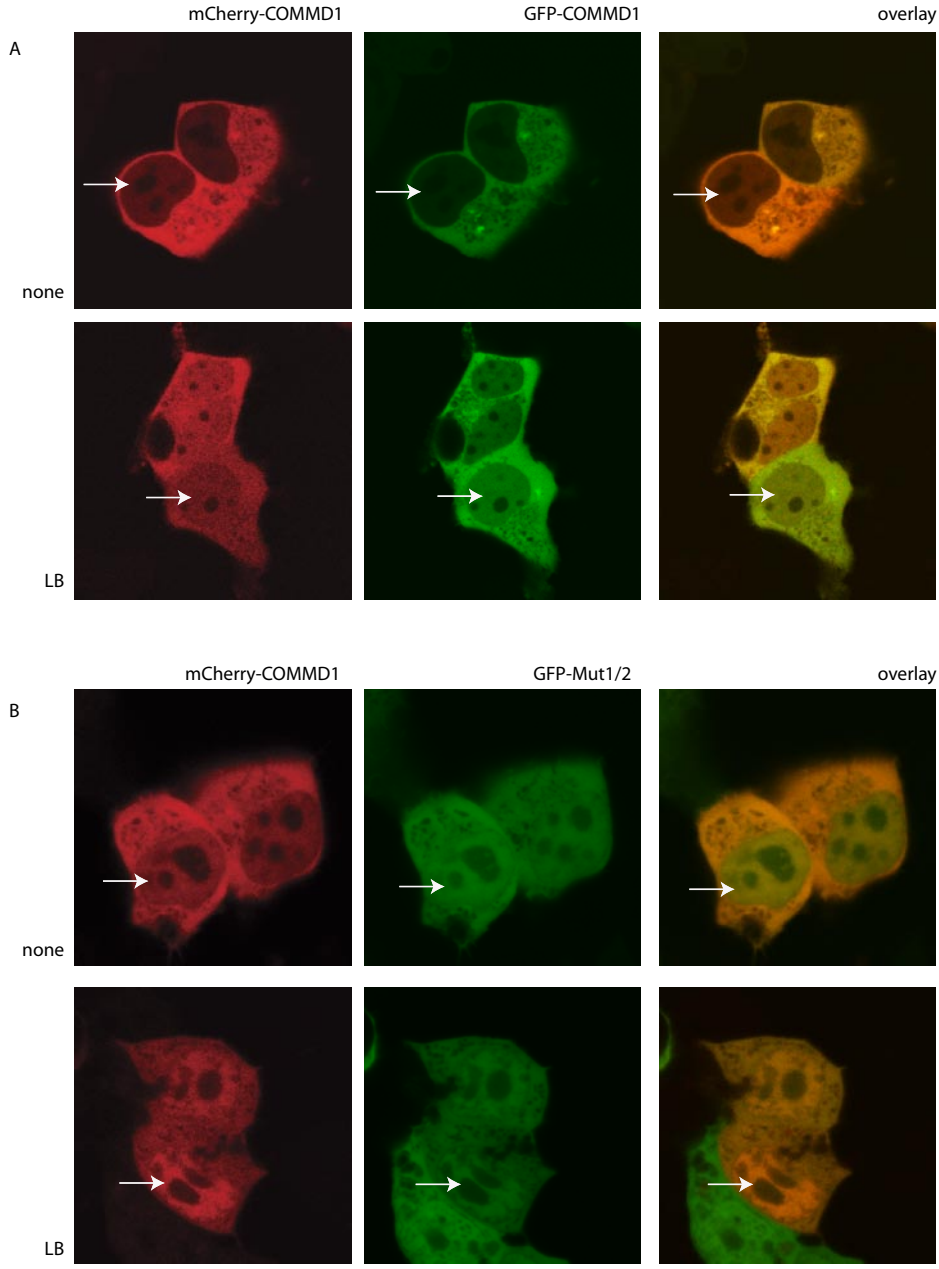

Figure 4 The COMMD1 NES mutants are irresponsive to LB exposure
A/B. The localization of COMMD1 and the COMMD1 NES double mutant was simultaneously investigated in individual HEK293T cells that were transfected with constructs encoding mCHERRY-COMMD1- WT (mCHERRY-COMMD1, red) in combination with GFP-COMMD1- WT (GFP-COMMD1, green) (A) as control or COMMD1-GFP-NES double mutant (GFP-COMMD1-Mut1/2, green) (B). 24 hrs post-transfection, the cells were incubated with LB where after the localization was determined by confocal live cell imaging microscopy. An overlay of the red and green channel is depicted in the right panels and arrows indicate the nucleus.

inhibited the NF-κB reporter approximately to 40%, similarly as described by Burstein *et al* [11]. Expression of Mut2 and Mut1/2 further significantly decreased NF-κB reporter activity approximately threefold compared to COMMD1-WT. These data suggest that nuclear accumulation of COMMD1 due to impaired nuclear export of COMMD1 resulted in an enhanced inhibition of NF-κB activity.

We wondered whether endogenous NF-κB target genes were similarly affected by expressing COMMD1-WT or the NES mutants. Previously, we performed genome-wide differential gene expression analysis in HEK293T cell that overexpressed COMMD1 and identified several downregulated genes of which some contained NF-κB binding sites in their upstream promoter sequences (PM and LK, unpublished results). The effects of COMMD1-WT or COMMD1 NES mutants on the expression of two of these genes, *ISG20* and *MGAM* were examined (figure 5D and 5E). Clearly, the mRNA expression of *ISG20* and *MGAM* was inhibited in a similar way as the NF-κB reporter construct.

Nuclear export of COMMD1 precedes COMMD1 ubiquitination and aggregate formation

Many transcriptional repressors, including p53 and p21 (Cip1), are transported into the cytosol via CRM1-mediated nuclear export followed by polyubiqutination and proteasomal degradation of these proteins [200, 201]. Previously, Burstein *et al* demonstrated that COMMD1 can undergo polyubiquitination and subsequent degradation under basal conditions [121]. The possible relation between nuclear export and polyubiquitination of COMMD1 was therefore investigated. The ubiquitination of COMMD1 was determined after incubation with TNF (8 hrs), LB and MG132 and compared to basal COMMD1 ubiquitination by a direct ubiquitination assay (figure 6A). Under basal conditions, monoubiquinated and polyubiquitinated COMMD1 species were readily detected. In contrast, LB-treatment strongly diminished polyubiquitination of COMMD1. These data suggest that nuclear export of COMMD1 precedes COMMD1 polyubiquitination. As expected, incubation with the proteasome inhibitor MG132 resulted in an increase in ubiquitinated COMMD1 species. Surprisingly, ubiquitination of COMMD1 was enhanced to a similar extent after TNF treatment. As it was previously shown that TNF incubation resulted in a moderate increase in nuclear expression of COMMD1 [11], we investigated the ubiquitination of COMMD1 after TNF or MG132 treatment when nuclear export was blocked by LB treatment. The combined incubation of LB with MG132 or TNF completely blocked COMMD1 polyubiquitination and strongly inhibited COMMD1 monoubiquitination compared to MG132 or TNF incubation alone (figure 6B).

Interestingly, we noticed that prolonged incubation with TNF for 12 hrs induced massive formation of perinuclear aggregates that colocalized with RFP-UB (figure 6C) The observation that both MG132 and TNF treatment resulted in polyubiquitination of COMMD1 provoked the question whether incubation with MG132 would affect the

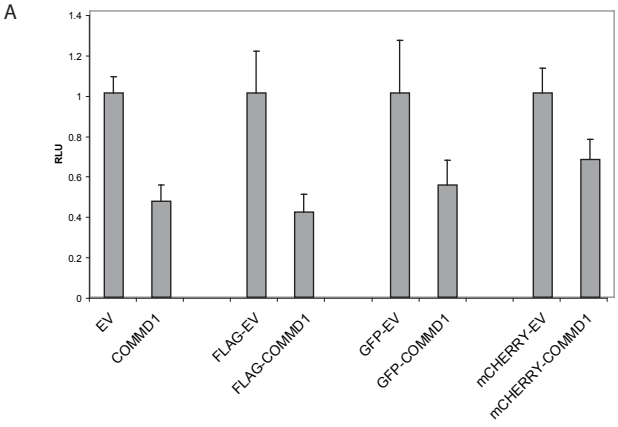
A
RLU
EV
COMMD1
FLAG-EV
FLAG-COMMD1
GFP-EV
GFP-COMMD1
mCHERRY-EV
mCHERRY-COMMD1

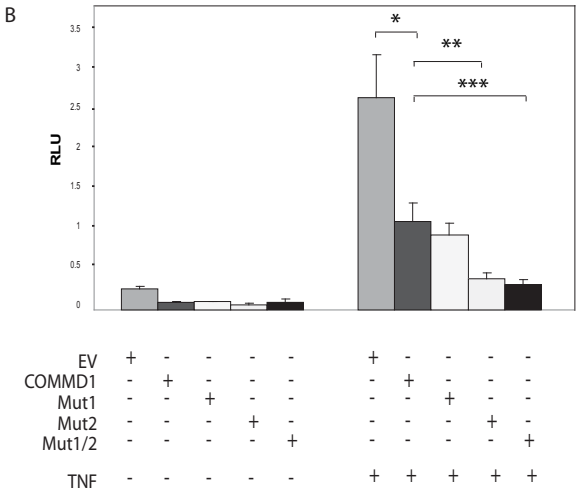
B
RLU
*
**
***
EV
COMMD1
Mut1
Mut2
Mut1/2
TNF

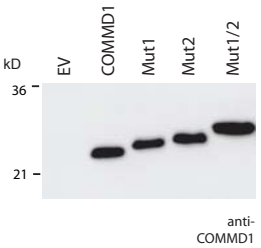
C
kD
EV
COMMD1
Mut1
Mut2
Mut1/2
36
21
anti-
COMMD1

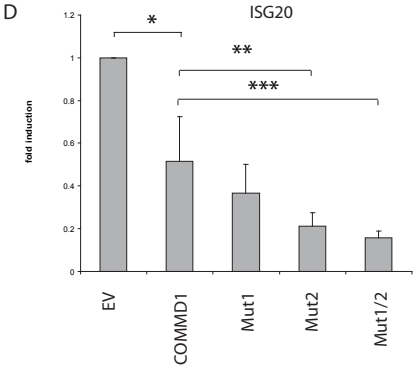
D
ISG20
fold induction
*
**
***
EV
COMMD1
Mut1
Mut2
Mut1/2

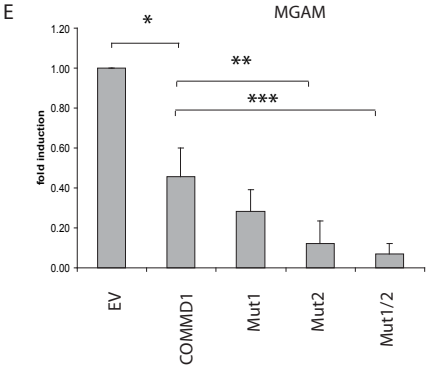
E
MGAM
fold induction
*
**
***
EV
COMMD1
Mut1
Mut2
Mut1/2

cellular localization of COMMD1. MG132 treatment resulted in a strikingly extensive, rapid and time-dependent accumulation of COMMD1-WT in the nucleus (figure 6D and data not shown). This MG132-dependent nuclear accumulation was reversible, since the nucleus became readily depleted of COMMD1 within a 3 hours after washing away MG132 (figure 6D). This process could be inhibited by LB-treatment, indicating active CRM1-mediated nuclear export (data not shown).

In addition to nucleocytoplasmic transport, disinhibition of the proteasome triggered massive aggregate formation of COMMD1 in perinuclear regions, indicated by arrowheads in figure 6D. Aggregate formation after MG132-withdrawal was observed when COMMD1-WT was expressed, but Mut1/2 was not detected in aggregates. This was most clearly demonstrated in co-expression experiments and indicated that aggregate formation was not the result of an overexpression artefact. HEK293T cells were co-transfected with constructs encoding mCHERRY-COMMD1-WT in combination with GFP-COMMD1-WT (Figure 6D), GFP -COMMD1-NES1 (data not shown), GFP -COMMD1-NES2 (data not shown) or GFP-COMMD1-NES1/2 (Figure 6D). Cells were subsequently treated with MG132 for 3 hr, followed by MG132 withdrawal. As a control, GFP-COMMD1-WT and mCHERRY-COMMD1-WT were perfectly colocalized in perinuclear aggregates. In contrast, these results demonstrated the complete absence of COMMD1 NES-mutants in cytoplasmic aggregates (figure 6D, right panels and data not shown). Collectively, these data suggest that the markedly increased polyubiquitination of COMMD1, detected in the presence of TNF, represents COMMD1 that has been exported out of the nucleus accumulate in aggregates. This implies that nuclear export of COMMD1 is a prerequisite for COMMD1 polyubiquitination and aggregate formation.

Figure 5 The NF-κB inhibitory activity of COMMD1 is enhanced by NES mutations
A. HEK293T cells were transfected with pEBB (EV), COMMD1-WT (WT), FLAG-pEBB (EV), FLAG-COMMD1-WT (FLAG-COMMD1), GFP (GFP-EV), GFP-COMMD1-WT (GFP-COMMD1), mCherry (mCherry-EV), mCherry-COMMD1-WT (mCherry-COMMD1) in combination with a 2κB-firefly luciferase reporter construct and a TK-renilla luciferase construct as transfection control. Cells were incubated for 16 hrs with TNF and luciferase was measured 24 hrs post-transfection in a luminometer. The NF-κB activity is depicted as RLUs (relative light units) that are corrected for renilla luciferase activity. Results are representative of three independent experiments performed in triplicate and error bars indicate standard deviations. B. HEK293T cells were transfected with pEBB (EV), FLAG -COMMD1-WT (WT), FLAG- Mut1-COMMD1 (Mut1), FLAG- Mut2-COMMD1 (Mut2) and FLAG-Mut1/2 -COMMD1 (Mut1/2) in combination with a 2κB-firefly luciferase reporter construct and a TK-renilla luciferase construct. Eight hrs post-transfection, cells were incubated with 500 Units/ ml TNF for 16 hrs and luciferase activity was measured in a luminometer. Results are representative of three independent experiments performed in triplicate and error bars indicate standard deviation. Asterisks (*) indicate statistically significant differences. C. The expression of COMMD1-WT and the mutants in the luciferase assay of B were verified by immunoblot analysis using anti-FLAG antibodies. The apparent molecular mass is indicated at the right in kDa. D/E. The mRNA expression of two COMMD1 target genes, *ISG20* (C) and *MGAM* (D) was determined by qRT-PCR in HEK293T cells transfected with pEBB (EV), FLAG -COMMD1-WT (WT), FLAG- Mut1-COMMD1 (Mut1), FLAG- Mut2-COMMD1 (Mut2) and FLAG-Mut1/2 -COMMD1 (Mut1/2). Results are representative of three independent biological triplicate experiments and error bars indicate the standard error of the mean. Statistical significance is indicated by an asterisk (*).

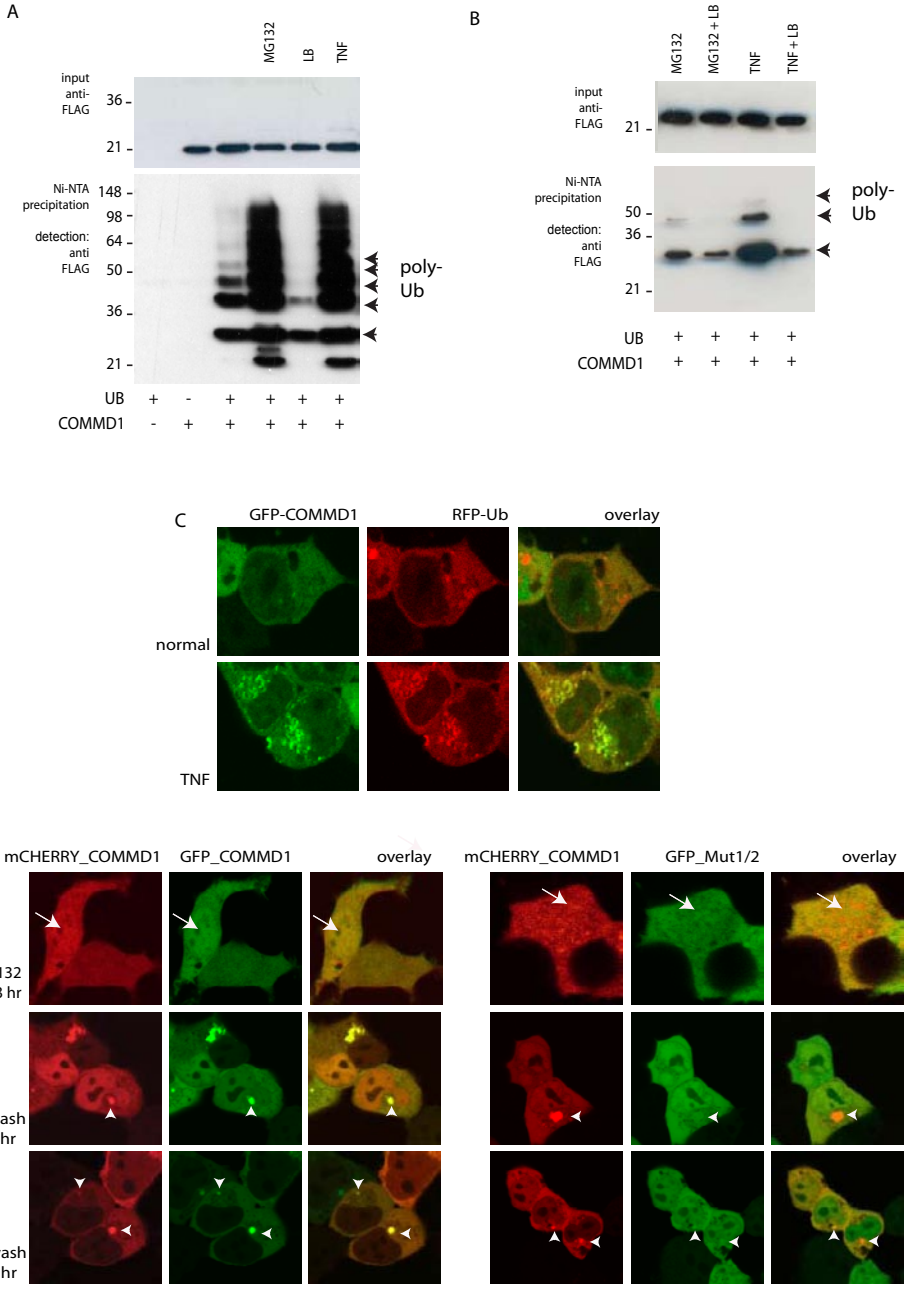
A
MG132
LB
TNF
input anti-FLAG
36
21
Ni-NTA precipitation
detection: anti FLAG
148
98
64
50
36
21
poly-Ub
UB + - + + + +
COMMD1 - + + + + +
B
MG132
MG132 + LB
TNF
TNF + LB
input anti-FLAG
21
Ni-NTA precipitation
detection: anti FLAG
50
36
21
poly-Ub
UB + + + +
COMMD1 + + + +
C
GFP-COMMD1
RFP-Ub
overlay
normal
TNF
D
mCHERRY_COMMD1
GFP_COMMD1
overlay
mCHERRY_COMMD1
GFP_Mut1/2
overlay
MG132 3 hr
wash 1 hr
wash 3 hr

Discussion

Several transcription factors and transcription regulatory proteins contain nuclear export signals, providing a means to rapidly down regulate the nuclear expression of these proteins. Amongst others, this mechanism is operative to fine-tune the NF-κB pathway. Several regulatory proteins within the NF-κB signalling cascade, including IKK proteins, NF-κB subunits and members of the IκB family, all contain NESs [189, 190, 192, 193]. In the present work, we demonstrate that COMMD1, a recently identified inhibitor of NF-κB signalling, also undergoes regulated nuclear export. Nuclear export appears to be linked to the ubiquitination and perinuclear aggregate formation of COMMD1, suggesting that it precedes COMMD1 degradation.

Together, we provide compelling evidence that COMMD1 undergoes constitutive nucleocytoplasmic transport. First, we identified two highly conserved classical NESs in the amino acid sequence of COMMD1. Second, mutation of critical amino acid residues within these NESs resulted in markedly increased nuclear expression of COMMD1, indicating that these NESs appeared necessary to induce nuclear export of COMMD1. Third, fusion of the putative NESs to GFP resulted in decreased nuclear accumulation of the reporter protein, indicating that the NESs are sufficient to induce nuclear export. Finally,

Figure 6 Nuclear export of COMMD1 is linked to ubiquitination and aggregate formation
A. HEK293T cells were transfected with constructs encoding HIS-UB (UB), FLAG-COMMD1-WT (COMMD1) or a combination of HIS-Ub and COMMD1-WT. The cells were incubated for 8 hrs with 5ng/μl LB, 3 μM MG132 (proteasome inhibitor) or 500 U/ml TNF. 36 hrs post-transfection cells were harvested in urea lysis buffer. Two percent of the lysate was used to detect input levels (upper panel A) and Histidine tagged protein complexes were precipated using Nickel-NTA beads. Proteins were separated by 10% SDS-PAGE and immunblotting with anti-FLAG antibodies was used to detect COMMD1-UB complexes in input lysates and precipitates. The molecular mass is indicated at the right in kDa and arrowheads indicate mono- and poly-ubiquitinated COMMD1. B. HEK293T cells were co-transfected with constructs encoding HIS-UB (UB) and FLAG-COMMD1-WT. Cells were incubated for 8 hrs 3 μM MG132 (proteasome inhibitor) or 500 U/ml TNF alone or in combination with 5ng/μl LB. 36 hrs post-transfection, cells were harvested and the ubiquitination of COMMD1 was determined in a ubiquitin assay as described above. Arrows indicate mono and polyubiquitinated COMMD1. In comparison to panel A, the exposure time in B is much shorter to allow better visualization of the LB-mediated inhibition in ubiquitination C. HEK293T cells were transfected with constructs encoding GFP-COMMD1-WT (GFP-COMMD1) in combination with RFP-Ubiquitin (RFP-UB). Cells were incubated with TNF for 12 hrs and the localization of COMMD1 and ubiquitin was determined by live cell imaging. An overlay of GFP-COMMD1 and RFP-UB is depicted in the right panels. D The localization of COMMD1 and the COMMD1 NES double mutant was simultaneously investigated in individual HEK293T cells that were transfected with constructs encoding mCHERRY-COMMD1-WT (mCHERRY-COMMD1, red) in combination with GFP-COMMD1-WT (GFP-COMMD1, green) as control (left panels) or COMMD1-GFP-NES double mutant (GFP-COMMD1-Mut1/2, green) (right panels). 24 hrs post-transfection, the cells were incubated with MG132 for 3 hrs, and the localization of COMMD1 and mut1/2 was determined by confocal live cell imaging microscopy. Subsequently, MG132 was replaced by fresh medium and the localization of COMMD1 and mut1/2 was determined after 1 or 3 hrs as depicted. An overlay of the red and green channel is depicted in the right panels, arrowheads indicate aggregates, arrows indicate the nucleus.

LB treatment, which is known to dissociate NESs from the CRM1-dependent nuclear export machinery, inhibited nuclear export of COMMD1.

A model to explain these findings is depicted in figure 7 and discussed below. COMMD1 is a relatively small 21-kDa protein that could passively diffuse through nuclear pore complexes to enter the nucleus [202]. Under normal conditions, the protein was detectable in the nucleus, but the localization of COMMD1 was predominantly cytoplasmic [11, 46, 166] (figure 1). Examination of the amino acid sequence of COMMD1 indeed failed to identify apparent nuclear localization signals. The nuclear content of COMMD1 increased when cells were treated with inhibitors of proteasomal degradation (this study). Nuclear COMMD1 expression was also somewhat increased after treatment of cells with TNF, a well-known stimulus of the NF-κB pathway [11]. This is an interesting observation, since COMMD1 was previously identified as an inhibitor of NF-κB activity in the nucleus by promoting ubiquitination of RelA by the ECS^{SOCS} complex and by accelerating the dissociation of RelA from κB dependent promoters [11, 168]. We therefore speculate that increased nuclear expression of COMMD1 might enhance the role of COMMD1 in repressing NF-κB activity. Consistent with this hypothesis, mutations of

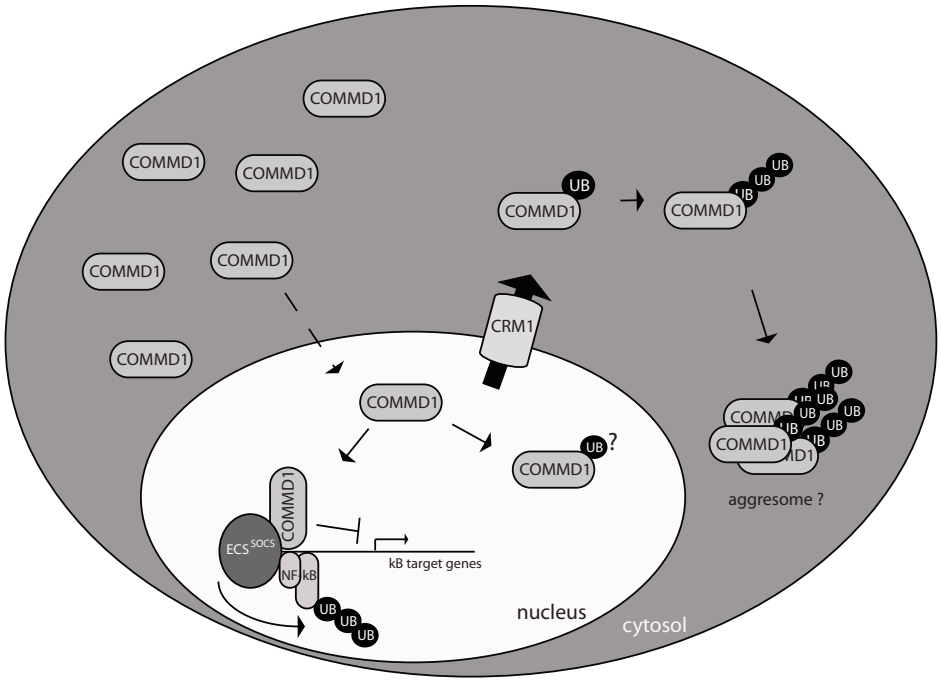

Figure 7 Schematic model of COMMD1 nuclear export and degradation
From our study, we propose a model in which nuclear expression of COMMD1 is maintained at a low level by constitutive CRM1-mediated nuclear export of COMMD1. COMMD1 that is exported out of the nucleus is subsequently or concomitantly ubiquitinated and localized to aggresomes to be degraded. See text for further explanation.

the NESs in COMMD1 resulted in nuclear expression of COMMD1 and a concomitant increased inhibition of NF-κB activity. These findings have important physiological implications, since NF-κB forms a key factor in many cellular processes, most prominently in innate and adaptive immune responses. Since prolonged activation of NF-κB signalling could be harmful for cells and lead to uncontrolled proinflammatory responses, negative feedback mechanisms to control NF-κB activity are crucial and include the induced expression of IκB proteins after TNF stimulation [203]. The nuclear increase in COMMD1 expression could therefore be a novel negative feedback mechanism to provide spatiotemporal control of NF-κB activity. This mechanism may be involved in the abrogation of HIV-1 replication in $CD4^+$ T-cells, since HIV-1 replication is dependent on NF-κB activity and is inhibited by overexpression of COMMD1 [123].

This study also provides information on the fate of COMMD1 after it has been exported from the nucleus. Blocking nuclear export by LB resulted in decreased ubiquitination of COMMD1 and prevention of the formation of cytoplasmic ubiquitin-positive aggregates that function as the proteolytic centre of a cell [204]. Mutations of the NESs in COMMD1 also prohibited the formation of these aggregates, indicating that this effect was not due to a general inhibition of nuclear export, but specific for COMMD1. Our data thus suggest that the nuclear function of COMMD1 in NF-κB signalling is constitutively terminated by regulated export from the nucleus, polyubiquitination and subsequent targeting of COMMD1 to aggresomes.

The molecular details of this newly identified regulation pathway remain to be further elucidated, but initial clues are provided in a parallel submission. Abolishment of the NESs of COMMD1 resulted in decreased interaction with XIAP and a decreased ubiquitination of COMMD1 (Maine *et al*, parallel submission). XIAP has previously been identified as an E3 ubiquitin ligase that interacts with and (poly)ubiquitinates COMMD1 to target the protein for proteasomal degradation [121]. Since XIAP is a cytoplasmic protein [205], we propose that XIAP ubiquitinates COMMD1 that has been exported from the nucleus.

Precedence for the link between nuclear export and ubiquitination is provided by many proteins. As one example, the nuclear expression of the tumor suppressor protein p53 is regulated by the oncoprotein MDM2 [200, 206]. Low levels of MDM2 promote the monoubiquitination of p53, which is subsequently exported to the cytoplasm in a CRM1-dependent fashion and degraded [200]. Similarly, the SUMO-specific protease SENP2 shuttles between the nucleus and the cytoplasm and shuttling is blocked by mutations in its canonical NES or by treatment of cells with LB. Restricting SENP2 in the nucleus by mutations in the NES impairs its polyubiquitination, whereas treating cells with MG132 leads to accumulation of polyubiquitinated SENP2, indicating that SENP2 is degraded through the 26S proteolysis pathway [207]. Finally, CRM1-mediated nuclear export is required for the proteasomal degradation of p21 (CIP1), p27Kip1 and Cyclin D1

[201, 208, 209]. Thus, the function of COMMD1 is regulated both by nucleocytoplasmic transport and polyubiquitin-mediated degradation, similar to a number of other transcriptional regulators.

In conclusion, these data characterize two functional NESs within COMMD1 that limit the role of COMMD1 in repressing NF-κB activity. In addition, nuclear export precedes ubiquitination and aggregate formation of COMMD1. As COMMD1 has been implicated in various other pathways, including hypoxia [167], its subcellular localization might affect HIF-1 activity in a similar fashion as NF-κB activity. Unravelling the precise mechanisms of COMMD1 nucleocytosolic transport will therefore be an important focus of future experiments. Finally, this mechanism may not be limited to COMMD1, since other COMMD proteins are equally effective inhibitors of NF-κB signalling and some of these also contain canonical NESs.

Chapter 7

COMMD1 expression is controlled by critical residues that determine XIAP binding

Gabriel N. Maine[1,2], Patricia A. Muller[3], Christine M. Komarck[1,2], Xicheng Mao[1,2], Leo W. Klomp[3], and Ezra Burstein[1,2,4,*]

Departments of [1]Internal Medicine and [2]Molecular Mechanisms of Disease Program, University of Michigan Medical School, Ann Arbor, Michigan, U.S.A.; [3]Laboratory of Metabolic and Endocrine Diseases, University of Utrecht, Utrecht, The Netherlands; [4]Gastroenterology Section at the Ann Arbor VA Medical Center, Ann Arbor, Michigan, U.S.A.

Submitted

Abstract

COMM domain-containing (or COMMD) proteins participate in several cellular processes, ranging from NF-κB regulation, copper homeostasis, sodium transport and adaptation to hypoxia. The best studied member of this family is COMMD1, but relatively little is known about its regulation, except that XIAP functions as its ubiquitin ligase. In this study, we identified that COMMD1 autoregulates its expression to maintain near physiologic protein levels through adaptive changes in the basal ubiquitination of COMMD1. Given that XIAP is a ubiquitin ligase for COMMD1, we examined the role of XIAP in this phenomenon. To that end, we mapped the interaction with XIAP to the COMM domain of COMMD1 and identified critical residues in this domain required for XIAP binding. A COMMD1 mutant unable to bind to XIAP demonstrated complete loss of basal ubiquitination and great stabilization of the protein. Interestingly, this also abrogated the autoregulatory increase in basal ubiquitination, highlighting that the COMMD1-XIAP interaction is critical for the regulation of COMMD1 expression.

Introduction

COMMD proteins are a group of evolutionarily conserved factors present in a wide range of organisms [11]. All ten members of this family are found in vertebrates and are also present in Dictyostelium discoideum. In addition, several COMMD genes are also identifiable in Drosophila and Caenorhabditis species, as well as in various unicellular protozoa [210]. The defining characteristic of all the members of the family is the presence of a highly conserved and unique domain in the extreme carboxyterminus of these proteins known as the Copper Metabolism MURR1 or COMM domain. The tertiary structure of this domain is not known, but it contains conserved tryptophan and praline residues, as well as a series of conserved leucines.

The COMM domain not only defines the protein family but provides a critical interface for proteinprotein interactions, such as COMMD1-COMMD1 dimer formation and binding to Cul2, Elongin C and SOCS1 [11, 166, 168, 211].

At the present time, a number of seemingly disparate functions have been ascribed to these factors. COMMD1 has been shown to inhibit HIV-1 replication and expression of several proinflammatory mediators through its suppression of NF-κB transcriptional activity [123, 168]. COMMD1 is also known to promote copper excretion, presumably by regulating the copper transporter ATP7B [9, 121, 212]. Indeed, a spontaneous mutation in COMMD1 is responsible for canine copper toxicosis, a disorder that resembles the effects of ATP7B mutations [8, 46]. COMMD1 has been implicated in intracellular sodium regulation through its inhibitory effects on the function of the epithelial sodium channel [122]. Recently, COMMD1 was also found to regulate the adaptation to hypoxia, by serving as an inhibitor of the HIF1α transcription factor [167]. Finally, COMMD5 has been reported to affect cell proliferation and gene expression but the precise targets responsible for these effects are unknown [213-215].

Little is known about the regulation of COMMD proteins themselves. We have previously reported that XIAP, a member of the Inhibitor of Apoptosis (IAP) family, functions as a ubiquitin ligase for COMMD1 [121]. However, the ultimate importance of this interaction in the regulation of COMMD1 protein expression and whether this paradigm is true for other COMMD proteins is not completely understood. In this study we report that basal levels of COMMD1 expression are tightly regulated, and the ability of COMMD1 to bind to XIAP seems to be required for this event. Stable overexpression of COMMD1 over time leads to protein levels than are close to the physiologic range and this process of autoregulation is accompanied by concomitant increase in COMMD1 ubiquitination. We subsequently mapped the interaction between COMMD1 and XIAP to the COMM domain and identified that leucine repeats within the COMM domain are required for this interaction. A mutant version of COMMD1 that cannot bind to XIAP lost any appreciable basal ubiquitination, was greatly stabilized and could be stably overexpressed. The data

collectively indicate that the XIAP-COMMD1 interaction is critical to the regulation of COMMD1 protein levels.

Materials and methods

Plasmids

The plasmids pEBB, pEBG, pEBBCOMMD1-Flag, pEBB-COMMD1-GST, pEBBCOMMD-GST have been previously described [11, 45, 121, 216, 217]. In addition, we utilized pEBBCOMMD1 N-term (amino acids 1-118) and pEBB COMMD1 COMM domain (amino acids 119-190) [168]. The plasmids pEBB-COMMD1 W/P (W124A, P141A), Mut1 (I145A, L147A, L149A), Mut2 (L172A, L175A, V178A) and Mut1/2 were generated by site directed mutagenesis. The expression vectors pEBB-XIAP, pEBB-Flag-XIAP pEBG-XIAP, pEBB-XIAP H467A and pEBG-XIAP H467A have been previously described [121]; pEBB Flag c-IAP1 H588A and pEBB Flag c-IAP2 H574A were kindly provided by Dr. Colin Duckett. The plasmid pCW7-His6-Myc-Ubiquitin was previously described [218].

Cell culture and transfection.

Human embryonic kidney 293 and 293T cells were obtained from ATCC. Those cell lines were cultured in DMEM supplemented with 10% FBS and L-glutamine. Treatment with the proteasome inhibitor MG-132 (Boston Biochem) consisted of culturing cells for 3 hour in media containing a 40 μM concentration of the drug (or the vehicle DMSO as a control). A standard calcium phosphate transfection protocol [45] was used to transfect plasmids into 293 and 293T cells. Generation of stable lines was performed after lentiviral infection and selection using the transient transfection of the pBABEPuro plasmid and the corresponding expression vector in a ratio of 1:5. Cells were then placed under Puromycin selection for 6 weeks. Hep3B cells were obtained from the ECACC (European collection of cell cultures) and cultured in high glucose DMEM supplemented with 10% FBS, Lglutamine, and 1% pen/strep. FLAG-COMMD1 and pBABE-Puro plasmids were co-transfected into Hep3B cells with lipofectamin at a ratio of 1:10. Upon reaching confluence, cells were split for colony growth under puromycin selection. After 1 week (293T cells) or 1.5 weeks (Hep3B) >20 colonies were picked and tested for COMMD1 expression levels.

RT-PCR

Total RNA was extracted from 293 cells using the RNeasy procedure (Qiagen) according to the manufacturer's instructions. Yield and purity was determined by measuring OD260/280 of RNA diluted in water. Quantitative RT-PCR of *COMMD1* utilizing Taqman probes has been previously described [11]. Quantitative RT-PCR for total and endog-

enous COMMD1 mRNA was performed with Sybr-Green based detection using primers located in the transcripts as indicated in Figure 1C: (1) GGACACTTTCCACGGGTAC, (2) ATCCATGTCTGCAGACGCAA, (3) TGTTGCCATTATAGAGCTGG, and (4)CTTAGAAAAGGTCAGTGGGG.

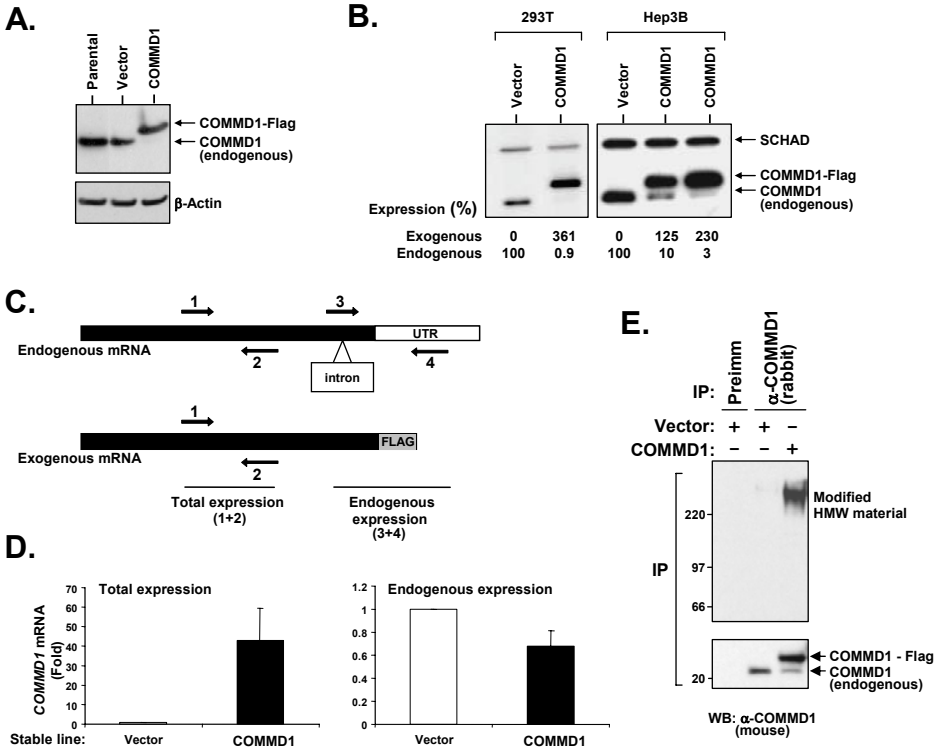

Figure 1 COMMD1 autoregulation is dictated by its ubiquitination.
(A) Stable overexpression of COMMD1 leads to near physiologic expression. A polyclonal populationof HEK 293 cells stably expressing COMMD1-Flag was generated. Lysates from the parentalline, the vector control and COMMD1-stable lines were subsequently prepared for COMMD1and β-Actin detection by immunoblotting. (B) COMMD1-Flag overexpression is associatedwith proportional suppression of endogenous COMMD1. Stable lines were generated as before in 293T and Hep3B cells. Single clones were isolated by limiting dilution and cell lysates were subsequently prepared for COMMD1 and SCHAD detection by immunoblotting. Relative protein levels were determined by densitometry. (C) RT-PCR detection strategy. Relative positions of oligonucleotides that recognize both endogenous and exogenous mRNA for COMMD1 are indicated. (D) Autoregulation is not associated with decreased endogenous mRNA expression. Utilizing the strategy depicted in (C), total and endogenous COMMD1 mRNA expression was determined by quantitative real-time RT-PCR. (E) overexpression results in the accumulation of high molecular weight modified COMMD1. Cell lysates prepared from stable lines and subjected to denatured immunoprecipitation with a preimmune serum or a COMMD1 specific rabbit antiserum. The precipitated material was subsequently resolved by SDS-PAGE and immunoblotted for COMMD1 with a mouse monoclonal antibody against COMMD1. Non-modified COMMD1 was detected in the lower part of the gel (bottom panel), whereas modified high molecular weight (HMW) material that is immunoreactive with this antibody was detected in the upper part of the gel (upper panel).

Immunoblotting and immunoprecipitation

Cell lysates were prepared by adding Triton lysis buffer [121]; immunoblotting and GSH precipitations were performed as previously described [121]. Denaturing immunoprecipitations were perfomed after boiling cell lysates for 10 minutes in a buffer containing 1% SDS, as previously described [168]. Antibodies against β-Actin (Sigma, A5441), COMMD1 [11, 46](Abnova, H00150684-M01), Flag (Sigma, A8592), GST (Santa Cruz, sc-459), SCHAD [46], Ubiquitin (Stressgen, SPA-205), and XIAP (BD Pharmingen, 610716) were used as indicated.

In vivo ubiquitination

293 cells were transfected with His6-Ubiquitin along with the indicated plasmids in each experiment. 48 hours later, the cells were lysed with a protein denaturing buffer (8M urea, 50mM Tris, pH 8.0, 300mM NaCl, 50 mM NaPO4, 0.5% NP-40). The lysate was sonicated for 20 seconds, and centrifuged to obtain a cleared lysate. This was applied to Ni-NTAAgarose beads (Invitrogen) and rocked at room temperature for 2 hours. The lysate was subsequently aspirated, and the beads washed 4 times in the same buffer at room temperature. The recovered ubiquitinated material was then resuspended in LDS gel loading buffer (Invitrogen) and separated by SDS-PAGE for subsequent immunoblotting.

Results

Stable expression of COMMD1 leads to near physiologic protein levels

In order to examine the effects of COMMD1 on gene expression, we attempted to generate cell lines that stably overexpress this protein through plasmid transfection or lentiviral infection. In either case, the polyclonal cell populations generated at the end of selection did not demonstrate significant overexpression at the protein level. In addition, expression of the endogenous protein was concomitantly suppressed such that the total levels of COMMD1 expression closely resembled those of the parental or vector transfected lines (Figure 1A). This observation was corroborated in other cell lines. Furthermore, derivation of monoclonal stable cell lines indicated that the level of suppression of endogenous COMMD1 expression correlated with the level of exogenously expressed protein (Figure 1B).

Autoregulation is the result of increased ubiquitination

In the stable cell lines generated, expression of endogenous and exogenous *COMMD1* was under the control of different promoters and UTR elements. Therefore, we reasoned that transcriptional mechanisms were unlikely to account for the reduction of

endogenous *COMMD1* expression and the concomitant near physiologic levels of exogenous *COMMD1* expression. To examine this notion, we devised a strategy to measure *COMMD1* mRNA levels resulting from transcription of the endogenous gene or the total expression resulting from transcription of both the endogenous and exogenous genes (Figure 1C). This approach demonstrated that the total levels of *COMMD1* transcripts were elevated by nearly 50-fold in the COMMD1 stable cell line, despite the fact that COMMD1 protein levels were similar to the control line. Importantly, mRNA expression of endogenous *COMMD1* was nearly identical to the vector control line, despite the fact that the endogenous protein was almost undetectable. These findings suggested that the regulation of COMMD1 protein levels might be mediated by a post-transcriptional mechanism. We have previously described that COMMD1 levels are regulated by ubiquitination and proteasomal degradation and therefore we explored the role of this process in the autoregulation of COMMD1.To that end, COMMD1 was immunoprecipitated from vector control or COMMD1 stable cell lines with a rabbit polyclonal antibody and the recovered material was immunoblotted with a mouse monoclonal antibody against COMMD1. Unmodified COMMD1 was recovered after immunoprecipitation with the rabbit antibody, but not the preimmune serum control (Figure 1E, bottom panel). In addition, significant amounts of modified high molecular weight COMMD1 was recovered only from the COMMD1 stable cell line and not the control line (Figure 1E, top panel). The identity of the modified form of COMMD1 is consistent with ubiquitinated COMMD1 and further confirmation that this high molecular

weight material corresponds to ubiquitinated COMMD1 is provided in later experiments (see below, Figure 5). This finding is consistent with the notion that increased ubiquitination of the protein might be responsible for maintaining COMMD1 levels near the physiologic range. The COMM domain mediates IAP binding We have previously reported that COMMD1 ubiquitination is regulated by XIAP, a RING domain containing member of the Inhibitor of Apoptosis family [219]. While XIAP is well recognized as a pro-survival factor, it is also an E3 ubiquitin ligase for several factors including COMMD1 [121, 220-222]. Therefore, we postulated that COMMD1-XIAP interactions might be important to mediate autoregulation. To test this possibility we first determined the domain in COMMD1 required for this interaction. The amino terminus (amino acids 1-118) or the COMM domain (amino acids 119-190) of COMMD1 were expressed in 293 cells in fusion with glutathione S-transferase (GST). The expressed proteins were subsequently precipitated from cell lysates with glutathione (GSH) sepharose beads. The presence of co-precipitated XIAP was determined by immunoblotting. As can be seen in Figure 2A, the COMM domain was necessary and sufficient for XIAP binding and proteasomal blockade enhanced the COMMD1-XIAP interaction, as previously described [121]. The identification of the COMM domain as the binding interface in the COMMD1-XIAP interaction suggested that other COMM-domain containing proteins might interact with

XIAP or other IAP proteins. We concentrated our attention on XIAP and its homologs c-IAP1 and c-IAP2, two other members of the family that also possess RING domains. All ten COMMD proteins fused to GST were expressed in 293 cells and subsequently precipitated from cell lysates. The presence of co-precipitated IAP proteins was determined by immunoblotting. The expressed IAPs contained a histidine to alanine point mutation in their RING domains that inactivate their ubiquitin ligase activity [222, 223]. This has been previously shown to stabilize the COMMD1-XIAP interaction [121], and allow for detectable expression of the very unstable c-IAP proteins [223]. As shown in Figure 2B, selected COMMD proteins, namely COMMD1, 2, 4, 5, and 10, demonstrated the ability to bind to IAP proteins, and interestingly, the binding patterns were similar for XIAP, c-IAP1 and c-IAP2.

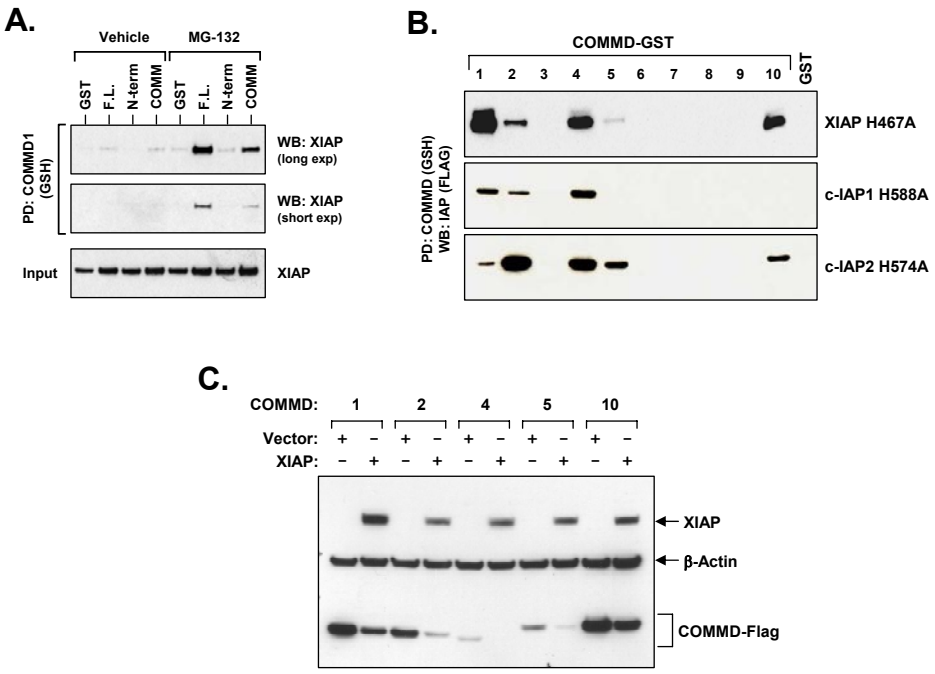

Figure 2 COMM domain containing proteins bind to IAP proteins.
(A) The COMM domain mediates the COMMD1-XIAP interaction. Wild-type XIAP was co-expressed with full-length COMMD1 (F.L.), the amino-terminal 118 amino acids (N-term), or the COMM domain (amino acids 119-190) in fusion with GST. Cells were treated with MG-132 or the corresponding vehicle, and cell lysates were subsequently prepared for COMMD1 precipitation using glutathione (GSH) beads. (B) Other COMMD proteins can interact with IAPs. As in (A), COMMD-GST fusion proteins and the indicated IAP protein were co-expressed in 293 cells. Point mutations in the RING domains of XIAP, c-IAP1 and c-IAP2 were utilized (see text for details). Cell lysates were subsequently prepared and COMMD-GST proteins were precipitated. The presence of co-precipitated IAP proteins was detected by immunoblotting. (C) XIAP mediates the degradation of interacting COMMDs. COMMD1, 2, 4, 5, or 10 were expressed in 293 cells along with XIAP. Cell lysates were subsequently subjected to SDS-PAGE and immunoblotting for COMMD levels (Flag antibody), β-Actin (loading control) or XIAP.

Consistent with their interaction with XIAP and the known role of this protein as a ubiquitin ligase, these COMMD proteins were expressed at lower levels in cells concomitantly transfected with wild-type XIAP (Figure 2C). The mutant XIAP H467A, which is devoid of ubiquitin ligase activity, did not promote COMMD degradation (data not shown), similar to its reported effect on COMMD1 [121]. Altogether, these findings indicate that like COMMD1, other COMMD proteins also interact with IAPs and undergo similar regulation.

Leucine repeats in the COMM domain are required for COMMD1-XIAP interactions

The identification that COMMD-IAP interactions are mediated by the COMM domain suggested that conserved elements in this domain were likely required for these interactions. The COMM domains of COMMD1, 2, 4, 5, and 10 were aligned as previously described [11]. As shown in Figure 3A, invariably conserved tryptophan and proline residues were identified. In addition, the same alignment demonstrated two conserved leucine repeats. Importantly, the leucine repeats were also evaluated for their possible role in determining the nucleocytoplasmic distribution of COMMD1 and were found to function as nuclear export signals (Muller and Klomp, unpublished observations). Point mutations in these areas of conservation were introduced to generate the indicated mutants (Figure 3B), and the ability of these mutants to bind to XIAP was evaluated. As shown in Figure 3C, COMMD1 wild-type demonstrated robust binding to XIAP H467A as expected. However, mutations on the first leucine repeat (Mut1 or Mut1/2) abrogated this interaction. The ability of COMMD1 wild-type or Mut1/2 to bind to XIAP was evaluated again, this time examining their ability to interact with XIAP wild-type as well as XIAP H467A. In both cases, COMMD1 Mut1/2 failed to bind to XIAP. Altogether, these experiments indicated that areas of conservation in the COMM domain, particularly its first leucine repeat, are critical for IAP binding.

Mutations that disrupt XIAP binding prevent basal ubiquitination of COMMD1

Since XIAP functions as an E3 ubiquitin ligase for COMMD1, the loss of COMMD1-XIAP interactions would be predicted to decrease the ubiquitination of COMMD1. To test this notion, we evaluated the basal rate of ubiquitination of wild-type COMMD1 or the COMM domain mutant forms. To that end, cells were transfected with His6-tagged ubiquitin along with COMMD1 wild-type or the indicated mutants. Ubiquitinated proteins were subsequently precipitated from cell lysates using Nickel-agarose beads and the recovered polyubiquitinated fraction was immunoblotted for COMMD1 (Fig 4A, upper panel). As can be appreciated, mutations in either leucine repeat (Mut1, Mut2 or Mut1/2) resulted in dramatic reductions in the amount of ubiquitinated COMMD1 recovered. This was the case even though there was equal recovery of polyubiquitinated proteins in each precipitation (Fig 4A, middle panel) and the expression levels for these mutants

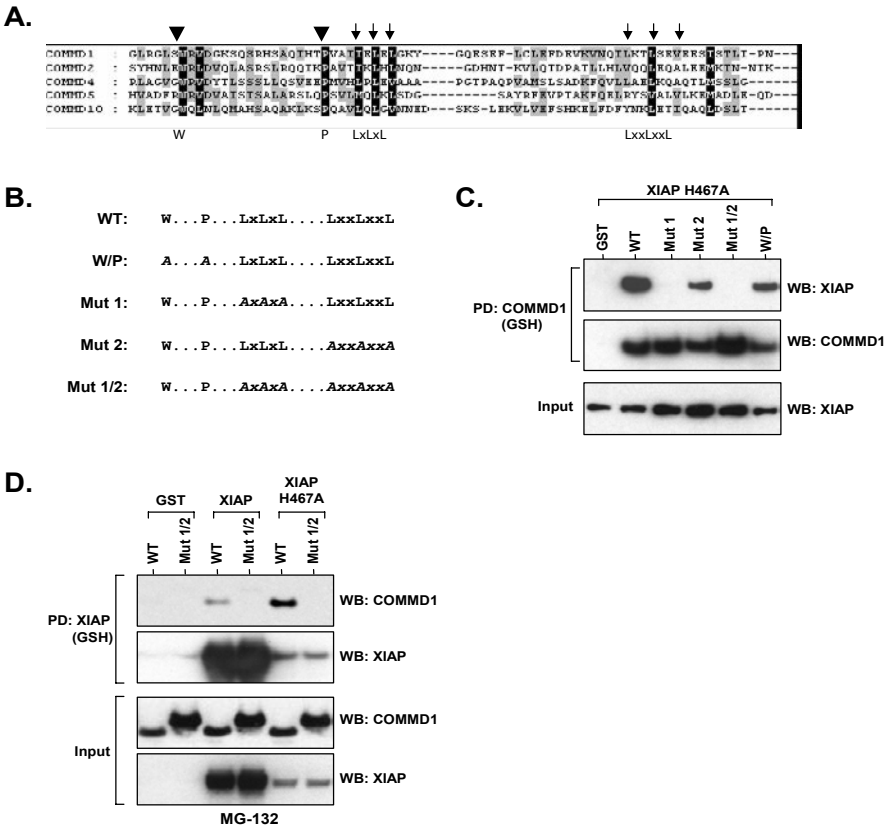

Figure 3: Leucine repeats in the COMM domain determine XIAP binding.
(A) Sequence alignment. The sequences for COMMD1, 2, 4, 5, and 10 were aligned across their COMM domains as previously described (1). Highly conserved motifs are noted in the alignment. (B) Mutations introduced in the COMM domain. The alanine substitutions introduced are depicted. The W/P mutant targets W124 and P141, Mut1 targets the first leucine repeat (I145, L147, and L149A), Mut2 targets the second leucine repeat (L172, L175, and V178). Mut1/2 targets both leucine repeats. (C) and (D) Effects of COMM domain mutations on XIAP binding. COMMD1 wild-type (WT) and the indicated mutations were expressed along with XIAP H467A in untreated cells (C) or along with either XIAP wild-type or XIAP H467A in cells treated with MG-132 for 3 hours (D). COMMD1 was subsequently precipitated from cell lysates and the presence of XIAP was determined by immunoblotting.

were comparable to the wildtype protein (Fig 4A, lower panel). Notably, the W/P mutant, which binds well to XIAP did not demonstrate this phenotype.

Our previous experiments (Figure 3B) demonstrated that Mut2 is capable of binding to XIAP, albeit with lesser efficiency than the wildtype protein when taking into account its input levels. Therefore, the apparent lack of basal ubiquitination for this mutant was initially surprising. To examine if some degree of ubiquitination of Mut2 was still possible, the mutants were expressed at increasing levels to detect basal polyubiquitination as before (Figure 4B). This experiment demonstrated that some degree of ubiquitination could be observed for Mut2, and to a lesser extent, Mut 1 could also be ubiquitinated.

However, a combined mutation in both leucine repeats (Mut1/2) was resistant to ubiquitination.

Consistent with their effects on ubiquitination, the mutations on the leucine repeats of COMMD1 greatly enhanced basal protein expression, an effect that was most pronounced for Mut1/2 (Figure 4C). Similarly, expression levels of wild-type COMMD1 were reduced after XIAP transfection, an effect mediated by the E3 ubiquitin ligase activity of XIAP [121]. However, Mut1/2 was resistant to XIAP-mediated degradation (Figure 4D) and the mutations in either leucine repeat (Mut 1 or Mut 2) demonstrated an intermediate phenotype. Altogether, these results indicated that disruption of the COMMD1-XIAP

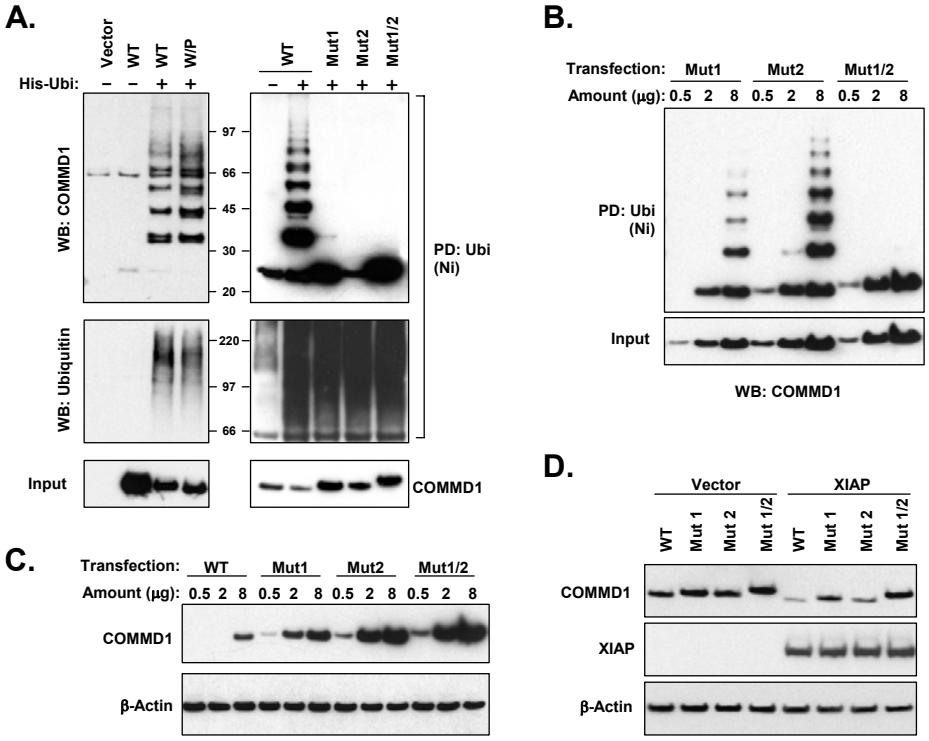

Figure 4 Mutations in the leucine repeats stabilize the protein by impairing COMMD1 ubiquitination
(A) and (B) Basal ubiquitination is greatly affected by mutations in the leucine repeats. COMMD1 was expressed in 293 cells and ubiquitinated proteins were subsequently precipitated from cell lysates with nickel-agarose beads (to precipitate expressed His6-tagged ubiquitin). The precipitated material was immunoblotted for COMMD1, and for ubiquitin (to ensure adequate precipitation). All mutants generated were tested in (A) and the mutations involving the leucine repeats were tested again in (B) in cells expressing increasing amounts of the COMMD1. (C) Mutations of the leucine repeats stabilize COMMD1. The wild-type protein or its mutants were transfected in a dose titrated manner and the resulting expression of COMMD1 was determined by immunoblotting. β-Actin was utilized as a loading control. (D) Mutations in the leucine repeats prevent XIAP-mediated degradation. COMMD1 wild-type or the indicated mutants were expressed along with XIAP and the levels of expression were determined by immunoblotting (upper panel). Expression of XIAP was confirmed (middle panel) and β-Actin was utilized as a loading control (bottom panel).

interaction resulted in decreased ubiquitination of COMMD1 and concomitant protein stabilization.

COMMD1 ubiquitination is required for autoregulation

Our initial studies identified that stable overexpression of COMMD1 is not feasible as it results in near physiologic protein levels. In fact, the endogenous protein is down-regulated in a manner proportional to the level of overexpression, consistent with the notion that COMMD1 autoregulates its expression. This process is post-transcriptional and is associated with the accumulation of high molecular weight modified COMMD1, which we speculated represents ubiquitinated COMMD1. This hypothesis predicts that expression of COMMD1 Mut1/2, which cannot be ubiquitinated, should result in stable overexpression of the protein. Therefore, 293 cells were transfected with COMMD1 wild-type or Mut1/2, and the cells were subjected to selection for one month. At that time point, protein and mRNA levels were determined (Figure 5A). Stable expression of wild-type COMMD1 or Mut1/2 resulted in similar elevations of mRNA levels. However, COMMD1 wild-type was again expressed at near physiologic levels, and the expression of endogenous COMMD1 was decreased as before. Interestingly, this was not true for Mut1/2, which displayed significant overexpression, and did not trigger autoregulation of the endogenous protein. We evaluated next whether stable expression of COMMD1 results in the accumulation of modified high molecular weight forms of COMMD1, as we had observed before in Figure 5E. We precipitated COMMD1 with a rabbit polyclonal antibody and immunoblotted the recovered material with a FLAG antibody, to specifically look at the effect on the overexpressed proteins. At the end of the immunoprecipitation greater amounts of unmodified COMMD1 Mut1/2 were recovered, consistent with its input level (Figure 5B, middle and lower panels). However, modified high molecular weight COMMD1 was only observed after precipitation of the wild-type protein. A western blot of the precipitated material with a polyubiquitin antibody was attempted but resulted in too much background signal to be interpretable (data not shown). Nevertheless, aided by the fact that Mut1/2 cannot be ubiquitinated under basal conditions as shown before (Figure 4), we concluded that this material is ubiquitinated COMMD1.

The notion that COMMD1 autoregulation is dictated by increased ubiquitination was examined further. To that end, we determined the recovery of COMMD1 from Triton-insoluble fractions, a common feature observed for polyubiquitinated proteins [224]. As can be appreciated in Figure 5C, Triton-insoluble COMMD1 was recovered from cells stably overexpressing wild-type protein and not the Mut1/2 version. This was true despite the fact that the latter was expressed at significantly higher levels. Similarly, the endogenous protein is largely excluded from the insoluble compartment even under conditions in which its expression levels are similar to those achieved in the COMMD1 wild-type transfected cells. Altogether, these findings indicate that stable expression of

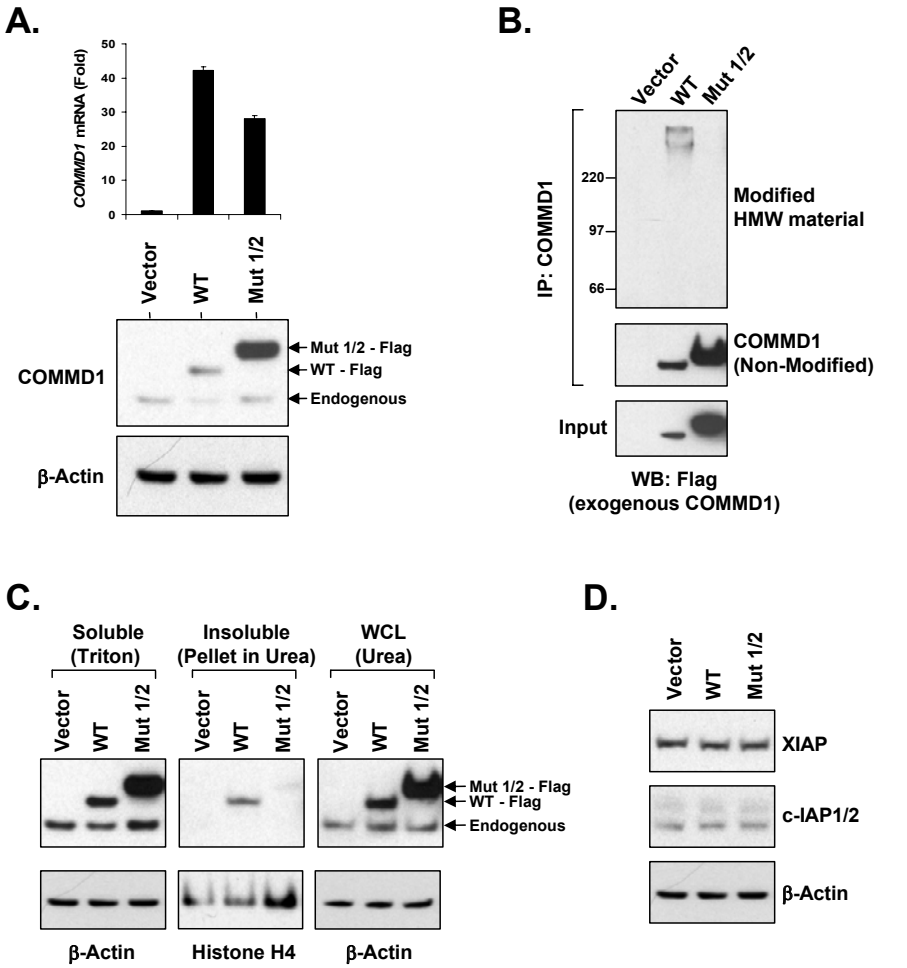

Figure 5: Impairment of COMMD1 ubiquitination prevents autoregulation

(A) COMMD1 Mut1/2 can be stably overexpressed. 293 cells were stably transfected with COMMD1 wild-type or Mut1/2 for over a month. Cell lysates for mRNA and protein extraction were prepared. COMMD1 mRNA levels were determined by qRT-PCR and normalized to the levels of GAPDH (top graph). COMMD1 protein levels were determined by immunoblotting, using β-Actin as a loading control (bottom panels). (B) Expression of wild-type COMMD1 results in modified high molecular weight forms. Cell lysates from the same cell lines were subjected to denaturing immunoprecipitation of COMMD1. The recovered material was immunoblotted for exogenously expressed COMMD1 using a Flag antibody: non-modified COMMD1 was readily detectable at the bottom of the gel (middle panel) and modified high molecular weight (HMW) material was noticeable at the top of the gel on the WT lane only (upper panel). (C) Recovery of COMMD1 from a Triton-insoluble compartment. Lysates from the indicated cell lines were prepared with a Triton containing buffer (soluble fraction, left panel), and the remaining pellet was lysed with an 8M urea buffer (insoluble fraction, middle panel). In addition, a whole cell lysate was prepared by lysing cells directly in an 8M urea buffer (WCL, right panel). COMMD1 levels were determined by immunoblotting; â-Actin and histone 4 were utilized as loading controls. (D) IAP expression levels were unaffected in COMMD1 stable lines. Cell lysates were subjected to SDS-PAGE and were immunoblotted with an XIAP antibody (top panel) and then re-probed with an antibody that reacts with both c-IAP1 and c-IAP2 (middle panel). β-Actin serves as a loading control.

COMMD1 triggers enhanced ubiquitination in order to reduce the protein levels to a near physiologic range. Finally, we examined whether this increase in COMMD1 ubiquitination was mediated by upregulation of IAP levels. Basal expression of XIAP, c-IAP1 or c-IAP2 was unchanged in the COMMD1 stable cell lines, indicating that the mechanism that accelerates the ubiquitination of COMMD1 is not simply the abundance of its ligase in the cell (Figure 5D).

Discussion

COMMD1, the prototype member of the *COMMD* family, was first identified due to its proximity to the imprinted *U2af1-rs1* gene in the mouse [134]. However, the first functional information about this gene was gleaned when it was identified that *COMMD1* participates in copper metabolism [8, 46]. Soon after that report, the ability of COMMD1 to inhibit NF-κB was identified, and presumably through this effect, COMMD1 was found to limit HIV-1 replication in CD4+ T cells [123]. Other functions for COMMD1 such as inhibition of HIF1α-mediated gene expression [167] and inhibition of the epithelial sodium channel [122] have been reported as well. The mechanism that underlies all these various functions is not completely understood, but COMMD1 has been shown to accelerate the rate of degradation of its interacting partners, namely NF-κB subunits [168] and ATP7B [10]. In the case of NF-κB, COMMD1 was found to be a subunit of a Cul2-containing ubiquitin ligase for this transcription factor, and presumably a similar mechanism may underlie its effects on ATP7B and other pathways.

Little is known about the regulation of COMMD1 itself. This factor is ubiquitously expressed and its basal levels are controlled by XIAP, a ubiquitin ligase that belongs to the Inhibitor of Apoptosis family. In this study we examined in greater detail the regulation of basal levels of COMMD1, stimulated by the surprising observation that COMMD1 levels are tightly regulated and stable ectopic overexpression of the protein could not be achieved. Our studies indicate that this latter event is due to increased ubiquitination of the protein, resulting in increased degradation and near physiologic COMMD1 protein levels.

The data presented here demonstrate that COMMD1-XIAP interactions are critical for this regulation. We mapped the binding site for XIAP to the COMM domain and introduced point mutations in its leucine repeats which abolished XIAP binding. As predicted, these mutations prevented XIAP-mediated degradation, greatly stabilized the protein, and abrogated basal ubiquitination of COMMD1. The latter finding highlights the importance of XIAP as a major regulator of COMMD1 levels.

It is unclear what upstream signals might stimulate the ubiquitination of COMMD1. Our studies indicate that ectopic overexpression of COMMD1 increased the level of ubiquitination of this protein, but increased expression of the IAP proteins themselves

does not account for this effect. Interestingly, the COMMD1 Mut1/2 version not only accumulated after stable overexpression but failed to induce autoregulatory degradation of the endogenous protein. The loss of autoregulation indicates that the ability of COMMD1 to interact with XIAP is either required for or correlates with the induction of increased ubiquitination. This highlights the importance of COMMD1 binding to XIAP in the regulation of its cellular levels. An additional corollary of our studies is the identification that a subset of COMMD proteins can similarly bind to IAP proteins, namely XIAP, c-IAP1 and c-IAP2. This suggests that IAP-mediated ubiquitination might be a mechanism of regulation for these factors, a notion that will need further investigation. Finally, COMMDs are involved in a growing number of protein-protein interactions and these have been frequently mapped to the COMM domain [9, 11, 121-123, 166, 168]. Attempts at obtaining structural information regarding the COMM domain have failed thus far, but the mutational analysis performed here indicates that conserved leucine repeats are critical for their ability to interact with XIAP. In addition, the same regions can function as nuclear export signals (Muller and Klomp, unpublished observations), suggesting that perhaps ubiquitination and cellular distribution might be linked events. Once structural information about the COMM domain is available, we anticipate that the leucine repeats will be found to be critical for the interface between COMMD and IAP proteins.

Acknowledgements

We are grateful to Rebecca Csomos andColin Duckett for kindly providing the c-IAP1 and c-IAP2 constructs utilized here. This work was supported in part by a Veterans Affairs Administration MREP Award, and a National Institutes of Health R01 grant DK073639-01A1 to E.B. and by the National Institutes of Health through the University of Michigan's Cancer Center Support Grant (5 P30 CA46592).

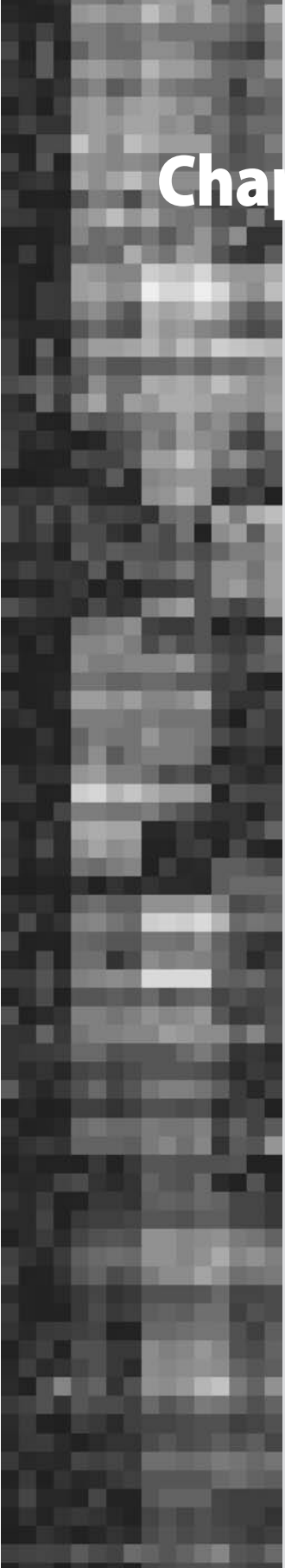

Chapter 8

Summarizing discussion

Gene expression profiling offers the possibility to objectively screen the complete genome for variations in gene expression in many different organisms. This technique has already proven valuable in several applications. As one example, recent studies suggest that genome-wide gene expression profiling as a tool in diagnosis, prognosis and therapy in cancer biology holds great future [225].Tissue-specific gene expression profiles have been used to determine the origin of cancer cells [86, 226]. Phenotypical characteristics of tumors (e.g. metastatic potential) can be classified by distinct gene expression profiles, providing a prognostic use of gene expression profiling [87, 227, 228]. Finally, gene expression profiling is useful in therapeutics to determine which patients can benefit from sometimes invasive therapies used to treat cancer [229-231]. In basic biomedical science, genome-wide gene expression studies can be applied to address a myriad of biological questions. These studies mostly aim to discover novel target genes or gene networks to better understand the physiology or pathophysiology of a system of interest. Caveats in the use of gene expression analyses comprise the limitations in differentiation between splice variants of genes, the fact that changes in mRNA expression are not always reflected in changes in protein levels and activities, and the additional post-transcriptional modifications often required by proteins to reach a specific cellular destination or to realize a specific function. An exciting aspect and yet another limitation of gene expression analysis resides in the fact that this technology is extremely powerful to identify novel genes in biological pathways, but the biomedical relevance of such findings need to be established by independent experiments. Nevertheless, compared to other systems biology approaches such as proteomics and metabolomics, transcriptomics currently offers the best opportunity to cover genome-wide changes. In this thesis, we used gene expression profiling to unravel novel aspects of copper metabolism. COMMD1 has originally been identified as a protein involved in copper homeostasis and was later implicated in various other processes (figure 1). We therefore used transcriptomics approaches to gain novel insights in the function of COMMD1 and COMMD proteins. Within the following sections the implications of these findings are discussed in the broader perspective of our current knowledge.

Gene expression profiling to unravel mammalian copper metabolism

The yeast strain *Saccharomyces cerevisiae,* has been extensively studied for gene expression variations in response to changing copper concentrations. Many genes involved in maintaining copper homeostasis were transcriptionally regulated as a result of copper overload or copper depletion [34, 36]. This mechanism is important for the yeast cell to properly maintain intracellular copper concentrations, since this metal is both essential to sustain life, but toxic in excess. Several studies in human cells, in animals and in patients

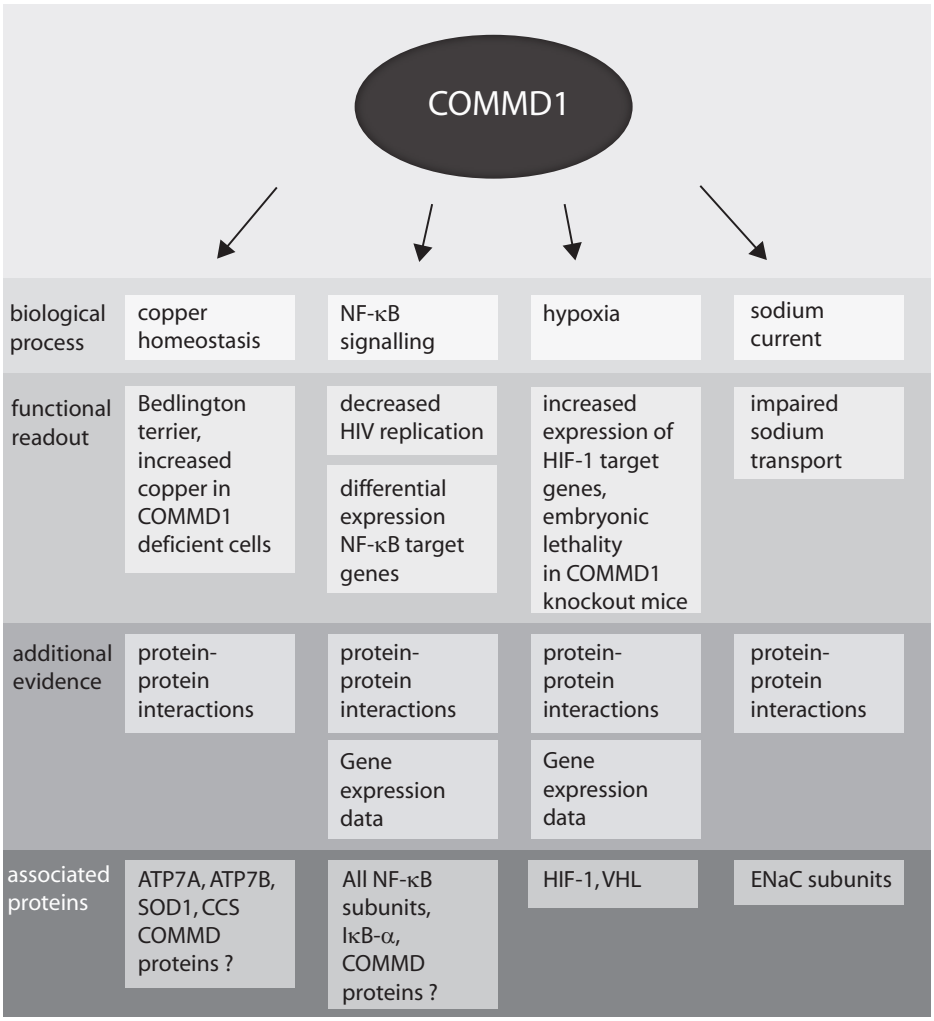

Figure 1 Schematic overview of the processes in which COMMD1 has been implicated
COMMD1 has been implicated in a variety of biological processes including copper homeostasis, NF-κB signalling, hypoxia and sodium transport. These data are based on functional experiments, protein-protein interaction data and/or gene expression data. In this figure, the functional and biochemical evidence for implicating COMMD1 in these processes, including interaction partners of COMMD1, involved in these processes are depicted. (ATP7A, Menkes disease protein; ATP7B, Wilson disease protein; COMMD, Copper metabolism MURR domain; NF-κB, nuclear factor kappa B, IκB, inhibitor of kappa B, HIF-1, hypoxia inducible factor 1; ENaC, epithelial sodium channel; HIV, human immunodeficiency virus)

have used extended sets of genes or genome-wide approaches to study differential gene expression as a result of primary or secondary copper shortage or copper overload [15, 16, 57, 92, 232]. Most of the copper overload studies were performed in cell lines at one time point or in Wilson disease animal models at specific stages of disease and are therefore limited. In chapter 2, we examined extensive time-dependent transcription

changes in liver cells and transcription changes in mice livers after a high copper diet. Our analysis in liver cells identified a rapid and marked response that was limited to just a few genes; the metal-responsive metallothionein genes, which were highly induced. Consistent with data from other gene expression studies after copper overload, our *in vivo* and *in* vitro analyses in combination with a qRT PCR (quantitative reverse transcription polymerase chain reaction) approach for candidate copper homeostasis genes did not reveal a differential expression of these candidate genes in response to copper (chapter 2) [57, 92, 232]. This suggests that, in comparison to yeast, mammalian cells only have limited capacity to regulate copper homeostasis by transcriptional mechanisms and indicate that intracellular mechanisms to rapidly withstand increasing copper concentrations are therefore probably mediated via post-transcriptional mechanisms.

Our time-resolved microarray analysis permitted us to identify a slower, probably secondary response to copper overload, which comprised over 100 genes involved in various processes. As individual gene expression studies can be prone to experimental variations, we then performed a transcriptomics meta-analysis on all publicly available gene expression changes as a result of copper overload in chapter 3, which included our own data of chapter 2. In this analysis we addressed the following two questions. Which biological processes are regulated by copper on the transcriptional level? To what extent are these transcriptional changes specific to copper overload? The first question was addressed by determining the overrepresentation of distinct genes based on functional classification by the gene ontology (GO) database [233], compared to the distribution of the GO-defined biological processes in all annotated genes. This analysis revealed that copper can regulate the expression of genes involved in various biological processes, including lipid metabolism, cell death and cell cycle progression. We addressed the second question by comparing the genome-wide hepatic gene expression changes after copper overload to the changes after iron overload (chapter 3). The rationale for this approach resides in the fact that both copper and iron are redox active transition metals. Furthermore, Wilson disease (hereditary copper overload disorder) and Hereditary hemochromatosis (iron overload disorder) are well known hepatic metal overload conditions characterized by a somewhat similar progression of liver disease [234]. This analysis revealed a copper-specific repression of genes involved in cholesterol biosynthesis. On a much broader scale, similar transcriptomics meta-analyses could be applied to understand and to distinguish between other well-defined disorders. For example, underlying differences in the pathology of other liver diseases, in phenotypically similar cancers and in various infectious diseases could be examined by such transcriptomics meta-analyses.

COMMD1 knockout mice have increased HIF-1 activity

In the course of the investigations described in this thesis, we decided to focus on the function of the recently discovered COMMD1 protein, because of four distinct arguments. First, the underlying genetic defect in Bedlington terriers affected with copper toxicosis is a deletion of part of the *COMMD1* gene, resulting in the absence of COMMD1 protein expression [8]. Second, increased intracellular amounts of copper were observed in HEK293T cells and in dog hepatocytes, in which COMMD1 expression was knocked down [121, 212]. Third, interaction studies identified COMMD1 as an interaction partner of ATP7B. Copper excretion into the bile is mediated via the copper transporting P-type ATPase ATP7B, which is expressed in the liver and mutated in patients with Wilson disease. The fact that COMMD1 is able to interact with ATP7B suggests a role for COMMD1 in cellular copper excretion [9, 10]. Finally, COMMD1 gene expression appeared to be repressed by prolonged copper treatment (Chapter 2).

In order to study the precise role of COMMD1, a *Commd1* knockout mouse was generated (chapter 4). Surprisingly, *Commd1* knockout mice embryos were delayed in embryonic development and died after 9.5 days postcoitum (dpc). Morphologically and developmentally, 9.5 dpc *Commd1* knockout mice embryos were comparable to 8.5 dpc wild type (WT) mice embryos. As COMMD1 is important in copper homeostasis in the Bedlington terrier, we examined whether *Commd1* knockout embryos suffered from a generalized copper overload, but specific histochemical copper staining did not reveal elevated copper concentrations in the knockout mice. The reason for the discrepancy between the phenotypes in the copper-toxicosis Bedlington terrier and in the *Commd1* knockout mice remains elusive. *Commd1* knockout mice embryos die before the liver is completely developed, indicating that these embryos probably die before copper accumulation can manifest. Most likely, species differences in *Commd* protein redundancy during embryogenesis are therefore responsible for the discrepancy in phenotypes. Currently, a liver-specific *Commd1* knockout mouse is generated in our laboratory that might be a better model for copper toxicosis in Bedlington terriers and might help to elucidate Commd1 function in liver copper homeostasis.

As we were puzzled by the unexpected phenotype of *Commd1* knockout embryos, we used a transcriptomics approach to obtain clues for underlying mechanisms leading to embryonic lethality. The successful use of transcriptomics approaches to gain novel insights into the role of the corresponding genes in mouse embryonic development has been demonstrated by others in the study of *Nfi-a* (nuclear factor I-A) and *(Hsf)-2* (heat shock transcription factor 2) knockout mice embryos [235, 236]. Since *Commd1* knockout embryos displayed growth retardation, we compared the gene expression profiles of knockout embryos to both those of 8.5 dpc and 9.5 dpc WT embryos. In a first analysis we compared differentially expressed genes between 8.5 dpc and 9.5 dpc WT mice embryos,

thus permitting us to delineate gene expression profiles related to differences in developmental stages. In a second analysis, the genome wide gene expression profiles between *Commd1* knockout mice embryos compared to both 8.5 and 9.5 dpc WT embryos were analyzed. In order to retrieve genes that were specifically related to embryonic lethality in *Commd1* knockout mice embryos we excluded the development related differentially expressed genes detected in the first analysis. In this way we identified an increased expression of several genes that are regulated by the transcription factor Hypoxia-inducible factor 1 (HIF-1) specifically in *Commd1* knockout embryos. HIF-1 is the key transcriptional regulator that mediates adaptive responses to reduced partial oxygen pressure. Consistent with our microarray data, COMMD1 could interact with HIF-1 and promote HIF-1 degradation. In addition, the expression of a known HIF-1 target gene, *BNIP3* (BCL2/adenovirus E1B 19 kD protein interacting protein 3) [237] was examined in a COMMD1 deficient cell line. Finally, *Commd1* deficient embryos displayed a placental biogenesis defect consistent with overactive HIF-1 target gene expression. Under normal oxygen concentrations, the expression of *BNIP3* was comparable between COMMD1 knockdown cells and control cells, but after hypoxia, the expression of *BNIP3* was further increased in COMMD1 knockdown cells as compared to control cells (chapter 4). Gene expression profiling in COMMD1 knockdown cells (HEK293T cells, HeLa cells and HT29 cells) under normal conditions did not reveal an increased expression of HIF-1 target genes (chapter 5, unpublished results). As mice embryos in general are subject to low oxygen levels [154], these combined data therefore suggest that COMMD1 can mainly regulate HIF-1 mediated gene expression under low oxygen levels, when HIF-1 is activated.

COMMD1 as a regulator of NF-κB activity

The findings that COMMD1 modulated gene expression in the HIF-1 pathway was even more interesting in the context of recent findings that COMMD1 is a regulator of NF-κB signaling. NF-κB is a transcription factor that can regulate the expression of a multitude of genes involved various processes including immune responses and regulated cell death [185, 186]. Protein-protein interaction studies and 2-κB luciferase assays clearly revealed a role for COMMD1 in NF-κB signaling and COMMD1 deficiency resulted in an enhanced expression of some NF-κB inducible genes after incubation with the NF-κB stimulus TNF [11, 123, 168]. These data therefore suggest that only subsets of TNF/ NF-κB target genes are inhibited by COMMD1. In COMMD1 deficient HT29 cells, we explored this possibility by analyzing the differential gene expression profiles in the presence and in the absence of TNF compared to control cells (chapter 5). Under normal conditions, we did not identify a differential expression of NF-κB target genes. After TNF exposure, however, many TNF target genes were statistically significantly differentially expressed

in the COMMD1 knockdown cell line compared to control cells. Together these data suggest that COMMD1 can be a modulator of NF-κB activity if NF-κB is activated.

Regulation and cellular localization of COMMD1

The role of COMMD1 as a transcriptional regulator in NF-κB or HIF-1 signaling appears to be especially prominent when these pathways are active. Many proteins that regulate NF-κB and HIF-1 activity shuttle between the nucleus and the cytoplasm and the localization of these proteins is mainly determined by NESs (nuclear export signals) and NLSs (nuclear localization signals) in their amino acid sequences [189-192, 238-240]. Interestingly, we identified two functional CRM-1-dependent nuclear export signals (NESs) in COMMD1, through which the cellular localization of COMMD1 appeared to be controlled (chapter 6). Under basal conditions, the nuclear expression of COMMD1 was low, indicative for constitutive nuclear export of COMMD1. Mutations in the NESs of COMMD1 increased the nuclear expression of COMMD1 and concomitantly resulted in an enhanced repression of NF-κB activity (chapter 6). Many proteins that contain NESs are regulated by relocalizing these proteins towards the cytoplasm or retaining these proteins in the nucleus in response to distinct stimuli [241]. TNF exposure resulted in a moderate increase in COMMD1 expression after 180 minutes [11], suggesting that such sophisticated regulatory mechanisms for COMMD1 might exist and have biological significance.

In collaboration with Dr. E. Burstein, we identified that nuclear export of COMMD1 is linked to COMMD1 polyubiquitination (chapter 6 and 7). For various other proteins, including p27Kip1, p21 (CIP1), Cyclin D1, RXRα and p53, a link between regulated nuclear export and protein degradation has been demonstrated [200, 201, 208, 209, 242]. These data are indicative for a common mechanism in which nuclear transcription regulators can be exported into the cytoplasm to be efficiently degraded. Previous studies identified XIAP (X-linked inhibitor of apoptosis) as an E3 ubiquitin ligase protein that adds ubiquitin chains onto COMMD1 and thus facilitates COMMD1 degradation [121]. Mutations in the NESs of COMMD1 disrupted the interaction between XIAP and COMMD1 (chapter 7). One explanation of this finding is the possibility that COMMD1-XIAP interaction *per se* is prevented. Alternatively, the interaction between mutant COMMD1 and XIAP could be abrogated because these two proteins are in different cellular compartments, mutant COMMD1 in the nucleus and XIAP in the cytoplasm [205]. Consistent with the latter possibility, inhibition of CRM-1-dependent nuclear export by leptomycin B (LB) resulted in decreased COMMD1 polyubiquitination (chapter 6). Based on these findings, we hypothesize that nuclear export of COMMD1 might be a prerequisite for COMMD1 degradation (figure 2). Future experiments, in which the interaction between

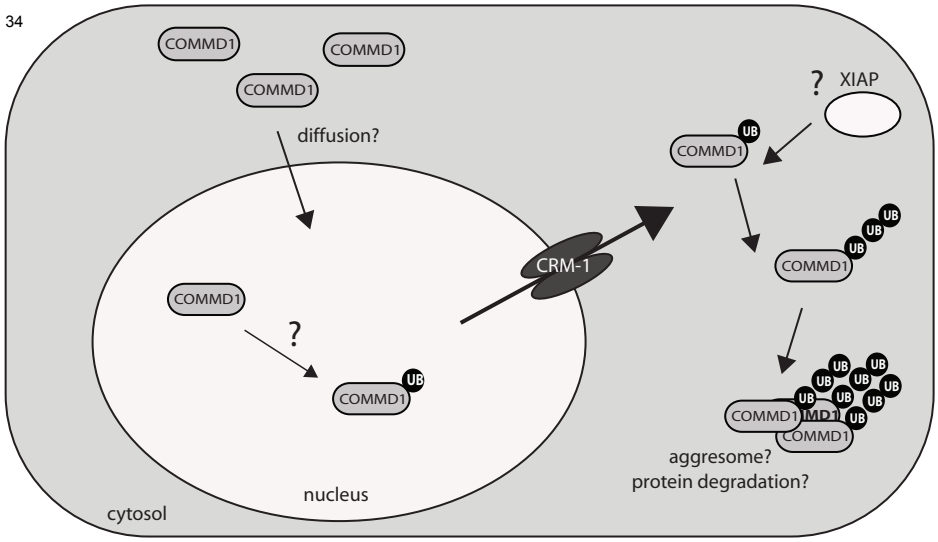

Figure 2 Model for COMMD1 function in relation to COMMD1 localization
Under normal conditions, COMMD1 is predominantly present in the cytoplasm. Import into the nucleus might occur via diffusion, but export can be facilitated by CRM-1, located on the nuclear envelope. In response to nuclear export, COMMD1 is ubiquitinated by XIAP in the cytoplasm.

in vitro translated XIAP and COMMD1 NES mutants is studied in a cell free environment, could discriminate between these two possibilities. Notably, nuclear export of COMMD1 was also associated with the formation of perinuclear COMMD1-containing aggregates (chapter 6). These aggregates co-localized with ubiquitin, suggesting that these aggregates might represent aggresomes that can function as the proteolytic centre of a cell [204]. Co-localization studies using antibodies to aggresome specific proteins such as γ-tubulin could test this hypothesis. TNF treatment resulted in an increased polyubiquitination of COMMD1 and an increased formation of aggregates, suggesting that nuclear export of COMMD1 is increased after TNF exposure (figure 2). In conclusion, our data illustrate that COMMD1 localization is dependent on NESs in COMMD1 and that the localization of COMMD1 affects NF-κB activation. Whether similar mechanisms underlie the regulatory role of COMMD1 in HIF1-mediated transcription during hypoxia is likely and is currently under investigation in our laboratory.

These findings raise the question of how COMMD1 exerts its role in regulating NF-κB and HIF-1 activity. NF-κB promoting stimuli induce the import of NF-κB dimer subunits into the nucleus to initiate transcription of genes with κB sites in the promoter sequence. Expression of NF-κB genes is highly dynamic due to negative feedback mechanisms that allow rapid termination of NF-κB activity [163]. These mechanisms include the synthesis of IκB proteins and the degradation of the NF-κB subunit RelA/p65 [203, 243]. Differential gene expression as a result of NF-κB activation is therefore a combined result of stimulating and inhibitory transcription events. The ubiquitin ligase complex ECS^{SOCS1}

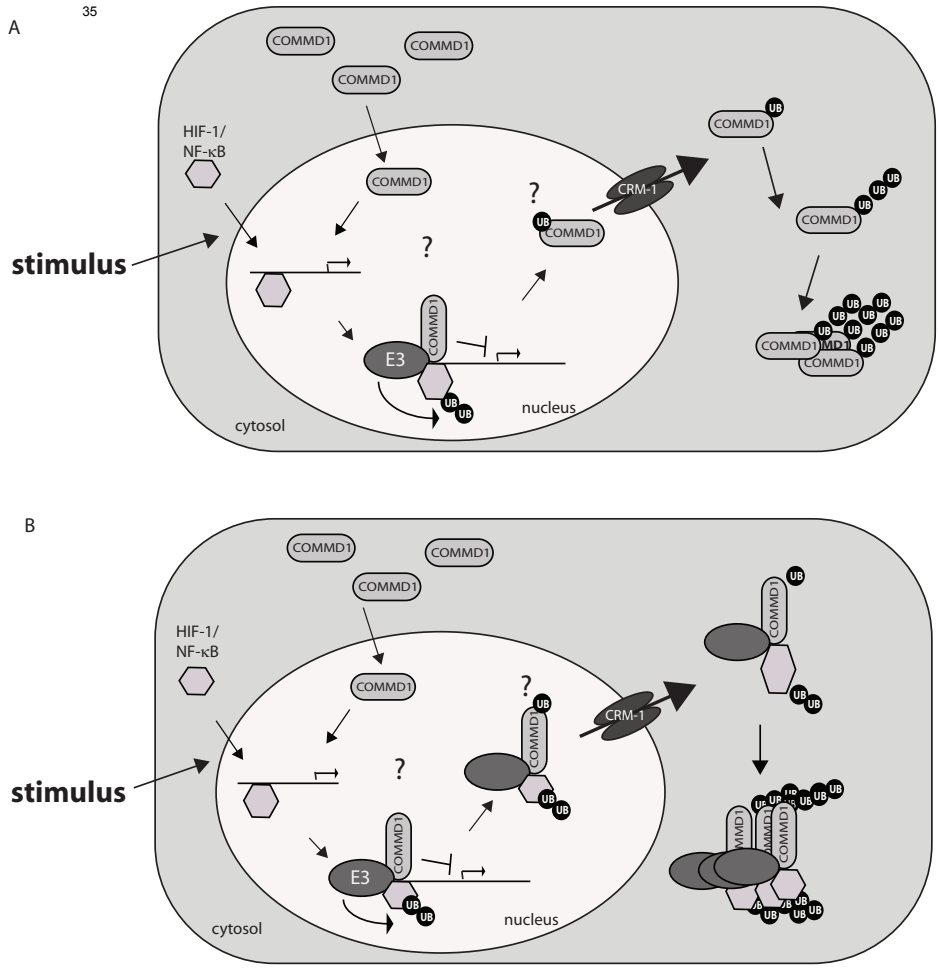

Figure 3. Models for the function of COMMD1 nuclear export
In response to stimuli, NF-κB subunits and HIF-1 are recruited into the nucleus to activate transcription. Nuclear COMMD1 recruits an E3 ubiquitin ligase complex to DNA-bound subunits to promote the degradation of these subunits upon activation of the corresponding pathways. After this recruitment we propose two possible scenarios that both result in the nuclear export of COMMD1 and subsequent degradation. In the first model (A), COMMD1 is detached from the subunit-DNA-ubiquitin-ligase complex to be exported out of the nucleus alone and to be degraded. In this model nuclear export of COMMD1 would prevent additional inhibition of transcription by COMMD1 (A). In a second model (B), COMMD1 together with the subunits and the ubiquitin ligase is detached from the DNA to be exported out of the nucleus and to be degraded together in perinuclear aggregates. This model would imply that COMMD1 is not only involved in the recruitment of an E3 ubiquitin ligase complex, but that COMMD1 also promotes the nuclear export of the subunits for efficient degradation in the cytoplasm.

involved in RelA degradation is composed of SOCS1, Elongin B/C and Cul2 [168]. COMMD1 can interact with DNA-bound RelA and can recruit ECS^{SOCS1}. Interactions between COMMD1 and proteins of ECS^{SOCS1}mediate the ubiquitination and subsequent degradation of RelA [11, 168].

Analogies between the regulation of NF-κB activity and the regulation of HIF-1 activity exist. HIF-1 regulates the expression of various genes involved in energy metabolism, cell growth and angiogenesis [244]. In normoxic conditions, the subunit HIF-1α is rapidly degraded, but during hypoxia, HIF-1α is stabilized, transported into the nucleus to form a dimer with HIF-1β, and initiates the transcription of genes with HREs (HIF-1 responsive elements) in the promoter region of target genes [245]. HIF-1 activity is also highly dynamic and is tightly controlled by VHL (von Hippel Lindau tumor suppressor protein), that can shuttle between the nucleus and the cytoplasm and can, in complex with other proteins, mediate the degradation of HIF-1 [240]. Remarkably, the ECS^{SOCS1} complex that regulates RelA stability is highly similar to the VHL ubiquitin complex that is composed of VHL, Elongin B/C and Cul2 [165, 246]. To terminate HIF-1 activity upon reoxygenation, VHL induces the nuclear export and ubiquitination of HIF-1 [240]. Upon reoxygenation, the absence of COMMD1 expression results in an increased stability of HIF-1 (chapter 4). In addition, COMMD1 interacts with VHL, suggesting a role for COMMD1 in VHL-mediated HIF-1 degradation (unpublished observations, B van de Sluis *et al.*).

As NF-κB and HIF-1 regulation reveals many similarities, we propose the following two models on how nuclear export of COMMD could play a role in regulating NF-κB or HIF-1 activity. In a first model, nuclear export of COMMD1 might provide a mechanism to terminate the inhibitory role of COMMD1 in the activated NF-κB and HIF-1 pathway (Figure 3A). Alternatively, in a second model we propose that COMMD1 might exert a role in mediating nuclear export of HIF-1 or NF-κB subunits to enhance their subsequent degradation into the cytoplasm (figure 3B). In this latter model, COMMD1 would serve a role as a nuclear export carrier protein. Consistent with this second model, increased nuclear expression of RelA was observed in COMMD1-deficient cells that were incubated with TNF [168]. Interaction studies that examine the association between COMMD1 and NF-κB subunits or HIF-1α in nuclear and cytosolic cell fractions after activation of these pathways should discriminate between these models.

The COMMD family of proteins; determinants of transcription specificity?

Recently, a group of 9 other COMMD proteins were identified that all share a homologous COMM domain [11, 210] (figure 4). All COMMD proteins are ubiquitously expressed and conserved in higher eukaryotes. Originally, some of these COMMD proteins were found in protein-proteins interaction studies as interacting partners of COMMD1 [11, 166]. Apart from their sequence conservation with COMMD1, many COMMD proteins can interact with proteins that interact with COMMD1 and similarly inhibit NF-κB activity as measured in κB luciferase assays [10, 11] (unpublished results of B. van de Sluis, W. Vonk, P. de Bie and L. Klomp). COMMD1 can interact with all five NF-κB subunits and is the only

COMMD protein to interact with c-Rel [11]. COMMD6 interacts with only the subunits NF-κB1 and RelA and COMMD9 interacts with only the subunits NF-κB1 and RelB [11, 166]. Using a transcriptomics approach we determined that COMMD1, COMMD6 and COMMD9 modulated the expression of distinct TNF-inducible genes. These data suggest distinct roles for COMMD proteins in modulating NF-κB-mediated transcription.

Precedence of proteins families that can modulate transcription is provided by the PIAS (protein inhibitor of activated STAT) proteins [247, 248]. Originally these proteins were identified as negative regulators of STAT (signal transducer and activator of transcription) signaling. Induction of gene expression by PIAS proteins and regulation of various other transcription factors, including NF-κB and has also been described [249, 250]. The PIAS family of proteins contains four members that can interact with the seven members of the STAT family to modulate transcription [247]. Protein-protein interaction studies revealed that both specificity and redundancy in PIAS-STAT interactions exist. Redundancy and specificity amongst PIAS proteins is also reflected in the regulation of

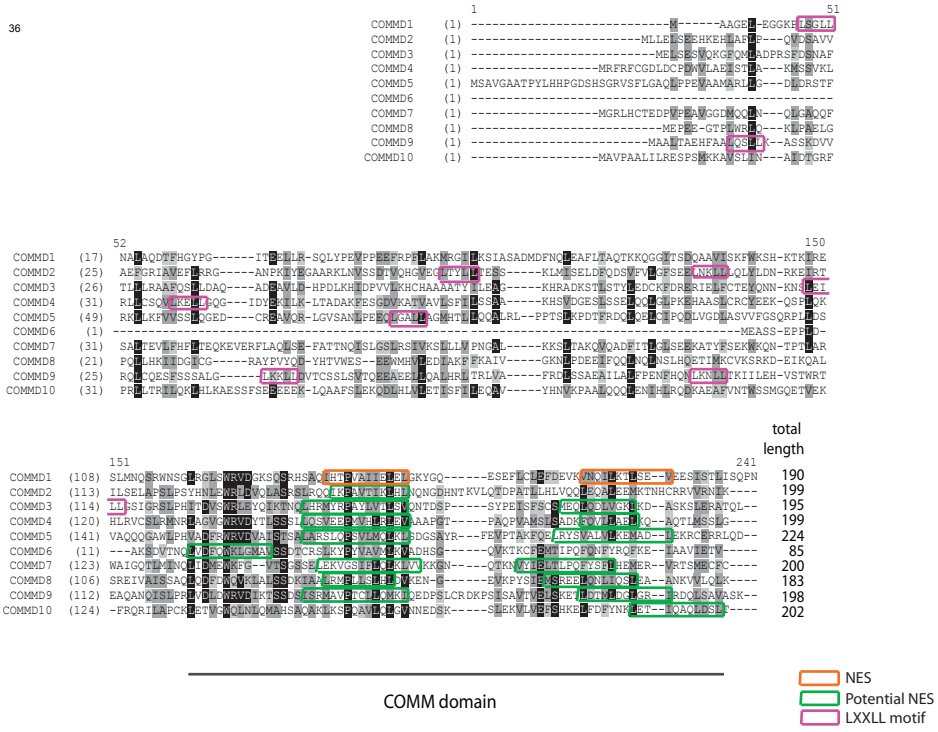

Figure 4 Conserved amino acid residues in COMMD proteins
In the alignment the protein sequences of all ten COMMD proteins is depicted. In black, conserved amino acids are denoted, in dark gray strongly similar amino acids are denoted and in light gray weakly similar amino acids are denoted. NESs are indicated by orange boxes, putativel NESs based on the consensus NES sequence of $HX_{2-3}HX_{2-3}HX_{1-2}H$ (in which H represents the hydrophobic amino acids L,I,V,M or F) are indicated by green boxes and LXXLL motifs are indicated in purple. The COMM domain is depicted below the sequences.

distinct subsets of genes [251]. Regulation of transcription by PIAS proteins is achieved via multiple molecular mechanism that include the prevention of transcription factor binding to the DNA, sumoylation of transcription factors and recruitment of other co-activators [247]. An LXXLL (in which L denotes Leucine and X denotes any amino acid) motif, which has been described as an important domain for interactions between nuclear receptors and co-regulators [252], was required for PIAS-mediated transcriptional modulation [253]. In summary, these findings have implicated PIAS proteins in fine-tuning immune responses and other biological processes through the modulation of transcription factor activities.

In analogy to the redundancy and specificity of PIAS proteins in transcriptional modulation, we identified distinct subsets of TNF-responsive genes that were repressed or further induced in one or more COMMD deficient cell lines (chapter 5). Many of the hydrophobic residues, important in nuclear export of COMMD1 are conserved among COMMD proteins (figure 4), which suggest that the localization of most COMMD proteins might be similarly regulated as COMMD1. Examination of the localization of COMMD6 revealed a similar cellular localization as COMMD1 [166], consistent with this hypothesis. In addition, one or multiple LXXLL motifs are present in the N-termini of most COMMD proteins except COMMD6, COMMD7, COMMD8 and COMMD10 (figure 4). Whether these domains are also important in COMMD protein function is unknown. Comparisons of the gene expression profiles of overexpressed WT-COMMD1 or LXXLL-mutated COMMD1 in cells could answer this question. In conclusion, our data suggest that comparable to PIAS proteins, COMMD proteins might modulate immune responses and other processes through regulation of transcription factors, including NF-κB, HIF-1 and possibly other transcription factors.

What is the function of COMMD1?

An important issue remains how COMMD1 can both be involved in copper metabolism and in transcriptional modulation (figure 1). A clue for a more pleiotropic function of COMMD1 in all these processes might reside in COMMD1-mediated regulation of protein degradation. In the NF-κB pathway, COMMD1 interacts with the five NF-κB subunits, with IκB-α and with the E3 ubiquitin ligase complexes [11, 123, 168]. The interaction of COMMD1 with the ECS^{SOCS} complex facilitates the degradation of RelA and thereby abrogates NF-κB mediated transcription. During hypoxia, COMMD1 interacts with HIF-1 and regulates HIF-1 stability [254]. In copper metabolism, overexpression of COMMD1 resulted in decreased stability of newly synthesized ATP7B [10]. In general, COMMD1 and possibly also other COMMD proteins might therefore fulfill a role as a chaperone that directs target proteins to ubiquitin ligase complexes to modulate degradation specificity.

Concluding remarks and future directions

In this thesis, our transcriptomics approaches have successfully revealed novel aspects of copper metabolism. In order to identify novel players in copper homeostasis, new unbiased approaches will be crucial. Systems biology approaches as discussed in chapter 1, can offer such a possibility. In relation to the gene expression signatures that are used in the diagnosis and the prognosis of cancers, transcriptomics approaches in the diagnosis and the prognosis of Wilson disease (an inherited copper overload disorder) and of Menkes disease (MD; an inherited copper deficiency disorder) might similarly yield valuable knowledge. In primary skin fibroblasts, obtained from Menkes disease patients, measurements of intracellular copper concentrations revealed an increased retention of copper compared to fibroblasts from healthy controls [255]. As an example of transcriptomics approaches in MD, the gene expression profiles in cultured Menkes disease patient fibroblasts could therefore be compared to the profiles of healthy control fibroblasts. Characterization of the genes that are differentially expressed specifically in Menkes fibroblasts could help in diagnosis and possibly in the prognosis of MD. An advantage of using cultured fibroblasts could reside in the fact that the transcriptional response of these fibroblasts can be monitored after incubation of these cells in the absence and in the presence of copper. In this way, changes in copper-dependent gene expression between Menkes disease fibroblasts and control fibroblasts can be examined. When growth conditions are kept sufficiently constant, gene expression profiles in these fibroblasts could also reveal novel transcriptional mechanisms that underlie in the pathophysiology of Menkes disease. Similar approaches could be used to study transcriptional copper-related responses in the livers of hepatocyte-specific Commd1 knockout mice kept on copper-deplete or copper-replete diets.

In a broader perspective, gene expression profiling offers great potential to reveal novel transcriptional mechanisms that underlie the pathogenesis of many hereditary and acquired diseases and such studies will provide important fundamental insight in the functions of genes of interest. In this way, transcriptomics can be an ideal tool to generate novel valuable and testable hypotheses. Consistent with this notion, we hypothesized from our gene expression studies in *Commd1* knockout mice that COMMD1 was involved in HIF-1 signaling. Additional experiments in a cellular system indeed supported this hypothesis. Furthermore, transcriptomics approaches described in this thesis have also been successful to establish a role for other COMMD proteins in NF-κB signaling.

In the future, improved reproducibility and combining DNA microarray data with various other techniques will expand the use of DNA microarrays to enhance our knowledge in understanding gene regulation networks and to generate more hypotheses. In this respect, ChIP-on-chip technology (an approach to isolate and characterize genomic

sites occupied by specific DNA-binding proteins in living cells) reveal the successful combination of DNA microarray with chromatin immuno-precipitation [256].

In addition to the modulatory role of COMMD1 in HIF-1 and NF-κB signaling, our observationsdescribed in this thesis that COMMD1 contains functional NESs have greatly contributed to our knowledge on COMMD1 function and regulation. Future studies should aim to dissect which physiological conditions affect the localization of COMMD1 and the precise mechanisms underlying this phenomenon. In addition, the NESs in COMMD1 are mostly conserved among other COMMD proteins. Other COMMD proteins might therefore similarly be subject to nuclear-cytoplasmic shuttling to regulate transcription. As distinct COMMD proteins affect the expression of distinct genes, the possibility that specific conditions might only affect the cellular localization of one or more COMMD proteins should be addressed. Finally, our data and data of others support the idea that COMMD1 might serve as a protein that promotes the degradation of distinct proteins. Identification of which proteins are prone to COMMD1-mediated degradation will help to understand the molecular function of COMMD1 in copper homeostasis, NF-κB activity, hypoxia, sodium transport and perhaps several more yet unidentified processes.

References

1 Chelly, J.; Tumer, Z.; Tonnesen, T.; Petterson, A.; Ishikawa-Brush, Y.; Tommerup, N.; Horn, N.; Monaco, A. P. (1993) Nat Genet 3 1 14-9
2 Mercer, J. F.; Livingston, J.; Hall, B.; Paynter, J. A.; Begy, C.; Chandrasekharappa, S.; Lockhart, P.; Grimes, A.; Bhave, M.; Siemieniak, D.; et al. (1993) Nat Genet 3 1 20-5
3 Vulpe, C.; Levinson, B.; Whitney, S.; Packman, S.; Gitschier, J. (1993) Nat Genet 3 1 7-13
4 Yamaguchi, Y.; Heiny, M. E.; Gitlin, J. D. (1993) Biochem Biophys Res Commun 197 1 271-7
5 Tanzi, R. E.; Petrukhin, K.; Chernov, I.; Pellequer, J. L.; Wasco, W.; Ross, B.; Romano, D. M.; Parano, E.; Pavone, L.; Brzustowicz, L. M.; et al. (1993) Nat Genet 5 4 344-50
6 Wijmenga, C.; Klomp, L. W. (2004) Proc Nutr Soc 63 1 31-9
7 Prohaska, J. R.; Gybina, A. A. (2004) J Nutr 134 5 1003-6
8 van De Sluis, B.; Rothuizen, J.; Pearson, P. L.; van Oost, B. A.; Wijmenga, C. (2002) Hum Mol Genet 11 2 165-73
9 Tao, T. Y.; Liu, F.; Klomp, L.; Wijmenga, C.; Gitlin, J. D. (2003) J Biol Chem 278 43 41593-6
10 de Bie, P.; van de Sluis, B.; Burstein, E.; van de Berghe, P. V.; Muller, P.; Berger, R.; Gitlin, J. D.; Wijmenga, C.; Klomp, L. W. (2007) Gastroenterology 133 4 1316-26
11 Burstein, E.; Hoberg, J. E.; Wilkinson, A. S.; Rumble, J. M.; Csomos, R. A.; Komarck, C. M.; Maine, G. N.; Wilkinson, J. C.; Mayo, M. W.; Duckett, C. S. (2005) J Biol Chem 280 23 22222-32
12 van den Berghe, P. V.; Folmer, D. E.; Malingre, H. E.; van Beurden, E.; Klomp, A. E.; van de Sluis, B.; Merkx, M.; Berger, R.; Klomp, L. W. (2007) Biochem J 407 1 49-59
13 Muller, P.; van Bakel, H.; van de Sluis, B.; Holstege, F.; Wijmenga, C.; Klomp, L. W. (2007) J Biol Inorg Chem 12 4 495-507
14 Huster, D.; Purnat, T. D.; Burkhead, J. L.; Ralle, M.; Fiehn, O.; Stuckert, F.; Olson, N. E.; Teupser, D.; Lutsenko, S. (2007) J Biol Chem 282 11 8343-55
15 Svensson, P. A.; Englund, M. C.; Markstrom, E.; Ohlsson, B. G.; Jernas, M.; Billig, H.; Torgerson, J. S.; Wiklund, O.; Carlsson, L. M.; Carlsson, B. (2003) Atherosclerosis 169 1 71-6
16 Armendariz, A. D.; Gonzalez, M.; Loguinov, A. V.; Vulpe, C. D. (2004) Physiol Genomics 20 1 45-54
17 Simpson, D. M.; Beynon, R. J.; Robertson, D. H.; Loughran, M. J.; Haywood, S. (2004) Proteomics 4 2 524-36
18 Tosco, A.; Siciliano, R. A.; Cacace, G.; Mazzeo, M. F.; Capone, R.; Malorni, A.; Leone, A.; Marzullo, L. (2005) J Proteome Res 4 5 1781-8
19 She, Y. M.; Narindrasorasak, S.; Yang, S.; Spitale, N.; Roberts, E. A.; Sarkar, B. (2003) Mol Cell Proteomics 2 12 1306-18
20 Roelofsen, H.; Balgobind, R.; Vonk, R. J. (2004) J Cell Biochem 93 4 732-40
21 Kulkarni, P. P.; She, Y. M.; Smith, S. D.; Roberts, E. A.; Sarkar, B. (2006) Chemistry 12 9 2410-22
22 Lim, C. M.; Cater, M. A.; Mercer, J. F.; La Fontaine, S. (2006) J Biol Chem 281 20 14006-14
23 Lim, C. M.; Cater, M. A.; Mercer, J. F.; La Fontaine, S. (2006) Biochem Biophys Res Commun 348 2 428-36
24 Ko, J. H.; Son, W.; Bae, G. Y.; Kang, J. H.; Oh, W.; Yoo, O. J. (2006) J Cell Biochem 99 3 719-34
25 Brooks, S. P.; Cockell, K. A.; Dawson, B. A.; Ratnayake, W. M.; Lampi, B. J.; Belonje, B.; Black, D. B.; Plouffe, L. J. (2003) J Nutr Biochem 14 11 648-55
26 Prohaska, J. R.; Brokate, B. (1999) J Nutr 129 12 2147-53
27 Jannaschk, D.; Burgos, M.; Centerlles, J. J.; Ovadi, J.; Cascante, M. (1999) FEBS Lett 445 1 144-8
28 Lucato, L. T.; Otaduy, M. C.; Barbosa, E. R.; Machado, A. A.; McKinney, A.; Bacheschi, L. A.; Scaff, M.; Cerri, G. G.; Leite, C. C. (2005) AJNR Am J Neuroradiol 26 5 1066-71
29 Valko, M.; Morris, H.; Cronin, M. T. (2005) Curr Med Chem 12 10 1161-208
30 Scheinberg, I. H.; Sternlieb, I. (1996) Am J Clin Nutr 63 5 842S-5S
31 Tanner, M. S. (1998) Am J Clin Nutr 67 5 Suppl 1074S-1081S
32 Araya, M.; Olivares, M.; Pizarro, F.; Gonzalez, M.; Speisky, H.; Uauy, R. (2003) Am J Clin Nutr 77 3 646-50
33 De Freitas, J.; Wintz, H.; Kim, J. H.; Poynton, H.; Fox, T.; Vulpe, C. (2003) Biometals 16 1 185-97

34 Gross, C.; Kelleher, M.; Iyer, V. R.; Brown, P. O.; Winge, D. R. (2000) J Biol Chem 275 41 32310-6
35 De Freitas, J. M.; Kim, J. H.; Poynton, H.; Su, T.; Wintz, H.; Fox, T.; Holman, P.; Loguinov, A.; Keles, S.; van der Laan, M.; Vulpe, C. (2004) J Biol Chem 279 6 4450-8
36 van Bakel, H.; Strengman, E.; Wijmenga, C.; Holstege, F. C. (2005) Physiol Genomics 22 3 356-67
37 Heuchel, R.; Radtke, F.; Georgiev, O.; Stark, G.; Aguet, M.; Schaffner, W. (1994) Embo J 13 12 2870-5
38 Bauerly, K. A.; Kelleher, S. L.; Lonnerdal, B. (2004) J Nutr Biochem 15 3 155-62
39 Bauerly, K. A.; Kelleher, S. L.; Lonnerdal, B. (2005) Am J Physiol Gastrointest Liver Physiol 288 5 G1007-14
40 Tennant, J.; Stansfield, M.; Yamaji, S.; Srai, S. K.; Sharp, P. (2002) FEBS Lett 527 1-3 239-44
41 Lee, J.; Prohaska, J. R.; Dagenais, S. L.; Glover, T. W.; Thiele, D. J. (2000) Gene 254 1-2 87-96
42 Paynter, J. A.; Grimes, A.; Lockhart, P.; Mercer, J. F. (1994) FEBS Lett 351 2 186-90
43 Song, M. O.; Freedman, J. H. (2005) Mol Cell Biochem 279 1-2 141-7
44 Birkey Reffey, S.; Wurthner, J. U.; Parks, W. T.; Roberts, A. B.; Duckett, C. S. (2001) J Biol Chem 276 28 26542-9
45 Duckett, C. S.; Gedrich, R. W.; Gilfillan, M. C.; Thompson, C. B. (1997) Mol Cell Biol 17 3 1535-42
46 Klomp, A. E.; van de Sluis, B.; Klomp, L. W.; Wijmenga, C. (2003) J Hepatol 39 5 703-9
47 Fuentealba, I. C.; Aburto, E. M. (2003) Comp Hepatol 2 1 5
48 Gentleman, R. C.; Carey, V. J.; Bates, D. M.; Bolstad, B.; Dettling, M.; Dudoit, S.; Ellis, B.; Gautier, L.; Ge, Y.; Gentry, J.; Hornik, K.; Hothorn, T.; Huber, W.; Iacus, S.; Irizarry, R.; Leisch, F.; Li, C.; Maechler, M.; Rossini, A. J.; Sawitzki, G.; Smith, C.; Smyth, G.; Tierney, L.; Yang, J. Y.; Zhang, J. (2004) Genome Biol 5 10 R80
49 Yang, Y. H.; Dudoit, S.; Luu, P.; Lin, D. M.; Peng, V.; Ngai, J.; Speed, T. P. (2002) Nucleic Acids Res 30 4 e15
50 Huber, W.; von Heydebreck, A.; Sultmann, H.; Poustka, A.; Vingron, M. (2002) Bioinformatics 18 Suppl 1 S96-104
51 Wu, H.; Kerr, K.; Cui, X.; Churchill, G. A., MAANOVA: A software package for the analysis of spotted cDNA microarray experiments. In *The analysis of gene expression data*, Springer: 2003.
52 Andrews, G. K. (1990) Prog Food Nutr Sci 14 2-3 193-258
53 Ishii, T.; Itoh, K.; Takahashi, S.; Sato, H.; Yanagawa, T.; Katoh, Y.; Bannai, S.; Yamamoto, M. (2000) J Biol Chem 275 21 16023-9
54 Blokhina, O.; Virolainen, E.; Fagerstedt, K. V. (2003) Ann Bot (Lond) 91 Spec No 179-94
55 Bauer, M.; Bauer, I. (2002) Antioxid Redox Signal 4 5 749-58
56 Leonard, S. S.; Harris, G. K.; Shi, X. (2004) Free Radic Biol Med 37 12 1921-42
57 Klein, D.; Lichtmannegger, J.; Finckh, M.; Summer, K. H. (2003) Arch Toxicol 77 10 568-75
58 Vyoral, D.; Petrak, J. (2005) Int J Biochem Cell Biol 37 9 1768-73
59 Shi, X.; Dong, Z.; Huang, C.; Ma, W.; Liu, K.; Ye, J.; Chen, F.; Leonard, S. S.; Ding, M.; Castranova, V.; Vallyathan, V. (1999) Mol Cell Biochem 194 1-2 63-70
60 Armendariz, A. D.; Olivares, F.; Pulgar, R.; Loguinov, A.; Cambiazo, V.; Vulpe, C. D.; Gonzalez, M. (2006) Biol Res 39 1 125-42
61 Anderson, S. P.; Howroyd, P.; Liu, J.; Qian, X.; Bahnemann, R.; Swanson, C.; Kwak, M. K.; Kensler, T. W.; Corton, J. C. (2004) J Biol Chem 279 50 52390-8
62 Kwak, M. K.; Wakabayashi, N.; Greenlaw, J. L.; Yamamoto, M.; Kensler, T. W. (2003) Mol Cell Biol 23 23 8786-94
63 Valko, M.; Rhodes, C. J.; Moncol, J.; Izakovic, M.; Mazur, M. (2006) Chem Biol Interact 160 1 1-40
64 Wang, X. W.; Hussain, S. P.; Huo, T. I.; Wu, C. G.; Forgues, M.; Hofseth, L. J.; Brechot, C.; Harris, C. C. (2002) Toxicology 181-182 43-7
65 Goh, J.; Callagy, G.; McEntee, G.; O'Keane, J. C.; Bomford, A.; Crowe, J. (1999) Eur J Gastroenterol Hepatol 11 8 915-9
66 Kumagi, T.; Horiike, N.; Abe, M.; Kurose, K.; Iuchi, H.; Masumoto, T.; Joko, K.; Akbar, S. F.; Michitaka, K.; Onji, M. (2005) Intern Med 44 5 439-43

67 Iwadate, H.; Ohira, H.; Suzuki, T.; Abe, K.; Yokokawa, J.; Takiguchi, J.; Rai, T.; Orikasa, H.; Irisawa, A.; Obara, K.; Kasukawa, R.; Sato, Y. (2004) Intern Med 43 11 1042-5

68 Steindl, P.; Ferenci, P.; Dienes, H. P.; Grimm, G.; Pabinger, I.; Madl, C.; Maier-Dobersberger, T.; Herneth, A.; Dragosics, B.; Meryn, S.; Knoflach, P.; Granditsch, G.; Gangl, A. (1997) Gastroenterology 113 1 212-8

69 Thorgeirsson, S. S.; Lee, J. S.; Grisham, J. W. (2006) Hepatology 43 2 Suppl 1 S145-50

70 Nairz, M.; Weiss, G. (2006) Wien Klin Wochenschr 118 15-16 442-62

71 Pietrangelo, A. (2006) Biochim Biophys Acta 1763 7 700-10

72 Deicher, R.; Horl, W. H. (2006) Eur J Clin Invest 36 5 301-9

73 Lee, P. L.; Beutler, E.; Rao, S. V.; Barton, J. C. (2004) Blood 103 12 4669-71

74 Papanikolaou, G.; Samuels, M. E.; Ludwig, E. H.; MacDonald, M. L.; Franchini, P. L.; Dube, M. P.; Andres, L.; MacFarlane, J.; Sakellaropoulos, N.; Politou, M.; Nemeth, E.; Thompson, J.; Risler, J. K.; Zaborowska, C.; Babakaiff, R.; Radomski, C. C.; Pape, T. D.; Davidas, O.; Christakis, J.; Brissot, P.; Lockitch, G.; Ganz, T.; Hayden, M. R.; Goldberg, Y. P. (2004) Nat Genet 36 1 77-82

75 Roetto, A.; Papanikolaou, G.; Politou, M.; Alberti, F.; Girelli, D.; Christakis, J.; Loukopoulos, D.; Camaschella, C. (2003) Nat Genet 33 1 21-2

76 Britton, R. S.; Leicester, K. L.; Bacon, B. R. (2002) Int J Hematol 76 3 219-28

77 Franchini, M.; Veneri, D. (2005) Hematology 10 2 145-9

78 Kitzberger, R.; Madl, C.; Ferenci, P. (2005) Metab Brain Dis 20 4 295-302

79 Das, S. K.; Ray, K. (2006) Nat Clin Pract Neurol 2 9 482-93

80 Ala, A.; Walker, A. P.; Ashkan, K.; Dooley, J. S.; Schilsky, M. L. (2007) Lancet 369 9559 397-408

81 Spellman, P. T.; Miller, M.; Stewart, J.; Troup, C.; Sarkans, U.; Chervitz, S.; Bernhart, D.; Sherlock, G.; Ball, C.; Lepage, M.; Swiatek, M.; Marks, W. L.; Goncalves, J.; Markel, S.; Iordan, D.; Shojatalab, M.; Pizarro, A.; White, J.; Hubley, R.; Deutsch, E.; Senger, M.; Aronow, B. J.; Robinson, A.; Bassett, D.; Stoeckert, C. J., Jr.; Brazma, A. (2002) Genome Biol 3 9 RESEARCH0046

82 Parkinson, H.; Kapushesky, M.; Shojatalab, M.; Abeygunawardena, N.; Coulson, R.; Farne, A.; Holloway, E.; Kolesnykov, N.; Lilja, P.; Lukk, M.; Mani, R.; Rayner, T.; Sharma, A.; William, E.; Sarkans, U.; Brazma, A. (2007) Nucleic Acids Res 35 Database issue D747-50

83 Edgar, R.; Domrachev, M.; Lash, A. E. (2002) Nucleic Acids Res 30 1 207-10

84 Bammler, T.; Beyer, R. P.; Bhattacharya, S.; Boorman, G. A.; Boyles, A.; Bradford, B. U.; Bumgarner, R. E.; Bushel, P. R.; Chaturvedi, K.; Choi, D.; Cunningham, M. L.; Deng, S.; Dressman, H. K.; Fannin, R. D.; Farin, F. M.; Freedman, J. H.; Fry, R. C.; Harper, A.; Humble, M. C.; Hurban, P.; Kavanagh, T. J.; Kaufmann, W. K.; Kerr, K. F.; Jing, L.; Lapidus, J. A.; Lasarev, M. R.; Li, J.; Li, Y. J.; Lobenhofer, E. K.; Lu, X.; Malek, R. L.; Milton, S.; Nagalla, S. R.; O'Malley J, P.; Palmer, V. S.; Pattee, P.; Paules, R. S.; Perou, C. M.; Phillips, K.; Qin, L. X.; Qiu, Y.; Quigley, S. D.; Rodland, M.; Rusyn, I.; Samson, L. D.; Schwartz, D. A.; Shi, Y.; Shin, J. L.; Sieber, S. O.; Slifer, S.; Speer, M. C.; Spencer, P. S.; Sproles, D. I.; Swenberg, J. A.; Suk, W. A.; Sullivan, R. C.; Tian, R.; Tennant, R. W.; Todd, S. A.; Tucker, C. J.; Van Houten, B.; Weis, B. K.; Xuan, S.; Zarbl, H. (2005) Nat Methods 2 5 351-6

85 Baranova, A.; Schlauch, K.; Gowder, S.; Collantes, R.; Chandhoke, V.; Younossi, Z. M. (2005) Liver Int 25 6 1091-6

86 Su, A. I.; Welsh, J. B.; Sapinoso, L. M.; Kern, S. G.; Dimitrov, P.; Lapp, H.; Schultz, P. G.; Powell, S. M.; Moskaluk, C. A.; Frierson, H. F., Jr.; Hampton, G. M. (2001) Cancer Res 61 20 7388-93

87 Chuma, M.; Sakamoto, M.; Yamazaki, K.; Ohta, T.; Ohki, M.; Asaka, M.; Hirohashi, S. (2003) Hepatology 37 1 198-207

88 Ji, X.; Cheung, R.; Cooper, S.; Li, Q.; Greenberg, H. B.; He, X. S. (2003) Hepatology 37 3 610-21

89 Tan, H.; Derrick, J.; Hong, J.; Sanda, C.; Grosse, W. M.; Edenberg, H. J.; Taylor, M.; Seiwert, S.; Blatt, L. M. (2005) J Interferon Cytokine Res 25 10 632-49

90 Kim, I. J.; Kang, H. C.; Park, J. G. (2005) Gastroenterology 129 5 1803; author reply 1803-4

91 Kim, J. W.; Ye, Q.; Forgues, M.; Chen, Y.; Budhu, A.; Sime, J.; Hofseth, L. J.; Kaul, R.; Wang, X. W. (2004) Hepatology 39 2 518-27

92 Huster, D.; Purnat, T. D.; Burkhead, J. L.; Ralle, M.; Fiehn, O.; Stuckert, F.; Olson, N. E.; Teupser, D.; Lutsenko, S. (2007) J Biol Chem
93 Backes, C.; Keller, A.; Kuentzer, J.; Kneissl, B.; Comtesse, N.; Elnakady, Y. A.; Muller, R.; Meese, E.; Lenhof, H. P. (2007) Nucleic Acids Res 35 Web Server issue W186-92
94 Mercer, J. F.; Grimes, A.; Rauch, H. (1992) J Nutr 122 6 1254-9
95 Muckenthaler, M.; Roy, C. N.; Custodio, A. O.; Minana, B.; deGraaf, J.; Montross, L. K.; Andrews, N. C.; Hentze, M. W. (2003) Nat Genet 34 1 102-7
96 Daffada, A. A.; Young, S. P. (1999) FEBS Lett 457 2 214-8
97 Laftah, A. H.; Ramesh, B.; Simpson, R. J.; Solanky, N.; Bahram, S.; Schumann, K.; Debnam, E. S.; Srai, S. K. (2004) Blood 103 10 3940-4
98 Mazur, A.; Feillet-Coudray, C.; Romier, B.; Bayle, D.; Gueux, E.; Ruivard, M.; Coudray, C.; Rayssiguier, Y. (2003) Metabolism 52 10 1229-31
99 Theurl, I.; Ludwiczek, S.; Eller, P.; Seifert, M.; Artner, E.; Brunner, P.; Weiss, G. (2005) J Hepatol 43 4 711-9
100 Barisani, D.; Meneveri, R.; Ginelli, E.; Cassani, C.; Conte, D. (2000) FEBS Lett 469 2-3 208-12
101 Wallander, M. L.; Leibold, E. A.; Eisenstein, R. S. (2006) Biochim Biophys Acta 1763 7 668-89
102 Rouault, T. A. (2006) Nat Chem Biol 2 8 406-14
103 Barzilai, A.; Yamamoto, K. (2004) DNA Repair (Amst) 3 8-9 1109-15
104 Ryter, S. W.; Kim, H. P.; Hoetzel, A.; Park, J. W.; Nakahira, K.; Wang, X.; Choi, A. M. (2007) Antioxid Redox Signal 9 1 49-89
105 Poli, G. (2000) Mol Aspects Med 21 3 49-98
106 Border, W. A.; Noble, N. A. (1994) N Engl J Med 331 19 1286-92
107 Bissell, D. M.; Roulot, D.; George, J. (2001) Hepatology 34 5 859-67
108 Houglum, K.; Bedossa, P.; Chojkier, M. (1994) Am J Physiol 267 5 Pt 1 G908-13
109 Tassabehji, N. M.; VanLandingham, J. W.; Levenson, C. W. (2005) Exp Biol Med (Maywood) 230 10 699-708
110 Pietrangelo, A.; Rocchi, E.; Schiaffonati, L.; Ventura, E.; Cairo, G. (1990) Hepatology 11 5 798-804
111 Gualdi, R.; Casalgrandi, G.; Montosi, G.; Ventura, E.; Pietrangelo, A. (1994) Gastroenterology 107 4 1118-24
112 Petrak, J.; Myslivcova, D.; Man, P.; Cmejla, R.; Cmejlova, J.; Vyoral, D.; Elleder, M.; Vulpe, C. D. (2007) Am J Physiol Gastrointest Liver Physiol
113 Brunet, S.; Thibault, L.; Delvin, E.; Yotov, W.; Bendayan, M.; Levy, E. (1999) Hepatology 29 6 1809-17
114 Rodo, M.; Czonkowska, A.; Pulawska, M.; Swiderska, M.; Tarnacka, B.; Wehr, H. (2000) Eur J Neurol 7 5 491-4
115 Klevay, L. M. (1987) Med Hypotheses 24 2 111-9
116 Levy, E.; Brunet, S.; Alvarez, F.; Seidman, E.; Bouchard, G.; Escobar, E.; Martin, S. (2007) Life Sci
117 Coronado, V. A.; Damaraju, D.; Kohijoki, R.; Cox, D. W. (2003) Mamm Genome 14 7 483-91
118 Hardy, R. M.; Stevens, J. B.; Stowe, C. M. (1975) Minnesota Veterinarian 15 13-24
119 Su, L. C.; Owen, C. A., Jr.; Zollman, P. E.; Hardy, R. M. (1982) Am J Physiol 243 3 G231-G236
120 Su, L. C.; Ravanshad, S.; Owen, C. A., Jr.; McCall, J. T.; Zollman, P. E.; Hardy, R. M. (1982) Am J Physiol 243 3 G226-30
121 Burstein, E.; Ganesh, L.; Dick, R. D.; van De Sluis, B.; Wilkinson, J. C.; Klomp, L. W.; Wijmenga, C.; Brewer, G. J.; Nabel, G. J.; Duckett, C. S. (2004) Embo J 23 1 244-54
122 Biasio, W.; Chang, T.; McIntosh, C. J.; McDonald, F. J. (2004) J Biol Chem 279 7 5429-34
123 Ganesh, L.; Burstein, E.; Guha-Niyogi, A.; Louder, M. K.; Mascola, J. R.; Klomp, L. W.; Wijmenga, C.; Duckett, C. S.; Nabel, G. J. (2003) Nature 426 6968 853-7
124 de Bie, P.; van de Sluis, B.; Burstein, E.; Duran, K. J.; Berger, R.; Duckett, C. S.; Wijmenga, C.; Klomp, L. W. (2006) Biochem J
125 Scheel, J. R.; Garrett, L. J.; Allen, D. M.; Carter, T. A.; Randolph-Moore, L.; Gambello, M. J.; Gage, F. H.; Wynshaw-Boris, A.; Barlow, C. (2003) Nucleic Acids Res 31 10 e57

126 Hofker, M. H.; van Deursen, J., *Transgenic Mouse Methods and Protocols*. Humana Press: 2002; Vol. 209, p 392.
127 Nada, S.; Yagi, T.; Takeda, H.; Tokunaga, T.; Nakagawa, H.; Ikawa, Y.; Okada, M.; Aizawa, S. (1993) Cell 73 6 1125-35
128 Lee, J.; Prohaska, J. R.; Thiele, D. J. (2001) Proc Natl Acad Sci U S A 98 12 6842-7
129 Brummelkamp, T. R.; Bernards, R.; Agami, R. (2002) Cancer Cell 2 3 243-7
130 Brummelkamp, T. R.; Bernards, R.; Agami, R. (2002) Science 296 5567 550-3
131 Vrljicak, P.; Myburgh, D.; Ryan, A. K.; van Rooijen, M. A.; Mummery, C. L.; Gupta, I. R. (2004) Am J Physiol Renal Physiol 286 4 F625-33
132 Wang, Y.; Joh, K.; Masuko, S.; Yatsuki, H.; Soejima, H.; Nabetani, A.; Beechey, C. V.; Okinami, S.; Mukai, T. (2004) Mol Cell Biol 24 1 270-9
133 Shibata, T.; Giaccia, A. J.; Brown, J. M. (2000) Gene Ther 7 6 493-8
134 Nabetani, A.; Hatada, I.; Morisaki, H.; Oshimura, M.; Mukai, T. (1997) Mol Cell Biol 17 2 789-98
135 Zhang, Z.; Joh, K.; Yatsuki, H.; Wang, Y.; Arai, Y.; Soejima, H.; Higashimoto, K.; Iwasaka, T.; Mukai, T. (2005) Gene
136 Wang, Y.; Joh, K.; Mukai, T. (2002) Genes Genet Syst 77 5 377-81
137 Haywood, S.; Fuentealba, I. C.; Kemp, S. J.; Trafford, J. (2001) J Small Anim Pract 42 4 181-5
138 Kuo, Y. M.; Zhou, B.; Cosco, D.; Gitschier, J. (2001) Proc Natl Acad Sci U S A 98 12 6836-41
139 Buiakova, O. I.; Xu, J.; Lutsenko, S.; Zeitlin, S.; Das, K.; Das, S.; Ross, B. M.; Mekios, C.; Scheinberg, I. H.; Gilliam, T. C. (1999) Hum Mol Genet 8 9 1665-71
140 Mercer, J. F. (1998) Am J Clin Nutr 67 5 Suppl 1022S-1028S
141 Theophilos, M. B.; Cox, D. W.; Mercer, J. F. (1996) Hum Mol Genet 5 10 1619-24
142 Aprelikova, O.; Chandramouli, G. V.; Wood, M.; Vasselli, J. R.; Riss, J.; Maranchie, J. K.; Linehan, W. M.; Barrett, J. C. (2004) J Cell Biochem 92 3 491-501
143 Lee, J. W.; Bae, S. H.; Jeong, J. W.; Kim, S. H.; Kim, K. W. (2004) Exp Mol Med 36 1 1-12
144 Greijer, A. E.; van der Groep, P.; Kemming, D.; Shvarts, A.; Semenza, G. L.; Meijer, G. A.; van de Wiel, M. A.; Belien, J. A.; van Diest, P. J.; van der Wall, E. (2005) J Pathol 206 3 291-304
145 Semenza, G. L. (1999) Annu Rev Cell Dev Biol 15 551-78
146 Vengellur, A.; Woods, B. G.; Ryan, H. E.; Johnson, R. S.; LaPres, J. J. (2003) Gene Expr 11 3-4 181-97
147 Bianchi, L.; Tacchini, L.; Cairo, G. (1999) Nucleic Acids Res 27 21 4223-7
148 Takeda, K.; Ho, V. C.; Takeda, H.; Duan, L. J.; Nagy, A.; Fong, G. H. (2006) Mol Cell Biol 26 22 8336-46
149 Greene, W. C. (2004) Nat Immunol 5 1 18-9
150 Murphy, B. J.; Sato, B. G.; Dalton, T. P.; Laderoute, K. R. (2005) Biochem Biophys Res Commun 337 3 860-7
151 Iyer, N. V.; Kotch, L. E.; Agani, F.; Leung, S. W.; Laughner, E.; Wenger, R. H.; Gassmann, M.; Gearhart, J. D.; Lawler, A. M.; Yu, A. Y.; Semenza, G. L. (1998) Genes Dev 12 2 149-62
152 Gnarra, J. R.; Ward, J. M.; Porter, F. D.; Wagner, J. R.; Devor, D. E.; Grinberg, A.; Emmert-Buck, M. R.; Westphal, H.; Klausner, R. D.; Linehan, W. M. (1997) Proc Natl Acad Sci U S A 94 17 9102-7
153 Hong, S. B.; Furihata, M.; Baba, M.; Zbar, B.; Schmidt, L. S. (2006) Lab Invest 86 7 664-75
154 Cowden Dahl, K. D.; Fryer, B. H.; Mack, F. A.; Compernolle, V.; Maltepe, E.; Adelman, D. M.; Carmeliet, P.; Simon, M. C. (2005) Mol Cell Biol 25 23 10479-91
155 Donadio, S.; Alfaidy, N.; De Keukeleire, B.; Micoud, J.; Feige, J. J.; Challis, J. R.; Benharouga, M. (2007) Placenta
156 Rossant, J.; Cross, J. C. (2001) Nat Rev Genet 2 7 538-48
157 Maine, G. N.; Mao, X.; Komarck, C. M.; Burstein, E. (2006) Embo J
158 Pause, A.; Lee, S.; Worrell, R. A.; Chen, D. Y.; Burgess, W. H.; Linehan, W. M.; Klausner, R. D. (1997) Proc Natl Acad Sci U S A 94 6 2156-61
159 Semenza, G. L. (2000) Genes Dev 14 16 1983-91
160 Hoffmann, A.; Natoli, G.; Ghosh, G. (2006) Oncogene 25 51 6706-16

161 Wang, J.; Wang, X.; Hussain, S.; Zheng, Y.; Sanjabi, S.; Ouaaz, F.; Beg, A. A. (2007) J Immunol 178 11 6777-88
162 Hoffmann, A.; Leung, T. H.; Baltimore, D. (2003) Embo J 22 20 5530-9
163 Natoli, G.; Saccani, S.; Bosisio, D.; Marazzi, I. (2005) Nat Immunol 6 5 439-45
164 Udalova, I. A.; Mott, R.; Field, D.; Kwiatkowski, D. (2002) Proc Natl Acad Sci U S A 99 12 8167-72
165 van de Sluis, B.; Groot, A. J.; Wijmenga, C.; Vooijs, M.; Klomp, L. W. (2007) Cell Cycle 6 17 2091-8
166 de Bie, P.; van de Sluis, B.; Burstein, E.; Duran, K. J.; Berger, R.; Duckett, C. S.; Wijmenga, C.; Klomp, L. W. (2006) Biochem J 398 1 63-71
167 van de Sluis, B.; Muller, P.; Duran, K.; Chen, A.; Groot, A. J.; Klomp, L. W.; Liu, P. P.; Wijmenga, C. (2007) Mol Cell Biol 27 11 4142-56
168 Maine, G. N.; Mao, X.; Komarck, C. M.; Burstein, E. (2007) Embo J 26 2 436-47
169 Sun, Z.; Andersson, R. (2002) Shock 18 2 99-106
170 Tian, B.; Nowak, D. E.; Jamaluddin, M.; Wang, S.; Brasier, A. R. (2005) J Biol Chem 280 17 17435-48
171 Sen, R.; Baltimore, D. (1986) Cell 47 6 921-8
172 dos Santos, C. C.; Han, B.; Andrade, C. F.; Bai, X.; Uhlig, S.; Hubmayr, R.; Tsang, M.; Lodyga, M.; Keshavjee, S.; Slutsky, A. S.; Liu, M. (2004) Physiol Genomics 19 3 331-42
173 Manos, E. J.; Jones, D. A. (2001) Cancer Res 61 2 433-8
174 Schwamborn, J.; Lindecke, A.; Elvers, M.; Horejschi, V.; Kerick, M.; Rafigh, M.; Pfeiffer, J.; Prullage, M.; Kaltschmidt, B.; Kaltschmidt, C. (2003) BMC Genomics 4 1 46
175 Zhou, A.; Scoggin, S.; Gaynor, R. B.; Williams, N. S. (2003) Oncogene 22 13 2054-64
176 Perkins, N. D. (1997) Int J Biochem Cell Biol 29 12 1433-48
177 Natoli, G.; De Santa, F. (2006) Cell Death Differ 13 5 693-6
178 Townley-Tilson, W. H.; Pendergrass, S. A.; Marzluff, W. F.; Whitfield, M. L. (2006) Rna 12 10 1853-67
179 Gorgoni, B.; Andrews, S.; Schaller, A.; Schumperli, D.; Gray, N. K.; Muller, B. (2005) Rna 11 7 1030-42
180 Zhao, X.; McKillop-Smith, S.; Muller, B. (2004) J Cell Sci 117 Pt 25 6043-51
181 Magder, S.; Neculcea, J.; Neculcea, V.; Sladek, R. (2006) J Vasc Res 43 5 447-61
182 Viemann, D.; Goebeler, M.; Schmid, S.; Nordhues, U.; Klimmek, K.; Sorg, C.; Roth, J. (2006) J Leukoc Biol 80 1 174-85
183 Black, D.; Bird, M. A.; Hayden, M.; Schrum, L. W.; Lange, P.; Samson, C.; Hatano, E.; Rippe, R. A.; Brenner, D. A.; Behrns, K. E. (2004) Surgery 135 6 619-28
184 Aggarwal, B. B. (2004) Cancer Cell 6 3 203-8
185 Hayden, M. S.; West, A. P.; Ghosh, S. (2006) Oncogene 25 51 6758-80
186 Dutta, J.; Fan, Y.; Gupta, N.; Fan, G.; Gelinas, C. (2006) Oncogene 25 51 6800-16
187 Perkins, N. D. (2006) Oncogene 25 51 6717-30
188 Scheidereit, C. (2006) Oncogene 25 51 6685-705
189 Johnson, C.; Van Antwerp, D.; Hope, T. J. (1999) Embo J 18 23 6682-93
190 Harhaj, E. W.; Sun, S. C. (1999) Mol Cell Biol 19 10 7088-95
191 Carlotti, F.; Dower, S. K.; Qwarnstrom, E. E. (2000) J Biol Chem 275 52 41028-34
192 Birbach, A.; Gold, P.; Binder, B. R.; Hofer, E.; de Martin, R.; Schmid, J. A. (2002) J Biol Chem 277 13 10842-51
193 Tanaka, T.; Grusby, M. J.; Kaisho, T. (2007) Nat Immunol 8 6 584-91
194 Bergink, S.; Salomons, F. A.; Hoogstraten, D.; Groothuis, T. A.; de Waard, H.; Wu, J.; Yuan, L.; Citterio, E.; Houtsmuller, A. B.; Neefjes, J.; Hoeijmakers, J. H.; Vermeulen, W.; Dantuma, N. P. (2006) Genes Dev 20 10 1343-52
195 Peng, J.; Schwartz, D.; Elias, J. E.; Thoreen, C. C.; Cheng, D.; Marsischky, G.; Roelofs, J.; Finley, D.; Gygi, S. P. (2003) Nat Biotechnol 21 8 921-6
196 la Cour, T.; Kiemer, L.; Molgaard, A.; Gupta, R.; Skriver, K.; Brunak, S. (2004) Protein Eng Des Sel 17 6 527-36
197 Bogerd, H. P.; Fridell, R. A.; Benson, R. E.; Hua, J.; Cullen, B. R. (1996) Mol Cell Biol 16 8 4207-14
198 Chung, J. H.; Ginn-Pease, M. E.; Eng, C. (2005) Cancer Res 65 10 4108-16

199 Stommel, J. M.; Marchenko, N. D.; Jimenez, G. S.; Moll, U. M.; Hope, T. J.; Wahl, G. M. (1999) Embo J 18 6 1660-72
200 Li, M.; Brooks, C. L.; Wu-Baer, F.; Chen, D.; Baer, R.; Gu, W. (2003) Science 302 5652 1972-5
201 Hwang, C. Y.; Kim, I. Y.; Kwon, K. S. (2007) Biochem Biophys Res Commun 358 1 219-25
202 Peters, R. (1983) J Biol Chem 258 19 11427-9
203 Brown, K.; Park, S.; Kanno, T.; Franzoso, G.; Siebenlist, U. (1993) Proc Natl Acad Sci U S A 90 6 2532-6
204 Wojcik, C.; DeMartino, G. N. (2003) Int J Biochem Cell Biol 35 5 579-89
205 Duckett, C. S.; Nava, V. E.; Gedrich, R. W.; Clem, R. J.; Van Dongen, J. L.; Gilfillan, M. C.; Shiels, H.; Hardwick, J. M.; Thompson, C. B. (1996) Embo J 15 11 2685-94
206 Nie, L.; Sasaki, M.; Maki, C. G. (2007) J Biol Chem 282 19 14616-25
207 Itahana, Y.; Yeh, E. T.; Zhang, Y. (2006) Mol Cell Biol 26 12 4675-89
208 Alao, J. P.; Gamble, S. C.; Stavropoulou, A. V.; Pomeranz, K. M.; Lam, E. W.; Coombes, R. C.; Vigushin, D. M. (2006) Mol Cancer 5 7
209 Zancai, P.; Dal Col, J.; Piccinin, S.; Guidoboni, M.; Cariati, R.; Rizzo, S.; Boiocchi, M.; Maestro, R.; Dolcetti, R. (2005) Oncogene 24 15 2483-94
210 Maine, G. N.; Burstein, E. (2007) Cell Mol Life Sci 64 15 1997-2005
211 Narindrasorasak, S.; Kulkarni, P.; Deschamps, P.; She, Y. M.; Sarkar, B. (2007) Biochemistry 46 11 3116-28
212 Spee, B.; Arends, B.; van Wees, A. M.; Bode, P.; Penning, L. C.; Rothuizen, J. (2007) Anim Genet 38 2 168-70
213 Solban, N.; Jia, H. P.; Richard, S.; Tremblay, S.; Devlin, A. M.; Peng, J.; Gossard, F.; Guo, D. F.; Morel, G.; Hamet, P.; Lewanczuk, R.; Tremblay, J. (2000) J Biol Chem 275 41 32234-43
214 Devlin, A. M.; Solban, N.; Tremblay, S.; Gutkowska, J.; Schurch, W.; Orlov, S. N.; Lewanczuk, R.; Hamet, P.; Tremblay, J. (2003) Am J Physiol Renal Physiol 284 4 F753-62
215 El Hader, C.; Tremblay, S.; Solban, N.; Gingras, D.; Beliveau, R.; Orlov, S. N.; Hamet, P.; Tremblay, J. (2005) Am J Physiol Renal Physiol 289 6 F1273-80
216 Duckett, C. S.; Li, F.; Wang, Y.; Tomaselli, K. J.; Thompson, C. B.; Armstrong, R. C. (1998) Mol Cell Biol 18 1 608-15
217 Richter, B. W.; Mir, S. S.; Eiben, L. J.; Lewis, J.; Reffey, S. B.; Frattini, A.; Tian, L.; Frank, S.; Youle, R. J.; Nelson, D. L.; Notarangelo, L. D.; Vezzoni, P.; Fearnhead, H. O.; Duckett, C. S. (2001) Mol Cell Biol 21 13 4292-301
218 Yu, H.; Kopito, R. R. (1999) J Biol Chem 274 52 36852-8
219 Holcik, M.; Korneluk, R. G. (2001) Nat Rev Mol Cell Biol 2 7 550-6
220 MacFarlane, M.; Merrison, W.; Bratton, S. B.; Cohen, G. M. (2002) J Biol Chem 277 39 36611-6
221 Suzuki, Y.; Nakabayashi, Y.; Takahashi, R. (2001) Proc Natl Acad Sci U S A 98 15 8662-7
222 Yang, Y.; Fang, S.; Jensen, J. P.; Weissman, A. M.; Ashwell, J. D. (2000) Science 288 5467 874-7
223 Yang, Q. H.; Du, C. (2004) J Biol Chem 279 17 16963-70
224 Li, X.; Yang, Y.; Ashwell, J. D. (2002) Nature 416 6878 345-7
225 Culhane, A. C.; Howlin, J. (2007) Cell Mol Life Sci
226 Ross, D. T.; Scherf, U.; Eisen, M. B.; Perou, C. M.; Rees, C.; Spellman, P.; Iyer, V.; Jeffrey, S. S.; Van de Rijn, M.; Waltham, M.; Pergamenschikov, A.; Lee, J. C.; Lashkari, D.; Shalon, D.; Myers, T. G.; Weinstein, J. N.; Botstein, D.; Brown, P. O. (2000) Nat Genet 24 3 227-35
227 Perou, C. M.; Sorlie, T.; Eisen, M. B.; van de Rijn, M.; Jeffrey, S. S.; Rees, C. A.; Pollack, J. R.; Ross, D. T.; Johnsen, H.; Akslen, L. A.; Fluge, O.; Pergamenschikov, A.; Williams, C.; Zhu, S. X.; Lonning, P. E.; Borresen-Dale, A. L.; Brown, P. O.; Botstein, D. (2000) Nature 406 6797 747-52
228 Buyse, M.; Loi, S.; van't Veer, L.; Viale, G.; Delorenzi, M.; Glas, A. M.; d'Assignies, M. S.; Bergh, J.; Lidereau, R.; Ellis, P.; Harris, A.; Bogaerts, J.; Therasse, P.; Floore, A.; Amakrane, M.; Piette, F.; Rutgers, E.; Sotiriou, C.; Cardoso, F.; Piccart, M. J. (2006) J Natl Cancer Inst 98 17 1183-92
229 Korrat, A.; Greiner, T.; Maurer, M.; Metz, T.; Fiebig, H. H. (2007) Cancer Genomics Proteomics 4 3 187-95

230 Fiebig, H. H.; Schuler, J.; Bausch, N.; Hofmann, M.; Metz, T.; Korrat, A. (2007) Cancer Genomics Proteomics 4 3 197-209
231 Gyorffy, B.; Surowiak, P.; Kiesslich, O.; Denkert, C.; Schafer, R.; Dietel, M.; Lage, H. (2006) Int J Cancer 118 7 1699-712
232 Takemura, F.; Inaba, N.; Miyoshi, E.; Furuya, T.; Terasaki, H.; Ando, S.; Kinoshita, N.; Ogawa, Y.; Taniguchi, N.; Ito, S. (2005) Anal Biochem 337 2 224-34
233 Jenssen, T. K.; Laegreid, A.; Komorowski, J.; Hovig, E. (2001) Nat Genet 28 1 21-8
234 Fink, S.; Schilsky, M. L. (2007) Curr Opin Gastroenterol 23 3 237-43
235 Wang, G.; Zhang, J.; Moskophidis, D.; Mivechi, N. F. (2003) Genesis 36 1 48-61
236 Wong, Y. W.; Schulze, C.; Streichert, T.; Gronostajski, R. M.; Schachner, M.; Tilling, T. (2007) Genome Biol 8 5 R72
237 Guo, K.; Searfoss, G.; Krolikowski, D.; Pagnoni, M.; Franks, C.; Clark, K.; Yu, K. T.; Jaye, M.; Ivashchenko, Y. (2001) Cell Death Differ 8 4 367-76
238 Shin, D.; Jeon, J. H.; Jeong, M.; Suh, H. W.; Kim, S.; Kim, H. C.; Moon, O. S.; Kim, Y. S.; Chung, J. W.; Yoon, S. R.; Kim, W. H.; Choi, I. (2007) Biochim Biophys Acta
239 Lee, S.; Neumann, M.; Stearman, R.; Stauber, R.; Pause, A.; Pavlakis, G. N.; Klausner, R. D. (1999) Mol Cell Biol 19 2 1486-97
240 Groulx, I.; Lee, S. (2002) Mol Cell Biol 22 15 5319-36
241 Fabbro, M.; Henderson, B. R. (2003) Exp Cell Res 282 2 59-69
242 Zimmerman, T. L.; Thevananther, S.; Ghose, R.; Burns, A. R.; Karpen, S. J. (2006) J Biol Chem 281 22 15434-40
243 Saccani, S.; Marazzi, I.; Beg, A. A.; Natoli, G. (2004) J Exp Med 200 1 107-13
244 Lopez-Lazaro, M. (2006) Faseb J 20 7 828-32
245 Koshiji, M.; Huang, L. E. (2004) Cell Cycle 3 7 853-4
246 Clifford, S. C.; Astuti, D.; Hooper, L.; Maxwell, P. H.; Ratcliffe, P. J.; Maher, E. R. (2001) Oncogene 20 36 5067-74
247 Shuai, K.; Liu, B. (2005) Nat Rev Immunol 5 8 593-605
248 Sharrocks, A. D. (2006) Genes Dev 20 7 754-8
249 Long, J.; Wang, G.; Matsuura, I.; He, D.; Liu, F. (2004) Proc Natl Acad Sci U S A 101 1 99-104
250 Gross, M.; Liu, B.; Tan, J.; French, F. S.; Carey, M.; Shuai, K. (2001) Oncogene 20 29 3880-7
251 Tahk, S.; Liu, B.; Chernishof, V.; Wong, K. A.; Wu, H.; Shuai, K. (2007) Proc Natl Acad Sci U S A 104 28 11643-8
252 Glass, C. K.; Rosenfeld, M. G. (2000) Genes Dev 14 2 121-41
253 Liu, B.; Gross, M.; ten Hoeve, J.; Shuai, K. (2001) Proc Natl Acad Sci U S A 98 6 3203-7
254 Huang, L. E.; Arany, Z.; Livingston, D. M.; Bunn, H. F. (1996) J Biol Chem 271 50 32253-9
255 Tumer, Z.; Horn, N. (1997) J Med Genet 34 4 265-74
256 Hawkins, R. D.; Ren, B. (2006) Hum Mol Genet 15 Spec No 1 R1-7

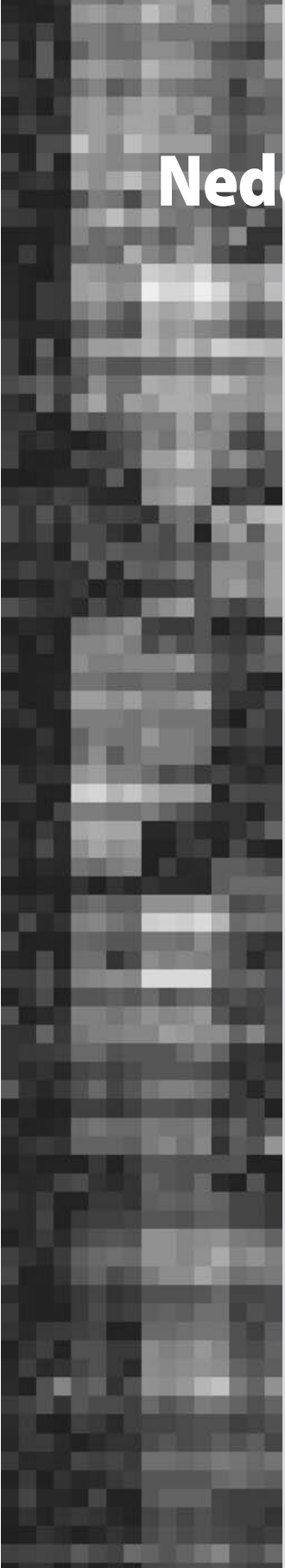

Nederlandse samenvatting

De studie naar de verandering in genexpressie in een organisme wordt aangeduid met de term transcriptomics. Recente ontwikkelingen in transcriptomicstechnieken maken het mogelijk om op een eenvoudige en tijdsbesparende manier een organisme te onderzoeken op variaties in genexpressie, waarbij het totale genoom gescand wordt. In dit proefschrift hebben wij transcriptomics toegepast om een beter inzicht te krijgen in kopermetabolisme en de functie van COMMD (copper metabolism MURR1 domein) eiwitten.

Koper is een sporenelement dat een essentiële rol speelt in belangrijke cellulaire processen. Koper fungeert als redox-cofactor in enzymatische reacties en katalyseert hierdoor de vorming van vrije zuurstofradicalen. Deze radicalen kunnen direct schade toebrengen aan DNA, eiwitten en lipiden. Het is daarom van levensbelang om een adequate balans in koperhomeostase, op zowel cellulair niveau als op het niveau van het organisme te handhaven. Indien eiwitten, die betrokken zijn bij het handhaven van de koperhomeostase, ontbreken of defect zijn, wordt deze balans verstoord en kunnen ernstige ziekteverschijnselen optreden. Mutaties in *ATP7A* (P-type ATPase 7A) en *ATP7B* (P-type ATPase 7B), die coderen voor koperexporterende eiwitten, leiden tot de erfelijke stoornissen als respectievelijk de ziekte van Menkes en de ziekte van Wilson. De ziekte van Menkes is vaak op jonge leeftijd lethaal en wordt veroorzaakt door een algemeen tekort aan koper dat gepaard gaat met groeiafwijkingen en neurologische verschijnselen. Patiënten met de ziekte van Wilson stapelen koper in de lever, waardoor ernstige leverschade kan ontstaan. Deze stoornissen illustreren het belang om koperhomeostase adequaat te reguleren.

Onze kennis over de exacte mechanismen, die de koperimport en koperexport reguleren, is echter beperkt. Het doel in het eerste deel in dit proefschrift is het vergroten van het inzicht in deze mechanismen met behulp van transcriptomics. In **hoofdstuk 1** van dit proefschrift zijn de meest recente ontwikkelingen op het gebied van de regulering van koperhomeostase uiteengezet. Tevens worden in dit hoofdstuk de mogelijkheden besproken om via systeembiologische technieken de pathofysiologische mechanismen die ten grondslag liggen aan koperstoornissen te identificeren.

In **hoofdstuk 2** hebben we in gekweekte humane levercellen en in muizenlevers de veranderingen in het totale genexpressieprofiel als gevolg van koperaccumulatie gekarakteriseerd. De tijdsafhankelijke veranderingen in genexpressie in levercellen werden gekenmerkt door een vroege inductie van metallothioneinegenen en een latere inductie van meer dan honderd genen, die voornamelijk betrokken zijn bij oxidatieve stress en gereguleerde eiwitafbraak. In muizenlevers konden we slechts een matige verandering in expressie van ongeveer twintig genen waarnemen nadat deze muizen een koperrijk dieet hadden gevolgd. Opmerkelijk genoeg vertoonden bekende genen, betrokken bij koperimport, -export, -distributie en -metabolisme geen veranderde expressie na koperbelasting van beide modelsystemen. Waarschijnlijk is bij zoogdieren het handhaven van koperhomeostase daarom voornamelijk op post-transcriptioneel niveau gereguleerd.

Genexpressiestudies zijn vaak onderhevig aan experiment-gebonden variaties. In **hoofdstuk 3** hebben we daarom alle publiekelijk toegankelijke data over genexpressieprofielen van levers en levercellen na koperbehandeling, inclusief onze data uit hoofdstuk 2, verzameld en opnieuw geanalyseerd in een transcriptomics meta-analyse. Met behulp van deze meta-analyse konden wij aantonen dat koperstapeling leidt tot een veranderde expressie van diverse genen. Om te bepalen hoe specifiek deze processen betrokken zijn bij koperstapeling, hebben we een vergelijkbare meta-analyse uitgevoerd op alle genen die als gevolg van ijzeraccumulatie in de lever of in levercellen veranderd tot expressie komen. Door deze twee analyses met elkaar te vergelijken, konden wij aantonen dat verlaagde expressie van vooral cholesterol-synthese geassocieerde genen, specifiek is voor koperaccumulatie.

Recent onderzoek in ons laboratorium heeft aangetoond dat het gen *COMMD1* een rol speelt in de regulatie van koperhomeostase. Bedlington terriers, die een mutatie in *COMMD1* hebben, stapelen koper in de lever. Deze data, in combinatie met het feit dat COMMD1 kan binden aan het koperexporterende eiwit ATP7B, suggereren een rol voor COMMD1 in cellulaire koperexcretie. De precieze manier waarop COMMD1 koperhomeostase kan reguleren is echter onbekend en om dit beter te bestuderen is in ons laboratorium een COMMD1 knockout muis gemaakt, die in **hoofdstuk 4** wordt beschreven. Opvallend genoeg blijkt de COMMD1 knockout muis embryonaal lethaal te zijn. Om een beter inzicht te krijgen in de biologische processen die een rol spelen in deze embryonale letaliteit, hebben we de genexpressieprofielen van COMMD1 knockout embryo's vergeleken met de genexpressieprofielen van wild-type muizenembryo's. COMMD1 knockout embryo's vertoonden een verhoogde expressie van genen die door HIF-1 (hypoxia inducible factor 1) gereguleerd worden. HIF1 reporter experimenten en genexpressiestudies in cellen bevestigden onze hypothese dat COMMD1 HIF-1 activiteit kan remmen.

Studies van anderen tonen aan dat COMMD1, naast een rol in koperexcretie en remming van HIF1 activiteit, ook een rol heeft in de remming van NF-κB (Nuclear factor kappa beta)- activiteit. NF-κB is een transcriptiefactor die de expressie van een groot aantal genen, betrokken in immuunreacties, celdood en celdeling, reguleert. NF-κB bestaat uit verschillende subunits en NF-κB-gemedieerde transcriptie wordt gereguleerd door diverse signaleringseiwitten. COMMD1 kan aan de meeste van deze eiwitten binden en daarmee de expressie van NF-κB-gereguleerde genen remmen. Naast COMMD1 blijken andere COMMD eiwitten, die een homoloog COMM-domein hebben, ook NF-κB-activiteit ook kunnen remmen. De exacte functie van de hele COMMD-eiwitfamilie is echter nog onbekend. Om de functie van de andere COMMD eiwitten te bestuderen hebben we in **hoofdstuk 5** transcriptomics toegepast in gekweekte darmcellen, waarin de expressie van COMMD1, COMMD6 of COMMD9 verlaagd was met behulp van RNA interferentie. De genexpressieprofielen in de COMMD1-, COMMD6- of COMMD9-deficiënte cellijnen

hebben we vergeleken met de profielen van controle cellen in de aan- en afwezigheid van de NF-κB-stimulus TNF (tumor necrosis factor). Na TNF behandeling konden we in alle deficiënte cellijnen een duidelijk afwijkend, zij het COMMDeiwit-specifiek, expressieprofiel van TNF-responsieve genen waarnemen ten opzichte van de controle cellijn.

De functie van NF-κB-regulerende eiwitten wordt bepaald door de cellulaire lokalisatie van deze eiwitten, die afhankelijk is van NESsen (nucleaire export signalen) in de aminozuursequentie van de desbetreffende eiwitten. In **hoofdstuk 6** hebben wij twee NESsen in COMMD1 geïdentificeerd, die het remmende effect van COMMD1 op de NF-κB-activiteit kunnen reguleren. Door COMMD1-constructen te genereren waarin we deze NESsen muteerden, konden we aantonen dat COMMD1 daadwerkelijk nucleaire export ondergaat en dat nucleaire export afhankelijk is van NESsen in COMMD1. Daarnaast konden we, in samenwerking met Dr. E. Burstein, aantonen dat deze domeinen betrokken zijn bij COMMD1-ubiquitinering, COMMD1-afbraak en de vorming van COMMD1-bevattende perinucleaire aggregaten (**hoofdstuk 6 en 7)**.

Kort samengevat heeft het werk in dit proefschrift twee belangrijke nieuwe inzichten opgeleverd. Allereerst hebben we door het analyseren van genexpressieprofielen en literatuurstudies nieuwe aspecten van de transcriptionele regulatie door koper in zoogdieren aangetoond . Daarnaast heeft dit werk bijgedragen aan de karakterisering van de functie van COMMD1 en andere COMMD eiwitten.

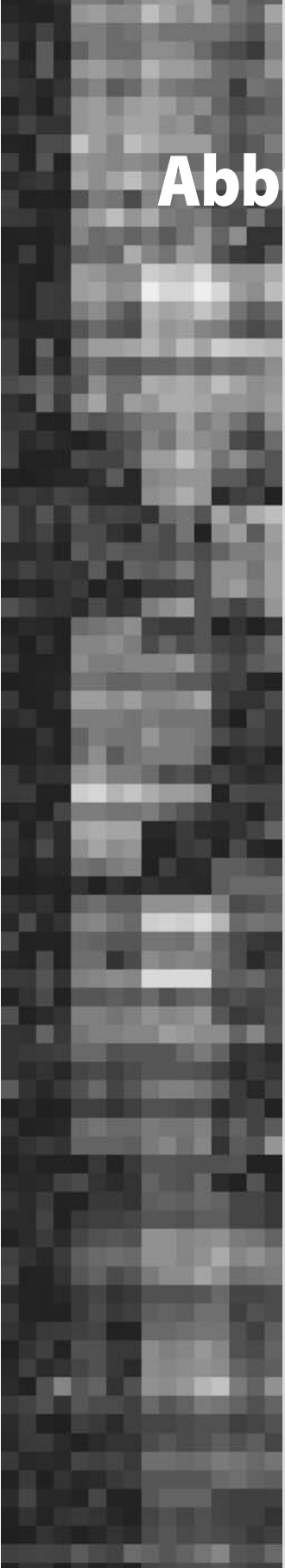

Abbreviations

ATP7A	p-Type ATPase 7A
ATP7B	p-Type ATPase 7B
BCS	Bathocuproine disulphonic acid
COMMD	COpper Metabolism MURR1 Domain
CYP	Cytochrome p450
DPC	Days post coitum
FAAS	Flame atomic absorption spectrometry
GEO	Gene expression omnibus
GFP	Green fluorescent protein
GO	Gene Ontology
HCC	Hepatocellular carcinoma
HEK293T	Human embryonic kidney cells
HH	Hereditary hemochromatosis
HIF-1	Hypoxia inducible factor-1
HMOX1	Heme oxygenase 1
I-κB	Inhibitor of kappa B
LB	Leptomycin B
LEC	Long Evans cinnamon
MAANOVA	Microarray analysis of variance
MD	Menkes disease
MIAME	Minimal information about a microarray experiment database
NES	Nuclear export signal
NF-κB	Nuclear transcription factor κB
NLS	Nuclear localization signal
qRT-PCR	quantitative Reverse Transcriptase Polymerase Chain Reaction
RLU	Relative light units
TNF	Tumor necrosis factor
VHL	Von Hippel Lindau protein
WD	Wilson disease
XIAP	X-linked inhibitor of apoptosis

Dankwoord

Nog even en dan vertrek ik naar Schotland, spannend hoor! Aangezien het dankwoord het meest gelezen deel van een proefschrift is, wil ik daarom iedereen die dit leest uitnodigen om als je toch in Schotland bent even langs te wippen. Maar voor het zo ver is, wil ik nog even stilstaan bij alle mensen die mij hier in Nederland hebben geholpen om te promoveren. Dus bij dezen iedereen enorm, super, geweldig bedankt. Maar dan heb ik me er iets te gemakkelijk van afgemaakt, toch?

Nou oké vooruit dan maar….. er zijn wel een aantal mensen, die ik in het bijzonder hier wil vermelden. Allereerst mijn co-promotor en directe begeleider Leo Klomp. Leo, al op een van de eerste dagen dat ik voor je kwam werken begon je met kleine plagerijtjes. Je vermeldde er wel bij dat je dat alleen deed als je mensen mocht en dat was voor mij het startsignaal voor een tegenoffensief. In de ogen van anderen kwam dit vaak over alsof ik je verschrikkelijk vond. Maar niets is minder waar, ik waardeer je enorm en ik heb veel van je geleerd. Je geduld en de ruimte die je biedt om te leren en zelfstandig te werken hebben me voldoende zelfvertrouwen gegeven om binnenkort als postdoc te kunnen beginnen.

Ook mijn 2 promotoren Cisca Wijmenga en Ruud Berger ben ik veel dank verschuldigd. Cisca, ik heb bewondering voor je opportunistische en strategische aanpak en je steun zelfs als je in dat verre Groningen zat. In het begin vond ik het moeilijk 'je' tegen je te zeggen, omdat je iemand bent die respect afdwingt. Je doet dat echter op zo'n lieve en rechtvaardige manier dat ik dat al snel afleerde. De besprekingen die we iedere maand met jou hadden, zelfs nadat je naar Groningen was verhuisd, waren een uitgelezen kans om alles even op een rijtje te zetten. Bedankt voor alles. Ruud, ongelooflijk knap hoe je vaak aan een paar woorden genoeg hebt om precies een probleem te doorgronden. Bedankt voor al je wijze woorden en dat ik met je mee mocht rijden naar de retraite in Limburg. Al een beetje gewend aan 6 versnellingen in een auto?

Paranimfjes, Willianne en Peter, allereerst vind ik het super dat jullie mijn paranimfen willen zijn. Peter, kamergenoot, je bent een prima boksbal om frustraties op af te reageren (voor sommigen zelfs letterlijk). Je bent een van de meest sociale personen die ik ken en ik vond het prettig met je samen te werken. Succes bij je promotie volgend jaar en je verdere carrière. Willianne, ik vond het erg leuk om naast je te pipetteren. Jij bent echt een keiharde werker en een ontzettend fijne collega. Ook jij succes met de rest van je promotietijd.

Alle andere collega's en ex-collega's van de kopergroep, Prim, Bart, Ellen van Beurden, Helga, Diana, Karen en alle studenten, bedankt. Bart, bedankt voor al je hulpvolle adviezen met pipetteer- en schrijfproblemen. Ik wens je een vruchtbare voortzetting van je carrière in Groningen. Prim, we zijn allebei begonnen als studenten bij Cisca en uiteindelijk als AIO bij Leo beland. Je begon als verlegen jochie in het lab, maar bent uiteindelijk helemaal ontdooid. Ik heb prettig met je samengewerkt en ik hoop dat je een succesvolle postdoc periode in Israel zult hebben. Naast Peter, Bart en Prim wil ik

ook m'n andere kamergenootjes Stan, Gemma en Rafaella bedanken voor een prettige, volgens sommigen te gezellige werksfeer in onze kamer. Veel succes de komende jaren. Gemma, denk nog eens aan me als je de witte wanden van je woonkamer bewonderd. Rafaella, if I drink an espresso, I will think of you. Good luck!

Alle andere stafmedewerkers, AIO's, postdocs en analisten van de afdeling metabole en endocriene ziekten, bedankt voor een fijne periode. Wendy, grappig dat we in dezelfde stad in dezelfde week geboren zijn, in hetzelfde jaargroepje van onze studie zaten en ook nog is een week na elkaar gaan promoveren. Ik wens je het allerbeste met je postdoc in Rotterdam. Lieke, ik zal je schaterlach niet gauw vergeten, eindelijk iemand die mijn kabaal kan overtreffen. Veel succes met de Illumina experimenten, ik weet zeker dat je die nu ook helemaal alleen kunt, hoor! Hannelie, je hebt vaak anti (vooroordeel)-artsen uitspraken van me moeten verduren, maar weet je … dat komt omdat je een echte onderzoeksmetaliteit hebt. Yuan, I enjoyed our dinners after work, even if I had to wait a little while…. Good luck the next years! Monique de Gooier, dank je dat je altijd zo snel klaarstond om een helpende hand toe te steken. Margriet, super dat je me vaak met statistische problemen hebt geholpen. Inge, ik kan je directe manier van dingen zeggen enorm waarderen en vond onze gesprekken vaak erg verhelderend. Truus, jouw motto is 'Voort wat, hoort wat' en daar heb ik regelmatig gebruik van gemaakt. Als ik je hielp met proeven, stond daar vaak een spoedbestelling tegenover, dank je.

In particular I would like to thank our collaborator Ezra Burstein and members of your lab for the fruitful collaboration and helpful discussions. I look forward to your visit in March.

Eric Reits, je enthousiasme is erg aanstekelijk en ik vond het fijn dat ik bij jullie in Amsterdam de live imaging microscoop mocht gebruiken. Dineke, ook jij bedankt voor alle hulp in Amsterdam en veel succes in Groningen.

In Utrecht deelde ik mijn woning met huisgenoten. Merkwaardig genoeg heb ik in de drie jaar dat ik daar woonde drie huisgenoten versleten, hmmm …zou het aan mij liggen? Ik heb in ieder geval prettig met jullie samen gewoond. Dineke, Ineke en Anne veel succes met jullie promoties of studies.

Genexpressiestudies heb ik voornamelijk in het stratenum uitgevoerd, dus ik wil ook de mensen van complex genetics groep en van de Holstege groep bedanken. Eric Strengman, wat een enorm geduld heb jij! Ontzettend bedankt dat je vaak direct klaar stond om mijn laptopproblemen op te lossen.

Mensen van de speciele endocrinologie, ik vond jullie prima buren! Gerard, Ad, Robert-Jan en Chris bedankt voor jullie steun en interesse en euh… Robert-Jan, ik heb volgens mij nog een fles wijn van je te goed!!

Verder wil ik bij de apotheek graag Siem en Vincent bedanken voor hun hulp bij het meten van koperconcentraties in mijn samples.

Als laatste, maar zeker niet in het minst wil ik mijn ouders bedanken. Vaak als ik gefrustreerd was door de vele tegenslagen die inherent zijn aan promoveren kwam ik chagrijnig in het weekend bij jullie logeren. Jullie hebben echter altijd voor me klaar gestaan. Pap en mam, bedankt voor jullie begrip en ik weet dat ik het niet vaak zeg maar bij deze zwart op wit 'ik hou van jullie'.

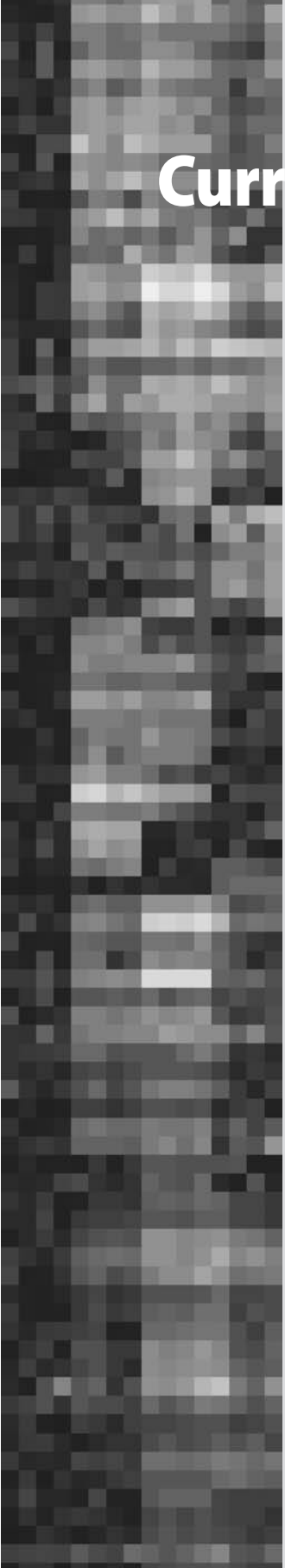

Curriculum Vitae

Patricia Muller is geboren op 7 oktober 1980 in Rotterdam. Na haar VWO examen aan het Willem de Zwijgercollege in Papendrecht is zij in 1998 begonnen aan de studie medische biologie aan de universiteit Utrecht.Voor deze studie heeft zij in 2002 haar hoofdvakstage afgerond aan het Eijkman-Winkler instituut in het UMC Utrecht onder begeleiding van Dr. Willem van Wamel. In deze stage heeft zij een gen met onbekende functie uit de bacterie *Staphylococcus aureus* gekloneerd en aangetoond dat het coderende eiwit potentieel betrokken is bij de remming van humane immuuncellen. Aansluitend heeft zij haar bijvakstage doorlopen aan de afdeling medische genetica onder begeleiding van Dr. Harm van Bakel en Prof. Dr. C. Wijmenga. Gedurende deze stage heeft zij de tijdsafhankelijke veranderingen in genexpressie in gekweekte levercellen na koperbehandeling gekarakteriseerd. Dit onderzoek heeft zij als AIO voortgezet bij de afdeling metabole en endocriene ziekten in het UMC Utrecht na het behalen van haar doctoraal examen medische biologie in 2003. Onder begeleiding van Dr. L. Klomp, Prof. dr. R. Berger en Prof. dr. C. Wijmenga heeft dit onderzoek uiteindelijk geleidt tot de resultaten beschreven in dit proefschrift. Patricia Muller zal haar wetenschappelijke carrière voortzetten aan het Beatson instituut in Glasgow, Schotland onder begeleiding van Prof. dr K. Vousden alwaar zij de mechanismen van p53-gemedieerde transcriptie zal bestuderen.

Patricia Muller was born on Ocotber 7th in 1980 in Rotterdam, the Netherlands. She attended the Willem de Zwijger college secondary school in Papendrecht, after which she started her study medical biology at the University of Utrecht in Utrecht, the Netherlands in 1998. For her major practical training in 2002, she studied the function of an unidentified gene of the bacterium *Staphylococcus aureus* at the Eijkman-Winkler institute in the UMC Utrecht under supervision of Dr. Willem van Wamel. This training was followed by a second practical training at the department of medical genetics under supervision of Dr. H. van Bakel and Prof. dr. C. Wijmenga. In this training she characterized the temporal gene expression profiles of cultured liver cells after copper exposure. In 2003, she graduated and continued this research work at the department of metabolic and endocrine diseases at the UMC Utrecht under supervision of Dr. L. Klomp, Prof. dr. R. Berger and Prof. dr. C. Wijmenga as a PhD-student. The results of this work are described in this thesis. Patricia Muller will continue her scientific carreer at the Beatson Institute in Glasgow, Scotland under supervision of Prof. dr. K. Vousden, where she will study the mechanisms of p53-mediated transcription.

List of publications

Muller PAJ, Klomp LW
Novel perspectives in mammalian copper homeostasis through the use of genome-wide approaches
Am. J. Clin. Nutr. in press

De Bie P, Muller PAJ, Wijmenga C, Klomp LW
Molecular pathogenesis of Wilson and Menkes disease: correlation of mutations with molecular defects and disease phenotypes.
J Med Genet. 2007 Nov;44(11):673-88

De Bie P, van de Sluis B, Burstein E, Van de Berghe PV, Muller PAJ, Berger R, Gitlin J, Wijmenga C, Klomp LW
Distinct Wilson-disease mutations in ATP7B are associated with enhanced binding to COMMD1 and reduced stability of ATP7B.
Gastroenterology 2007 Oct;133(4):1316-26

Muller PAJ, van Bakel H, van de Sluis B, Holstege F, Wijmenga C, Klomp LW
Gene expression profiling of liver cells after copper overload in vivo and in vitro reveals new copper-regulated genes.
J Biol Inorg Chem. 2007 May;12(4):495-507

van de Sluis B, Muller PAJ, Duran K, Chen A, Groot AJ, Klomp LW, Liu PP, Wijmenga C.
Increased activity of hypoxia-inducible factor 1 is associated with early embryonic lethality in Commd1 null mice.
Mol Cell Biol. 2007 Jun;27(11):4142-56

Muller PAJ, , van de Sluis B, Verbeek D, Vonk W, Wijmenga C, Burstein E, Reits E, Klomp LW
Nuclear-cytosolic transport of COMMD1 regulates NF-κB activity
Submitted

Muller PAJ, de Bie P, Wijmenga C, Klomp LW
Novel insights in the pathophysiology of Wilson disease and Hereditary hemochromatosis by a transcriptomics meta-analysis.
Submitted

Maine G, Muller PAJ, Komarck C, Mao X, Klomp LWJ, Burstein E
COMMD1 expression is controlled by critical residues that determine XIAP binding
Submitted

Muller PAJ, Repaka A, Mao X , Maine G, Sluis B, Wijmenga C, Klomp LWJ, Burstein E
Distinct COMMD proteins regulate the expression of specific subsets of NF-κB target genes
Manuscript in preparation